

**LONG-RANGE TRANSPORT CLUSTERS, FINE PARTICULATE  
MATTER (PM<sub>2.5</sub>) AND SOOT CONCENTRATIONS OF AIR MASSES  
IN CAPE TOWN, SOUTH AFRICA**

by

JOHN PETER WILLIAMS

Thesis submitted to the Department of Chemical Sciences of the University of the Western  
Cape in fulfilment of the requirements for the degree of



Supervisor: Prof. L. Petrik

Co-supervisor: Prof. J. Wichmann

**Keywords:** APM, PM<sub>2.5</sub>, Soot, Cape Town, Long-Range Transport, HYSPLIT, Cluster Analysis, Gravimetric Analysis, SSR, IC, ICP-OES, SEM, TEM, Kruskal-Wallis, Pearson Product-Moment Correlation, Shapiro-Wilks, Spearman Rank-Order Correlation

*Copyright 2018, John Peter Williams*

## **DECLARATION**

I, John Peter Williams, hereby declare that this master's thesis represents my own work and has been written by me in its entirety using referenced literature and other sources of information. This thesis has not been submitted to any institute of learning or examining authority for the purposes of obtaining a degree and has not been published before.



---

Signature

UWC, 14 September 2018

---

Place and Date



UNIVERSITY *of the*  
WESTERN CAPE

## **ABSTRACT**

Ambient air pollution is the biggest environmental threat to human health. According to the World Health Organisation (WHO), ambient air pollution kills millions of people worldwide every year. Airborne particulate matter (APM) affects more people than any other air pollutant and has been linked with various adverse health outcomes, especially fine fractions (commonly abbreviated to PM<sub>2.5</sub>). PM<sub>2.5</sub> penetrates lung tissue to enter the cardiovascular system where it poses the greatest risk. Detailed ambient APM studies are rare in Africa. Such studies are needed to better understand the characteristics, origins and trends of particulate pollution. This study was conducted in Cape Town (the first of its kind for the area) as part of a bigger project on ambient PM<sub>2.5</sub> and soot concentrations in South Africa. PM<sub>2.5</sub> filter samples were collected at a fixed sampling site in the suburb of Kraaifontein from April 2017 to April 2018, yielding 121 days of data. PM<sub>2.5</sub> mass concentration and absorption coefficient determinations were done using gravimetric analysis and smoke stain reflectometry (SSR). Mean PM<sub>2.5</sub> concentration for the study period was  $13.4 \pm 8.1 \mu\text{g}\cdot\text{m}^{-3}$  (range: 1.17-39.1  $\mu\text{g}\cdot\text{m}^{-3}$ ) that fell below the South African National Ambient Air Quality Standard (SA NAAQS) annual limit of 20  $\mu\text{g}\cdot\text{m}^{-3}$  but exceeded the WHO annual limit of 10  $\mu\text{g}\cdot\text{m}^{-3}$ . Mean absorption coefficient for the same period was  $1.38 \pm 1.23 \text{ m}^{-1}\cdot 10^{-5}$  (range: 0.00-5.38  $\text{m}^{-1}\cdot 10^{-5}$ ) which did not exceed any limits. Source-region analyses were performed using single, 24-hour backward trajectories and trajectory clusters derived from the Hybrid Single Particle Lagrangian Integrated Trajectory (HYSPLIT) model. Six single trajectories were identified; the most frequent were trajectories Atlantic-Ocean (38.8 %) and Indian-Ocean (26.4 %). Cluster analyses yielded three to four clusters per season. Dominating clusters were Atlantic-Ocean (61.8 %) and Indian-Ocean (29.5 %) and Inland (8.50 %). Contributions by local sources (within 40 km of the sampling site) to PM mass in samples far exceeded those of distant sources through long-range transport (LRT).

## **PREFACE**

This thesis is the culmination of my master's study conducted at the University of the Western Cape (UWC) and documents the research carried out from April 2017 until April 2018. It presents data on ambient PM<sub>2.5</sub> and soot concentrations in Cape Town, South Africa, and focuses specifically on the effects of meteorological parameters, and local, regional and long-range transport on ambient APM concentrations whilst investigating correlation, normality and significance, not only between data of the aforementioned particulate pollutants but also between these pollutants and gaseous air pollutants. Air pollution is an environmental issue that impacts everyone and I am grateful to have been afforded the opportunity of making a contribution towards the better understanding of the issue in my home city of Cape Town.



## **ACKNOWLEDGMENTS**

This study was a learning experience and not without its challenges. Fortunately for me the journey was made simpler by a few individuals and institutions whom I would like to acknowledge. Firstly, I would like to thank God for presenting me with this opportunity for self-improvement and contribution to the understanding of particulate pollution in Cape Town. I would like to thank my supervisors, Prof. Leslie Petrik and Prof. Janine Wichmann for their assistance, guidance and support during this study. A word of thanks goes out to the National Research Foundation (provision of funding), the City of Cape Town: Air Quality Division (provision of air pollution data), the South African Weather Services (provision of meteorological data), Dr. Nico Claassens (air sampling induction), Mr. Adrian Josephs (SEM work), Ms. Natasha Peterson (TEM work), and Mr. Adewale Ademyi, Ms. Thizwilondi Madzaga and Ms. Ilse' Wells (assistance with laboratory works) for their contributions to this study. I would like to thank my partner, Ms. Nicole Mouton, for her patience and support. A special word of thanks goes out to my parents, Mr. John and Periette Williams, for their motivation, support, warm meals, and reduced boarding costs. The above-mentioned all contributed to this study and I thank them all wholeheartedly.

# **TABLE OF CONTENTS**

	Page
LIST OF FIGURES .....	xii
LIST OF TABLES .....	xv
ABBREVIATIONS .....	xvii
CHEMICAL SPECIES .....	xx
REAGENTS AND SOLVENTS.....	xxi
UNITS.....	xxii
STATISTICAL OPERATORS .....	xxiii
<b>CHAPTER 1: INTRODUCTION.....</b>	<b>1</b>
1.1 Background.....	1
1.2 Problem statement.....	2
1.3 Hypothesis.....	3
1.4 Research objectives.....	4
1.5 Research questions .....	5
1.6 Study design.....	6
1.7 Research approach .....	7
1.8 Scope of study.....	8
1.9 Thesis layout .....	9
<b>CHAPTER 2: LITERATURE REVIEW.....</b>	<b>10</b>
2.1 Air pollution.....	10
2.1.1 What is air pollution? .....	10
2.1.2 Historical perspective .....	11
2.1.3 UN Sustainable Development Goals .....	12
2.1.4 Sources of air pollution.....	13
2.1.5 Classification of air pollutants .....	13
2.1.6 Air quality monitoring in South Africa .....	15
2.2 Airborne particulate matter .....	16
2.2.1 Physical attributes .....	16
2.2.1.1 Size and morphology.....	16
2.2.1.2 Formation processes and size modes .....	19
2.2.1.3 Particulate size distribution.....	21
2.2.2 Chemical properties.....	24



2.2.3 Soot.....	25
2.2.4 APM deposition and health effects.....	27
2.2.4.1 Deposition mechanisms in the lungs.....	27
2.2.4.2 Health effects of APM.....	30
2.2.5 Atmospheric dispersion of APM.....	32
2.3 Dispersion, transport and origins of particulate pollution.....	35
2.3.1 HYSPLIT.....	35
2.3.1.1 Calculation method.....	36
2.3.1.2 Backward trajectory analysis.....	37
2.4 Study site description.....	39
2.4.1 South Africa.....	39
2.4.2 Cape Town, Western Cape.....	41
2.4.3 Emission sources in Cape Town.....	43
2.5 Air quality management legislation in South Africa.....	44
2.5.1 Air Pollution Prevention Act.....	44
2.5.2 National Environmental Management: Air Quality Act.....	45
2.5.2.1 National ambient air quality standards.....	45
2.5.2.2 Atmospheric emissions licensing.....	46
2.6 Air quality monitoring.....	47
2.6.1 Global air quality monitoring.....	47
2.6.2 Air quality monitoring in Cape Town.....	48
2.6.3 Ambient APM monitoring.....	49
2.6.3.1 Alternative methodologies of ambient APM monitoring.....	50
2.6.3.2 Prospective methodologies of ambient APM monitoring.....	54
2.7 Gap analysis.....	55
<b>CHAPTER 3: METHODOLOGY.....</b>	<b>56</b>
3.1 Field work.....	56
3.1.1 Sampling site.....	56
3.1.2 Sampling period.....	59
3.1.3 Training and procedures.....	59
3.1.4 Sampling equipment and materials.....	59
3.1.4.1 Sampling station.....	61
3.1.4.2 Collection medium.....	62

3.1.4.3	Air samplers .....	62
3.1.4.4	Air flow calibrators .....	62
3.1.4.5	Miscellaneous items .....	63
3.1.5	Sampling technique .....	63
3.2	Analysis of filter samples.....	65
3.2.1	Chronological information .....	65
3.2.2	Methods and techniques .....	65
3.2.2.1	Gravimetric analysis.....	65
3.2.2.1.1	Equipment and materials .....	66
3.2.2.1.2	Conditioning of filters .....	66
3.2.2.1.3	Laboratory conditions .....	67
3.2.2.1.4	Weighing of filters.....	67
3.2.2.2	Smoke stain reflectometry .....	68
3.2.2.2.1	Equipment and materials .....	69
3.2.2.2.2	Reflection measurements.....	70
3.2.2.3	Inductively coupled plasma-optical emission spectrometry .....	71
3.2.2.3.1	Equipment and materials .....	71
3.2.2.3.2	Cleaning of glassware.....	72
3.2.2.3.3	Working standards and control solution preparation.....	72
3.2.2.3.4	Sample preparation.....	73
3.2.2.3.5	Pre-analysis checks.....	74
3.2.2.3.6	Analysis .....	75
3.2.2.4	High-performance liquid chromatography.....	77
3.2.2.4.1	Equipment and materials .....	77
3.2.2.4.2	Cleaning of glassware.....	78
3.2.2.4.3	Working standards and control solution preparation.....	78
3.2.2.4.4	Sample preparation.....	79
3.2.2.4.5	Eluent preparation.....	80
3.2.2.4.6	Pre-analysis checks .....	80
3.2.2.4.7	Analysis .....	80
3.2.2.5	Scanning electron microscopy .....	82
3.2.2.5.1	Equipment and materials .....	82
3.2.2.5.2	Sample preparation.....	83
3.2.2.5.3	Stub preparation.....	83



3.2.2.5.4 Photomicrography .....	84
3.2.2.6 Transmission electron microscopy .....	85
3.2.2.6.1 Equipment and materials .....	85
3.2.2.6.2 Sample preparation.....	86
3.2.2.6.3 Grid preparation.....	86
3.2.2.6.4 Photomicrography .....	86
3.2.2.7 HYSPLIT modelling .....	87
3.2.2.7.1 Equipment and materials .....	87
3.2.2.7.2 Backward trajectory analysis.....	87
3.3 Air pollution data collected by the City of Cape Town .....	89
3.4 Air pollution data for Pretoria and Thohoyandou.....	90
3.5 Statistical analysis .....	91
3.5.1 Study data .....	91
3.5.1.1 Data management.....	91
3.5.1.2 Determination of outliers in data sets.....	91
3.5.1.3 Normality analysis .....	92
3.5.1.4 Correlation and significance analyses.....	92
3.5.2 Air pollution data collected by the CoCT.....	91
3.5.2.1 Normality analysis .....	91
3.5.2.2 Correlation and significance analyses.....	91
<b>CHAPTER 4: RESULTS .....</b>	<b>94</b>
4.1 Calendar samples .....	94
4.1.1 PM <sub>2.5</sub> mass concentration data.....	94
4.1.2 Absorption coefficient and soot concentration data .....	98
4.1.3 Statistical information.....	102
4.1.3.1 Descriptive statistics and normality analyses.....	102
4.1.3.2 Correlation, linear regression and significance analyses .....	108
4.2 Meteorological data for Cape Town for the study period.....	113
4.3 Origins and trajectories of air masses in Cape Town.....	122
4.3.1 Trajectories .....	122
4.3.2 Trajectory frequencies .....	124
4.4 Correlation between study data and air pollution data collected by the CoCT.....	128
4.4.1 Seasonal air pollution data.....	128
4.4.2 Statistical analyses .....	130

4.2.2.1 Normality analyses .....	130
4.2.2.2 Correlation and significance analyses .....	130
4.4.3 Air pollution data for Pretoria and Thohoyandou .....	134
4.5 Composite samples .....	136
4.5.1 Anion profiling .....	136
4.5.2 Elemental profiling .....	138
4.5.3 Inorganic carbon content .....	140
4.5.4 Chemical composition of PM in composite samples.....	141
4.5.5 Microscopic information .....	144
4.5.5.1 Coagulated and agglomerate particulates .....	144
4.5.5.2 Particulate morphology .....	145
<b>CHAPTER 5: DISCUSSION .....</b>	<b>149</b>
5.1 Calendar samples .....	149
5.1.1 Relationship between PM <sub>2.5</sub> concentrations and absorption coefficients .....	149
5.1.2 The effects of meteorological conditions on ambient APM concentrations.....	152
5.1.2.1 Meteorological conditions for Cape Town.....	153
5.1.2.2 Change of ambient APM concentrations with temperature .....	153
5.1.2.3 Change of ambient APM concentrations with Rh and precipitation.....	154
5.1.2.4 Change of ambient APM concentrations with air velocity and UV exposure .....	155
5.1.2.5 Summary .....	156
5.1.3 The effects of air mass transport on ambient APM concentrations.....	158
5.1.4 Correlation between study data and air pollution data from the CoCT.....	160
5.1.5 Correlation between air pollution data for Cape Town, Pretoria and Thohoyandou .....	163
5.2 Composite samples .....	164
5.2.1 The effects of meteorological conditions on composite samples .....	165
5.2.2 The effects of air mass transport on composite samples .....	167
5.2.3 Summary.....	167
<b>CHAPTER 6: CONCLUSION.....</b>	<b>170</b>
6.1 Outcomes of the study.....	170
6.2 Research questions .....	172
6.3 Research delimitations and limitations .....	174
6.4 Recommendations .....	175

<b>BIBLIOGRAPHY .....</b>	<b>176</b>
<b>APPENDICES .....</b>	<b>187</b>
1A Sampling information (calendar samples).....	187
1B Seasonal sampling information .....	188
1C Sampling information (composite samples).....	189
2 Ambient APM sampling instructions .....	190
3 Chronology of analyses .....	194
4 Filter weighing procedure.....	195
5 Reflectometry procedure .....	196
6A Gravimetric analysis data .....	197
6B Gravimetric analysis quality control data (pre-sampling) .....	207
6C Gravimetric analysis quality control data (post-sampling).....	208
7A Reflectometric data.....	209
7B Reflectometric quality control data (primary control filter).....	214
7C Reflectometric quality control data (samples rechecked).....	215
8 Outliers in PM <sub>2.5</sub> concentration and absorption coefficient data sets .....	216
9 Descriptive statistics (monthly data) .....	217
10 Descriptive statistics (weekday and weekend day data).....	218
11A Shapiro-Wilks normality test (autumn) .....	219
11B Shapiro-Wilks normality test (winter).....	220
11C Shapiro-Wilks normality test (spring).....	221
11D Shapiro-Wilks normality test (summer) .....	222
11E Shapiro-Wilks normality test (full study).....	223
12 Trajectory clusters and corresponding sampling dates .....	225
13A Air pollution data from the Atlantis AAQM station.....	226
13B Air pollution data from the City Hall AAQM station .....	227
13C Air pollution data from the Goodwood AAQM station .....	228
13D Air pollution data from the Somerset-West AAQM station.....	230
13E Air pollution data from the Tableview AAQM station .....	231
13F Air pollution data from the Wallacedene AAQM station.....	232
14A Mean monthly concentrations for Atlantis and City Hall.....	234
14B Mean monthly concentrations for Goodwood and Somerset-West.....	235
14C Mean monthly concentrations for Tableview and Wallacedene.....	236

15	Meteorological conditions (mean monthly values) for September 2017 and January 2018 .....	237
16	Standardisation curves (ICP-OES) .....	238
17	Standardisation curves (IC) .....	240
18	Chromatograms (IC) .....	242



UNIVERSITY *of the*  
WESTERN CAPE

## **LIST OF FIGURES**

Figure number	Page
2.1 Air polluting emissions in Bellville, Cape Town.....	10
2.2 Smog in Donora, Pennsylvania .....	11
2.3 UN Sustainable Development Goals .....	12
2.4 Photochemical smog in Cape Town .....	14
2.5 SAWS AAQM station at Hantam National Botanical Garden, Northern Cape .....	15
2.6 Particulate diameters compared to a human hair .....	16
2.7 Particulate shapes .....	17
2.8 Formation processes of APM .....	20
2.9 Particulate size distribution, formation processes and multi-modal distribution of APM at ambient conditions .....	22
2.10 Log-normal particulate distribution curves .....	23
2.11 Photomicrographs of soot.....	26
2.12 Soot coagulation processes.....	26
2.13 Mechanisms of PM deposition in the lungs.....	29
2.14 Possible mechanisms for cardiovascular effects by PM.....	31
2.15 Ground-level temperature inversion.....	33
2.16 Atmospheric elapse rates for surface level and aloft inversions .....	34
2.17 Ground-level inversion for urban areas at the coast and in valleys .....	34
2.18 Examples of backward trajectories derived from the HYSPLIT model.....	38
2.19 Map of South Africa .....	39
2.20 Total primary energy consumption in South Africa for 2012 .....	39
2.21 Percentage energy demand in Africa for 2001 .....	40
2.22 Air quality in South Africa .....	41
2.23 Map of Cape Town .....	42
2.24 Ambient PM <sub>2.5</sub> contribution by Eskom's coal-fired power stations.....	43
2.25 Locations of known AAQM stations that report to the WAQI .....	48
2.26 Map of AAQM network in Cape Town.....	49
2.27 Aeroqual AQM 65 station .....	50
2.28 LORAX instrument .....	51
2.29 LiDAR scanning and detection by aeroplane .....	51
2.30 Thermo Scientific model 5028i continuous particulate monitor .....	52

2.31	Methods and technologies for APM monitoring .....	53
3.1	Locations of local sources of ambient APM .....	57
3.2	Location of the sampling site.....	58
3.3	Sampling equipment and materials.....	60
3.4	Sampling station at the sampling site .....	61
3.5	Schematic representations of the sampling station and cyclone assembly with filters before and after exposure to ambient air .....	64
3.6	Mettler-Toledo XP6 Ultra-Microbalance .....	66
3.7	Laboratory conditions .....	67
3.8	Handling of filters.....	68
3.9	Diffusion Systems Ltd. EEL model.43 Smoke Stain Reflectometer.....	69
3.10	Principle of reflectometry.....	70
3.11	Areas (1-5) where the light beam should approximately strike during reflectance measurement.....	70
3.12	Varian 710-ES Inductively Coupled Plasma-Optical Emission Spectrometer and sample analysis process .....	72
3.13	Components inspected during pre-analysis checks of the 710-ES .....	75
3.14	Dionex ICS-1600 High-Performance Liquid Chromatograph and anion analysis process.....	78
3.15	Components physically inspected during pre-analysis checks of the ICS-1600 .....	80
3.16	Zeiss Auriga 4527 Scanning Electron Microscope .....	82
3.17	Stub preparation for SEM photomicrography .....	83
3.18	FEI Tecnai G <sup>2</sup> F20 Scanning Transmission Electron Microscope .....	85
3.19	Mesh grid preparation for TEM photomicrography .....	86
3.20	Locations of the six AAQM stations whose data was used for correlation purposes.....	89
3.21	Locations of the Cape Town, Pretoria and Thohoyandou sampling sites .....	90
4.1	PM <sub>2.5</sub> concentrations for period 2017/04/18 to 2017/10/18 .....	95
4.2	PM <sub>2.5</sub> concentrations for period 2017/10/21 to 2018/04/16 .....	96
4.3	Monthly PM <sub>2.5</sub> concentrations .....	97
4.4	Seasonal PM <sub>2.5</sub> concentrations.....	98
4.5	Absorption coefficients for period 2017/04/18 to 2017/10/18.....	99
4.6	Absorption coefficients for period 2017/10/21 to 2018/04/16.....	100
4.7	Monthly absorption coefficient and eBC values .....	101
4.8	Seasonal absorption coefficient and eBC values .....	102

4.9	PM <sub>2.5</sub> concentrations and absorption coefficients for the study period.....	103
4.10	BW plots of seasonal PM <sub>2.5</sub> concentration data.....	105
4.11	BW plots of seasonal PM <sub>2.5</sub> concentration data (outliers omitted).....	106
4.12	BW plots of seasonal absorption coefficient data .....	106
4.13	BW plots of seasonal absorption coefficient data (outliers omitted).....	107
4.14	BW plots of A/P ratios.....	108
4.15	PM <sub>2.5</sub> concentration v. absorption coefficient data for the study period .....	109
4.16	PM <sub>2.5</sub> concentration v. absorption coefficient data (seasonal) .....	110
4.17	PM <sub>2.5</sub> concentration v. absorption coefficient data (weekday and weekend day) .....	111
4.18	Meteorological data for Cape Town for the study period .....	113
4.19	Seasonal wind direction frequencies .....	116
4.20	Seasonal wind direction frequencies (continued).....	117
4.21	Seasonal ambient APM concentrations v. temperature .....	118
4.22	Seasonal ambient APM concentrations v. Rh and precipitation .....	119
4.23	Seasonal ambient APM concentrations v. air velocity .....	120
4.24	Seasonal ambient APM concentrations v. wind direction.....	120
4.25	Seasonal ambient APM concentrations v. percentage clear skies .....	121
4.26	Dominating trajectories derived from the HYSPLIT model .....	123
4.27	Single trajectory frequencies .....	124
4.28	Seasonal cluster plots.....	125
4.29	Seasonal trajectory frequency plots.....	126
4.30	Seasonal trajectory frequency plots (Zoom factor: 2) .....	127
4.31	PM <sub>10</sub> concentrations v. absorption coefficients .....	132
4.32	Locations of AAQM stations.....	133
4.33	Percentage recovery for anions in control solution .....	136
4.34	Total anion masses in composite samples .....	137
4.35	Percentage recovery for metals in control solution .....	138
4.36	Total metals masses in composite samples.....	139
4.37	Total inorganic carbon mass in composite samples .....	140
4.38	Chemical make-up of PM in composite samples .....	143
4.39	SEM photomicrographs of weekday composite samples for September 2017 .....	144
4.40	TEM photomicrographs of PM collected on weekend days during January 2018.....	146
4.41	TEM and SAED.....	147
4.42	EDS spectrum of weekend day composite sample for January 2018.....	148

## **LIST OF TABLES**

Table number	Page
2.1	Most abundant air pollutants in the atmosphere ..... 13
2.2	$D_a$ for differently-shaped particulates and different particulate densities ..... 18
2.3	Effects of particulate size on number of particulates and surface area for a given mass of a single spherical particulate ..... 23
2.4	NAAQS for ambient air in South Africa ..... 45
3.1	Sampling equipment and materials..... 60
3.2	Composition of VHG Labs multi-element standard solution 1586 ..... 73
3.3	710-ES operating conditions ..... 76
3.4	Elements, emission wavelengths and standardisation equations ..... 76
3.5	Composition of Inorganic Ventures anion calibration standard 59 ..... 79
3.6	ICS-1600 operating conditions ..... 81
3.7	Anions, retention times and standardisation equations ..... 81
3.8	Auriga 4527 operating conditions ..... 84
3.9	Tecnai G <sup>2</sup> F20 operating conditions ..... 86
3.10	HYSPLIT user settings for single backward trajectory plots ..... 87
3.11	HYSPLIT user settings for backward trajectory cluster plots ..... 88
4.1	Quality control information for gravimetric analyses ..... 94
4.2	Quality control information for reflectometric analyses ..... 98
4.3	Descriptive statistics of seasonal PM <sub>2.5</sub> concentration and absorption coefficient data..... 104
4.4	Correlation information ..... 112
4.5	Significance information ..... 112
4.6	Mean temperature, air velocity, Rh and precipitation for the study period..... 114
4.7	Monthly and seasonal wind direction information ..... 115
4.8	Mean PM <sub>2.5</sub> concentration and absorption coefficient values for three temperature ranges..... 118
4.9	Mean PM <sub>2.5</sub> concentration and absorption coefficient values for three Rh and precipitation ranges..... 119
4.10	Mean PM <sub>2.5</sub> concentration and absorption coefficient values for three air velocity ranges..... 120
4.11	Cluster frequencies (%) for each season and full study period ..... 128



4.12	Mean seasonal concentrations for six AAQM stations in Cape Town.....	129
4.13	Spearman correlation coefficients ( $\rho$ ).....	130
4.14	Spearman correlation coefficients ( $\rho$ ) for pollutants NO <sub>2</sub> , SO <sub>2</sub> and PM <sub>10</sub> .....	132
4.15	Descriptive statistics of seasonal PM <sub>2.5</sub> concentration and absorption coefficient data for Pretoria and Thohoyandou.....	135
4.16	Anion concentrations in control solution.....	136
4.17	Experimental data and anion masses for 1.00 cm <sup>2</sup> sub-samples .....	137
4.18	Metal concentrations in control solution .....	138
4.19	Experimental data and metal masses for 4.28 cm <sup>2</sup> sub-samples .....	139
4.20	Experimental data and inorganic carbon concentrations in composite samples.....	140
4.21	Chemical compositions of weekday and weekend day composite samples .....	142



UNIVERSITY *of the*  
WESTERN CAPE

## **ABBREVIATIONS**

3D	Three-dimensional
a.m.	Ante meridiem (before midday)
AEL	Atmospheric Emission Licenses
AIDS	Acquired Immune Deficiency Syndrome
APM	Airborne Particulate Matter
AQI	Air Quality Index
AQM	Air Quality Monitoring
AAQM	Ambient Air Quality Monitoring
ARL	Air Resources Laboratory
BC	Black Carbon
CAPCO	Chief Air Pollution Control Officer
CBD	Central Business District
CDC	Global reanalysis meteorological data model
CMB	Chemical Mass Balance
CoCT	City of Cape Town
CPC	Condensation Particle Counter
CPMA	Centrifugal Particle Mass Analyser
CTIA	Cape Town International Airport
DEA	Department of Environmental Affairs
DMS	Dioxin Monitoring System
DNA	Deoxyribonucleic acid
EDB	Ethylene Dibromide Sampler
EHT	Electron High Tension
ELPI	Electrical Low Pressure Impactor
EMU	Electron Microscopy Unit
EN	Standard Reference Method: Environmental
ENS	Environmental and Nano Sciences
FIMS	Flow Injected Mercury System
GAW	Global Atmosphere Watch
GDAS	Global Data Assimilation System
HPLC	High-performance liquid chromatography

HYSPLIT	Hybrid Single Particle Lagrangian Integrated Trajectory
IC	Ion chromatography
ICP-OES	Inductively coupled plasma-optical emission spectrometry
ISO	International Organisation for Standardisation
LII	Emission band of x-ray spectrometry
LiDAR	Light Detection and Ranging
LORAX	LiDAR On-Road Aerosol eXperiment
LRT	Long-Range Transport
MES	Minimum Emission Standards
N/A	Not applicable
NAAQS	National Ambient Air Quality Standard
NCAR	National Centres for Environmental Prediction
NCAS	National Centre for Atmospheric Sciences
NCEP	National Centre for Atmospheric Research
ND	Not detected
Nd: YAG	Neodymium-doped Yttrium Aluminium Garnet
NEMAQA	National Environmental Management: Air Quality Act
NOAA	National Oceanic and Atmospheric Administration
NWU	North-West University
OPC	Optical Particle Counter
PAH	Polycyclic Aromatic Hydrocarbons
PAN	Peroxyacyl Nitrates
PASS	Passive Sampling
PM	Particulate Matter
PM <sub>1</sub>	Particulate Matter (aerodynamic diameters ≤ 1 µm)
PM <sub>2.5</sub>	Particulate Matter (aerodynamic diameters ≤ 2.5 µm)
PM <sub>10</sub>	Particulate Matter (aerodynamic diameters ≤ 10 µm)
PMF	Positive Matrix Factorisation
PMT	Photomultiplier Tube
PP	Polypropylene
PPE	Personal Protective Equipment
PTFE	Polytetrafluoroethylene (or Teflon)
RF	Radio frequency

Rh	Relative humidity
REVIHAAP	Review of Evidence on Health Aspects of Air Pollution
ROSA	Romanian Space Agency
RUPIOH	Relationship between Ultrafine and fine Particulate matter in Indoor and Outdoor air and respiratory Health
SAAO	South African Astronomical Observatory
SAAQIS	South African Air Quality Information System
SA NAAQS	South African National Ambient Air Quality Standard
SANS	South African National Standard
SAWS	South African Weather Service
SEM	Scanning electron microscopy
SHSPH	School of Health Systems and Public Health
SMPS	Scanning Mobility Particle Sizer Spectrometer
SOP	Standard Operating Procedure
SSR	Smoke stain reflectometry
TEM	Transmission electron microscopy
TEOM	Tapered Element Oscillating Microbalance
TSP	Total Suspended Particulates
UK-AIR	United Kingdom Air Information Resource
UN	United Nations
UNEP	United Nations Environmental Programme
UniVen	University of Venda
UP	University of Pretoria
UTC	Universal Coordinated Time
UV	Ultraviolet
U.S. EPA	United States Environmental Protection Agency
USA	United States of America
UWC	University of the Western Cape
VOC	Volatile Organic Compound
V/V	Volume-to-volume
WAQI	World Air Quality Index
WD	Working Distance
WHO	World Health Organisation
WMO	World Meteorological Organisation

## CHEMICAL SPECIES

Al	Aluminium	Mg	Magnesium
NH <sub>3</sub>	Ammonia	Mn	Manganese
NH <sub>4</sub> <sup>+</sup>	Ammonium	Mo	Molybdenum
NH <sub>4</sub> NO <sub>3</sub>	Ammonium nitrate	Ni	Nickel
(NH <sub>4</sub> ) <sub>2</sub> SO <sub>4</sub>	Ammonium sulfate	NO <sub>3</sub> <sup>-</sup>	Nitrate
Ar	Argon	HNO <sub>3</sub>	Nitric acid
As	Arsenic	NO <sub>2</sub> <sup>-</sup>	Nitrite
Ba	Barium	NO <sub>2</sub>	Nitrogen dioxide
C <sub>6</sub> H <sub>6</sub>	Benzene	NO <sub>x</sub>	Nitrogen oxides
Be	Beryllium	O <sub>3</sub>	Ozone
B	Boron	PO <sub>4</sub> <sup>3-</sup>	Phosphate
Br <sup>-</sup>	Bromide	P	Phosphorous
Cd	Cadmium	K	Potassium
Ca	Calcium	Rd	Radon
CaSO <sub>4</sub>	Calcium sulfate	Si	Silicon
CO <sub>2</sub>	Carbon dioxide	Na	Sodium
CO	Carbon monoxide	NaCl	Sodium chloride
CO <sub>x</sub>	Carbon oxides	NaNO <sub>3</sub>	Sodium nitrate
Cl <sup>-</sup>	Chloride	Sr	Strontium
Cr	Chromium	SO <sub>4</sub> <sup>2-</sup>	Sulfate
Co	Cobalt	SO <sub>2</sub>	Sulfur dioxide
Cu	Copper	SO <sub>x</sub>	Sulfur oxides
N <sub>2</sub>	Diatomic nitrogen	H <sub>2</sub> SO <sub>4</sub>	Sulfuric acid
O <sub>2</sub>	Diatomic oxygen	O <sub>2</sub> <sup>-</sup>	Superoxide
F <sup>-</sup>	Fluoride	Ti	Titanium
·OH	Hydroxyl radical	C <sub>6</sub> H <sub>5</sub> CH <sub>3</sub>	Toluene
Fe	Iron	V	Vanadium
Pb	Lead	Xe	Xenon
Li	Lithium	Zn	Zinc

## **REAGENTS AND SOLVENTS**

Milli-Q water	Deionised water (conductivity = 20-25 $\mu\text{S}\cdot\text{cm}^{-1}$ )
$\text{C}_2\text{H}_5\text{OH}$	Ethanol
HCl	Hydrochloric acid
HF	Hydrofluoric acid
$\text{CH}_3\text{OH}$	Methanol
$\text{HNO}_3$	Nitric acid
$\text{NaHCO}_3$	Sodium bicarbonate
$\text{Na}_2\text{CO}_3$	Sodium carbonate



UNIVERSITY *of the*  
WESTERN CAPE

## UNITS

cm	Centimetre	$\mu\text{m}$	Micrometre
$\text{m}^3$	Cubic metre	$\mu\text{S}$	Microsiemens
$^{\circ}\text{C}$	Degrees Celsius	$\mu\text{S}\cdot\text{cm}^{-1}$	Microsiemens per centimetre
Gt	Gigatonne	mA	Milliampere
$\text{g}\cdot\text{cm}^{-3}$	Grams per cubic centimetre	$\text{mg}\cdot\text{kg}^{-1}$	Milligrams per kilogram
g	Gram	$\text{mg}\cdot\text{L}^{-1}$	Milligrams per litre
keV	Kilo electronvolt	mL	Millilitre
km	Kilometre	$\text{mL}\cdot\text{min}^{-1}$	Millilitres per minute
$\text{km}\cdot\text{h}^{-1}$	Kilometres per hour	mm	Millimetre
kPa	Kilopascal	mM	Millimolar
kt	Kilotonne	M	Molar
kW	Kilowatt	$\text{ng}\cdot\mu\text{g}^{-1}$	Nanograms per microgram
L	Litre	nm	Nanometre
$\text{L}\cdot\text{min}^{-1}$	Litres per minute	%	Percentage
Mt	Megatonne	$\text{m}^{-1}$	Reciprocal metre
m	Metre	rpm	Revolutions per minute
$\text{m}\cdot\text{s}^{-1}$	Metres per second	s	Second
$\mu\text{g}$	Microgram	$\text{cm}^2$	Square centimetre
$\mu\text{g}\cdot\text{m}^{-3}$	Micrograms per cubic metre	$\text{m}^2$	Square metre
$\mu\text{g}\cdot\text{kg}^{-1}$	Micrograms per kilogram	sr	Steradians
$\mu\text{g}\cdot\text{L}^{-1}$	Micrograms per litre	wt. %	Weight percentage
$\mu\text{L}$	Microlitre		



## **STATISTICAL OPERATORS**

$\mu$	Arithmetic mean
H	H-statistic (Kruskal-Wallis significance test)
t	t-statistic (Student's T-test)
r	Pearson correlation coefficient
RSD	Relative standard deviation (or coefficient of variation)
$\rho$	Spearman correlation coefficient
$\sigma$	Standard deviation (population)
s	Standard deviation



UNIVERSITY *of the*  
WESTERN CAPE



## **CHAPTER 1: INTRODUCTION**

### 1.1 Background

We all breathe in air daily, 10-20 times per minute in fact. The United States Environmental Protection Agency (U.S. EPA), in the 2011 edition of its exposure factors handbook, has calculated the mean volumes of air males and females (aged 1-96 years) inhale in 24 hours to be 12 m<sup>3</sup> and 10 m<sup>3</sup> respectively. With such large quantities of “life-supporting fluid” filling our lungs every day it is imperative that we continuously breathe clean, unpolluted air to prevent adverse health outcomes. Air pollution is a major health problem the world over (UN, 2017). One reason why air pollution is such a threat to human health is that there is no alternative to the air we breathe (Koenig, 2000). Ambient air pollution with high concentrations of fine particulate matter (or PM<sub>2.5</sub>) is linked to various short- and long-term adverse health outcomes. The World Health Organisation (WHO) estimated that air pollution was the direct cause of 6.5 million deaths worldwide every year in 2012 of which three million deaths was attributable to chronic exposure to ambient PM<sub>2.5</sub>. Closer to home, a Global Burden of Disease study found that exposure to ambient PM<sub>2.5</sub> was the direct cause of an estimated 1,800 deaths in South Africa every year in 2012 (Altieri et al., 2016). South Africa is Africa’s second largest economy, bested only by Nigeria (International Monetary Fund, 2016). South Africa’s economy, like most economies, is built on energy. Because of its abundant reserves (estimated to be 50-55 Gt), 75-80 % of the country’s electricity needs are provided by coal (Eskom, 2017). The biggest disadvantage of coal combustion for electricity generation activities is the excessive amounts of waste products produced. Coal-fired power stations in South Africa emitted an estimated 100-110 kt of airborne particulate matter (APM) every year in 2014 (Myllyvitra, 2014). These emissions are deposited into the atmosphere where they undergo local, regional and long-range transport (LRT) by air masses. Under suitable meteorological conditions, APM is capable of travelling thousands of

kilometres from its origin (Molnár et al., 2017). Cape Town's population exposure to pollutants emitted by coal power stations is miniscule (Myllyvitra, 2014), however, Cape Town is the second most populous city in South Africa boasting urban population and economic growth rates of 1.1 % and 0.3 % per annum respectively (Western Cape Government, 2017). As urban populations increase so do power consumption and generation activities, as demand for electricity, transportation and other human needs increases (WHO, 2013). Increased demand ultimately leads to a rise in air pollution levels that deteriorates air quality and adversely affects human health (U.S. EPA, 2012).

## 1.2 Problem statement

Each year the Department of Environmental Affairs (DEA) presents its 'State of Air Report' which gives an analysis of local and provincial air quality in South Africa [based on data and findings provided by the South African Ambient Air Quality Information System (SAAQIS)]. Typically, ambient APM information contained within these reports is limited to PM<sub>10</sub> and PM<sub>2.5</sub> mass concentrations, and local and regional particulate pollution "hotspots" (DEA, 2015). Particulate pollution originates from various anthropogenic (or human) and natural sources (WHO, 2013). It is important to identify these sources and their overall contribution to ambient APM concentrations so that cost-effective mitigation strategies are pursued (Molnár et al., 2017). Studies investigating air pollutant origins and transport are common internationally but very rare in the entire Africa; only a few publications in peer-reviewed scientific journals (Wichmann, 2017). There is a need for detailed ambient APM studies in South Africa that will yield useful information on the characteristics, origins and trends of ambient PM<sub>2.5</sub> and soot in the region so that effective mitigating strategies are implemented.

### 1.3 Hypothesis

The general population in Cape Town and the region is exposed to ambient APM every day. Ambient air pollutants  $PM_{2.5}$  and soot are hazardous to human health. The effects of  $PM_{2.5}$  on human health are observed in epidemiology studies where  $PM_{2.5}$  levels are well below the strict limits imposed by WHO standards and European Union guidelines [see page 4 of the Review of Evidence on Health Aspects of Air Pollution (REVIHAAP) report of 2013] that are more stringent than South African National Ambient Air Quality Standard (SA NAAQS) safety standards. There is high correlation between ambient  $PM_{2.5}$  concentration and absorption coefficient (proxy for soot content). As  $PM_{2.5}$  concentrations rise so do soot concentrations. Meteorological parameters affect ambient  $PM_{2.5}$  and soot concentrations differently. Air velocity (or wind speed) has the greatest effect on  $PM_{2.5}$  and soot concentrations, followed by temperature, precipitation (or rainfall), relative humidity and UV exposure in that order. Wind direction and air mass transport from local sources have pronounced effects on ambient  $PM_{2.5}$  and soot concentrations in a region and, to lesser extent, long-range transport (LRT) from distant sources. Contributions to ambient  $PM_{2.5}$  and soot concentrations by local sources (within a 40 km radius) far exceed those by LRT. Correlation between ambient  $PM_{2.5}$  and soot concentrations (study data) and air pollution data collected by the City of Cape Town (CoCT) dwindles the farther ambient air quality monitoring (AAQM) stations are located from the sampling site.

#### 1.4 Research objectives

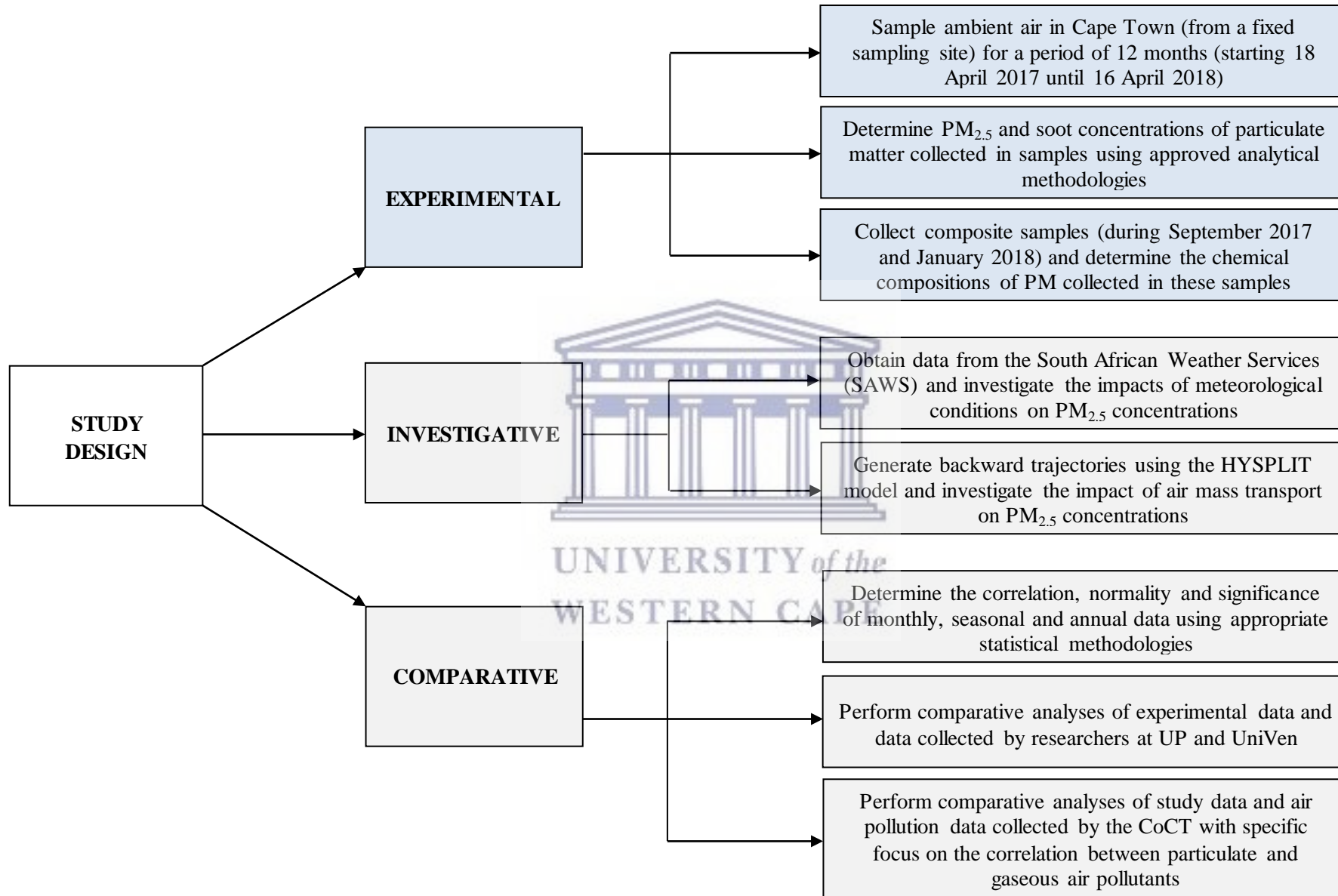
The objectives of this study were to:

1. Determine ambient  $PM_{2.5}$  mass and soot concentrations in filter samples, collected at a fixed sampling site in Kraaifontein, Cape Town, using gravimetric analysis and smoke stain reflectometry (SSR).
2. Investigate the impact of meteorological conditions on ambient APM data and data collection.
3. Determine air masses that passed over Cape Town and the region using Hybrid Single Particle Lagrangian Integration Trajectory (HYSPLIT) backward trajectory analysis.
4. Compare  $PM_{2.5}$  concentration and absorption coefficient data for Cape Town with data for Pretoria and Thohoyandou.
5. Determine the correlation between study data and air pollution data collected by the City of Cape Town (CoCT)
6. Evaluate compliance to WHO and SA NAAQS safety limits.
7. Determine the chemical compositions and particulate morphologies of composite samples collected during September 2017 and January 2018.

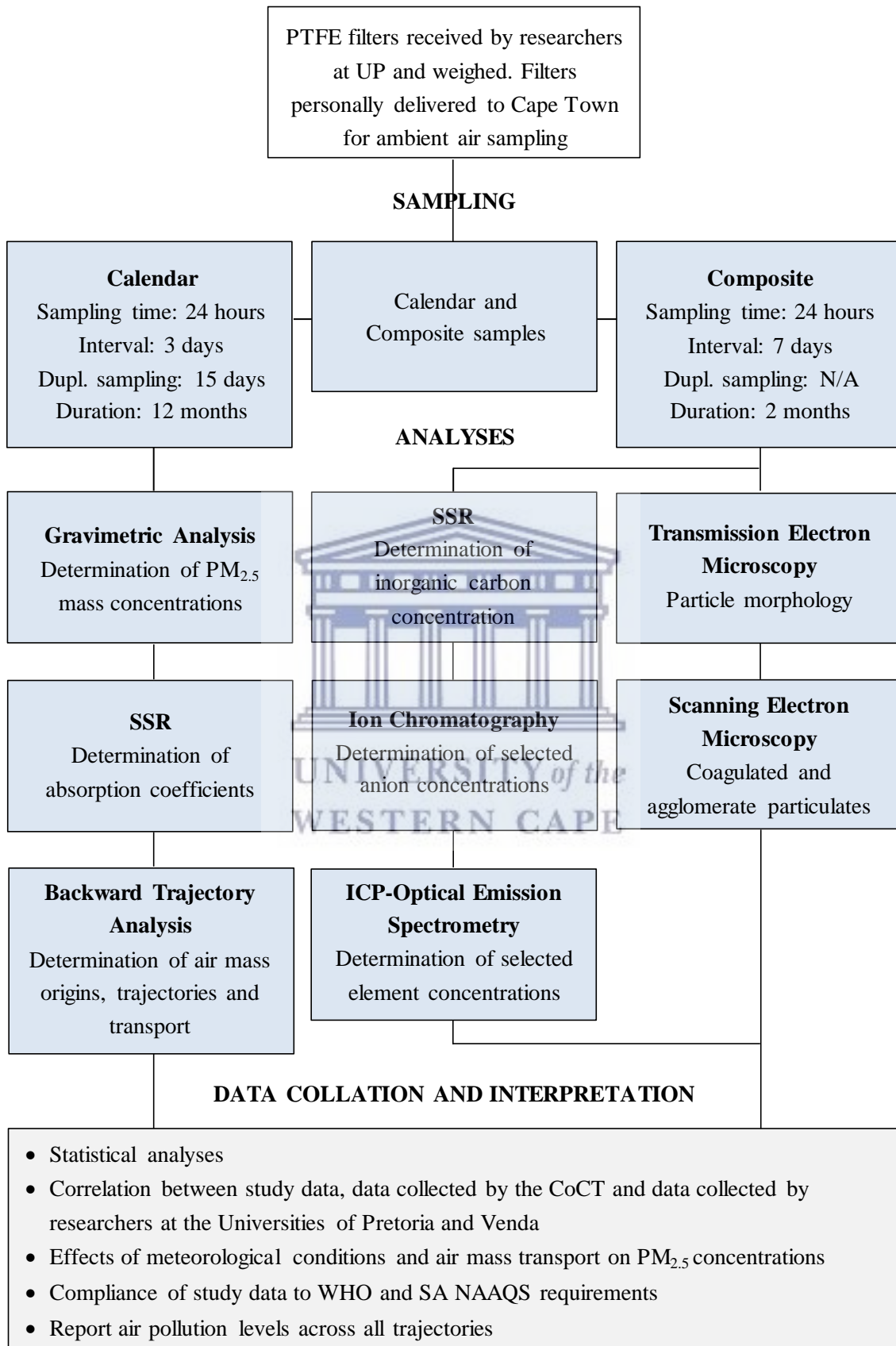
## 1.5 Research questions

Some of the questions this study addressed were:

1. Is ambient  $PM_{2.5}$  and soot (or black carbon) data, collected at a fixed sampling site, representative of an entire area or region?
2. What are the probable sources of ambient  $PM_{2.5}$  and soot in Cape Town?
3. Are there associations between ambient  $PM_{2.5}$  and soot concentrations for monthly and seasonal data sets? Why are there differences between monthly and seasonal associations?
4. Are there associations between study data and air pollution data produced by the CoCT? Why do associations between study data and data from individual AAQM stations differ with direction and distance of these stations from the sampling site?
5. Do ambient  $PM_{2.5}$  and soot concentrations for the study period fall below or exceed WHO and SA NAAQS limits? Why do APM concentrations in Cape Town differ from concentrations in Pretoria and Thohoyandou?
6. Is HYSPLIT an effective tool for determining air mass origins? Why was it used for trajectory and cluster analyses?
7. Do meteorological parameters impact ambient APM concentrations? Why do some meteorological parameters affect APM concentrations more than others?
8. Is air quality in Cape Town impacted by LRT? Is the impact of LRT on air pollution levels in the city significant?



1.7 Research approach



## 1.8 Scope of study

This study formed part of a bigger collaborative study investigating the health effects, geographical origins and source apportionment of ambient  $PM_{2.5}$  and soot in South Africa between the Environmental and Nano Sciences (ENS) group of the University of the Western Cape (UWC), the School of Health Systems and Public Health (SHSPH) of UP, UniVen and Occupational and Environmental Medicine of the University of Gothenburg (Sweden). The contents herein are limited to data and findings of research conducted in Cape Town. Ambient  $PM_{2.5}$  sampling was performed in the suburb of Kraaifontein (27 km ENE of the city centre) for a period of 12 months from 18 April 2017 until 16 April 2018. Sampling times and intervals were fixed at 24 and 72 hours respectively, with duplicate samples taken every 15 days. In all, a total of 146 ambient  $PM_{2.5}$  filter samples were collected (including 25 duplicate samples) over 121 days. Ambient  $PM_{2.5}$  mass concentrations and absorption coefficients were determined using gravimetric analysis and SSR. Additionally, the chemical compositions and particulate morphologies of composite samples (collected during September 2017 and January 2018) were determined using inductively coupled plasma-optical emission spectrometry (ICP-OES), ion chromatography (IC), SSR and transmission electron microscopy (TEM). HYSPLIT backward trajectories were used to determine air masses that passed over Cape Town and the region during the study period. Seasonal variations, the effects of meteorological parameters on ambient  $PM_{2.5}$  data, and the correlation between  $PM_{2.5}$ , soot and other air pollutants ( $PM_{10}$ ,  $SO_2$ ,  $NO_2$  and  $O_3$ ) were also investigated. Lastly, study data was evaluated for compliance to WHO and SA NAAQS safety limits. This study provides information about ambient APM mass concentrations and air mass transport in Cape Town and the region that can be useful to future source apportionment studies in the area.



## 1.9 Thesis layout

This paper contains six chapters in total. They are:

1. Introduction
2. Literature Review
3. Methodology
4. Results
5. Discussion and
6. Conclusion

The next chapter is Literature Review (chapter two). Literature Review elaborates on the current knowledge and substantive findings on the physical and chemical properties, health effects, atmospheric lifetimes, dispersion and transport of ambient APM in Cape Town. Valuable theoretical and methodological contributions to this atmospheric chemistry topic are also cited here. Next up is Methodology (chapter three). This chapter covers, in detail, i) how field work and laboratory activities were carried out, ii) which sampling equipment and materials, and analytical techniques were used and iii) precisely how each activity was performed indicating successes and shortcomings so that efforts are reproducible. Methodology is followed by Results (chapter four). All field work and experimental data are captured in this chapter. Experimental data is presented in text, numeral or graphical formats. The penultimate chapter, Discussion (chapter five), as the name suggests, is an in-depth discussion of field and laboratory data and findings, and how the data and findings either support or contradict current knowledge and theories on the subject matter. Conclusion (chapter six) is the final chapter of this study and culmination of the study as a whole. An extension of the Discussion chapter, it summarises the objectives of the study and draws conclusions on the presented findings. Suggested future research priorities are also listed here.

## **CHAPTER 2: LITERATURE REVIEW**

### 2.1 Air pollution

#### 2.1.1 What is air pollution?

The term air pollution does not have a single definition. The WHO defines air pollution as “the contamination of an indoor or outdoor environment by a biological, chemical or physical agent that alters the natural atmospheric properties of that environment” while the Natural Resources Defense Council defines it as “the release of a chemical or particulate species into the atmosphere that is hazardous to humans and the Earth as a whole”. The atmosphere is the planet’s largest shared resource. It



*Fig. 2.1: Air polluting emissions in Bellville, Cape Town (Image: own).*

protects life by absorbing harmful ultraviolet (UV) radiation (DEA, 2017). The crucial role the atmosphere plays is under threat by anthropogenic (or human) activities that lead to the deposition of pollutants into the atmosphere (Hunter et al. 2002). Air pollutants do not only disrupt the temperature-regulating role of the atmosphere but also “taint” the air we breathe, threatening the well-being of all life on Earth. A frightening fact about air pollution is that it can be found anywhere making indoor and outdoor (or ambient) air potential sources of exposure to hazardous substances (U.S. EPA, 2015). In 2012, air pollution diseases were responsible for 6.5 million deaths worldwide, more deaths than from acquired immune deficiency syndrome (AIDS), tuberculosis and malaria combined (WHO, 2016). In 2015, this death toll rose to nine million (mean increase of 13 % year-on-year). Air pollution is, without a doubt, the largest environmental cause of disease and mortality in the world today (Landrigan et al., 2017).

### 2.1.2 Historical perspective

Air pollution has a long history with the first ever recorded event dating back to 13<sup>th</sup> century London when emissions from coal combustion led to severe air pollution in the region (Helfand, 2001). Centuries had past and air pollution continued to lie under the radar because its harmful effects were poorly understood. It was not until the mid-20<sup>th</sup> century when air pollution was exposed as a major threat to human health that people began to act (U.S



**Fig. 2.2:** Smog in Donora, Pennsylvania (Image: [alleghenyfront.org/wp-content/uploads/2017/04/AP\\_4810300105-2-1800\\_px.jpg](http://alleghenyfront.org/wp-content/uploads/2017/04/AP_4810300105-2-1800_px.jpg)).

EPA, 2017). The first episode of significance occurred in Meuse River Valley (Belgium) in 1930 but it was not until 1948 when the events of Donora (Pennsylvania, USA) showcased the consequences of industrial and urban growth to the world (U.S. EPA, 2017). In 1948, the small American town was covered in an inversion layer of sulfurous smog originating from an acid plant, mills and smelters. Over a period of one week, approximately 40-50 lives were lost and thousands reported to have suffered adverse health outcomes. Air pollution crises, like that of Donora and London (1952), led to the discovery of the link between air pollution and health (U.S. EPA, 2017). In 1970, the WHO and United Nations Environmental Programme (UNEP) established regulations for air pollution control worldwide so that the catastrophic events of Donora and others would not be repeated (Calkins, 1998). “Restrictions on tailpipe and smokestack emissions have improved air pollution control,” says Prof. M. Jacobson, Senior Fellow at the Precourt Institute of Energy. “However, air pollution still kills thousands of people each year,” he added. Today, many institutions recognise air pollution as a great risk to environmental and human health.

### 2.1.3 UN Sustainable Development Goals

Air pollution is recognised as a major threat to the health and well-being of all at all ages by many institutions across the world, , so-much-so that the United Nations (UN) has listed it as a contributing factor under sustainable development goal 3. In 2015, more than 150 world leaders gathered for an annual UN Sustainable Development summit. During this summit, Sustainable Development Goals were adopted with one goal in mind - achieving sustainable development for all people, in all countries of the world by the year 2030. These goals (Fig. 2.3) were designed to primarily combat <sup>1</sup>extreme poverty, <sup>2</sup>injustice and inequality and <sup>3</sup>fixing climate change (UN, 2017). Air pollution is listed under sustainable development goal 3 (Good health and well-being, subcategory 3.9). Indoor and ambient air pollution is the greatest environmental risk to human health. In 2012, ambient air pollution from vehicles, industry and fossil fuel and waste combustion led to the premature deaths of some 6.5 million people, 20 % of which were from respiratory illnesses and cancers related to exposure to PM<sub>2.5</sub>, the most harmful air pollutant to human health. World leaders have vowed to enforce measures that would drastically reduce air pollution by the year 2030 and improve the health and well-being of all of the world's citizens (UN, 2017).



**Fig. 2.3:** UN Sustainable Development Goals. There are a total of 17 goals. Air pollution is listed as a contributing factor under sustainable development goal 3 (Image: UN).

#### 2.1.4 Sources of air pollution

Air pollution emanates from various sources. Most air pollutants are the undesired by-products of power generation and consumption activities. Sources of air pollution (including precursors) are divided into four main groups: area, mobile, stationary and natural (U.S. EPA, 2017). Major sources include biomass and fuel combustion for cooking and heating purposes (area), coal power stations, industrial facilities, factories, refineries (stationary), and inefficient modes of transport (mobile) (WHO, 2017). Although the largest sources of air pollution are anthropogenic, not all air pollutants stem from human activities. Natural sources like sandstorms, volcanoes and wildfires can also affect air quality (WHO, 2017). The three largest sources of ambient air pollution globally are electricity generation, transportation and industrial processes (WHO, 2017). The most abundant air pollutants, their sources and percentage derived from power generation and consumption activities are shown in Table 2.1.

**Table 2.1:** Most abundant air pollutants in the atmosphere (Source: WHO).

Pollutant	Principal sources	Percentage from power activities
Sulfur dioxide (SO <sub>2</sub> )	Power and industry	> 99
Nitrogen oxides (NO <sub>x</sub> )	Transport and industry	> 99
Carbon monoxide (CO)	Residential and transport	> 90
Fine particulates (PM <sub>2.5</sub> )	Industry and residential	> 80
Secondary organic aerosols	Industry and transport	> 50

#### 2.1.5 Classification of air pollutants

Air pollutants are chemically and physically diverse (WHO, 2017). The majority of air pollutants in the atmosphere are oxides of carbon, nitrogen and sulfur (CO<sub>x</sub>, NO<sub>x</sub> and SO<sub>x</sub>). These are what are called gaseous air pollutants, one of two main air pollutant groups. The second group is airborne suspensions that includes, but is not limited to, very small liquid droplets and solid particles called particulate matter or PM (e.g. aerosols, fly ash and soot) (Encyclopedia Britannica, 2017). Collectively, these are called primary air pollutants. Primary air pollutants are deposited directly into the atmosphere from a source where they

undergo chemical transformations, in the presence of an energy source (typically UV), to form new secondary air pollutants [e.g. ozone ( $O_3$ ), peroxyacyl nitrates (PAN), sulfate ( $SO_4^{2-}$ )] (Duan et al., 2008). Photochemical smog (Fig. 2.4) is a noxious mixture of primary and secondary air pollutants that forms when industrial and vehicular emissions concentrate in the atmosphere and undergo photochemical reactions with sunlight (Encyclopedia Britannica, 2017). Photochemical smog, a common phenomenon near major freeways and urban-industrial areas, is saturated with  $NO_x$ ,  $O_3$  and volatile organic compounds (VOC) that give it a brownish-grey colour (Hallquist et al., 2016).



**Fig. 2.4:** Photochemical smog in Cape Town. Photochemical smog photographed from the N1 freeway (left) and Sir Lowry's pass (right) [Images: own (left) and Getty (right)].

Moreover, air pollutants are categorised into three classes: air toxics, biological pollutants and criteria air pollutants (Australian Department of the Environment and Energy, 2005). Air toxics (or hazardous air pollutants) are gaseous or particulate pollutants that are present in air in low concentrations with toxicity levels so as to be a hazard to humans, plants and animals. Biological pollutants are living materials that can become airborne and impact air quality (e.g. pollen). 'Criteria air pollutants' collectively describes six pollutants used internationally as indicators of air quality (Australian Department of the Environment and Energy, 2005). Criteria air pollutants can injure human health, harm the environment and cause property damage and thus are strictly regulated (U.S. EPA, 2017). The six criteria pollutants are:

- Carbon monoxide (CO)
- Lead (Pb)
- Nitrogen dioxide (NO<sub>2</sub>)
- Ozone (O<sub>3</sub>)
- Particulate matter (PM)
- Sulfur dioxide (SO<sub>2</sub>)

#### 2.1.6 Air quality monitoring in South Africa

South Africa is one of 13 African countries with known ambient air quality monitoring (AAQM) stations but more importantly it is the only country on the continent to actively contribute to the WAQI in real-time (World Air Quality, 2017). The National Environmental Management: Air Quality Act (NEMAQA)

stipulates that authorities must monitor and manage South Africa's outdoor air quality. To

achieve this, the "Outdoor Air Quality Monitoring Module" [within the South African Air Quality Information System (SAAQIS) network] was developed (DEA, 2017). The "Outdoor Air Quality Monitoring Module" is an online tool that allows users access to accurate, up-to-date air quality data from various AAQM stations that report to SAAQIS. As at August 2017, there were more than 50 fully operational AAQM stations supplying real-time data to SAAQIS across the country (SAAQIS, 2017). The South African Weather Service (SAWS) is also actively involved in AAQM in the country. A member of the World Meteorological Organisation (WMO), the SAWS is the authority for weather forecasting in South Africa but also participates in research initiatives with local and foreign academic and research institutes. SAWS AAQM stations, like the one installed at Hantam National Botanical Garden (Fig. 2.5), continuously monitor for CO, NO<sub>x</sub>, SO<sub>2</sub>, PM<sub>10</sub>, PM<sub>2.5</sub> and black carbon (DEA, 2017). The extent of research activities at the SAWS was evident during a visit to the



*Fig. 2.5: SAWS AAQM station at Hantam National Botanical Garden, Northern Cape (Image: [sanbi.org/sites/default/files/images/dsc00923](http://sanbi.org/sites/default/files/images/dsc00923)).*

Global Atmosphere Watch (GAW) station at Cape Point, Cape Town. Headed by Dr. S. Labuschagne, it is one of 31 stations in the GAW network that monitor several atmospheric pollutants including CO<sub>x</sub>, NO<sub>x</sub>, SO<sub>x</sub>, O<sub>3</sub>, PM<sub>10</sub>, PM<sub>1</sub>, xenon (Xe) and radioactive isotopes of radon (Rd), generating data for both the SAWS and the WMO. South Africa has a capable AAQM network and is ahead of its African counterparts, contributing to both domestic and international databases.

## 2.2 Airborne particulate matter

Airborne particulate matter (APM) is a general term used to describe liquid droplets and solid particles suspended in air (U.S. EPA, 2012). APM is characterised by both physical attributes and chemical properties (Dockery et al., 1993).

### 2.2.1 Physical attributes

#### 2.2.1.1 Size and morphology

The physical size of APM varies greatly. Some are large enough to be seen with the naked eye while others are so small that they can only be seen with a powerful electron microscope (U.S. EPA, 2012). Two size ranges are widely monitored, PM<sub>10</sub> and PM<sub>2.5</sub>. Fig. 2.6 gives an indication of just how small PM<sub>10</sub> (aerodynamic diameter  $\leq 10 \mu\text{m}$ ) and PM<sub>2.5</sub> (aerodynamic diameter  $\leq 2.5 \mu\text{m}$ ) are in relation to a strand of human hair.

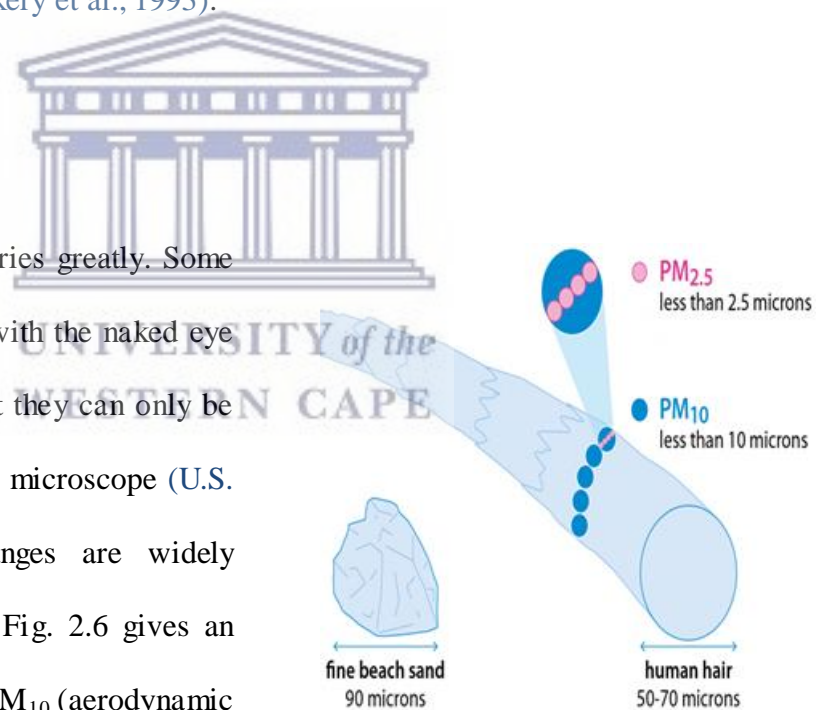


**Fig. 2.6:** Particulate diameters compared to a human hair (Image: [blf.org.uk/support-for-you/air-pollution/types](http://blf.org.uk/support-for-you/air-pollution/types)).

APM in both ranges act differently in air. Coarse particulates (subset of PM<sub>10</sub> larger than 2.5  $\mu\text{m}$ ) do not remain airborne for long and are deposited downwind of their emission sources within hours. The lighter, finely-divided PM<sub>2.5</sub> can remain suspended in air



for much longer periods of time and travel several hundreds, even thousands of kilometres from its emission sources (U.S. EPA, 2012). Like physical size, the morphology (or shape) of APM also vary. According to the Environmental Protection Agency (U.S. EPA), there are seven prominent particulate morphologies (Fig. 2.7). Because particulates are not all spherically-shaped, particulate diameters are best described as equivalent

	Solid Sphere
	Hollow Sphere
	Solid Irregular
	Flake
	Fiber
	Condensation Floc
	Aggregate

**Fig. 2.7:** Particulate shapes (Source: [epa.gov/eogapiti1/module3/diameter/diameter.htm](http://epa.gov/eogapiti1/module3/diameter/diameter.htm)).

diameter. The equivalent diameter is the diameter of a sphere with the same value for a specific physical property as a non-spherical particulate being measured (Willeke et al., 1993). The type of equivalent diameter used depends on the importance of the ‘physical process’ the particulate undergoes. Dominating processes for fine (subset  $\leq 0.3 \mu\text{m}$ ) and large particulates are diffusion and gravitational settling respectively (Willeke et al., 1993). Particulate diameters  $\leq 0.3 \mu\text{m}$  are best described by Stokes diameter ( $D_s$ ) while larger diameters (greater than  $0.3 \mu\text{m}$ ) are best described by aerodynamic diameter ( $D_a$ ).  $D_a$  is a standardised measure for irregular particulates (Bèrubè et al., 1999) and is the diameter of unit-density sphere with same gravitational settling velocity as the particulate being measured (Willeke et al., 1993). The relationship between  $D_s$  and  $D_a$  is shown in equation 1:

$$D_a = D_s \sqrt{\frac{d \cdot C_s}{C_a}} \quad (1)$$

Where  $d$  is particle density and  $C_s$  and  $C_a$  are Cunningham correction factors for  $D_s$  and  $D_a$ . The Cunningham correction factor is the ratio between particulate diameter and mean free path length of air molecules. For smaller particulates, C-values are greater than 1. For larger

particulates the diameters are greater than the mean free path length of air molecules ( $\lambda$ ) meaning all particulates collide with air molecules (Willeke et al., 1993). In this case, it is estimated that  $C_s = C_a = 1$ , hence the  $D_a$  of particulates where  $D_s \gg \lambda$  and  $D_s \ll \lambda$  is represented by equations 2 and 3:

$$D_a = D_s \sqrt{\rho} \quad (2)$$

$$D_a = D_s \cdot \rho \quad (3)$$

Observed  $D_a$  values for three examples of differently-shaped particulates and three different particulate densities are shown in Table 2.2:

**Table 2.2:**  $D_a$  for differently-shaped particulates and different particulate densities (Source: U.S. EPA).

<b>Aerodynamic diameters for differently-shaped particulates</b>		
Solid sphere	$\rho = 2.0 \text{ g.cm}^{-3}$ , $D_s = 1.4 \text{ }\mu\text{m}$	
Hollow sphere	$\rho = 0.5 \text{ g.cm}^{-3}$ , $D_s = 2.8 \text{ }\mu\text{m}$	$D_a = 2.0 \text{ }\mu\text{m}$
Irregular shape	$\rho = 2.4 \text{ g.cm}^{-3}$ , $D_s = 1.3 \text{ }\mu\text{m}$	
<b>Aerodynamic diameters for different particulate densities</b>		
Low density	$\rho = 1.0 \text{ g.cm}^{-3}$ , $D_s = 1.4 \text{ }\mu\text{m}$	$D_a = 2.0 \text{ }\mu\text{m}$
Medium density	$\rho = 2.0 \text{ g.cm}^{-3}$ , $D_s = 2.8 \text{ }\mu\text{m}$	$D_a = 2.8 \text{ }\mu\text{m}$
High density	$\rho = 3.0 \text{ g.cm}^{-3}$ , $D_s = 1.3 \text{ }\mu\text{m}$	$D_a = 3.5 \text{ }\mu\text{m}$

Inhalable coarse particulates like those found in emissions near roadways and industry are found within the equivalent diameter subset  $2.5 \text{ }\mu\text{m} \leq x \leq 10 \text{ }\mu\text{m}$ . Fine particulates such as those found in smoke and smog have equivalent diameters  $\leq 2.5 \text{ }\mu\text{m}$  (U.S. EPA, 2012). Equivalent diameters are important parameters in aerosol physics and chemistry and are useful for:

- Calculating deposition rates and atmospheric lifetimes of airborne particulates
- Determining the characteristics, origins and trends of APM and
- Determining the mechanisms of interaction and systemic effects of PM on living organisms (U.S. EPA, 2012)

### 2.2.1.2 Formation processes and size modes

APM are divided into three fundamental size modes: nucleation, accumulation and coarse-mode (Kittelson et al., 2014). The smallest mode is *nucleation* (diameters  $\leq 0.05 \mu\text{m}$ ). Nucleated particulates (or nuclei) are formed by condensation in the atmosphere or by nucleation processes within emissions from high-temperature sources. Nuclei-mode particulates are solids with very low-vapour pressures. The atmospheric lifetimes of nuclei-mode particulates are short (1-2 hours) because they spontaneously coagulate into larger particles or settle-out onto surfaces due to their diffusive nature resulting from very low particulate mass and their susceptibility to Brownian motion (Aerosol Science and Engineering program, 2017). The next mode is *accumulation* (diameters between 0.05 and 2.5  $\mu\text{m}$ ). Nuclei grow to larger sizes by condensation or coagulation processes to form accumulation-mode (or fine) particulates. Accumulation-mode particulates include combustion, smog and some nuclei-mode particulates. These particulates are extremely light and do not readily settle-out neither do they coagulate quickly enough into larger particulates and thus have long atmospheric lifetimes (up to a month) (Aerosol Science and Engineering program, 2017). Particulates in this size-mode are hazardous to human health (WHO, 2017). The largest mode is *agglomeration* (diameters greater than 2.5  $\mu\text{m}$ ). These particulates are created through mechanical processes (e.g. farming and mining). Gravitational settling rates are appreciable within this size range. Coarse-mode particulates include ash, dust, mold, pollen, sand and salt (sea spray) and some anthropogenic particulates. Because of their physical size (2.5-100  $\mu\text{m}$ ), these particulates have short atmospheric lifetimes. Deposition (or sedimentation) occurs within a couple of hours (Aerosol Science and Engineering program, 2017). Fig. 2.8 (page 20) shows the formation processes of the three APM size modes.

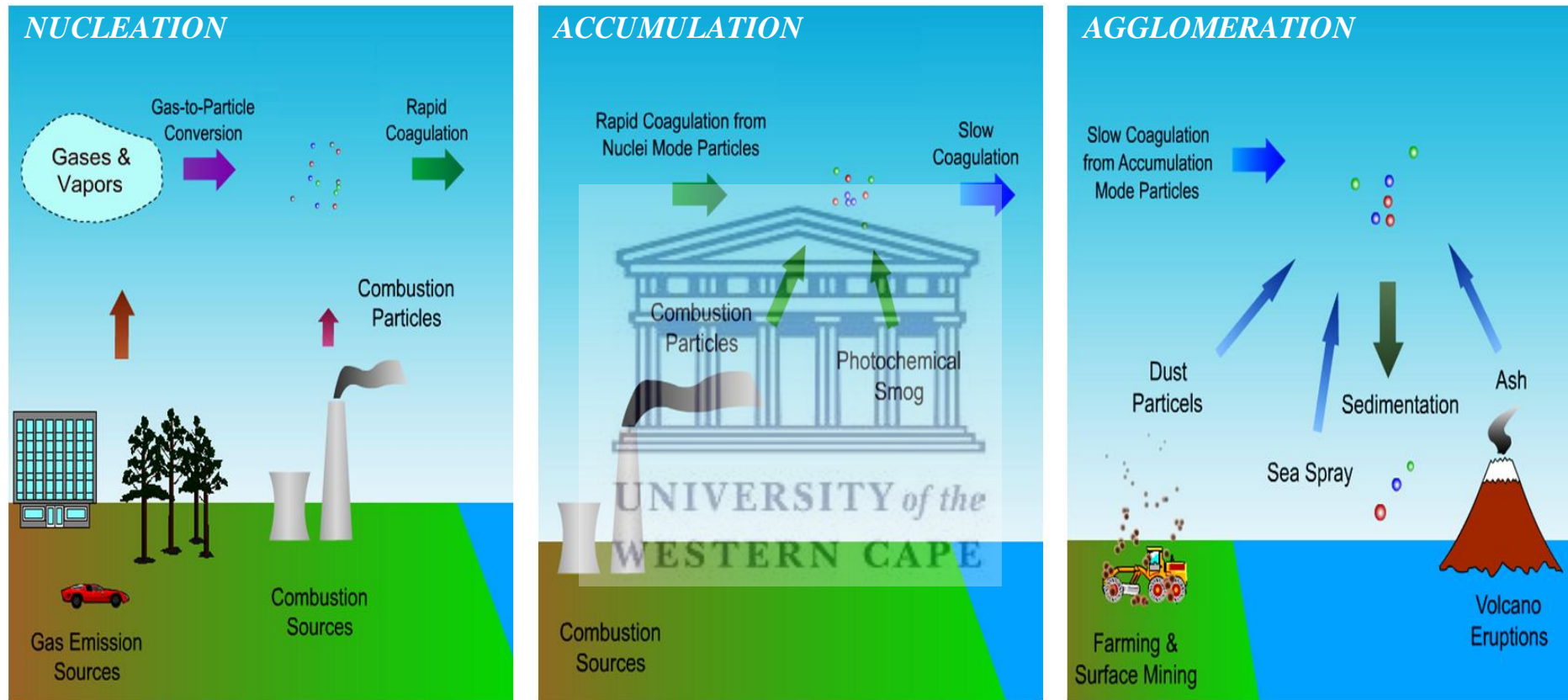


**Fig. 2.8:** Formation processes of APM. From left to right are nucleation (nuclei-mode), accumulation (accumulation-mode) and agglomeration (coarse-mode) (Images: Aerosol Science and Engineering program).

### 2.2.1.3 Particulate size distribution

Particulate size distribution is an important parameter for investigating APM behaviour. For monodisperse aerosols (particulates of equivalent sizes produced in the laboratory), particulate diameter is sufficient for describing particulate size. However, for particulate sizes in polydisperse aerosols, like those found in the environment, particulate size distribution is needed. Particulate size distribution defines the amounts of particulates in polydisperse aerosols and sorts them according to size/diameter (Hinds, 1999). A common approach to particulate size distribution is the splitting of the entire size range into intervals and calculating the amount of particulates in each interval. The number of particulates in each size interval can be plotted in a histogram, with the area of each bar representing the amount of particulates in that specific size range. For normalisation purposes, the number of particulates in each size range is divided by the width of that range, the area of each bar is now proportionate to number of particulates in size range it represents (Hinds, 1999). When the width of the bar approaches zero (0), equation 4 applies:

$$df = f(dp) \cdot d(dp) \quad (4)$$

Where  $dp$  is the particulate diameter,  $df$  is the fraction of particulates with diameters (between  $dp$  and  $dp + d(dp)$ ) and  $f(dp)$  is the frequency function (Hinds, 1999). The area below the frequency curve between sizes  $x$  and  $y$  is the total fraction of particulates in that size range:

$$f_{xy} = \int_x^y f(dp) \cdot d(dp) \quad (5)$$

Normal distribution does not describe particulate size distribution because of the skewness of the long tail of larger particulates (Hinds, 1999). A widely-used log-normal distribution for particulate number frequency is preferred:

$$df = \frac{1}{\alpha\sqrt{6.2832}} e^{-\frac{(dp-\bar{dp})^2}{2\sigma^2}} d(dp) \quad (6)$$

Where  $\sigma$  is the standard deviation of the size distribution and  $\bar{d}_p$  is the mean particulate diameter (Hinds, 1999). Size-based multi-modal particulate distributions have been recognised since the late 1970s. Whitby (1978) hypothesised that fine and coarse modes are physically and chemically different, that dynamics in fine particulate growth would have prevented it from growing larger than 1.0  $\mu\text{m}$  and that the distinction between fine and coarse modes was fundamentally important to any discussion on aerosol physics and chemistry. Particulates display consistent multi-modal distribution (Fig. 2.9) over several metrics including mass and volume, specific distributions may differ over area, conditions and time because of the number of sources, meteorological conditions and topography (Kittelson et al., 2014). Combustion and atmospheric chemical reactions of gases that create ‘low saturation vapour pressure’ are the major routes for the formation of ambient  $\text{PM}_{2.5}$  (accumulation mode) (U.S. EPA, 2012). Particulates in the accumulation mode do not grow into the coarse mode (Whitby’s hypothesis) but in high humidity conditions ‘hygroscopic-accumulation’ particulates grow, that bridges accumulation and coarse modes (U.S. EPA, 2012).

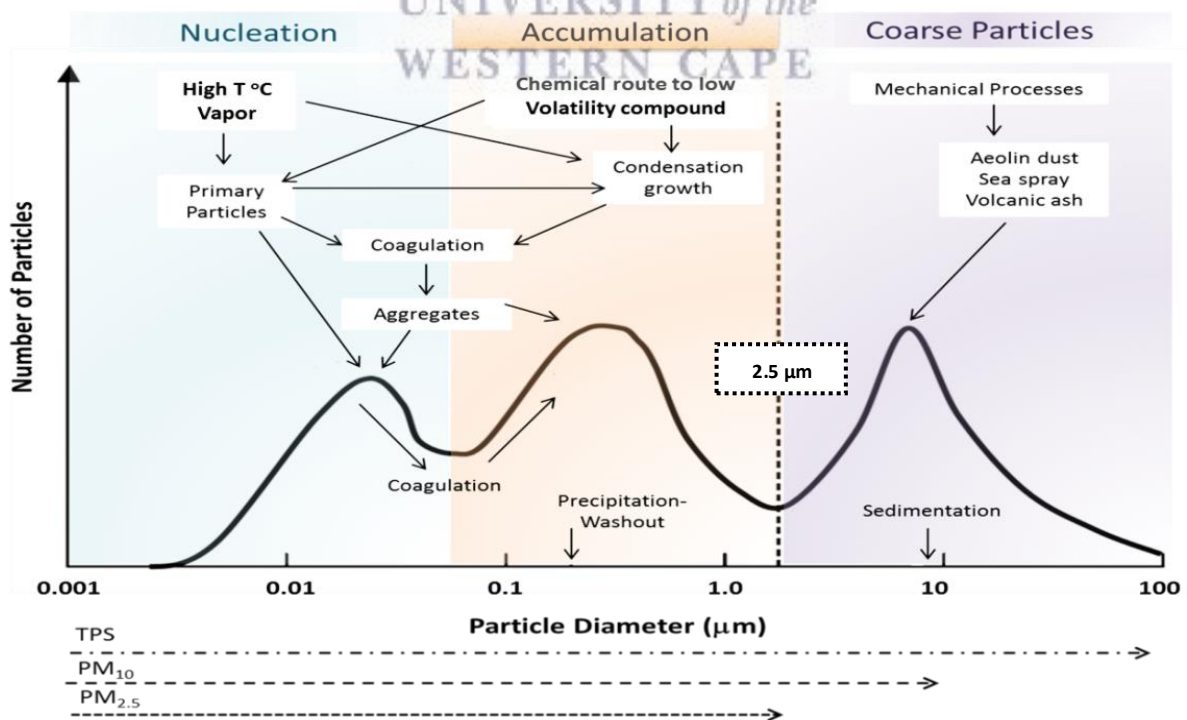


**Fig. 2.9:** Particulate size distribution, formation processes and multi-modal distribution of APM at ambient conditions (Image: Guarieiro et al., 2015).

Fig. 2.9 is acceptable for typical particulate size distributions but size distribution is dependent on whether it is expressed as particulate number, surface area or volume (Hinds, 1999). In a sample of ambient air,  $\pm 75\%$  of particulates are ultrafine. Particulates in this size range are abundant but they have small surface areas and are very light compared to larger particulates thus plots of distribution of surface area and volume according to particle size look quite different from the distribution of particulate numbers against particle size (Hinds, 1999). This is illustrated in Fig. 2.10. When particulate density changes are negligible with size, the particulate size distribution of mass is identical to the volume (Hinds, 1999). The

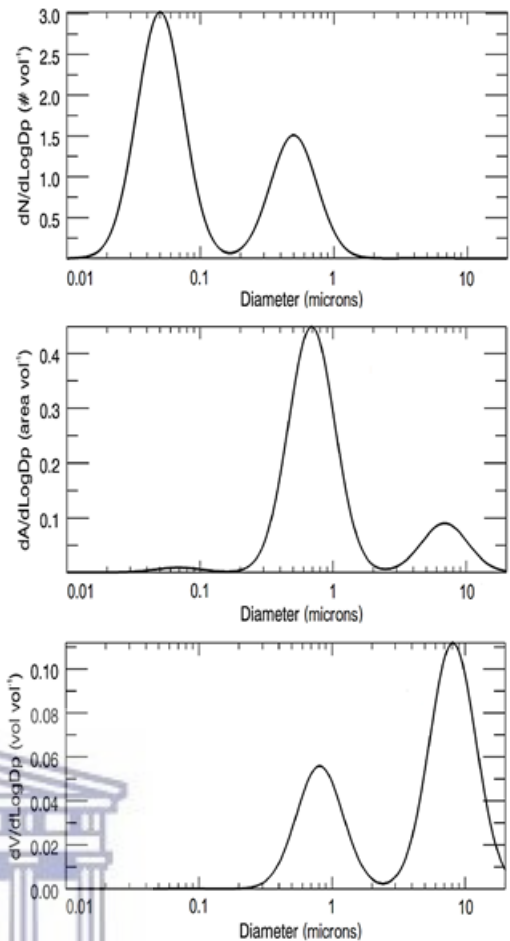


**Fig. 2.10:** Log-normal particulate distribution curves. From top to bottom are number vs. diameter, surface area vs. diameter and volume vs. diameter (Image: Hinds, 1999).

changes in relative number of particulates and surface area when a 10  $\mu\text{m}$  particulate is divided into three sizes: 0.01, 0.1 and 1.0  $\mu\text{m}$  are shown in Table 2.3.

**Table 2.3:** Effects of particulate size on number of particulates and surface area for a given mass of a single spherical particulate (Source: Hinds, 1999).

Diameter ( $\mu\text{m}$ )	Relative number of particulates	Relative surface area
10	1	10
1.0	$10^3$	$10^2$
0.1	$10^6$	$10^4$
0.01	$10^9$	$10^6$

### 2.2.2 Chemical properties

APM has diverse chemical compositions. The most common constituents of APM are biological matter, inorganic and organic species, minerals, stable radicals of carbon and transition metals (Valavanidis et al., 2008). Chemical constituents are divided into two groups - major and minor. Major constituents make up, at least, a few percentages of the total particulate mass and typically include the following:

i. Ammonium ( $\text{NH}_4^+$ )

Mainly present ammonium nitrate ( $\text{NH}_4\text{NO}_3$ ) or ammonium sulfate [ $(\text{NH}_4)_2\text{SO}_4$ ],  $\text{NH}_4^+$  forms when ammonia ( $\text{NH}_3$ ) neutralises gaseous nitric acid ( $\text{HNO}_3$ ) and gaseous sulfuric acid ( $\text{H}_2\text{SO}_4$ ) in the atmosphere.

ii. Chloride ( $\text{Cl}^-$ )

Major component of sea spray.

iii. Inorganic carbon and organic compounds

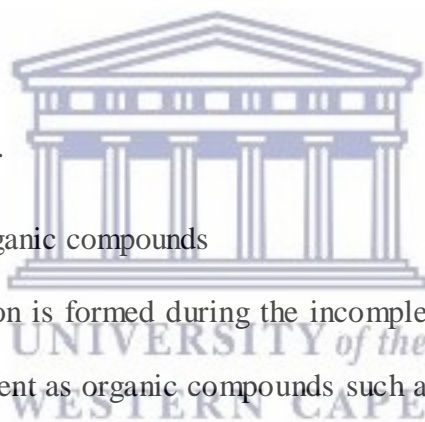
Inorganic (or elemental) carbon is formed during the incomplete combustion of fossil fuels. Organic carbon is mainly present as organic compounds such as benzene ( $\text{C}_6\text{H}_6$ ) and toluene ( $\text{C}_7\text{H}_8$ ), emitted from various primary sources including industry and vehicles, or as VOCs such as PAN and polycyclic aromatic hydrocarbons (PAH).

iv. Minerals

Crustal materials (rock, soil, etc.) contain elements such as aluminium (Al), iron (Fe) and several earth metals. Minerals (mainly coarse-mode particulates) are generated mechanically (construction works, erosion, farming and mining) or by highly turbulent wind.

v. Nitrate ( $\text{NO}_3^-$ )

Mainly present as  $\text{NH}_4\text{NO}_3$  or sodium nitrate ( $\text{NaNO}_3$ ) [displacement of hydrochloric acid (HCl) from sodium chloride (NaCl) by gaseous  $\text{HNO}_3$ ].





vi. Sodium ( $\text{Na}^+$ )

Like chloride,  $\text{Na}^+$  is mainly present in sea spray.

vii. Sulfate ( $\text{SO}_4^{2-}$ )

Largely present as secondary pollutants formed by the atmospheric oxidation of sulfur dioxide ( $\text{SO}_2$ ). Small amounts of sulfate also arise from atmospheric gypsum (or  $\text{CaSO}_4$ ) and sea spray.

viii. Water

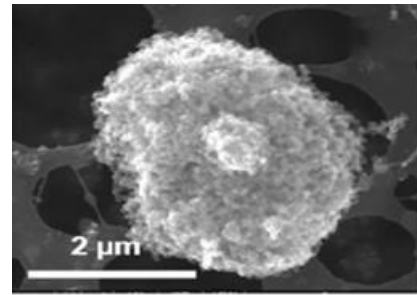
Water often accounts for a large proportion of particulate mass (UK-AIR, 2005).

In addition to the major chemical constituents, there are minor chemical constituents. Minor constituents include metals and organic compounds. Many metals are used in a variety of industrial processes. Some metals are found as additives or impurities in fuels while others are used in consumer products. Emissions from these processes are deposited into the atmosphere. Fortunately these metals that include chromium (Cr), lead (Pb), nickel (Ni) and zinc (Zn) are emitted in extremely low quantities. APM can also consist of several organic compounds. These compounds include aliphatic (straight-chain) and aromatic (cyclic) hydrocarbons, ketones and carboxylic acids. A large percentage of organic particulates are generated by power generation and consumption activities. These compounds are also emitted in very low quantities (UK-AIR, 2005).

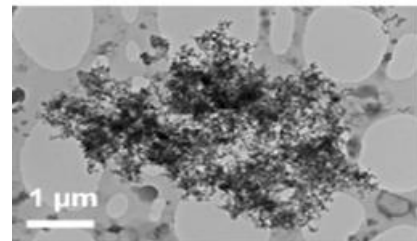
### 2.2.3 Soot

Soot (Fig. 2.11, page 26) is the most abundant particulate pollutant in the atmosphere accounting for 25 % of the total hazardous pollution in air (Omidvarborna et al., 2015). Soot (or black carbon, commonly abbreviated to BC) is mostly found in high concentrations near urban-industrial areas and busy transport routes. Soot consists mainly of finely-divided amorphous carbon produced by the incomplete combustion of biomass, coal or other fuels

(Omidvarborna et al., 2015) but can also contain acids, metals, organics and toxic chemical species such as PAHs, that are known mutagens and human carcinogens (Spengler et al., 2001). In fact, research has shown that soot, derived from wood burning, can share as many as 100 chemicals found in cigarette smoke (WHO, 2017). Soot is a hazardous air pollutant and for good reason. Soot particulates are tiny ( $\leq 2.5 \mu\text{m}$ ), when inhaled, travels deep into the lungs where the chemical constituents can do damage



SEM picture of soot



TEM picture of soot

**Fig. 2.11:** Photomicrographs of soot (Images: R'Mili et al., 2011).

Once soot has entered the blood it can cause serious health issues from bronchitis and asthma to cancer, stroke and even death (WHO, 2017). Not only is soot dangerous to human health but it can be coated with  $\text{HNO}_3$  or  $\text{H}_2\text{SO}_4$  which acidifies water forming acid rain that can damage crops and soil, affect water quality and impact the nutrient balance of ecosystems (Cashins & Associates Inc., 2013). In nature, soot exists as either accumulation- or coarse-mode particulates. Fig. 2.12 shows the formation of soot agglomerates from monomers.

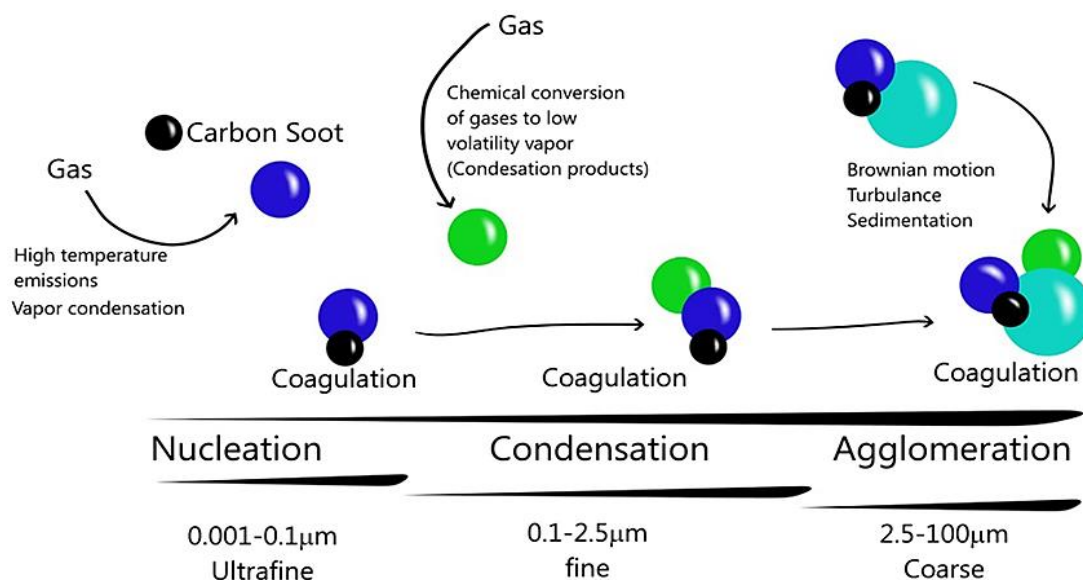


**Fig. 2.12:** Soot coagulation processes (Image: C Falcon-Rodriquez et al., 2016).

#### 2.2.4 APM deposition and health effects

A vast majority of the world's population live in areas with excessive air pollution levels. In 2016, the WHO estimated that 90-92 % of all people live in areas within countries that exceeded WHO safety limits. "Ambient air pollution, particularly in low- to middle-income countries, continues to rise at an unprecedented rate, impacting human health severely" says Dr. F. Bustreo (WHO Assistant-Director General of Family, Women and Children Health). "For people to live healthy lives they must continuously breathe clean air," she added. APM affects more people than any other air pollutant. It is the combination of chemical composition and particle size that makes APM such a serious health concern (WHO, 2016). Research has shown that there is a direct relationship between exposure to high concentrations of ambient PM<sub>2.5</sub> and increased mortality and morbidity (WHO, 2016). PM<sub>2.5</sub> can deeply penetrate lung tissue to enter the cardiovascular system where they pose the greatest risk. Once it has entered the body, PM<sub>2.5</sub> has both short-term (mortality and infections) and long-term or accumulative (cardiopulmonary diseases, lung cancer, etc.) effects (Valavanidis et al., 2008). Concentration, particulate size, residence time and toxicity all determine the impact APM has on health (WHO, 2016). The "Review of Evidence of Health Aspects of Air Pollution" (or REVIHAAP) project, undertaken by the WHO and published in 2013, showed the adverse effects of air pollution on human health in Europe. Information in the REVIHAAP report would later be used to establish air quality guidelines.

##### 2.2.4.1 Deposition mechanisms in the lungs

The human respiratory system is responsible for the exchange of gases between the circulatory system and the air we breathe. O<sub>2</sub> and CO<sub>2</sub> enter and exit our blood stream through the process of gaseous diffusion. The respiratory system is an important system of the human body and plays a life-supporting role but, unfortunately, it also provides a pathway for APM to enter into the body. The respiratory system is divided into three regions:

1) nasopharyngeal, 2) tracheobronchial and 3) alveolar regions (see Fig. 2.13, page 29). As APM enter the airways they are retained. Retention is dependent on the physiochemical properties, deposition location and clearance mechanisms ([Aerosol Science and Engineering program, 2017](#)). Cranial and lung airways are lined with mucous that traps APM bigger than 10  $\mu\text{m}$  in diameter. Once trapped, APM is transported to the stomach by mucociliary transport. In a similar fashion, particulates with diameters of 4-10  $\mu\text{m}$  in diameter are trapped, only this time by the mucous linings of airways and forced back to the oral cavity by billions of microscopic hairs. Particulates smaller than 4  $\mu\text{m}$  in diameter bypass natural removal systems and enter the alveoli ([Aerosol Science and Engineering program, 2017](#)). The alveolar airways are not mucous-lined and thus cannot expel APM by mucociliary transport. Instead, foreign materials are sent to the lymph nodes where it can take months or even years for them to be expelled. The four important deposition mechanisms in alveolar and bronchial regions are: impaction (i), settling (ii), diffusion (iii) and interception (iv). Impaction and settling are of primary concern to the bronchial airways. Impaction occurs when inertia causes large particulates to deviate from high velocity air streamlines (at curves) and continue along the original linear trajectory. Settling occurs when large particulates in slow velocity streamlines within narrow, horizontally-orientated bronchial passages settle-out under gravity. Diffusion is an important mechanism for the deposition of very small particulates (less than 0.5  $\mu\text{m}$  in diameter) in small airways where residence time is long and distance is short. Particulates are driven out of the air streamlines by Brownian movement to the walls of the airways. The effectiveness of this mechanism is adversely proportional to particulate size. Interception occurs when long fibres continue in the direction of the air streamlines (without deviation) but because of their size deposit onto the surfaces of airways, obstructing them ([Aerosol Science and Engineering program, 2017](#)).

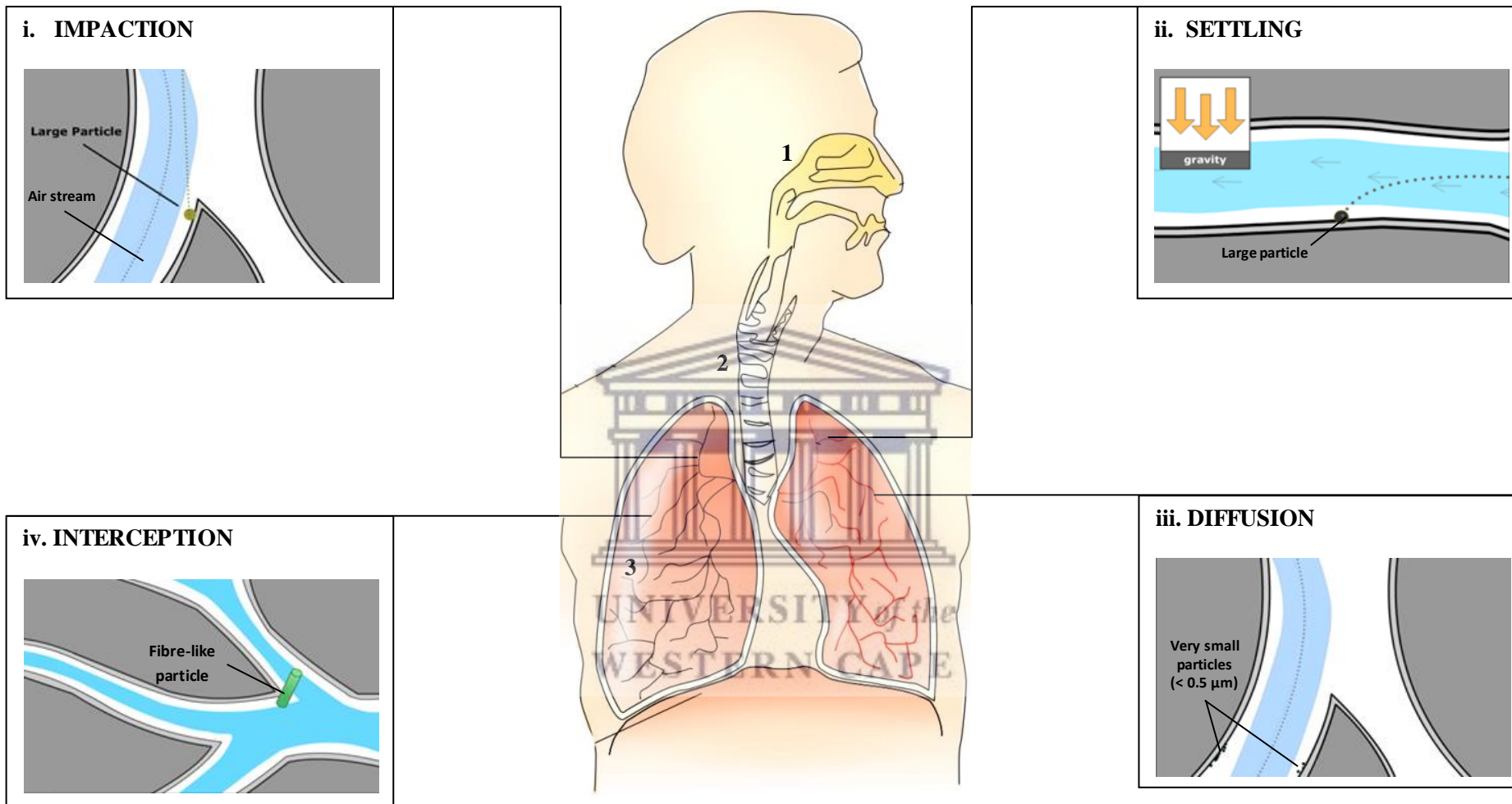


**Fig. 2.13:** Mechanisms of PM deposition in the lungs. Deposition mechanisms are, clockwise from top-left, impaction, settling, diffusion and interception (Image: Aerosol Science and Engineering program).

#### 2.2.4.2 Health effects of APM

Since the 1980s, many papers have been published correlating APM to adverse health outcomes such as decreased lung function in children, increased cases of respiratory infections and elevated mortality rates (WHO, 2017). APM is hazardous to human health. In section 2.1.1 it was discussed that nine million people died prematurely every year from air pollution in 2015, three million from exposure to high levels of ambient APM. APM has only one entry route into the body and that is via inhalation. This makes the respiratory system a central point for investigating all aspects of APM on human health (U.S. EPA, 2017).

##### i. Respiratory effects

According to the U.S. EPA, we breathe in, on average,  $11.4 \text{ m}^3$  of air every day. If it is considered that for 2016, the lowest recorded mean annual ambient  $\text{PM}_{2.5}$  concentration was  $2.0 \mu\text{g}\cdot\text{m}^{-3}$  (Powell River, Canada) and the highest recorded mean annual concentration was  $217 \mu\text{g}\cdot\text{m}^{-3}$  (Zabol, Iran), the average person inhales roughly 1,200  $\mu\text{g}$  of  $\text{PM}_{2.5}$  every day. In the section 2.2.4.1, the four mechanisms of APM deposition in the lungs was discussed. Damage caused by deposited APM can either be immediate or prolonged and may also lead to respiratory diseases. Obstructive lung diseases occur when particulates block airways, preventing air from reaching the alveolar region. Examples of obstructive lung disease are asthma and bronchitis (U.S. EPA, 2017). Restrictive lung diseases result from harmful activity within the gas-exchange tissue of the alveoli and are common in cases of chronic exposure to APM. Asthma, chronic bronchitis and lung inflammation are three ailments commonly associated with exposure to APM. Several studies have also linked lung cancer amongst adults to APM. According to the WHO, APM accounted for 3-5 % of new lung cancer cases every year in 2014. The respiratory effects of APM, especially  $\text{PM}_{2.5}$ , on human health can be devastating but APM-related cardiac effects may be as severe as or even more severe than those attributed to respiratory causes (U.S. EPA, 2017).

ii. Cardiovascular effects

In 2004, the inaugural American Heart Association meeting concluded that APM exposure contributes to mortality and morbidity. In recent years, evidence from several epidemiological and experimental studies has linked APM, especially the finest fractions, to increases in cardiovascular diseases and deaths (U.S. EPA, 2017). Arrhythmias, arteriosclerosis, heart failure, pulmonary and systemic inflammation, and stroke are just some of the adverse health effects associated with ambient PM<sub>2.5</sub> (Pope et al., 2002 and Martinelli et al., 2013). Expectedly, it is the most vulnerable of populations – the elderly, diabetics and those with coronary artery disease who are particularly susceptible to health effects triggered by APM exposure (Martinelli et al., 2013). Cardiovascular mortality and morbidity effects are observed for both acute and chronic exposure (U.S. EPA, 2017). In 2010, the American Heart Association concluded that PM<sub>2.5</sub> can trigger cardiovascular mortality and non-fatal events. Long-term exposure to PM<sub>2.5</sub> increases the risk of cardiovascular mortality to a greater extent and reduces life expectancy amongst highly exposed members of the population. Mechanisms for cardiovascular effects by APM are shown in Fig. 2.14.

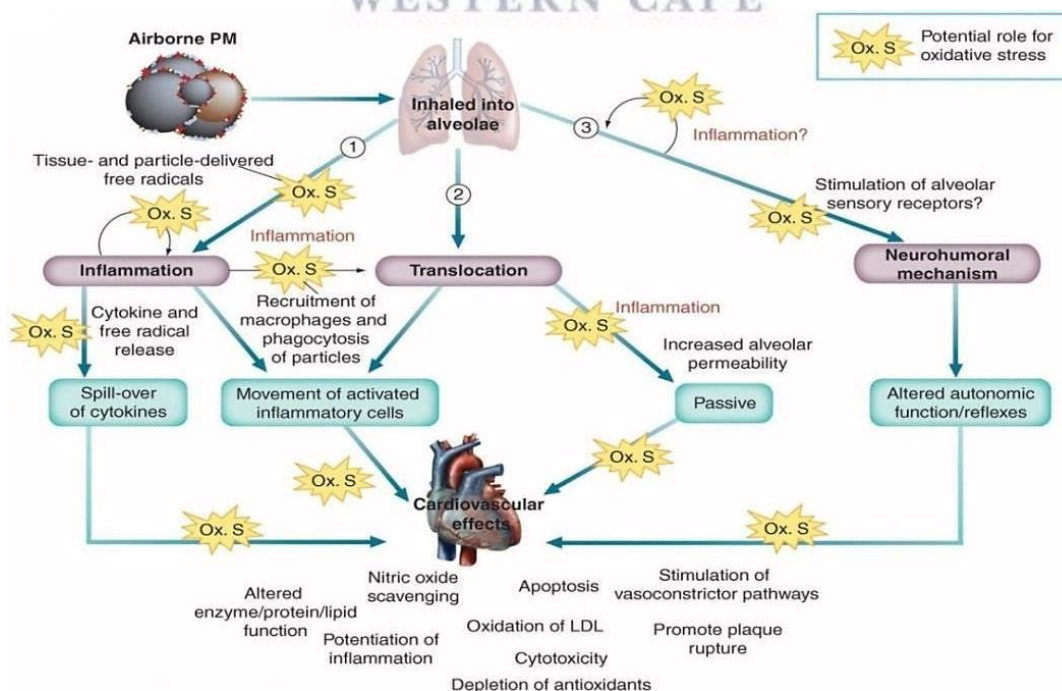


Fig. 2.14: Possible mechanisms for cardiovascular effects by PM (Image: U.S. EPA).

### iii. Mutagenic effects

APM originating from traffic and incomplete combustion of fuels contains large numbers of mutagenic chemical constituents (Valavanidis et al., 2008). In fact, emissions from combustion activities are associated with most of the mutagenicity and carcinogenicity of urban APM (Gábelová et al., 2004). In decades past, epidemiological studies used various short-term assays to provide evidence for the mutagenic properties of APM. Studies found that the mutagenicity of APM was due to at least 500 different organic compounds from varying classes including nitroaromatics (or polycyclic aromatic hydrocarbons), aromatic amines and aromatic ketones (Claxton et al., 2004). These compounds, especially nitroaromatics, have been found to cause deoxyribonucleic acid (DNA) damage (including oxidative DNA damage), micronuclei sister chromatid exchange, single-strand breaks and promote malignant neoplasms (Healey et al., 2005). Populations with frequent cases of lung cancer have been linked to the nitroaromatic component of coal smoke (U.S. EPA, 2017). Water-soluble species (mainly transition metals) have been found to induce oxidative DNA damage more readily than organic compounds. When inhaled, these species are deposited into the lungs which lead to the formation of reactive oxygen species, species like hydroxyl radicals ( $\cdot\text{OH}$ ) and superoxides ( $\text{O}_2^-$ ), that play an important role in the destruction of cell lipid membranes, enzymes and DNA (Gutiérrez-Castillo et al., 2006).

#### 2.2.5 Atmospheric dispersion of APM

The dispersion (concentration) and atmospheric lifetimes (residence time) of particulates are largely affected by meteorological parameters. Meteorological parameters play an important role in the extent of human exposure to particulate pollution (U.S. EPA, 2015). Elevated temperatures and low relative humidities (Rh) provide ideal conditions for long residence times. As Rh increases, ambient APM concentrations (particularly fine and ultrafine fractions) decrease due to the highly diffusive nature of these pollutants. Air velocity (or



wind speed) impacts dispersion. Particulate dispersion is indirectly proportional to air velocity. When air velocity is high then particulate pollution levels should be low and vice versa. This is not always true. Research has shown that particulate pollution levels do not decrease as quickly as expected (U.S. EPA, 2015). Surface topography (or roughness) is a physical characteristic of APM that can impact concentration. The roughness coefficient is defined as the extent of surface roughness i.e. the distribution of microscopic projections on the surface of particulates (Mondy et al., 1987). As air molecules pass over the surfaces of particulates they collide with these projections (like the sail on a yacht) causing the particulates to move about. Pollutant dispersion is directly proportional to the roughness coefficients of pollutants. In addition to air velocity, wind direction and vertical mixing of air masses can also impact ambient APM concentrations. Vertical mixing is impacted by atmospheric stability which is, in turn, is controlled by thermal buoyancy. Thermal buoyancy occurs when air heated near the Earth's surface rises rapidly. As the air rises it cools and expands because air pressure drops with elevation. Air ascension rate affects vertical mixing and the extent thereof (Stephens, 1965). Ground level thermal inversion and aloft inversion are two phenomena that inhibit ambient APM dispersion. Ground level inversion (Fig. 2.15) occurs when the layer of air, nearest to the ground, is cooled by the ground overnight. This

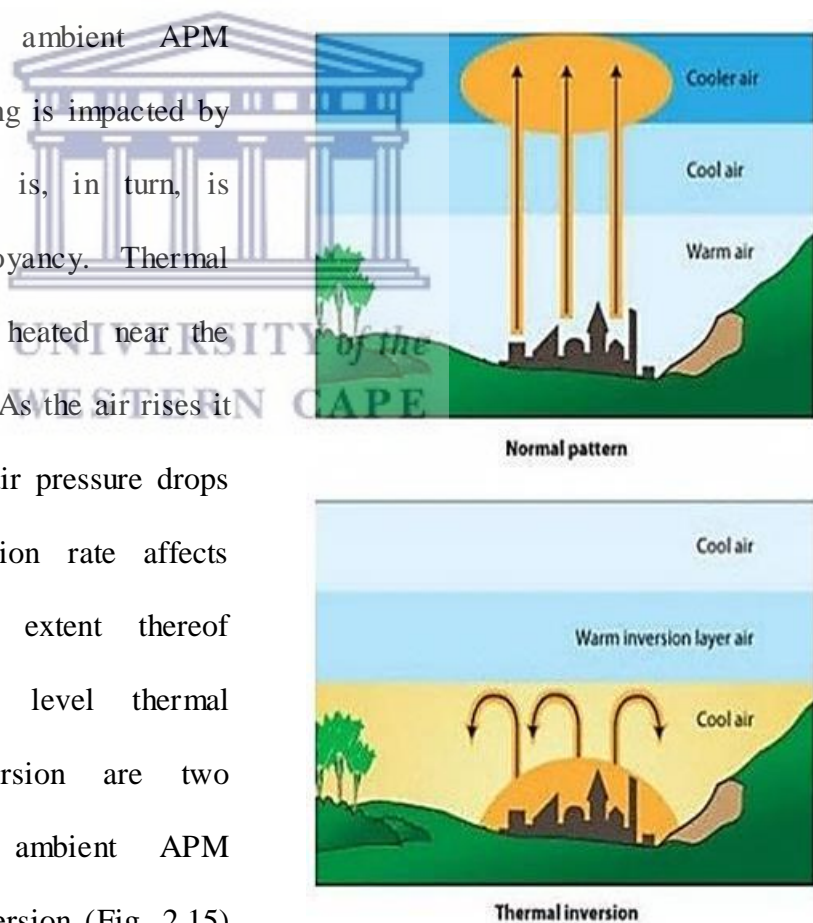


**Fig. 2.15:** Ground-level temperature inversion (Image: [bumc.bu.edu/otlt/MPH-Modules/PH/RespiratoryHealth/Temperature-inversion.jpg](http://bumc.bu.edu/otlt/MPH-Modules/PH/RespiratoryHealth/Temperature-inversion.jpg)).

cooler layer cannot ascend past the warm inversion layer above it as it is warmed by the sun and becomes stagnant, concentrating the pollutants within it (Stephens, 1965). Aloft inversion is entirely different. Aloft inversion occurs when air of a high pressure system descends from the centre of the inversion system and warms as it passes through the

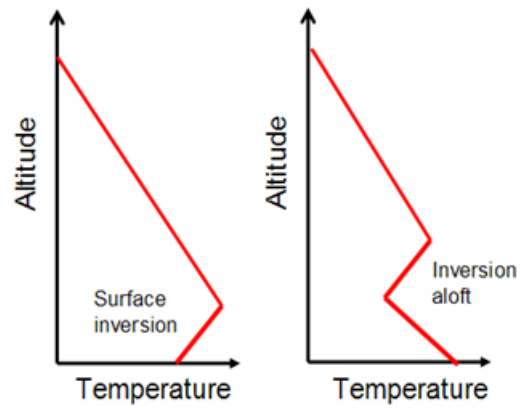


**Fig. 2.16:** Atmospheric elapse rates for surface level and aloft inversions (Image: [pataga.net/WhetherToFly.html](http://pataga.net/WhetherToFly.html)).

warmer layer. Warm air mixes with the cooler layer near the ground and disperses the particulates in that layer to an altitude where the inversion layer begins. Fig. 2.16 shows the changes in air temperature with altitude for ground level and aloft inversion events. Episodes of air pollution are worse for ground level inversion. Geography and topography can also affect air pollution dispersion. Urban settlements (coastal and valleys) are susceptible to higher air pollution levels resulting from ground level inversion (Fig. 2.17). For valleys, cool air moves in at night and at the coast, cool sea breezes blow across the land forcing it below warm terrestrial air increasing dispersion below the inversion layer (Gramsch et al., 2014).

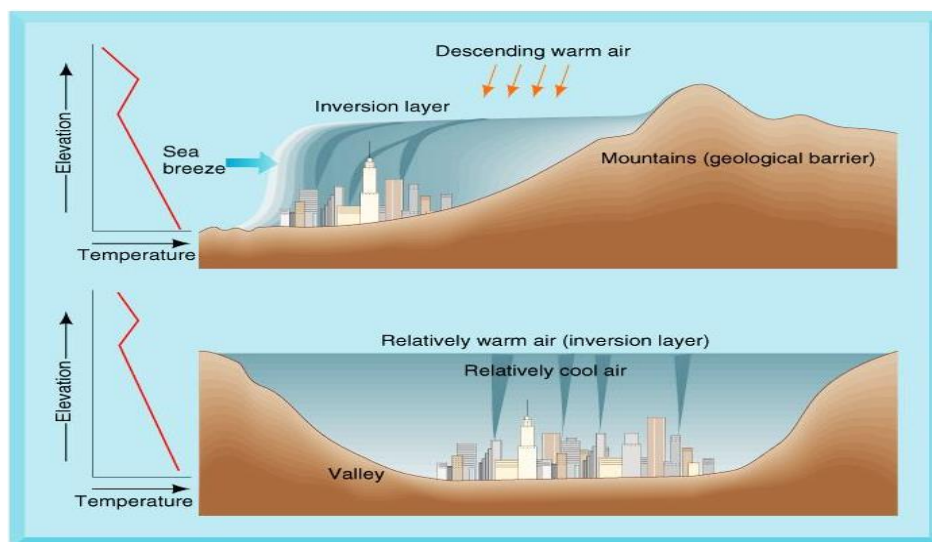


**Fig. 2.17:** Ground level inversion for urban areas at the coast and in valleys (Image: [ksuweb.kennesaw.edu/~jdirnber/scienceII/OutlineAir/OutlineAirNotes.html](http://ksuweb.kennesaw.edu/~jdirnber/scienceII/OutlineAir/OutlineAirNotes.html)).

Hartbeespoort, a small resort town situated in the North-West Province of South Africa, is a perfect example of how air pollutants “migrate”. In 2016, the WHO estimated that the town had a mean annual ambient PM<sub>2.5</sub> concentration of 60 µg.m<sup>-3</sup> (six times higher than the recommended limit of 10 µg.m<sup>-3</sup>), strange considering that there are no major industrial activities to speak of in the area. The only plausible explanation for such high PM<sub>2.5</sub> concentrations is that ambient APM was transported to the area from neighbouring provinces Gauteng (economic hub) and Mpumalanga (12 coal-fired power stations) by wind advection.

### 2.3 Dispersion, transport and origins of particulate pollution

Air pollution studies have rocketed in the last two decades, especially in highly industrialised countries in the Americas, Asia and Europe (WHO, 2016). Awareness of the risks of air pollution, or “invisible killer” as the WHO calls it, has seen interest in the matter soar. As the risks of air pollution to human health and climate change intensify, concerted efforts are being made to better understand air pollution trends (WHO, 2016). Detailed air quality studies are required to better understand air pollutant characteristics and trends. Such studies provide researchers who seek to advance their understanding of the causes and remedies of air pollution with important information (National Research Council, 2002). Detailed ambient APM studies are uncommon in Africa but the tools do exist for those wanting to investigate the dispersion, transport and source distribution of ambient APM in “data-sparse” regions. Hybrid Single Particle Lagrangian Integrated Trajectory (HYSPLIT) backward trajectory analysis is a technique widely used in the air quality and atmospheric chemistry communities.

#### 2.3.1 HYSPLIT

The HYSPLIT model, developed by the National Oceanic and Air Administration’s (NOAA) Air Resources Laboratory (ARL), is a tool that helps describe how air pollutants and harmful substances are transported, dispersed and deposited. It was designed to be used for both

single particle and complex dispersion and deposition simulations (Draxler et al., 1998). The foundation for HYSPLIT's trajectory capabilities can be traced back to 1949 when the United States (US) weather bureau was tasked with determining the source of radionuclides originating from the first Soviet nuclear tests. Over the past 67 years, the model has undergone several upgrades and is widely used throughout the scientific community. Some of the examples of its applications include tracking and forecasting the release of radioactive substances, dust and smoke from natural sources, and pollutants from various mobile and stationary sources (Draxler et al., 1998).

### 2.3.1.1 Calculation method

The calculation method HYSPLIT uses is a combination of the Lagrangian approach (moving frame of reference for calculating advection and diffusion as air parcels move from their origins) and the Eulerian approach [fixed three-dimensional (3D) grid for frame of reference for calculating air pollutant concentrations] (Draxler et al., 1998). Equation 7 is the basic calculation of particle parcel trajectories. The position of a particle at time  $(t + \Delta t)$  by wind advection is determined by the trajectory of the particle and is computed as follows:

$$p_{\text{mean}}(t + \Delta t) = p_{\text{mean}}(t) + \frac{1}{2} [v(p_{\text{mean}} \cdot t) + [v(p_{\text{mean}} \cdot t)\Delta t], (t + \Delta t)]\Delta t \quad (7)$$

Where  $p_{\text{mean}}$  is change in position vector with time and  $v$  is 3D velocity vectors. Dispersion equations are formulated in terms of turbulent velocity. Particle dispersion is computed by adding a turbulent factor to the mean velocity obtained from meteorological data as follows:

$$x_{\text{final}}(t + \Delta t) = x_{\text{mean}}(t + \Delta t) + U'(t + \Delta t)\Delta t \quad (8)$$

$$z_{\text{final}}(t + \Delta t) = z_{\text{mean}}(t + \Delta t) + W'(t + \Delta t)\Delta t \quad (9)$$

Where  $x_{\text{final}}$ ,  $z_{\text{final}}$  are the final particle positions in the 3D grid,  $x_{\text{mean}}$ ,  $z_{\text{mean}}$  are mean particle positions and  $U'$ ,  $W'$  are turbulent velocity factors. Factors  $U'$ ,  $W'$  are calculated based on

the modified discrete-time Langevin equation expressed as a function of velocity variance (derived from meteorological data and Langevin time scale) (Draxler et al., 1998).

### 2.3.1.2 Backward trajectory analysis

Backward trajectory analysis is the most commonly used feature of HYSPLIT. It depicts air flow patterns and allows for the interpretation of pollutant transport over spatial and temporal ranges (Fleming et al., 2012). Backward trajectory analysis is a surrogate measure (or proxy) for long-range transported air pollution and distant sources, and is particularly useful in air pollution studies where air mass origin and trajectory predictions are required (Molnár et al., 2017). Although useful for source-receptor relationship, a single backward trajectory does not represent mixing during transport and must be coupled to a Lagrangian dispersion component to give an accurate representation of particle concentration at the receptor and the sources influencing it (Lin et al., 2003). For backward-in-time calculations, equations 8 and 9 are assumed to be reversible when integrated from  $t + \Delta t$  (first-guess position) to  $t$  (initial position). With this approach, the wider distribution of Lagrangian particles released from a receptor undergoing backward transport represents the geographical influence and extent of possible pollution sources affecting the location of interest (or receptor) (Lin et al., 2003). From a computational perspective, backward calculation from a few receptor locations is more effective than forward calculation from more potential source locations to find the best match with receptor data (Lin et al., 2003). Fig. 2.18 (page 38) shows 24-hour and 72-hour backward trajectories for the coastal town of Atlantis, Cape Town, for April 2017. HYSPLIT uses the Global Data Assimilation System (GDAS), the same system used by the National Centre for Environmental Prediction Global Forecast System, to plot air mass data on a 2D map (i), showing the origin, trajectory (at user-specified intervals) and end position of air masses. The third plane (z-axis) is located below the map (ii). Here, altitude (calculated with the vertical motion method) is plotted against time.

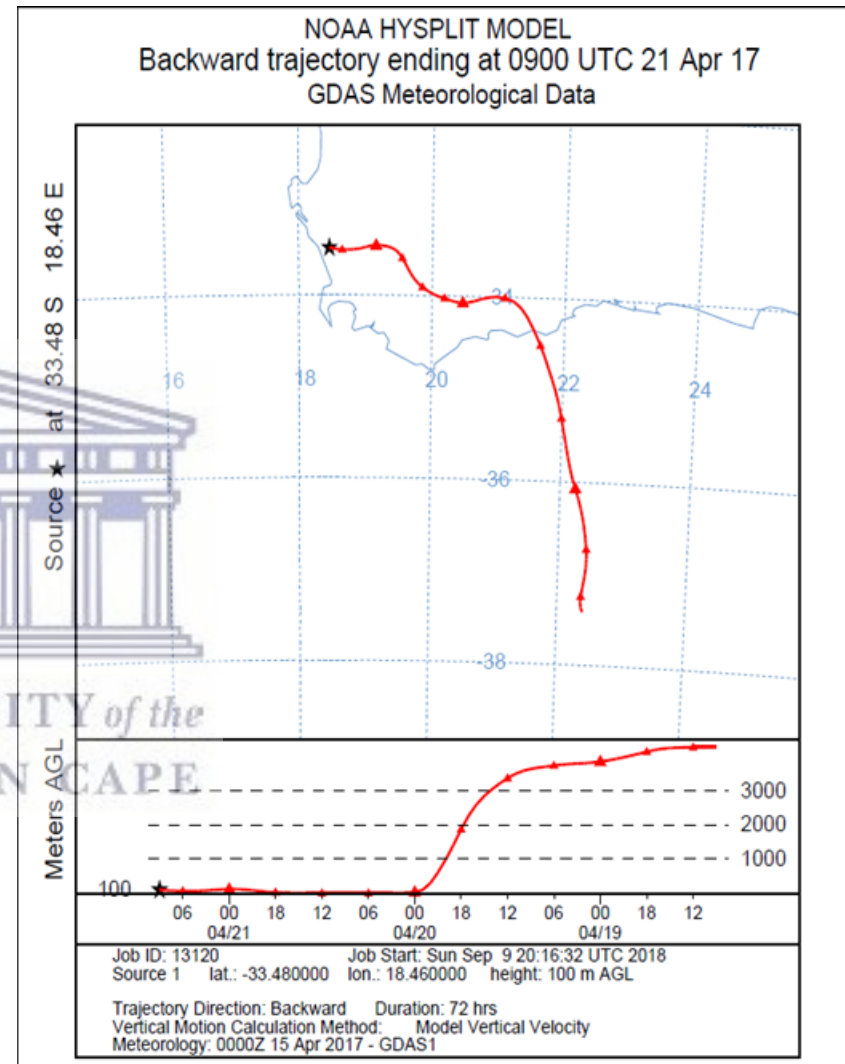
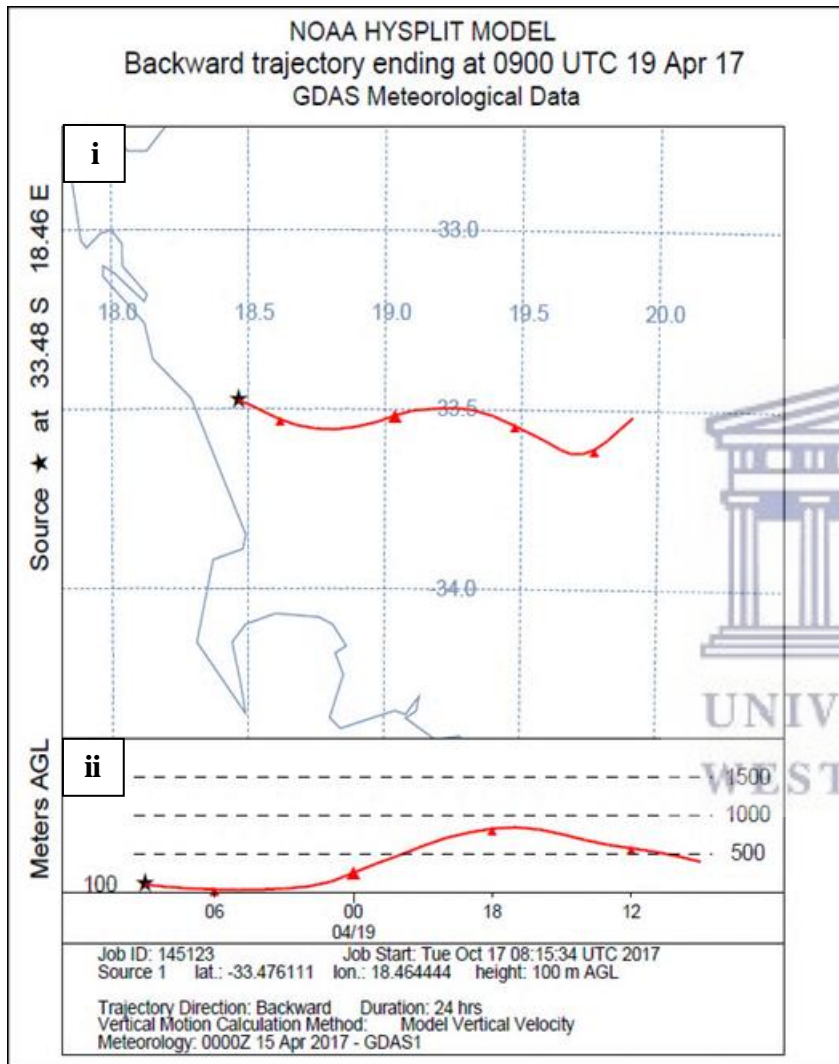


**Fig. 2.18:** Examples of backward trajectories derived from the HYSPLIT model. Above are 24-hour (left) and 72-hour (right) backward trajectories (six-hour intervals) for Atlantis - a small town 45 km N of the city centre on Cape Town's West Coast (Images: NOAA ARL HYSPLIT model).

## 2.4 Study site description

### 2.4.1 South Africa

South Africa (Fig. 2.19) is the southernmost country in Africa. It is home to 57 million inhabitants making it the sixth-most populous country on the continent and 25<sup>th</sup> in the world ([worldometers.com](http://worldometers.com)). South Africa is a developing nation boasting population and urban population growth rates of 1.6 % (1.3 % in 2007) and 2.4 % (2.2 % in 2007) per annum respectively ([tradingeconomics.com](http://tradingeconomics.com)). 64 % of the country's population is urban ([worldometers.com](http://worldometers.com)).



**Fig. 2.19:** Map of South Africa (Image: [municipalities.co.za/img/frontend/provincial\\_map.gif1503668364](http://municipalities.co.za/img/frontend/provincial_map.gif1503668364)).

If the urban population continues to grow at the current rate of 2.4 % per annum, the urban population will surpass the 80 % mark by 2023-2024. Coal is South Africa's largest primary energy source. The country's overwhelming dependence on fossil fuels can be seen in Fig. 2.20. Coal accounted for 72 % of the total fuel consumed in 2012, 140 % higher than the mean global coal dependence (30 %) over the same period (BP Statistical Review of

World Energy, 2013). Eskom, South Africa's only power utility and biggest consumer of coal, recently announced that due to the lack of suitable replacements and the costs of renewable energy technologies it is highly unlikely that the country's dependence on coal for electricity generation will change in the next 10 years. Coal combustion for electricity generation

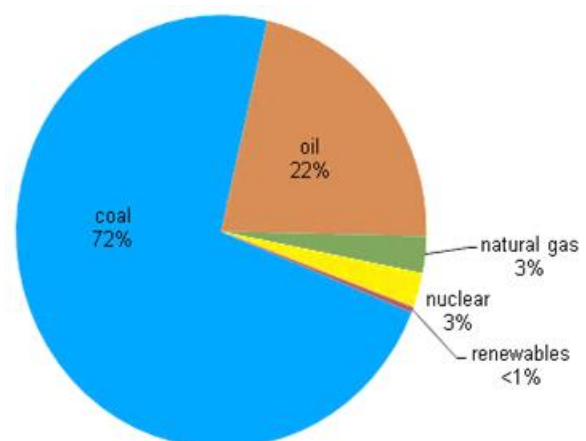


**Fig. 2.20:** Total primary energy consumption in South Africa for 2012 (Image: BP Statistical Review of World Energy, 2013).

activities accounted for 83 % of the total coal consumed nationwide in 2015 (Eskom, 2017). Fig. 2.21 shows Africa’s energy demands for 2001. In 2001, electricity generation activities accounted for 25 % of South Africa’s total coal consumption. This figure rose to 83 % in 2015, an increase of more than 230 %. The quantities of nitrogen oxides (NO<sub>x</sub>), SO<sub>2</sub> and PM<sub>10</sub> emitted by coal power stations in South Africa during 2014 were enormous, in the order of 1.1 Mt, 2.3

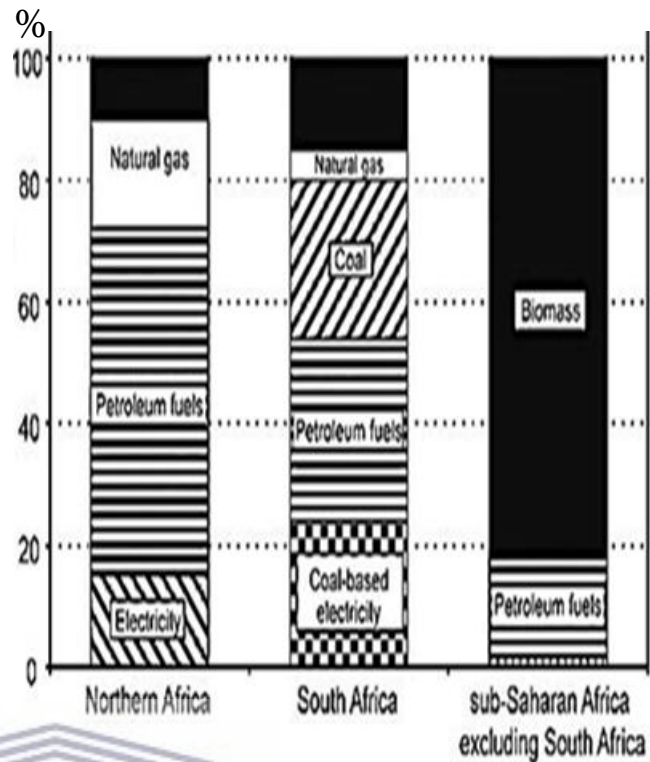


**Fig. 2.21:** Percentage energy demand in Africa for 2001 (Image: [scielo.org.za/img/revistas/sajs/v105n5-6/a09fig01.gif](http://scielo.org.za/img/revistas/sajs/v105n5-6/a09fig01.gif)).

Mt and 108 kt respectively (Myllyvitra, 2014). These pollutants are deposited directly into the atmosphere, deteriorating air quality in the region. Speaking at the National Environmental Management Air Quality Act (NEMAQA) colloquium, held at the Parliament of South Africa in Cape Town on 13 July 2017, Mr. T. Govender (Eskom Group Executive for Transmissions and Sustainability) stated that Eskom had begun retrofitting the biggest emitters in its coal station fleet with the latest in ‘scrubbing technology’ that would reduce emissions by 50 %. “Retrofitting activities should conclude sometime during 2023,” he added. In recent times Eskom has had many ‘postponements’ approved, exempting the utility from laws setting minimum emission standards (MES) for power stations. These postponements entail higher than acceptable air pollution emissions in the region. Ambient APM emissions are expected to cause approximately 20,000 deaths over the remaining life of coal power plants (Myllyvitra, 2014). In a recent update of its Global Urban Ambient Air



Pollution Database, the WHO released a map of the world (Fig. 2.22) with shades of yellow, orange, red and purple indicating regions whose air quality levels exceeded WHO recommended safety limits. South Africa ranked amongst the top 200 most air-polluted regions in the world.

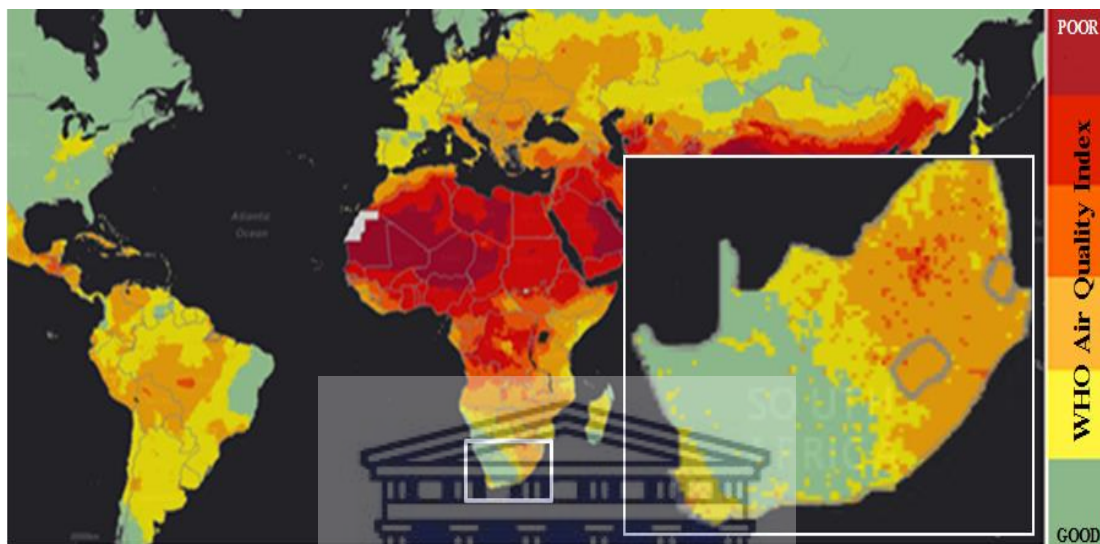


*Fig. 2.22: Air quality in South Africa (Image: WHO).*

It must be said that South Africa has recognised its air pollution problems and has invested substantially in improving air quality (United States Department of Commerce, 2016). Coal station upgrades, “Go Green” funding, policy amendments, reviews of ambient air pollution limits and proactive planning by authorities are some of the initiatives taken. Despite all efforts, ambient  $PM_{2.5}$  levels continue to exceed both daily and annual health safety limits (as much as 40 % of the days in the year) (DEA, 2017).

#### 2.4.2 Cape Town, Western Cape

Cape Town (Fig. 2.23, page 42) is situated  $-33.9250^{\circ}$ ,  $18.4240^{\circ}$  and occupies the southwesternmost point of the Western Cape Province. It is the legislative capital and second-most populous city in South Africa behind Johannesburg (Western Cape Government, 2017). The city is home to some four million residents, the majority of whom dwell in urban

environments (worldpopulationreview.com, 2017). Cape Town has a Mediterranean climate with warm summers and wet winters. Temperatures in the region vary from 7.1 °C (July) to 27 °C (February) with most of the rainfall occurring during the winter months of June through August. Average precipitation for the region is 515 mm per annum (SAWS, 2017). Cape Town started experiencing its worst drought in 100 years from 2015 (v. Dam, 2017) which has seen rainfall dwindle in recent



**Fig. 2.23:** Map of Cape Town (Image: [westerncape.gov.za/image/2012/10/cape\\_town\\_metro\\_map.jpg](http://westerncape.gov.za/image/2012/10/cape_town_metro_map.jpg)).

times. Rh is 50-70 % (worldweatheronline.com, 2017). Air velocity in the region averages

between 12-28 km.h<sup>-1</sup> (roughly 3.3-7.8 m.s<sup>-1</sup>) with south-easterly (21 % of the days in 2016) and north-westerly (13 % of the days in 2016) wind directions predominating (windfinder.com, 2017). The “Cape Doctor” is a name given to the former by the locals. It

originates in False Bay and channels through to Cape Town and Blouberg, clearing the peninsula of air pollution. Topographically, Cape Town is situated 40-50 m above sea level and has many peaks exceeding 300 m within its limits, the most well-known being Table Mountain (1,000-1,100 m above sea level) (topographic-map.com, 2017). In 2016, the WHO ranked Cape Town the 13<sup>th</sup> most polluted city in South Africa with a mean ambient PM<sub>2.5</sub> concentration of 16 µg.m<sup>-3</sup> (national mean: 28 µg.m<sup>-3</sup>). Unlike its northerly counterparts, Cape Town benefits from its geographical position in that the impact of air pollution from coal power station emissions is very low. Fig. 2.24 (page 43) shows the distribution of APM emitted by coal power stations in South Africa.

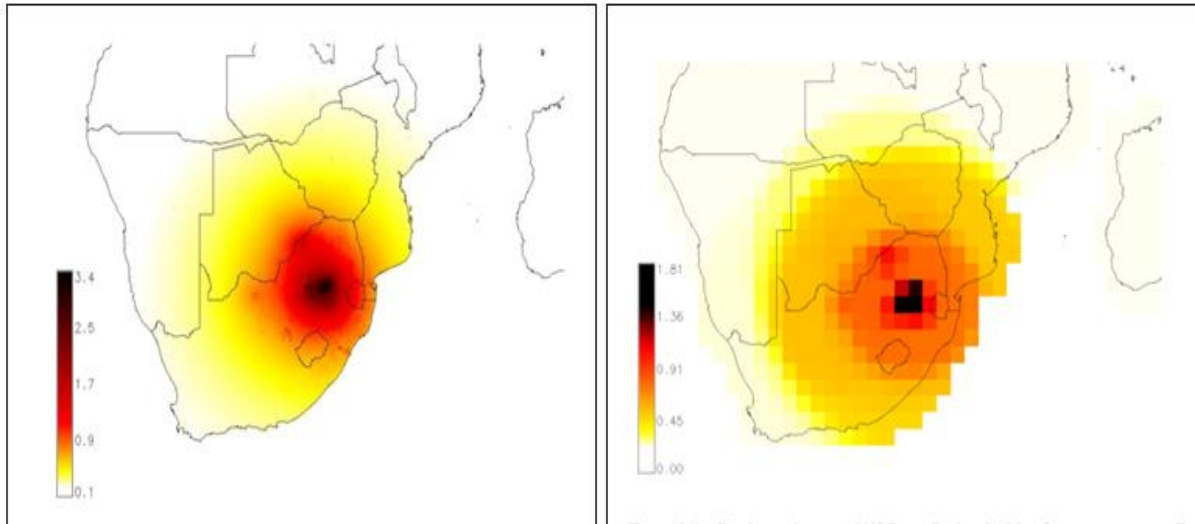


**Fig. 2.24:** Ambient  $PM_{2.5}$  contribution by Eskom's coal-fired power stations. Ambient  $PM_{2.5}$  contributions are based on Baker & Foley (left) and Zhou et al. (right) regression models of 2011 and 2014 (Image: Myllyvitra, 2014).

### 2.4.3 Emission sources in Cape Town

Air pollution in Cape Town originates mainly from mobile and stationary sources. Automobile emissions are the largest source of air pollution in the city. “Road-faring vehicles top the list of air polluters in Cape Town,” says Mr. S. Mamkeli (mayoral committee member for health at the city). “Traffic makes up two-thirds of the visible portion of air pollution in the city,” he added. Vehicular emissions deteriorate Cape Town’s air quality significantly. In urban areas, vehicular emissions can account for 90-95 % of CO, 60-70 % of NO<sub>x</sub> and a significant amount of soot in the atmosphere (Schwela, 2004). As Cape Town’s urban population continues to grow, so does the need for business and private transportation. In December 2016, a total of 1.28 million vehicles were registered by the City of Cape. By December 2017, this number grew to 1.31 million - an increase of 2.34 % year-on-year (eNaTIS, 2017). Aviation also impacts air quality in Cape Town, particularly areas within ± 10 km of the suburb of Matroosfontein (17 km ESE of the city centre), the location of Cape Town International Airport (CTIA). CTIA is the third largest airport in Africa. In 2017 it serviced 10 million passengers with some 65,000 flights (CTIA, 2017). Stationary sources of air pollution in Cape Town are subdivided into three categories: domestic, commercial and

industrial. Domestic emissions (combustion of biomass and fossil fuels for cooking and heating) are the largest stationary source of air pollution in the city. Natural sources of air pollution like open area burns, veld and wildfires, common occurrences in the region during the blistering summer months, also affect air quality. Daily temperatures in the mid- to high 20s, strong north-westerly and south-easterly winds combined with human carelessness and the continuation of the worst drought in over a century had resulted in many fires in Cape Town during 2017. According to the Volunteer Wildfire Services, 250+ open area, veld and wildfires occurred in the city and region during 2017.

## 2.5 Air quality management legislation in South Africa

### 2.5.1 Atmospheric Pollution Prevention Act

In 1970, the WHO and UNEP implemented regulations for air quality control around the world. Five years earlier, in South Africa, the APPA was drafted. The APPA (Act 45 of 1965) was implemented to regulate and management ambient air quality in the country. From the mid-1950s, South Africa experienced rapid growth in industrial development. Industrial growth led to increased air pollution levels, particularly in urban-industrial areas (SAAQIS, 2014). The APPA was largely based on the British Alkali Act (drafted in the late 1800s) which primarily focused on industrial emissions and controlled significant polluters with the traditional “command and control” method (SAAQIS, 2014). In the early 1990s, the efficacy of APPA at protecting ambient air quality was argued. It had become clear that a modern approach, one that was aligned to South Africa’s new constitution, was needed to effectively regulate ambient air quality thus protecting the human right to an environment that is not harmful to health and well-being (Constitution of South African, 1996). The Government’s Integrated Pollution and Waste Management committee initiated the development of an Air Quality Bill in late 2001 (DEA, 2000) with one desired outcome: national air quality that was not harmful to health and well-being (DEA, 2001). After a three-year developmental process

(that included discussions and debate), the NEMAQA (Act 39 of 2004) was made law in February 2005 and brought into effect in September 2005 (SAAQIS, 2014).

## 2.5.2 National Environmental Management: Air Quality Act

The APPA was replaced by the National Environmental Management: Air Quality Act (NEMAQA). The main objective of the NEMAQA is to regulate air quality and protect the environment. NEMAQA (Act 39 of 2004) provides measures to prevent pollution and ecological degradation for securing ecologically sustainable development, while promoting economic and social development, and standards to regulate air quality monitoring, management and control at all spheres of government (SAAQIS, 2014).

### 2.5.2.1 National Ambient Air Quality Standards

National Ambient Air Quality Standards (NAAQS) were authorised by the NEMAQA to protect public health in South Africa. The NEMAQA currently enforces NAAQS for PM<sub>10</sub>, PM<sub>2.5</sub>, NO<sub>2</sub>, SO<sub>2</sub>, CO, O<sub>3</sub>, lead (all criteria pollutants) and benzene. Table 2.4 (continues on page 46) shows the NAAQS currently enforced in South Africa.

**Table 2.4:** NAAQS for ambient air in South Africa (Source: DEA). Concentrations are in  $\mu\text{g}\cdot\text{m}^{-3}$

Pollutant	Averaging period	Concentration (max. limit)	Frequency of exceedances (max. limit)	Compliance date	Reference method(s)
PM <sub>10</sub>	24 hours	75	4	2015/01/01	EN 12341
	1 year	40	0	2015/01/01	
PM <sub>2.5</sub>	24 hours	40	4	2016/01/01	EN 14907
	1 year	20	0	2016/01/01 to	
	1 year	15	0	2030/01/01	
NO <sub>2</sub>	1 hour	200	88	2005/09/11	ISO 7996
	1 year	40	0	2005/09/11	
SO <sub>2</sub>	10 mins	500	526	2005/09/11	ISO 6767
	1 hour	350	88	2005/09/11	
	24 hours	125	4	2005/09/11	
	1 year	50	0	2005/09/11	

Pollutant	Averaging period	Concentration (max. limit)	Frequency of exceedances (max. limit)	Compliance date	Reference method(s)
Ground-level O <sub>3</sub>	8 hours	120	11	2005/09/11	SANS 13964
CO	1 hour	30	88	2005/09/11	ISO 4224
	8 hours	10	11	2005/09/11	
Lead (Pb)	1 year	0.5	0	2005/09/11	ISO 9855
Benzene	1 year	5	0	2015/01/01	ISO 9487

### 2.5.2.2 Atmospheric emissions licensing

The inception of NEMAQA (Act 39 of 2004) in February 2005 placed additional obligations and responsibilities on all three spheres of government in terms of air quality management in South Africa (DEA, 2016). Before the APPA (Act 65 of 1965) was annulled, the issuing of Registration certificates (as listed in Schedule 2 of APPA) remained the responsibility of the Chief Air Pollution Control Officer (CAPCO) at the DEA (APPA, 1965). Schedule 2 of the APPA listed 70+ processes that emitted air pollutants into the atmosphere. Any individual, company, corporation or organisation that operated any one of these processes should have been in possession of a valid APPA registration certificate that specified the operating parameters (as per set of guidelines) (APPA, 1965). Schedule 2 was replaced entirely by Section 21 of NEMAQA. Section 21 lists the 70+ processes (originally listed in APPA) into groups with each group having its own unique set of emission standards. A major difference between NEMAQA, as opposed to APPA, is that the NEMAQA requires Atmospheric Emission Licences (AEL) be issued by the Licensing Officer as opposed to the registration processes undertaken by the CAPCO under APPA (DEA, 2005). The responsibilities of the issuing AEL is vested in Metropolitan and District municipalities. The Act provides information for occasions when the municipality is an applicant stating that the Province (in which the municipality is located) becomes the licensing authority. Management of APPA registration processes was ineffective. There were many instances where emissions exceeded limits as scheduled processes were being operated outside of guideline limits. The DEA

investigated various industrial sectors, in this regard, to review and, if necessary, align registration certificates with new AELs and specific NAAQS requirements as per the NEMAQA (DEA, 2005).

## 2.6 Air quality monitoring

### 2.6.1 Global air quality monitoring

Many countries struggle with rapidly deteriorating air quality. Exposure to air pollution has become an inescapable part of urban living. The first efforts to monitor air pollution date back to 1970 when a partnership between the WHO and UNEP was formed (see section 2.1.2). This partnership coordinated all operations of the Global Air Quality Monitoring (AQM) Program with a view to total global AQM (Calkins, 1998). By the mid-90s, the program oversaw the operations of more than 250 AAQM stations across 50 countries. In 2007, the UN sought a different approach and after consultations with several institutions (including the WHO) the World Air Quality Index (WAQI) project was born (World Air Quality, 2017). The WAQI is an open (free-to-all) data framework that supplies accurate air quality data to the citizens of the world. The WAQI team is made up of professionals working in the areas of air quality, health and epidemiology studies and visual design. As at December 2017, air quality data from 9,000 stations in over 600 cities across more than 90 countries was published to the WAQI in real-time (World Air Quality, 2017). The effects of air pollutants on human health are not published on the WAQI website, however, visitors to the website are provided with an Air Quality Index (AQI) scale. The AQI scale is easy to use and provides the user with important information such as health implications (multiple pollutants) and cautionary statements (PM<sub>2.5</sub> only) based on the pollution levels in their geographical area. Fig. 2.25 (page 48) shows the locations of AAQM stations that supply data to the WAQI network. It should be noted that South Africa is the only African nation to actively contribute to the WAQI in real-time (see section 2.1.6).



**Fig. 2.25:** Locations of known AAQM stations that report to the WAQI (Image: World Air Quality).

### 2.6.2 Air quality monitoring in Cape Town

Cape Town boasts a network of 13 AAQM stations (Fig. 2.26, page 49) scattered across the region that continuously supply air quality information to SAAQIS in real-time. The city monitors CO, NO<sub>x</sub>, SO<sub>2</sub>, PM<sub>10</sub> and PM<sub>2.5</sub>, and compares daily readings to international guidelines (Western Cape Government, 2017). In 2017, the accuracy and validity of data obtained from these stations were scrutinised after it was discovered that station maintenance regimes were allegedly in contravention of procedural guidelines. Speaking at the NEMAQA colloquium, Mr. I. Gildenhuys [Head of Specialised Environmental Health Services at the City of Cape Town (CoCT)] addressed these concerns by reiterating that all stations were compliant and that data was accurate and reliable. “Given that AAQM equipment is imported, there is an inevitable loss of data when units fail,” he added. Cape Town’s AAQM network is the most comprehensive of all local authorities (Western Cape Government, 2017). “Cape Town is committed to better air quality and continues to set the standard for AAQM, both regionally and nationally,” says Mr. A. Smith (Mayoral Committee Member for Safety, Security and Social Service at the city). In addition to AAQM equipment, Scientific Services has installed an antenna camera on Tygerberg Hill for remote monitoring of air



pollution and our Diesel Emission Testing Programme had tested over 7,500 vehicles in the last financial year,” he explained in an article written by Mari Macnamara (published 21 November 2017).

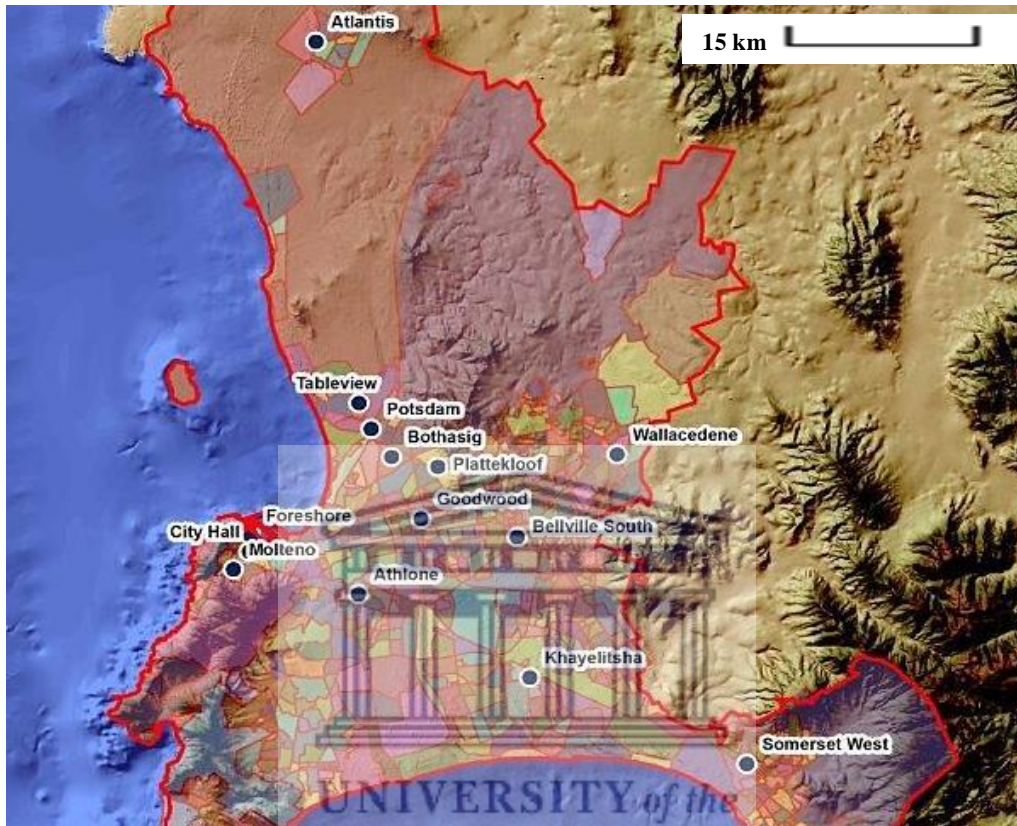


*Fig. 2.26: Map of AAQM network in Cape Town (Image: City of Cape Town).*

### 2.6.3 Ambient APM monitoring

Ambient APM monitoring is necessary to determine the ambient air quality of a region, provide data to regulatory bodies to determine whether a region has attained the National Ambient Air Quality Standard (NAAQS) and to assess the progress of mitigation strategies toward achieving ambient air quality goals (U.S. EPA, 2017). Since regulation requires information, continuous and reliable methods of ambient APM monitoring are essential (WHO, 2017). Cape Town has an adequate AAQM programme. AAQM stations monitor  $PM_{10}$  and  $PM_{2.5}$  using tapered element oscillating microbalance (TEOM) technology. TEOM measures ambient APM in real-time by measuring the mass concentrations. This technique,

approved by the U.S. EPA for environmental AQM, uses a vibrating glass tube. As APM is deposited onto its surface, it changes the oscillation frequency of the tube. The reduction in oscillation frequency is proportional to PM mass (Queensland Department of Environment and Heritage Protection, 2017). TEOM technology was first used introduced by Rupprecht and Patashnick Co. in 1981 and was the preferred choice for APM monitoring for three decades (Mischler et al., 2017). Modern AQM stations, like Aeroqual's AQM 65 station



*Fig. 2.27: Aeroqual AQM 65 station. The station can be outfitted with a laser nephelometer particle sensor (i) or particle counter (ii) (Image: Aeroqual).*

(Fig. 2.27), use particle sensors or optical particle counters to determine particulate mass and size. These devices are capable of detecting a wide range of PM<sub>2.5</sub> and PM<sub>10</sub> concentrations (0-2,000 µg.m<sup>-3</sup>) with accuracy and detectable limits of ± 2 µg.m<sup>-3</sup> and less than 1 µg.m<sup>-3</sup> respectively. The AQM 65 is a popular choice because it can continuously monitor 10 pollutants simultaneously, has low detectable limits and is remotely accessible from anywhere on the planet (Aeroqual, 2017).

### 2.6.3.1 Alternative methodologies of ambient APM monitoring

#### i. Light scattering and optical scintillation

Light scattering occurs when light is reflected or refracted from the surfaces of particulates. The amount of light scattered is dependent on the properties of particulates (concentration, size and shape) in the path of the light beam (U.S. EPA, 2017). An example of an instrument that uses light scattering is LiDAR (Light Detection and Ranging). This laser sensing instrument uses a solid-state Nd: YAG (Neodymium-doped yttrium aluminium garnet) laser

to detect tiny particulates in the atmosphere (Gaudio et al., 2015). In 2002, the Desert Research Institute experimented with one of the very first LiDAR instrument in Las Vegas, Nevada. The LORAX (LiDAR On-Road Aerosol eXperiment) (Fig. 2.28) was designed to measure particulate emissions (diameters of 0.1-0.2  $\mu\text{m}$ ) emitted by diesel-fuelled vehicles in the state. The goal of the study was to test the



*Fig. 2.28: LORAX instrument (Image: Desert Research Institute).*

instrument and iron out “teething” problems but ultimately to determine the feasibility of LiDAR compared to conventional sampling techniques at the time (Desert Research Institute, 2002). In 2010, collaboration between North-West University (NWU) and the University of Helsinki led to the establishment of an air pollution and climate change monitoring station in the city of Potchefstroom (North-West Province). According to Prof. P. Beukes, an

atmospheric chemistry researcher at NWU, the station uses LiDAR technology to monitor ambient APM pollution in the area. In 2014, the Romanian National Institute for Research and Development in Optoelectronics headed the development of Europe’s first multi wavelength high spectral resolution LiDAR system. The instrument, that took two years to build, scans the atmosphere from an aeroplane (Fig. 2.29) to detect and map aerosols containing minute particulates (ROSA, 2014). One limitation of

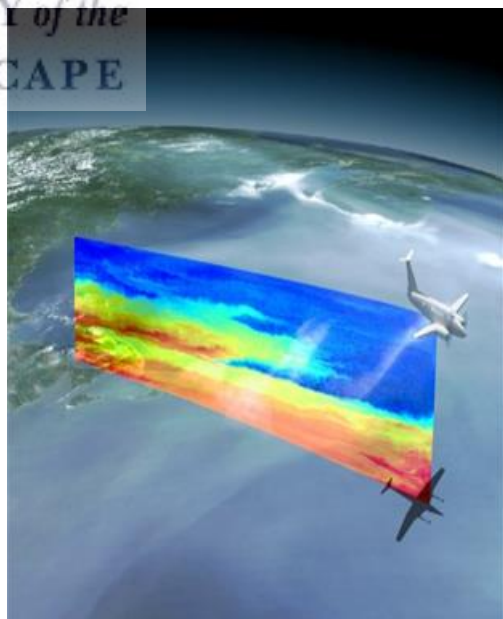


*Fig. 2.29: LiDAR scanning and detection by aeroplane (Source: ROSA).*

LiDAR is that APM detection is almost exclusive for elemental and organic carbon (Desert Research Institute, 2002). Another method of APM monitoring is optical scintillation. Unlike light scattering that uses focused laser beams for APM detection, scintillation uses a wide beam of light. When particulates pass through the light beam they momentarily disrupt it, causing fluctuations in amplitude of light signal received. Particulate concentration is directly proportional to the variation of light received (U.S. EPA, 2017).

ii. Beta ( $\beta$ ) attenuation

The principle of  $\beta$ -attenuation in particulate sampling instruments is that energy is absorbed from beta radiation as the rays pass through the PM sample collected on a filter medium. The attenuation (or weakening) of beta radiation intensity is proportional to the amount of material present (Thermo Scientific, 2017). The

Thermo Scientific model 5028i (Fig. 2.30) uses beta attenuation. The main components of any



Fig. 2.30: Thermo Scientific model 5028i continuous particulate monitor (Image: Thermo Scientific).

$\beta$ -attenuation measuring system are the  $\beta$ -source and detector. The preferred source is carbon-14 because of its abundance, high energy-level and long half-life. The gauge works by measuring beta counts before (clean filter) and after (exposed filter) sampling to provide a PM mass concentration.  $\beta$ -attenuation is especially useful to those monitoring airborne toxic metals (beta attenuation is identical for most materials, except hydrogen and toxic metals) (Thermo Scientific, 2017). Light scattering, optical oscillation and beta attenuation are only three examples of methodologies used by the air quality and atmospheric chemistry communities today. Fig. 2.31 (page 53) shows the various APM measurement and monitoring methodologies available to researchers.

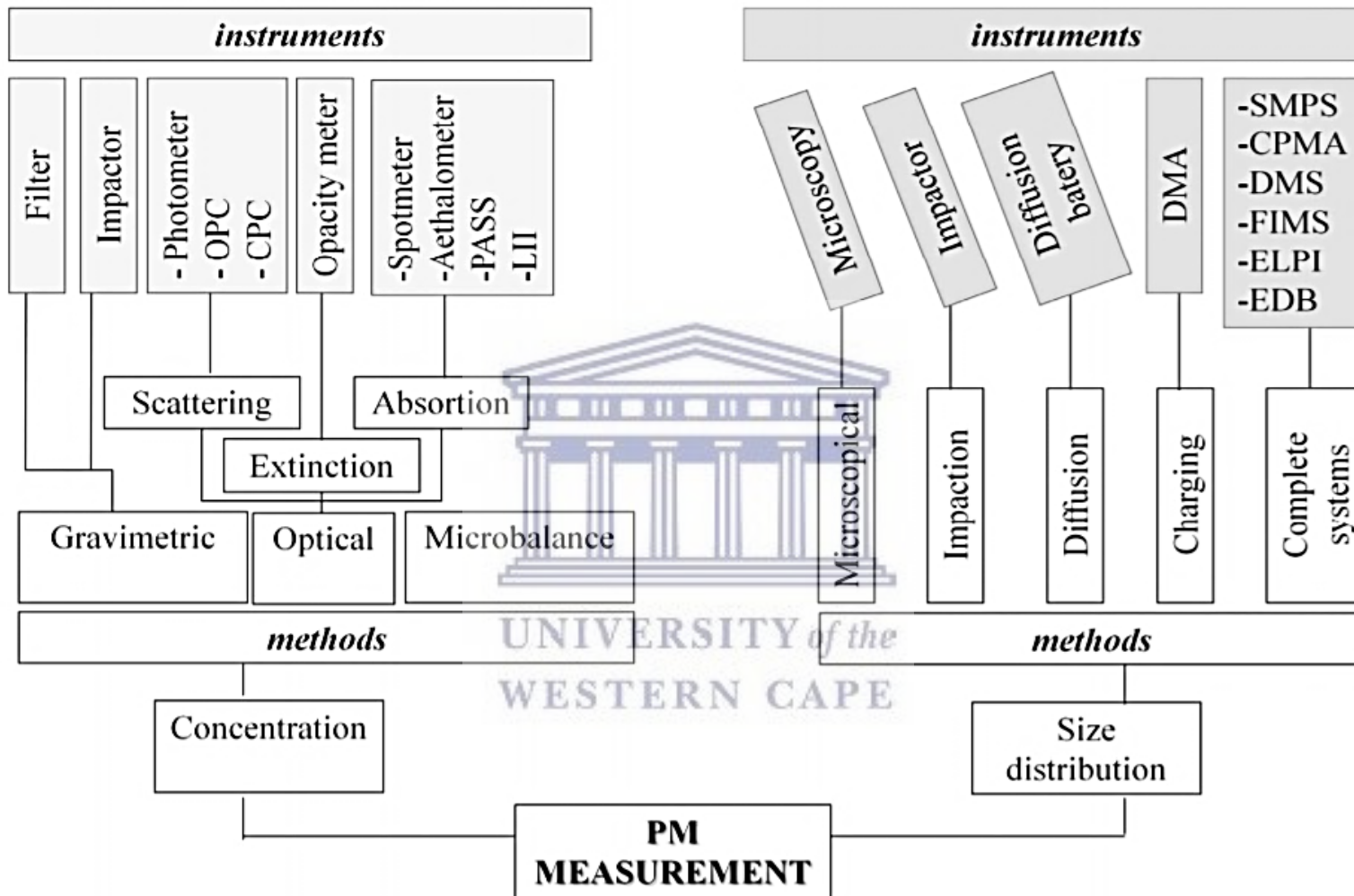


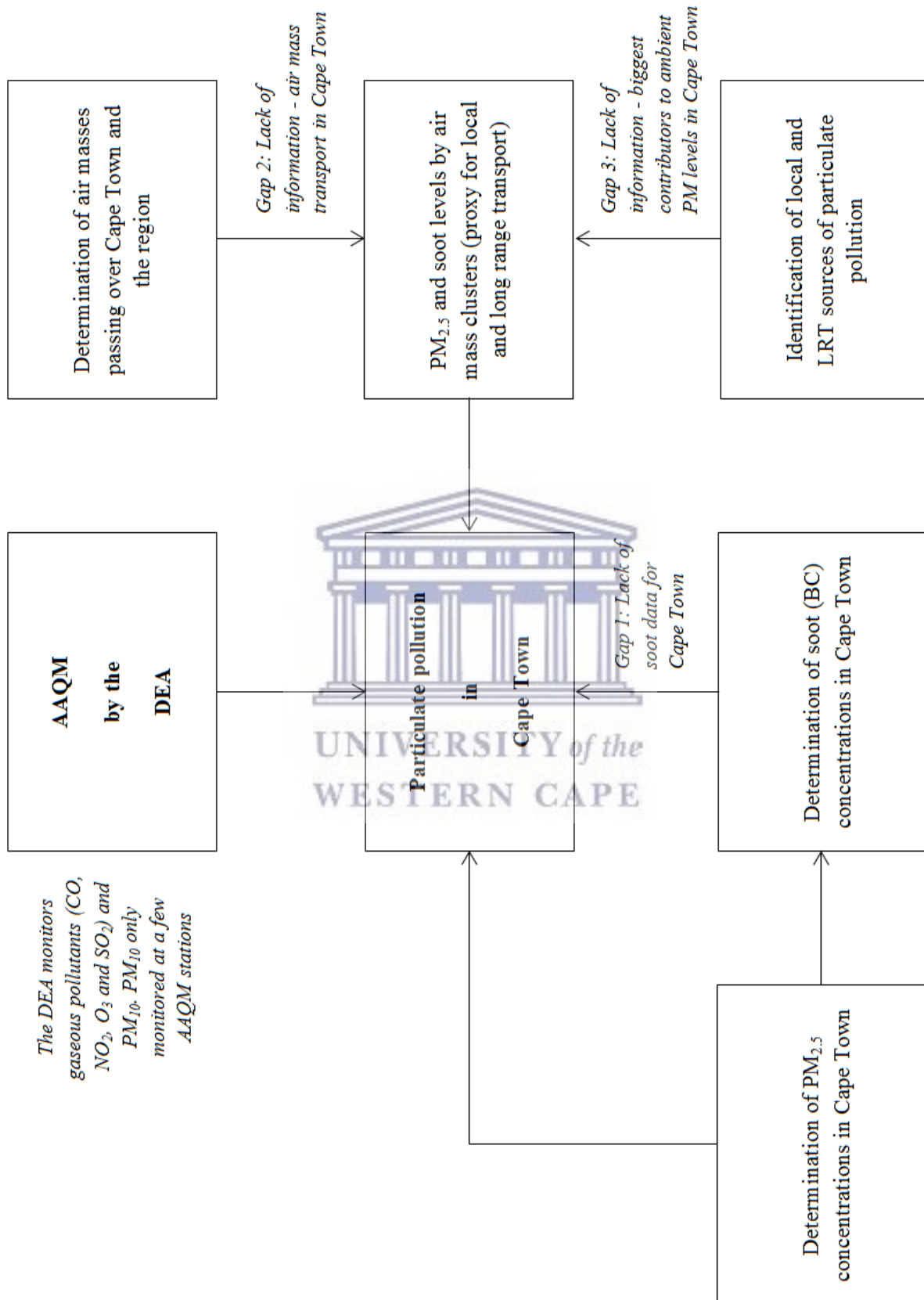
Fig. 2.31: Methods and technologies for APM monitoring (Source: Amaral et al., 2015).

### 2.6.3.2 Prospective methodologies of ambient APM monitoring

The U.S. EPA is responsible for air monitoring, measuring and emissions research in the USA. The agency is the leader in the development of instruments and techniques to monitor air quality and continually conducts research for improving monitoring capabilities not only in the USA, but worldwide too. Listed below are U.S. EPA technologies currently in development or undergoing field testing.

- i. **Black carbon samplers** (status: in development) - low cost, low power, high-time resolution samplers that provide continuous monitoring of black carbon in various environments.
- ii. **Fence samplers** (status: field testing) - low cost, solar-powered air sampling device (called S-pod) that is mounted to a fence or perimeter boundary and provides real-time data on VOCs (such as benzene). Because the device is solar-powered it can be utilised in areas that have limited or complete absence of electrical infrastructure.
- iii. **Mobile air measurements** (status: field testing) - geospatial measurement of air pollution using mobile sensor technology to quantify source emissions and trends near harbours, industrial facilities, railways and roadways using Google street view vehicles that will provide insight into air quality at ground level.
- iv. **Wildfire system** (status: field testing) - quantification of emissions from wildfires and open area burns using an instrument (called Aerostat). A helium-filled balloon is used to lift the Aerostat into the smoke plumes where it is capable of quantifying many gaseous and particulate pollutants including CO, CO<sub>2</sub>, black carbon, elemental and organic carbon and VOCs to name only a few (U.S. EPA, 2017).

2.7 Gap analysis



## **CHAPTER 3: METHODOLOGY**

This chapter is divided into two main sections, section 3.1 and section 3.2. Section 3.1 covers field work (how ambient APM was sampled) and section 3.2 describes the analytical methodologies used (how filter samples were analysed).

### 3.1 Field work

This section provides an overview of the field work (or sampling) phase of this study. Sampling site, times and intervals, procedures, equipment and materials, and sampling methodologies used are presented in this section.

#### 3.1.1 Sampling site

Ambient PM<sub>2.5</sub> filter samples were collected in the residential suburb of Kraaifontein, Cape Town (27 km ENE of the city centre). The sampling site (coordinates: -33.8429, 18.7026) was located in the western outskirts of Kraaifontein. Kraaifontein had an urban background. The N1 freeway (a major traffic route in the area) and Buh-Rein Estate construction site were 0.6 and 2 km from the sampling site respectively. The campus of the University of the Western Cape (UWC), situated 12 km SSW of the sampling site, could not serve as the sampling site because of its close proximity to Cape Town International Airport (CTIA), Consol Glass and industria, all large emitters of PM in the area. Fig. 3.1 (page 57) is a map of the greater Cape Town area. Markers have been added to identify large sources of ambient APM within 40 km of the sampling site. Admittedly, there were thousands of ambient APM sources scattered across Cape Town but only large sources, those with a high likelihood of impacting ambient PM<sub>2.5</sub> mass concentrations, were identified. An aerial photograph of the sampling site is shown in Fig. 3.2 (page 58)



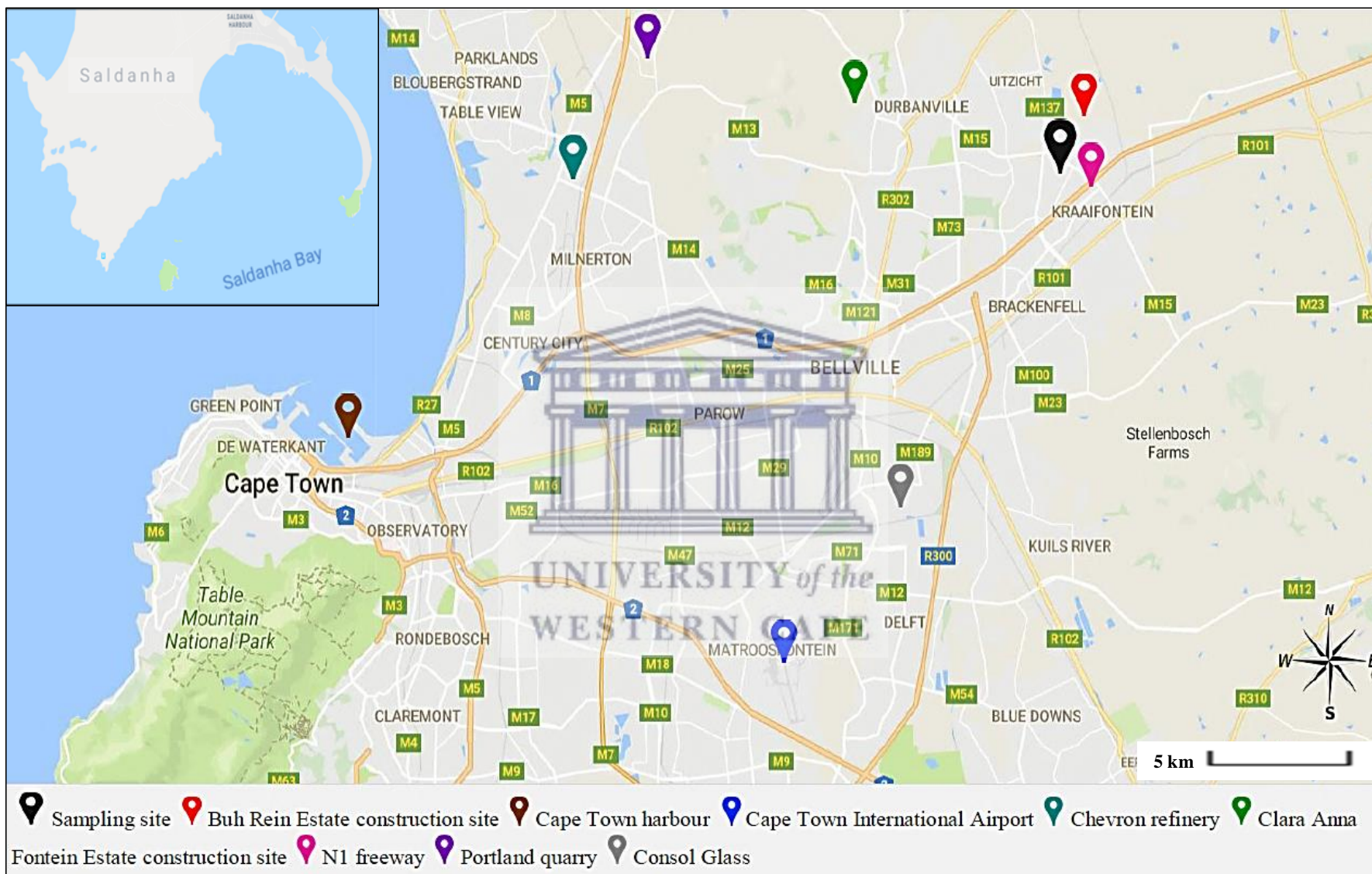


**Fig. 3.1:** Locations of local sources of ambient APM. The coastal town of Saldanha (top-left), 116 km NNW of the sampling site, was a probable source of LRT (Source: Google Maps).



**Fig. 3.2:** Location of the sampling site. The sampling site (yellow arrow) was on the roof of a dwelling in Kraaifontein, 3 m above ground level. An aerial photograph of the western parts of Kraaifontein (top-left) shows the proximity of the sampling site to the N1 freeway (pink marker) (Images: Google Maps).

### 3.1.2 Sampling period

Ambient PM<sub>2.5</sub> filter samples were collected for a period of 12 months from 18 April 2017 until 16 April 2018. Filters were exposed for 24 hours (09:00 a.m. to 09:00 a.m., UTC + 2 hours). Sampling and duplicate sampling intervals were three (3) and 15 days respectively. In all, sampling was performed over 121 days. Minor deviations from the initially proposed sampling dates were incurred because of human error (see Appendix 1A). In addition to the calendar samples, four composite (two weekdays and two weekend days) samples were collected over four consecutive weeks (09:00 a.m. to 09:00 a.m. at seven day intervals) during September 2017 and January 2018. Composites samples were analysed to determine the chemical compositions of PM collected.

### 3.1.3 Training and procedures

Air sampling training was provided by Dr. N. Claassens at the Air Quality Lab of the School of Health Systems and Public Health (SHSPH) in Pretoria on 11 April 2017. *GilAir-5 Air Sampling Systems Operation Manual* and *Ambient APM Sampling Instructions* were the two guides used for air sampling. The *Operation Manual* contained information on GilAir-5 maintenance, operation and troubleshooting, and would have served as a useful reference document in the event of sampler failure or inoperability. Fortunately, no technical issues were encountered for the duration of this study. *Ambient APM Sampling Instructions* was a step-by-step procedure containing information required to perform ambient APM sampling in a safe and consistent manner. It was used regularly during the field work phase of this study.

### 3.1.4 Sampling equipment and materials

No fewer than 13 individual items were used in this study. To assure accurate PM<sub>2.5</sub> measurements, equipment was thoroughly inspected for defects before field deployment. Only equipment and materials from reputable manufacturers were used. Equipment and

materials shown listed in Table 3.1.

**Table 3.1:** Sampling equipment and materials

Item	Type	Manufacturer	Part number
Air sampling cassette	Polystyrene (37 mm)	Casella	P101026
Cassette tubing adapter	Polystyrene (6.4 mm)	Zefon International	ZA0005
Connecting tube	Tygon	SKC Ltd.	225-1346
Cyclone	Aluminium	Sensidyne	GK 2.69
Filters (with PP supports)	PTFE	Zefon International	FPTPT237
Insulation tape	Light duty	Nitto Denko Corp.	No.21 series
Personal air samplers	GilAir-5	Sensidyne	800883-171
Petri slide	Polystyrene (51 mm)	Merck Millipore	Z355445
Primary calibrator	Gilibrator-2	Sensidyne	850190-1
Sampling station	Polystyrene	-	-
Screwdriver	Flat	-	-
Secondary calibrator	Air flow meter	Brooks Instrument	2500 series
Surgical gloves	Latex (powder free)	Supernax Healthcare Limited	-
Tweezers	Flat-nosed	-	-

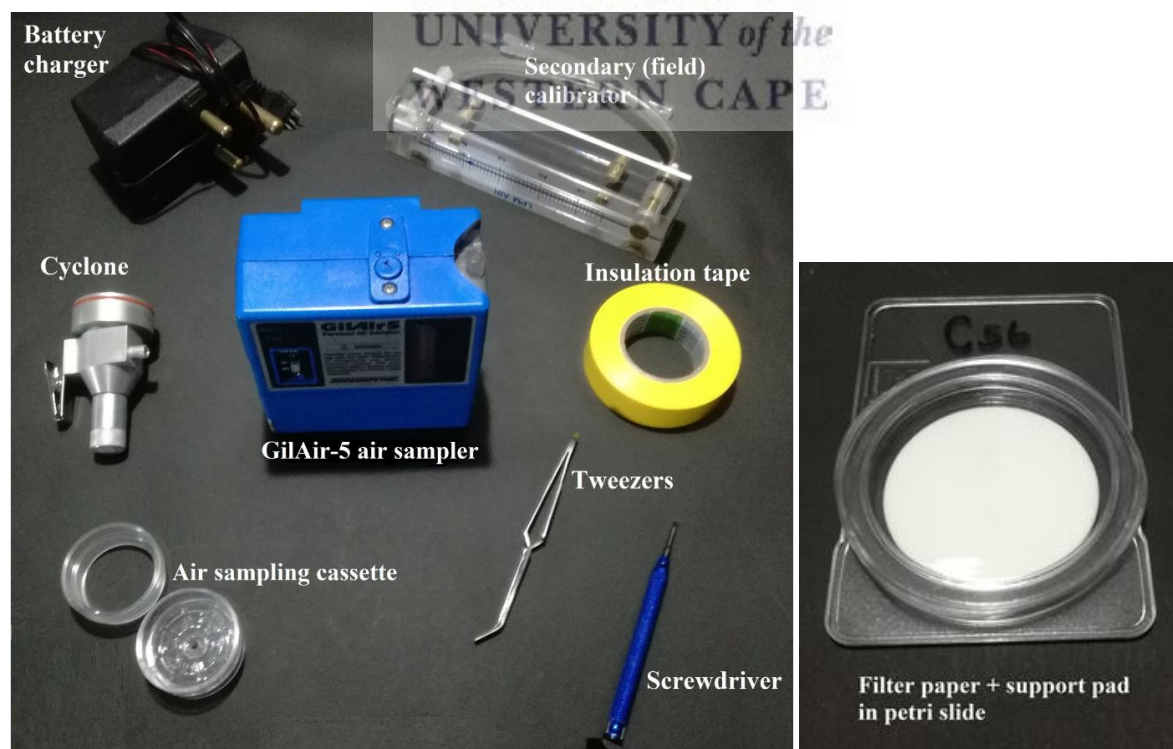


**Fig. 3.3:** Sampling equipment and materials (Images: own).

#### 3.1.4.1 Sampling station

Before sampling activities could commence, a suitable container was required to serve as a sampling station. The container had to be durable (protection from the elements), lightweight (easy to handle) and waterproof but still allow for sufficient air flow into its interior to cool the air samplers and chargers within. A repurposed polystyrene container (Fig. 3.4) was chosen as it met all the requirements.



*Fig. 3.4: Sampling station at the sampling site (Images: own).*

To assure equipment protection and uninterrupted sampling during field deployment, minor modifications were made. First, air holes were punched into its walls that allowed for sufficient air flow into the container. Air holes meant that the station was no longer completely waterproof. To prevent the little water that had entered from causing any damage, electrical equipment was placed on and wrapped in plastic bags. This intervention was successful. Then, two lids (salvaged from disposed ice-cream containers) were fastened to the top cover. These lids prevented rain water from entering the cyclones during sampling, mitigating filter and pump damage. Finally, instead of anchoring it to the roof of the dwelling, the station was weighted down with bricks as fall protection from the notoriously strong gusts in Cape Town. Unlike fixed monitoring stations, this station was mobile and could be orientated and positioned as per user requirements.

#### 3.1.4.2 Collection medium

Zefon International 37 mm (2 µm pore size) PTFE membrane filters (part number: FPTPT237, lot: 45849) were used as collection media in this study. These filters were durable and chemical-resistant making them a good choice for ambient APM sampling. PTFE filters were the preferred choice for several ambient APM studies [Vallius et al. (2000); Davy et al. (2017); Molnár et al. (2017)].

#### 3.1.4.3 Air samplers

Two GilAir-5 personal air samplers were used in this study. Manufactured by Sensidyne, the GilAir-5 (part number: 800883-171) had a flow range of 0.1-5 L.min<sup>-1</sup> and was powered by a built-in nickel-cadmium battery or DC input. Studies conducted by v. Roosbroeck et al (2006) and Molnár et al. (2017), used pumps similar to the GilAir-5 for ambient air monitoring. The samplers were given primary and secondary (duplicate) designations that were changed continually (once every seven weeks) to reduce mechanical wear-and-tear thus prolonging pump life. A feature of the GilAir-5 air sampler was “automatic constant flow” that assured air flow was maintained within 5 % of a set point. Maximum discrepancy between the initial set point and post-sampling air flows was ± 0.1 L.min<sup>-1</sup> (deviation of ± 2.5 %). Great care was taken during the handling and storage of these samplers.

#### 3.1.4.4 Air flow calibrators

Primary air flow calibrators are NIST-certified devices used to check the accuracy and performance of air sampling equipment (NIOSH, 1973). The device used in this study was the Gilian Gilibrator-2. The Gilibrator-2 (part number: 850190-1) was Sensidyne’s flagship primary air flow calibrator with an air flow range of 1-30,000 mL.min<sup>-1</sup>. Secondary (or field) calibrators are devices whose calibrations are traceable to a primary calibrator. Secondary calibrators can maintain their accuracy for extended periods of time (up to one year) with safe

handling and care (NIOSH, 1973). The device used (Brooks Instrument, 2500 series), was calibrated on 11 April 2017. A discrepancy, between the measured and true air flows, was observed during induction. Measured air flow was 5 % lower than true air flow. This discrepancy was eliminated with normalisation during final sample volume calculations (see section 4.1).

#### 3.1.4.5 Miscellaneous items

Other equipment used for sampling was:

- Air sampling cassettes
- Cassette tubing adapters
- Connecting tubes
- Cyclones
- Flat-nosed tweezers
- Flat screwdriver
- GilAir-5 battery charger
- Insulation tape
- Multi-plug (optional)
- Permanent marker
- Petri slides
- Power cord (optional)

#### 3.1.5 Sampling technique

The technique chosen for ambient PM<sub>2.5</sub> measurements was well documented and easy to setup. v. Roosbroeck et al. (2006) and Molnár et al. (2017) used similar approaches in their respective studies. Ambient air sampling was performed in accordance with *Ambient APM Sampling Instructions* (Appendix 2). The process began with checks of overall equipment condition, operability and performance. In addition, initial set point air flow rates and meteorological parameters were captured. To assure uninterrupted sampling, DC input was preferred to battery operation. Sampler operation created suction that drew in air from the environment. As ambient air entered the cyclone assembly, it permeated the filter. Particulate sizes > 2 µm in diameter were unable to permeate the filter and were caught. Larger, heavier particulates (aerodynamic diameters > 2.5 µm) and debris ended up in the grit trap preventing unwanted sample contamination. Fig. 3.5 (page 64) shows the inner workings of the cyclone

assembly during sampling. Filters were exposed for 24 hours at  $4.0 \text{ L}\cdot\text{min}^{-1}$ . When 24 hours had elapsed, filter samples were retrieved and post-sampling air flow rates captured. Filter samples were returned to their petri slides and refrigerated to prevent any unwanted loss of PM. The air sampling cassettes, connecting tubes and cyclones were all thoroughly cleaned with a fine-bristled brush and anti-static cloth (this process was performed before and after sampling activities). One filter sample (C40, collected on July 23, 2017) was discarded due to equipment failure (loss of vacuum due to cracked fitting). In all, 146 samples (including 25 duplicate samples) were collected.

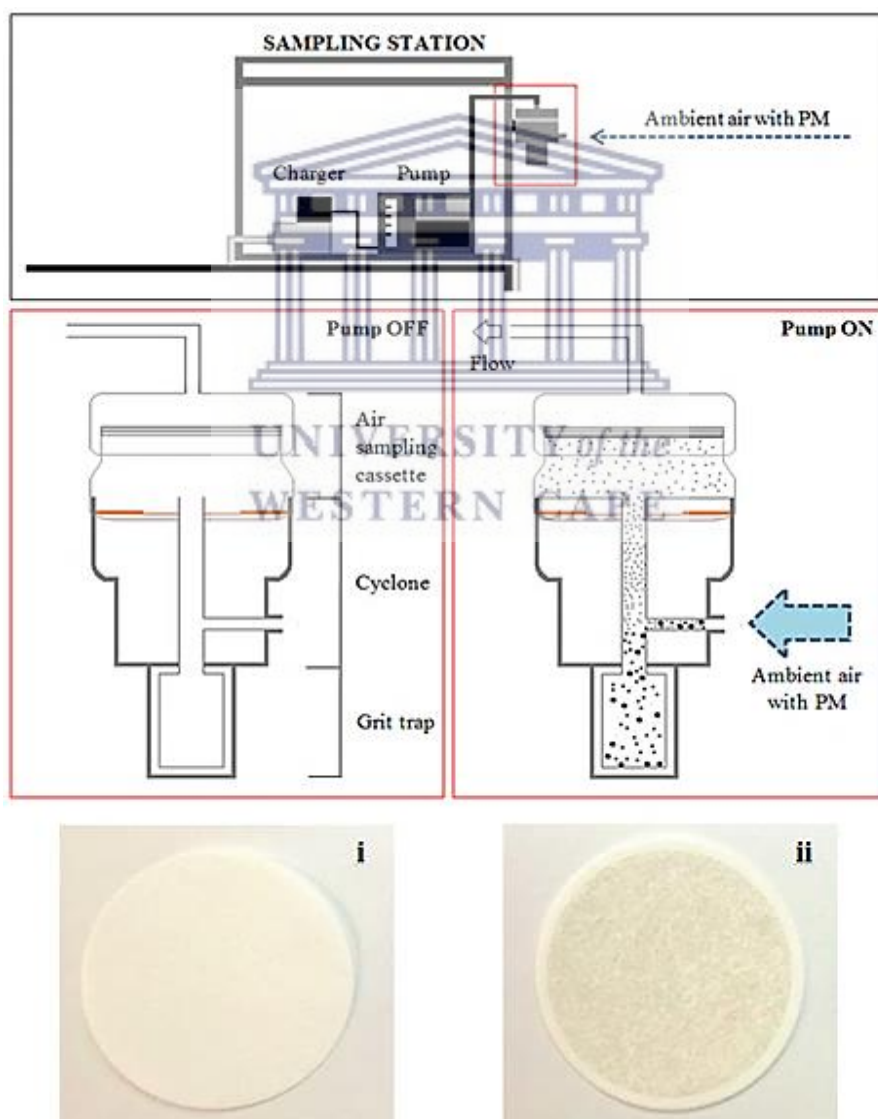


**Fig. 3.5:** Schematic representations of the sampling station and cyclone assembly with filters before (i) and after (ii) exposure to ambient air (Images: own).



## 3.2 Analysis of filter samples

This section provides an overview of the laboratory (or analysis) phase of this study. Chronology of analyses, methods and techniques used, and analytical methodology are presented in this section. Note: Powder free latex surgical gloves were used at all times for all sampling and laboratory activities.

### 3.2.1 Chronological information

Analyses were performed over a period of 16 months (from April 2017 until July 2018). The chronology of analyses is shown in Appendix 3.

### 3.2.2 Methods and techniques

Pre- and post-sampling filters were collected by co-supervisor or lab assistant (in batches of 20 filters) for gravimetric and smoke stain reflectometry (SSR) analyses. Gravimetric and SSR analyses were mostly conducted by a trained lab assistants at the SHSPH. Inductively coupled plasma-optical emission spectrometry (ICP-OES), ion chromatography (IC), scanning and transmission electron microscopy (SEM/TEM), selected area electron diffraction (SAED) and electron dispersive x-ray spectroscopy (EDS) were conducted at the University of the Western Cape (UWC) by myself and trained operators and lab assistants.

#### 3.2.2.1 Gravimetric analysis

Gravimetric analysis is an analytical technique used to determine analyte mass by measuring a change in mass. Analyte mass ( $m$ ) is expressed as:

$$m = m_f - m_i - m_r \quad (10)$$

Where  $m_i$  is the mean pre-sampling filter mass ( $\mu\text{g}$ ),  $m_f$  is the mean sample filter mass ( $\mu\text{g}$ ) and  $m_r$  is the mean mass change ( $\mu\text{g}$ ) of the reference (or control) filters at the start and end of each measurement session.

### 3.2.2.1.1 Equipment and materials

Filter samples were weighed with a Mettler-Toledo XP6 Ultra-microbalance (Fig. 3.6). The XP6 has readability and repeatability of 1 and 0.6  $\mu\text{g}$  (at 0.2 g) and was calibrated by an authorised technician on a six-monthly basis. An ioniser (c) was used to eliminate the effects of electrostatic charges on mass measurements. In addition to the balance, a flat-nosed tweezers, latex surgical gloves and data logbook were also used.



**Fig. 3.6:** Mettler-Toledo XP6 Ultra-Microbalance. The XP6 (left) has three main components - the control unit (a), weighing chamber (b) and AC adaptor (d). Pre- and post-sampling filters were conditioned for 24 hours before being weighed (right) (Images: own).

### 3.2.2.1.2 Conditioning of filters

Before filters were weighed they underwent conditioning (or normalisation). A clean carton box with spine base was used for this purpose. The box was carefully sealed and placed in a clean, climate-controlled laboratory (Temperature: 20.1-22.0  $^{\circ}\text{C}$ , Rh: 43-54 %, barometric pressure: 101-103 kPa) where filters (in batches of 20-30) were allowed to condition for a period of 24 hours, before and after exposure to ambient air.

### 3.2.2.1.3 Laboratory conditions

Gravimetric analyses were performed in a climate-controlled laboratory using working procedure *Mettler-Toledo ultra-microbalance weighing procedure* (Appendix 4) and *Weighing of Teflon Filters to determine Particle Mass Concentrations* [SOP 3.0 (2009)]. According to the former, laboratory temperature of  $21 \pm 1.0$  °C and Rh of  $50 \pm 5$  % were recommended for the weighing of filters. Laboratory conditions are shown in Fig. 3.7.

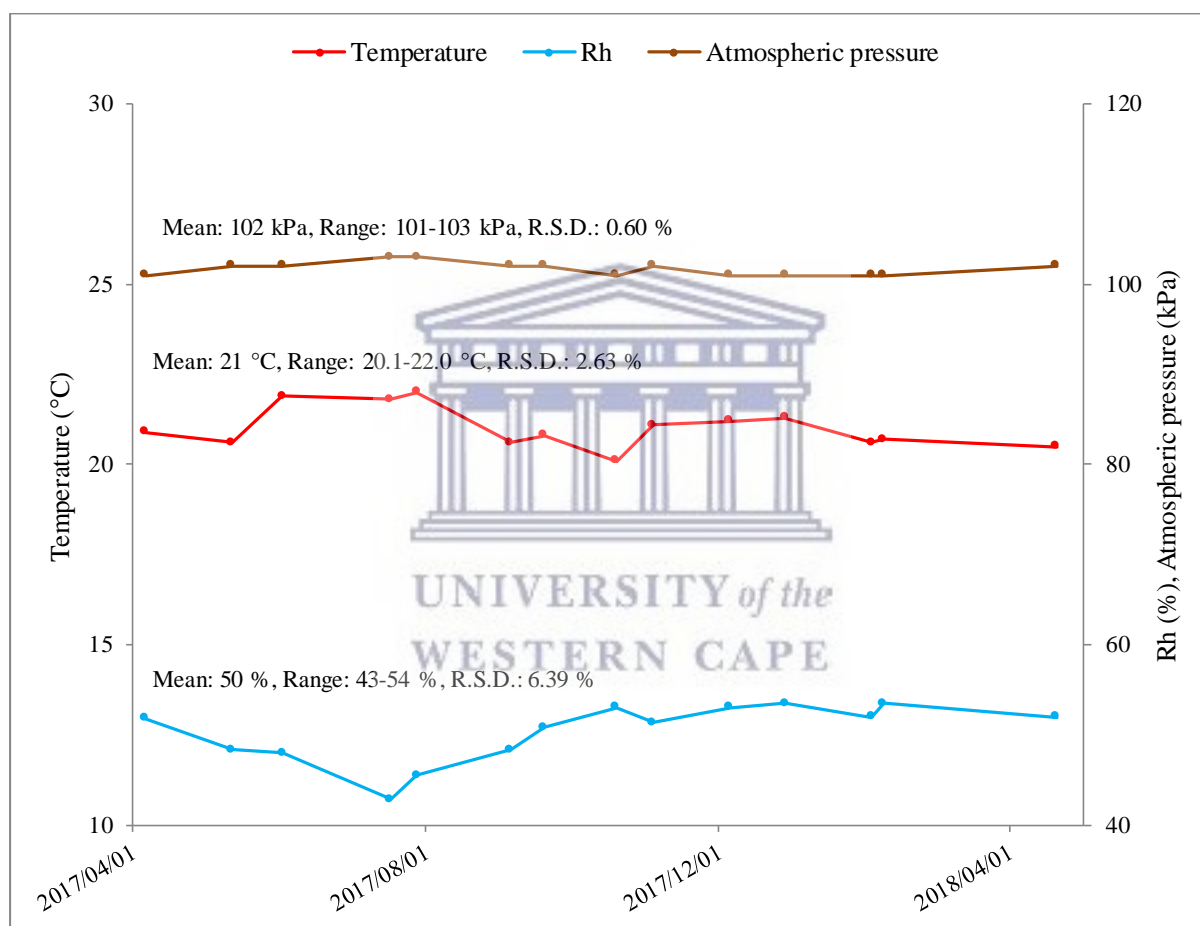


**Fig. 3.7:** Laboratory conditions (R.S.D. is relative standard deviation).

### 3.2.2.1.4 Weighing of filters

A flat-nosed tweezers was used at all times when handling filters. At the start and end of each weighing session, quality control checks were performed. If the checks were unsatisfactory, action was required before continuing. Additionally, control filters were checked at intervals of 10 consecutive filter measurements and at the end of each session. If the mean mass of

control filters had deviated by  $\pm 15 \mu\text{g}$ , or the percentage difference between minimum/maximum filter mass and mean mass was  $> 0.001 \%$ , the masses of the 10 filters that preceded that check was nullified and measurements repeated. Filters were weighed individually with measurements performed in triplicate (repeated three times). Samples were handled at the unexposed outer ring (Fig. 3.8) while avoiding contact with the exposed area.



**Fig. 3.8:** Handling of filters. Samples were handled at the unexposed outer ring (Image: own).

The final step was to recheck the control filters. The mean mass change ( $m_r$ ) was deducted from sample filters masses measured during that corresponding session. Mean and standard deviation values were calculated. If standard deviation was  $\geq 3 \mu\text{g}$ , readings were nullified and the individual filters reweighed. If a standard deviation of  $\geq 3 \mu\text{g}$  persisted, the entire process, starting with the control filter check, was repeated.

### 3.2.2.2 Smoke stain reflectometry

Smoke stain reflectometry (SSR) is an analytical technique used to determine the absorption coefficient (proxy for soot concentration) of a sample by measuring the intensity of light reflected from its surface. Reflectance (R) is expressed as:

$$R = \ln \left( \frac{R_0}{R_s} \right) \quad (11)$$

Where  $R_0$  is the amount of light reflected from the surface of a blank filter (%) and  $R_s$  is the amount of light reflected from the surface of the sample filter (%). Absorption coefficient (a) is expressed as:

$$a = \left( \frac{A}{2V} \right) \times R \quad (12)$$

Where  $A$  is the area of exposed filter ( $m^2$ ),  $V$  is the volume of air sampled ( $m^3$ ) and  $R$  is reflectance.

### 3.2.2.2.1 Equipment and materials

A Diffusion Systems Ltd. EEL model 43D Smoke Stain Reflectometer (Fig. 3.9) was used to determine the reflectance of filter samples. The model 43 D is a reference instrument indicated by the European Directive 80/799/EEC for the measurement of smoke stain reflectance. In addition to the reflectometer, cleaning equipment, a flat-nosed tweezers, latex surgical gloves, grey and white standard plate and a mask were also used.



**Fig. 3.9:** Diffusion Systems Ltd. EEL model 43D Smoke Stain Reflectometer. The model 43D has two main components – a measuring head (a) and control unit (b) (Image: own).

### 3.2.2.2.2 Reflection measurements

Reflectometric analyses were performed using *Determination of Absorption Coefficients using Reflectometric Method* (Appendix 5). SOP 4.0 (2002) was compiled under the guidelines of international standard ISO 9835 of 1993. The first step was to prepare the reflectometer for analysis. The measuring head, mask and grey/white standard plate were cleaned and the instrument adjusted for maximum sensitivity with the standard plate. A selenium disc, at the base of the measuring head, was highly photo-sensitive so extra care was taken when manoeuvring this component. The effects of light were eliminated by working in low-light conditions. Filters were handled with a flat-nosed tweezers at all times while avoiding contact with the exposed area to prevent contamination or PM loss. Measurements were performed in quintuplicate (repeated five times) using a five-point configuration (Fig. 3.11).

Before filters were analysed a primary control filter was selected from three unexposed blank filters (this filter would be used as the control filter for all subsequent sessions that followed). With this filter, fine adjustments were made so that the reading was as close to 100.0 as possible. Sample measurements followed. It was an instruction of the procedure to recheck

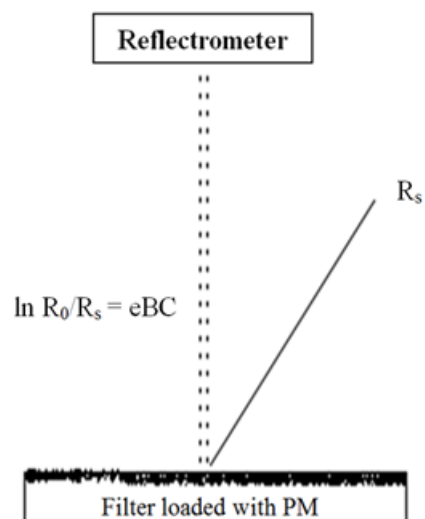


**Fig. 3.10:** Principle of reflectometry. Reflectance is indirectly proportional to soot content on the filter surface (Source: Davy et al., 2017).

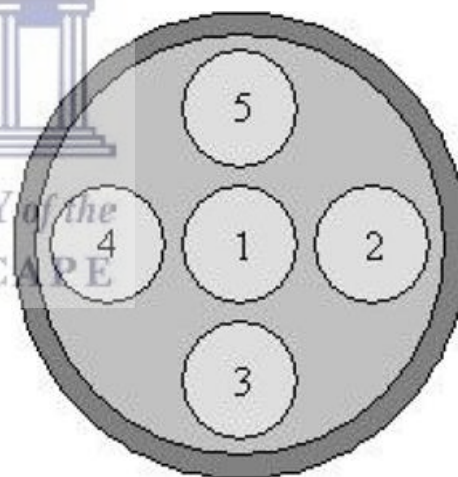


**Fig. 3.11:** Areas (1-5) where the light beam should approximately strike during reflectance measurements (Source: SOP 4.0, 2009).

the control filter after 20 consecutive sample measurements and again at the end of the session. If the control filter deviated by 3 % or more from its original value, results of the 20 filters that preceded that check were nullified and measurements repeated. If standard deviation was  $\geq 3$  %, results were nullified and the individual filters rechecked. If a standard deviation of  $\geq 3$  % persisted, the entire analysis process, starting with reflectometer adjustments, was repeated. It was a requirement to check 10 % of samples analysed during the session as a secondary check. The same acceptance criteria applicable to the control filter had applied. Soot concentration (eBC) was calculated using equation 19 (Davy et al., 2017).

$$\text{eBC } (\mu\text{g. m}^{-3}) = \frac{A \times 10^6}{2 \times V \times \sigma_{\text{ATN}}} \times \ln\left(\frac{R_0}{R_s}\right) \times [1 + k \times \ln\left(\frac{R_0}{R_s}\right)] \quad (13)$$

Where  $A$  is the area of exposed filter ( $8.55 \times 10^{-4} \text{ m}^2$ ),  $V$  is volume of ambient air sampled ( $\text{m}^3$ ),  $\sigma_{\text{ATN}}$  is black carbon extinction coefficient ( $19.5 \text{ m}^2 \cdot \text{g}^{-1}$  for PTFE filters),  $k$  is the loading correction factor (0.3 for PTFE filters) and  $R$  is reflectance.

### 3.2.2.3 Inductively coupled plasma-optical emission spectrometry

Inductively coupled plasma-optical emission spectrometry (ICP-OES) is an analytical technique used to determine the concentrations of elements in samples by measuring light emitted by analyte atoms when returning to a lower energy state (Hitachi Tech., 2017).

#### 3.2.2.3.1 Equipment and materials

A Varian 710-ES inductively coupled plasma-optical emission spectrometer (Fig. 3.12, page 72) was used to determine the concentrations of select elements in composite samples. The 710-ES has a wavelength range of 177-785 nm and low detection limits ( $1 \mu\text{g} \cdot \text{L}^{-1}$ ). In addition to the spectrometer, beakers (100 mL), volumetric flasks (100 and 250 mL), micropipettes (1,000 and 5,000  $\mu\text{L}$ ), centrifuge tubes (15 mL), a flat-nosed tweezers, hotplate, latex surgical gloves, a scalpel and various reagents were also used.

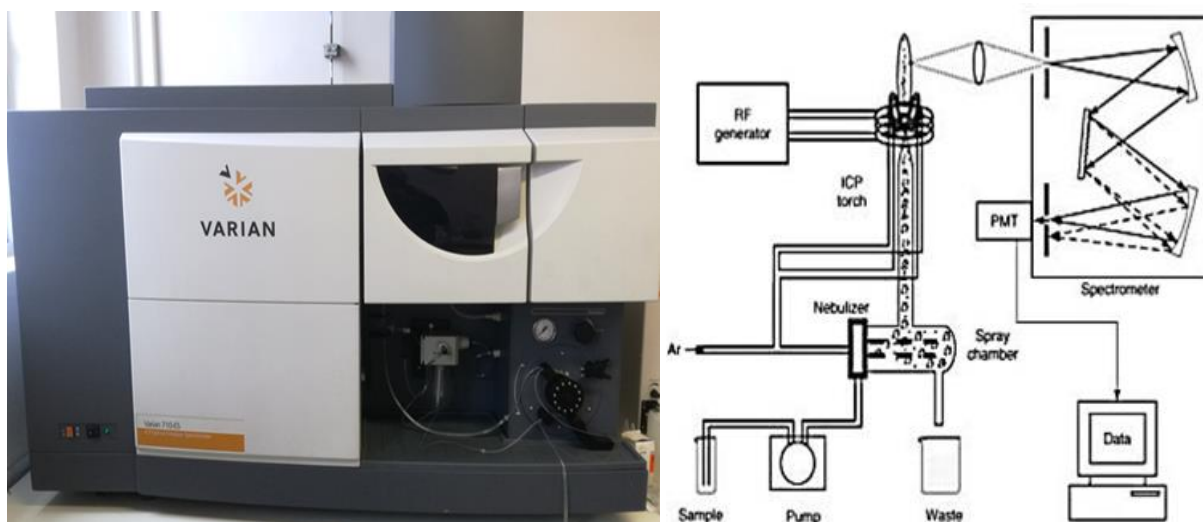


**Fig. 3.12:** Varian 710-ES Inductively Coupled Plasma-Optical Emission Spectrometer (left) and schematic representation of the sample analysis process (right) [Images: own (left) and [slideshare.net/firdousasma/ipc-632379381466407594](http://slideshare.net/firdousasma/ipc-632379381466407594) (right)]

### 3.2.2.3.2 Cleaning of glassware

Standard and control solutions were prepared in 100 mL volumetric flasks. Volumetric flasks were cleaned by rinsing three times with Milli-Q water. Elemental extraction was performed in 100 mL beakers. Five beakers were cleaned with a dilute solution of nitric acid ( $\text{HNO}_3$ , 5 wt. %). 250 mL of the  $\text{HNO}_3$  solution was prepared by transferring 90-100 mL of Milli-Q water to a clean 250 mL volumetric flask then adding 14 mL of 69%  $\text{HNO}_3$  (Merck Millipore, part number: 1018322500, lot: 1041704) before making up to the mark with Milli-Q water. 40-50 mL of the acid solution was added to the beakers and boiled for 10 minutes on a hotplate. After 10 minutes, the beakers were removed and allowed to cool to ambient temperature. Once cooled, the residual acid solutions were discarded and beakers rinsed three times with Milli-Q water.

### 3.2.2.3.3 Working standards and control preparation

Three working standards and a control (or check standard) were prepared using Custom multi-element standard solution 1586 (part number: VHG-ZLGC-1586-500), 1000  $\text{mg.L}^{-1}$  sodium ( $\text{Na}^+$ ) standard (part number: VHG-INAW1K-500) and 1000  $\text{mg.L}^{-1}$  calcium ( $\text{Ca}^{2+}$ )



standard (part number: VHG-ICAW1K-500) manufactured by VHG Labs. Standard solution 1586 contained 24 elements in a 5 wt. % HNO<sub>3</sub>/0.2 wt. % hydrofluoric acid (HF) matrix. Metal concentrations in the standard solution are shown in Table 3.2.

**Table 3.2:** Composition of VHG Labs multi-element standard solution 1586

Element	Concentration (mg.L <sup>-1</sup> )	Element	Concentration (mg.L <sup>-1</sup> )	Element	Concentration (mg.L <sup>-1</sup> )
Al	100	Cu	100	P	100
As	100	Fe	100	K	1000
Ba	100	Pb	100	Si	100
Be	100	Li	100	Sr	100
B	100	Mg	100	Ti	100
Cd	100	Mn	100	V	100
Cr	100	Mo	100	Zn	100
Co	100	Ni	100		

Working standards were prepared by pipetting 2.0, 5.0 and 10 mL of standard solution 1586 (lot: 10059633-1), 1.0, 2.5 and 5.0 mL of 1000 mg.L<sup>-1</sup> Ca<sup>2+</sup> (lot: 73924) and 1.0, 2.5 and 5.0 mL of Na<sup>+</sup> (lot: 30701264) standards into three 100 mL volumetric flasks, and making up to the mark with Milli-Q water. A control solution was prepared by pipetting 2.0 mL of standard solution 1586 (lot: 10059633-2) and 1.0 mL of the 1000 mg.L<sup>-1</sup> Ca<sup>2+</sup> (lot: 73925) and Na<sup>+</sup> (lot: 30701265) into a fourth 100 mL volumetric flask, and making up to the mark with Milli-Q water. Solution preservation was not performed because analysis was carried out immediately.

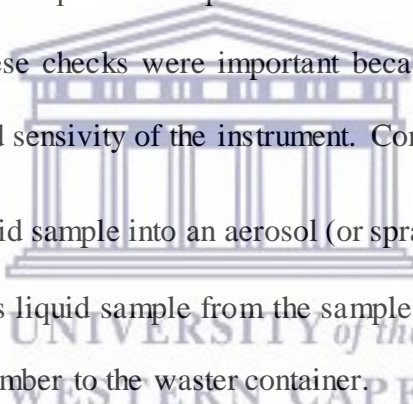
#### 3.2.2.3.4 Sample preparation

Hot acid extraction using a mixture of dilute nitric acid and hydrochloric acid (or aqua regia) (3 wt. % HNO<sub>3</sub>/8 wt. % HCl) as per EPA Compendium Method IO-3.1 (1999) was used to extract metals from samples. 100 mL of aqua regia was prepared by transferring 40-50 mL of Milli-Q water to a clean 100 mL volumetric flask then adding 3.5 mL of 69% HNO<sub>3</sub> and 22

mL of 32 % HCl (Kimix, part number: n/a, lot: NO6244980) before making up to the mark with Milli-Q water. Four composite samples and blank filter were cut into two halves with a scalpel. One half of each sample was placed exposed side face-down into four separate beakers containing 15 mL of aqua regia (blank was placed in a fifth beaker). The beakers were covered with watch glasses and acid solutions refluxed for 15 minutes (at 120-130 °C) using a hotplate. After 15 minutes, the beakers were removed and allowed to cool to ambient temperature. Once cooled, 10 mL of each solution was decanted into five 15 mL centrifuge tubes. Sample preservation was not performed because samples were analysed immediately.

#### 3.2.2.3.5 Pre-analysis checks

Pre-analysis checks were done on specific components to ensure that they were clean and ‘fit-for-use’ prior to analysis. These checks were important because of the number of samples analysed on a weekly basis and sensitivity of the instrument. Components inspected were:

- 
- Nebuliser - converts liquid sample into an aerosol (or spray).
  - Peristaltic pump - pumps liquid sample from the sample container to the nebuliser and waste from the spray chamber to the waste container.
  - Radio frequency (RF) coil - transmits radio frequencies (RF generator) to ignite the plasma.
  - Sample cone - directs ion beam from torch to the orifice of skimmer cone whilst deflecting larger liquid droplets and debris.
  - Skimmer cone - directs ion beam to the photomultiplier and any droplets or debris that has entered through the orifice of the sample cone.
  - Torch - uses a plasma to desolvate and ionise analyte atoms.
  - Spray chamber - condenses large liquid droplets (sent to waste container) and allows only fine spray to enter the torch.

- Tygon tubing - flexible tubing used to carry liquid samples and waste throughout the system. Ensure that tubing is properly connected to the pump before proceeding. If flow is reversed, waste will enter the spray chamber causing it to fill. If filling continues, liquid will flow into the torch and extinguish the plasma.

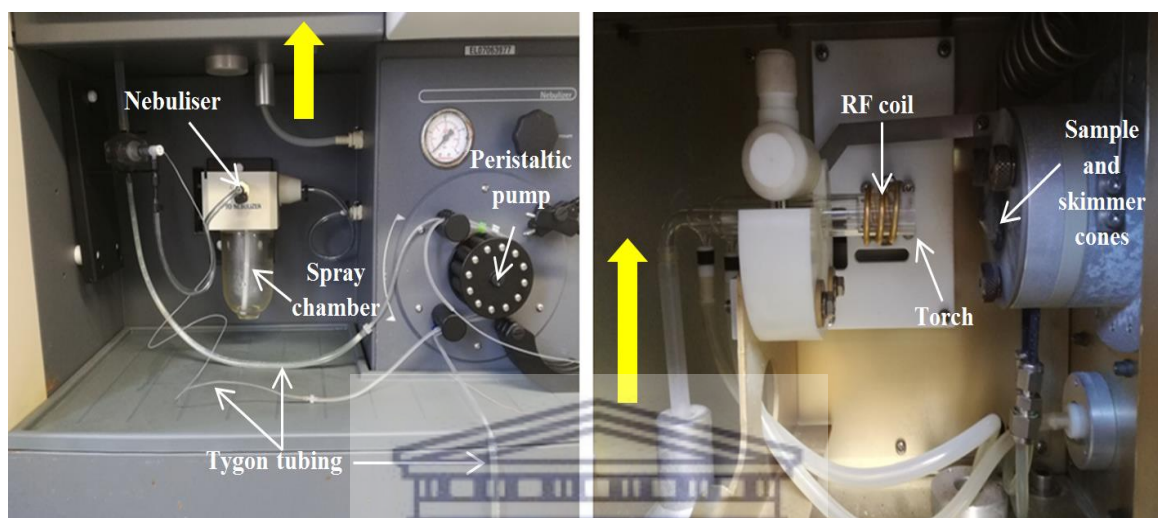


**Fig. 3.13:** Components inspected during pre-analysis checks of the 710-ES. Additionally, Ar pressure, connectors, fittings and waste container level were also checked (Images: own).

#### 3.2.2.3.6 Analysis

Instrument operations were performed in accordance with procedure *Elemental analysis using the Varian 710-ES Inductively Coupled-Plasma Optical Emission Spectrometer* (compiled by the ENS group) using ICP Expert II software. Three optimisation steps were carried out during instrument setup: torch alignment, drift and select wavelength ( $\lambda$ ) intensity calibrations. Torch alignment was done using a  $5.0 \text{ mg.L}^{-1}$  Mn solution. The intensity was  $> 300,000$  counts (expected). Instrument drift was checked with Milli-Q water and was acceptable (if the drift fluctuates, check the torch). Finally, selective  $\lambda$  intensity calibration was done using the  $5.0 \text{ mg.L}^{-1}$  working standard solution (if intensities are too low, calibration will abort. Check gas supply and repeat). When setup was complete, the instrument was standardised. The operating conditions of the spectrometer are shown in Table 3.3 (page 76).

**Table 3.3:** 710-ES operating conditions

Condition	Unit	Value
Ar pressure	kPa	550 ( $\pm$ 50)
RF power	kW	1.2
Nebuliser pressure	kPa	200
Plasma gas flow rate	L.min <sup>-1</sup>	15
Auxillary gas flow rate	L.min <sup>-1</sup>	1.2
Pump speed	rpm	6
Replicate read time	s	5
Sample delay time	s	45
Stabilisation time	s	15
Rinse time	s	30

Working standards, control and samples were analysed in triplicate without background correction. The sample introduction needle was rinsed with dilute HNO<sub>3</sub> (2 wt. %) and Milli-Q water between acquisitions to prevent cross-contamination between samples. Linear and quadratic standardisation equations were used when the concentration of the highest standard was  $\leq 10$  mg.L<sup>-1</sup> and  $> 10$  mg.L<sup>-1</sup> respectively (see Table 3.4). Standard deviation  $< 3$  % was considered acceptable (if  $\geq 3$  %, results were nullified and samples rechecked).

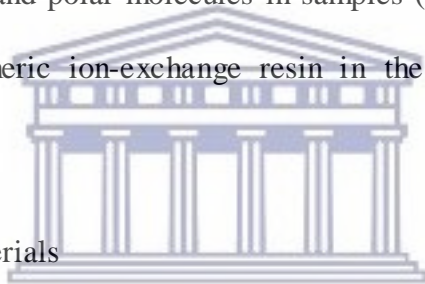
**Table 3.4:** Elements, emission wavelengths and standardisation equations

Element	Emission $\lambda$ (nm)	Standardisation equation	Element	Emission $\lambda$ (nm)	Standardisation equation
Al	394.4	Linear	Mg	280.3	Linear
As	193.7	Linear	Mn	257.6	Linear
Be	313.0	Linear	Mo	202.0	Linear
Cd	214.4	Linear	Ni	221.6	Linear
Ca	315.9	Quadratic	P	213.6	Linear
Cr	267.7	Linear	K	769.9	Quadratic
Co	238.9	Linear	Si	250.7	Linear
Cu	327.4	Linear	Na	568.3	Quadratic
Fe	238.2	Linear	Sr	407.8	Linear
Pb	220.4	Linear	Ti	336.1	Linear
Li	670.8	Linear	Zn	213.9	Linear

If the concentration of an element in the control (first check) deviated by 30 % or more from the expected value, sample analysis was aborted and standardisation repeated. If the problem persisted, the instrument was shut down and further actions taken. If the concentration of an element in the control (second check) deviated by 30 % or more, the result (of that particular element) was nullified and sequence repeated. The control values of all elements tested were within acceptable limits.

#### 3.2.2.4 Ion chromatography

High-performance liquid chromatography (HPLC) is an analytical technique used to determine the concentrations of ions in samples. Also known as ion chromatography (IC), this technique separates ions and polar molecules in samples (injected into an eluent) based on their affinities for polymeric ion-exchange resin in the separator column. (Thermo Scientific, 2017).



##### 3.2.2.4.1 Equipment and materials

A Dionex ICS-1600 ion chromatograph (Fig. 3.14, page 78) was used to determine the concentrations of select anions in composite samples. The ICS-1600 is designed for solid IC performance and ease-of-use with electrolytic suppression and front panel control. In addition to the chromatograph, beakers (100 mL), volumetric flasks (100 and 2,000 mL), watch glasses, micropipettes (1000 and 5000  $\mu$ L), centrifuge tubes (15 mL), a flat-nosed tweezers, hotplate, latex surgical gloves, a scalpel and various reagents were also used. Equipment used for preparatory activities were rinsed thoroughly with Milli-Q water to eliminate any possibility of chemical cross-contamination.

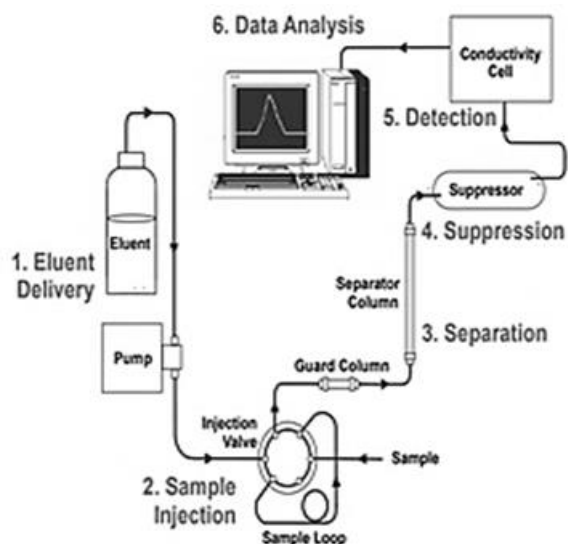
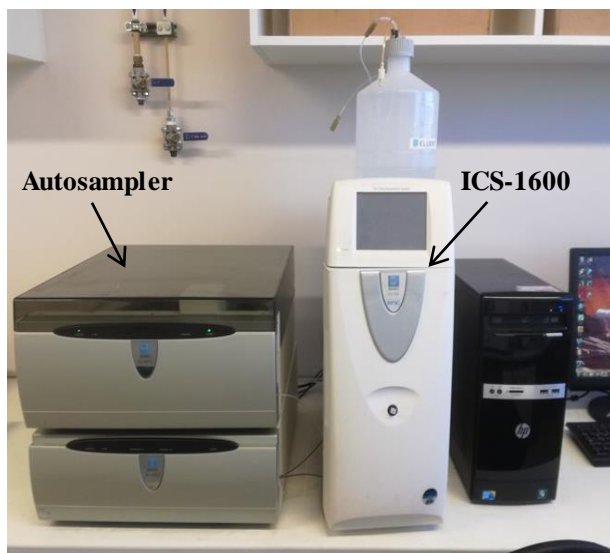


**Fig. 3.14:** Dionex ICS-1600 High-Performance Liquid Chromatograph (left) and schematic representation of the anion analysis process [Images: own (left) and Thermo Scientific (right)].

#### 3.2.2.4.2 Cleaning of glassware

Working standards, control and eluent solutions were prepared in volumetric flasks. Volumetric flasks were cleaned by rinsing three times with Milli-Q water. Extraction of anions from samples was performed in 100 mL beakers. Like the volumetric flasks, beakers were cleaned by rinsing with Milli-Q water three times. Milli-Q rinsing was preferred to chemical cleaning to prevent unwanted contamination. Dedicated glassware was used so there was no need for a chemical cleaning regime.

#### 3.2.2.4.3 Working standards and control preparation

Three working standards and a control were prepared using anion calibration standard 59 (part number: IV-STOCK-59) manufactured by Inorganic Ventures Incorporated. The calibration standard contained seven anion species in a water matrix. Anion concentrations in the calibration standard are shown in Table 3.5 (page 79).

**Table 3.5:** Composition of Inorganic Ventures anion calibration standard 59

Anion	Concentration (mg.L <sup>-1</sup> )	Anion	Concentration (mg.L <sup>-1</sup> )
Br <sup>-</sup>	1000	NO <sub>2</sub> <sup>-</sup>	1000
Cl <sup>-</sup>	1000	PO <sub>4</sub> <sup>3-</sup>	1000
F <sup>-</sup>	1000	SO <sub>4</sub> <sup>2-</sup>	1000
NO <sub>3</sub> <sup>-</sup>	1000		

2, 5 and 10 mg.L<sup>-1</sup> working standards were prepared by pipetting 0.2, 0.5 and 1 mL of calibration standard (lot: H2-MEB537138) into three dedicated 100 mL volumetric flasks, and making up to the mark with Milli-Q water. A 5 mg.L<sup>-1</sup> control was prepared by pipetting 0.5 mL of calibration standard (lot: H2-MEB537139) into a fourth 100 mL volumetric flask, and making up to the mark with Milli-Q water. Because standards and control solutions were prepared 10 minutes before analysis, preservation was not required.

#### 3.2.2.4.4 Sample preparation

Warm water extraction as proposed by D. Jenke (1983) was used to extract anions from samples. 1 cm<sup>2</sup> sub-samples were cut from the remaining halves of the four composite samples and blank filter (see section 3.2.2.3.4) with a scalpel. With flat-nosed tweezers, the sub-samples were placed into five separate 100 mL beakers containing 15 mL of Milli-Q water (pre-heated to 50-60 °C). Each beaker was covered with a watch glass. D. Jenke (1983) indicated that 15 minutes of sonicating was sufficient. Because of the unavailability of an ultrasonic bath, the heated solutions were agitated (by swirling) for 15 minutes whilst maintaining temperatures between 50-60 °C. After 15 minutes, the beakers were allowed to cool to ambient temperature. Once cooled, 10 mL of each solution was transferred to five separate 15 mL centrifuge tubes. Chemical preservation was not performed to prevent contaminant ingress, instead, samples were refrigerated overnight at 4-6 °C.

#### 3.2.2.4.5 Eluent preparation

2.0 L of sodium carbonate/sodium bicarbonate eluent (4.5 mM Na<sub>2</sub>CO<sub>3</sub>/1.4 mM NaHCO<sub>3</sub>) was prepared by pipetting 20 mL of Na<sub>2</sub>CO<sub>3</sub> (0.45 M)/NaHCO<sub>3</sub> (0.14 M) AS22 eluent concentrate (Thermo Scientific, part number: 063965, lot: 170512) into 700-800 mL of Milli-Q water and stirring well before making up to the mark in a 2.0 L volumetric flask.

#### 3.2.2.4.6 Pre-analysis checks

Tubing and connectors were checked for leaks before start-up. Once checks were completed, the instrument was primed. Priming is a process of manually expelling trapped gases that can alter the conductivity of an eluent thus impacting retention times. Once priming was completed, the priming valve was shut and the instrument started-up. It took approximately 30-45 minutes for the instrument to stabilise with a baseline conductivity of < 0.1 μS.cm<sup>-1</sup>.



**Fig. 3.15:** Components inspected during pre-analysis checks of the ICS-1600. Tubing, connectors (left) and eluent reservoir level (right) were checked (Images: own).

#### 3.2.2.4.7 Analysis

Instrument operations were performed in accordance with procedure *Anion analysis using the Dionex ICS-1600 Ion Chromatograph* (compiled by the ENS group) using Chromeleon software. The operating conditions of the chromatograph are shown in Table 3.6 (page 81).



**Table 3.6:** ICS-1600 operating conditions

Condition	Unit	Value
Pump pressure	kPa	13,700 ( $\pm$ 500)
Suppressor current	mA	50
Column heater temperature	$^{\circ}$ C	35
Eluent flow rate	mL.min <sup>-1</sup>	1.2
Sample volume	$\mu$ l	25
Sample run time	s	900
Rinse time	s	60

Samples were injected into the chromatograph by an autosampler (Dionex AS-DV). An Dionex AS22 separator column was installed. A Milli-Q water rinse step of the sample introduction, between acquisitions, prevented cross-contamination between samples. Linear standardisation equations were used (see Table 3.7). Standard deviation  $<$  3 % was considered acceptable (if  $\geq$  3 %, results were nullified and samples rechecked).

**Table 3.7:** Anions, retention times and standardisation equations

Anion	Retention time (minutes)	Standardisation equation	Anion	Retention time (minutes)	Standardisation equation
F <sup>-</sup>	2.38	Linear	NO <sub>3</sub> <sup>-</sup>	5.09	Linear
Cl <sup>-</sup>	3.30	Linear	PO <sub>4</sub> <sup>3-</sup>	6.93	Linear
NO <sub>2</sub> <sup>-</sup>	3.91	Linear	SO <sub>4</sub> <sup>2-</sup>	7.88	Linear
Br <sup>-</sup>	4.57	Linear			

The same acceptance criteria (applicable to ICP-OES) applied to IC. If the concentration of an anion in the control (first check) deviated by 30 % or more from the expected value, sample analysis was aborted and standardisation repeated. If the problem persisted, the instrument was shut down and further actions taken. If the concentration of an element in the control (second check) deviated by 30 % or more, the result (of that particular anion) was nullified and sequence repeated. The control values of all anions tested were within acceptable limits.

### 3.2.2.5 Scanning electron microscopy

Scanning electron microscopy (SEM) is a magnification technique that uses focused beams of electrons to obtain compositional, topographical and morphological information of samples (Zeiss International, 2017).

#### 3.2.2.5.1 Equipment and materials

A Zeiss Auriga 4527 field emission scanning electron microscope (Fig. 3.16) was used for microscopic and spectroscopic analyses. The Auriga 4527 uses Gemini objective, electrostatic and magnetic lenses to provide excellent high resolution images and a range of 20-500,000x normal magnification (Zeiss International, 2017). In addition to the electron microscope, a micropipette (100  $\mu$ L), adhesive carbon tabs (9 mm), centrifuge tubes (15 and 50 mL), flat-nosed and pointed tweezers, sputter coater, latex surgical gloves, ultrasonic bath, a scalpel and alcoholic reagents were also used.

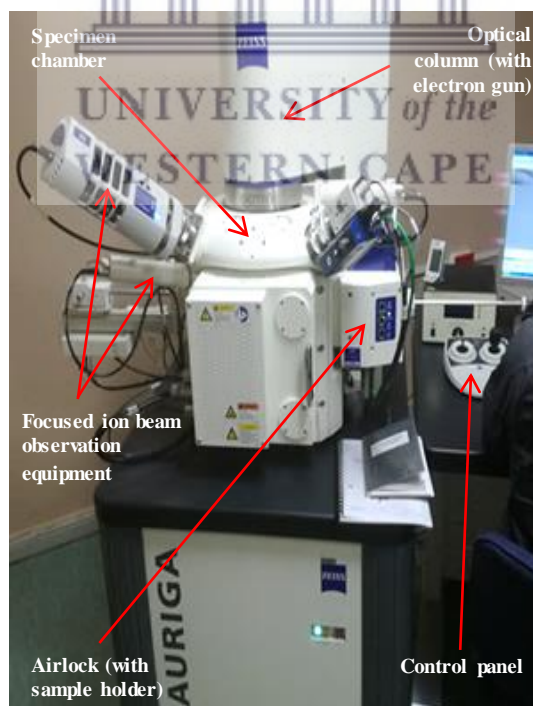


**Fig. 3.16:** Zeiss Auriga 4527 Scanning Electron Microscope (Image: own).

### 3.2.2.5.2 Sample preparation

Methanol ( $\text{CH}_3\text{OH}$ ) extraction proposed by Roper et al. (2015) was used to extract PM from filter samples. The extraction solvent used was nine parts 99.9 %  $\text{CH}_3\text{OH}$  (Sigma-Aldrich, part number: 34860, lot: SZBD315BV) and one part Milli-Q water (9:1, v/v). 50 mL of the solution was prepared by transferring 45 mL of  $\text{CH}_3\text{OH}$  to a 50 mL centrifuge tube and making up to the mark with Milli-Q water. 0.2-0.3  $\text{cm}^2$  sub-samples were cut from the four composite samples and blank filter using the remaining halves of each filter. With a flat-nosed tweezers, the sub-samples were transferred to five 15 mL centrifuge tubes (pre-rinsed with Milli-Q water) containing 5 mL of extraction solvent and labelled. Roper et al. (2015) indicated that two minutes of sonication was sufficient. Because of an appointment postponement by the Electron Microscopy Unit (EMU), extraction solutions stood for 10 days at ambient conditions before been imaged.

### 3.2.2.5.3 Stub preparation

Before samples were photomicrographed, they were prepared on stubs (Fig. 3.17). Prior to assembly, extraction solutions were sonicated for two minutes and the stub surfaces cleaned with absolute ethanol ( $\text{C}_2\text{H}_5\text{OH}$ ) (Merck Millipore, part number: 107017) to remove surface contaminants. A stub assembly consists of three parts: an adhesive carbon tab (Agar Scientific, part number: AGG3357N), a stub and a base. Each part was carefully handled with a pointed tweezers during preparation with extra caution taken not to touch the surface of the

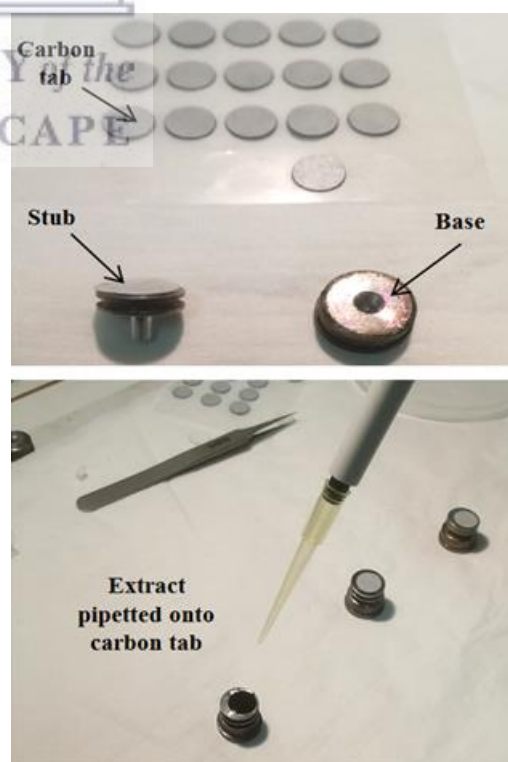


**Fig. 3.17:** Stub preparation for SEM photomicrography (Images: own).

carbon tab. Carbon tabs were used to hold specimens firmly in place and any contact to this area would have affected adhesion and also left impressions on the tab surface. A drop of each extraction solution was dropped onto four different carbon tabs. Stubs were then put under a heat lamp to dry. The final step of sample preparation was sputter coating. Sputter coating is a process used to coat specimens with a thin layer of conducting material (Au/Pd alloy was used). Electrons are negatively-charged hence the more negatively-conducting (i.e. positively-charged) the sample, the greater the image resolution (Zeiss International, 2017).

#### 3.2.2.5.4 Photomicrography

SEM photomicrography was performed in a climate-controlled laboratory (temperature: 22-23 °C, Rh: 47-48 %) using Zeiss Atlas-5 software. Photomicrographs of the stubs revealed a layer of PM deposited on the surfaces (i.e. solutions were saturated with particulates). Unfortunately, morphologies of fine particulates could not be studied so solutions were diluted with Milli-Q water and sent for TEM (see section 3.2.2.6). 0.1-0.2 cm<sup>2</sup> sub-samples were cut from the remaining halves of each composite sample and blank filter which provided an opportunity to capture photomicrographs of coagulated and agglomerate particulates. These particulates were large (2.5-100 µm) and because of their physical size they were easy to identify. Sub-samples were micrographed at various magnifications. The operating conditions of the microscope are shown in Table 3.8.

**Table 3.8:** Auriga 4527 operating conditions

Parameter	Unit	Value
Electron high tension (EHT)	kV	5.00
Signal	-	InLens
Working distance (WD)	mm	4.7
Magnification	-	10k-100k

### 3.2.2.6 Transmission electron microscopy

Transmission electron microscopy (TEM) is a magnification technique that transmits a focused beam of electrons through a specimen to form an image (Thermo Scientific, 2017). Unlike SEM that produces high-resolution 3D images of specimens, TEM only generates 2D images. TEM has a greater magnification range than SEM and is capable of producing photomicrographs down to the 2 nm range.

#### 3.2.2.6.1 Equipment and materials

An FEI Tecnai G<sup>2</sup> F20 field emission Scanning Transmission Electron Microscope (Fig. 3.18) was used for particulate morphology analysis. The G<sup>2</sup> F20 uses a 200 kV field emission gun and X-TWIN objective lens to provide excellent point and lattice resolutions (0.25 and 0.10 nm respectively) and a range of 25-930,000x normal magnification (FEI Company, 2007). In addition to the electron microscope, a micropipette (100  $\mu$ L), copper mesh grids (3 mm), a pointed tweezers, latex surgical gloves and ultrasonic bath were also used.

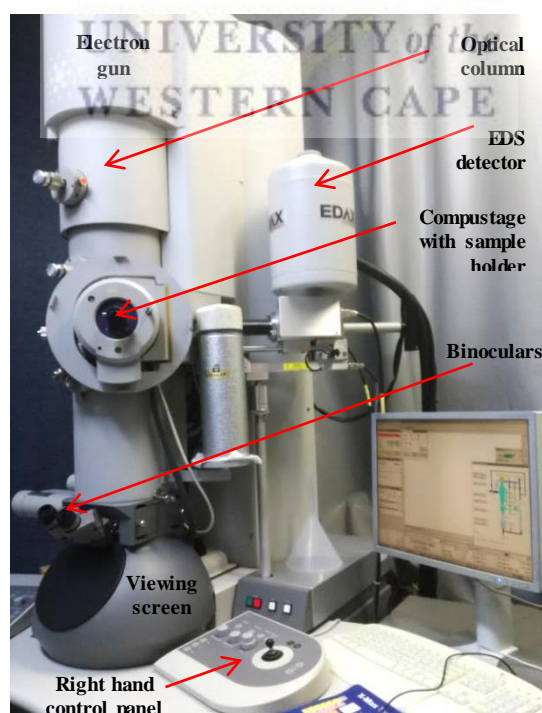


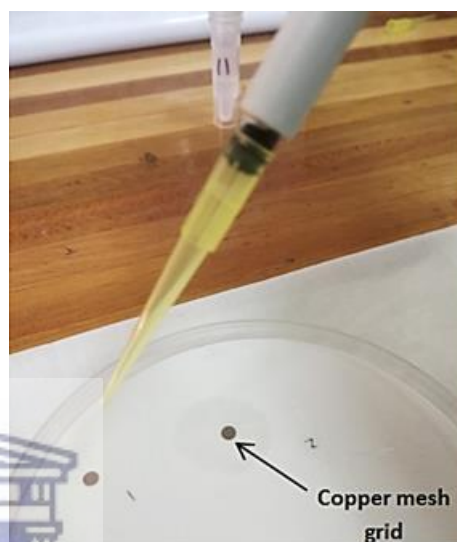
**Fig. 3.18:** FEI Tecnai G<sup>2</sup> F20 Scanning Transmission Electron Microscope (Image: own).

### 3.2.2.6.2 Sample preparation

One extraction solution (weekend day composite sample for January 2018) was sent for TEM photomicrography (see section 3.2.2.5.2 for preparatory activities).

### 3.2.2.6.3 Mesh grid preparation

The extraction solution was sonicated for two minutes prior to mesh grid preparation. Two copper mesh grids (SPI supplies, part number: 3540C-MB) were used (Fig. 3.19). A drop of extraction solution was dropped onto mesh grid (1). The solution was diluted 1:10 (1 part extraction solution: 9 parts Milli-Q water) and a drop dropped onto grid (2).



Mesh grids were then put under a heat lamp for 10 minutes to dry. A pointed tweezers was used at all times to prevent unwanted contamination.

*Fig. 3.19: Mesh grid preparation for TEM photomicrography (Images: own).*

### 3.2.2.6.4 Photomicrography

TEM photomicrography was performed in a climate-controlled laboratory (temperature: 24-25 °C, Rh: 45-46 %) using Tecnai G<sup>2</sup> software (version 4.4). Mesh grids (1) and (2) were micrographed at various magnifications. The operating conditions of the microscope are shown in Table 3.9. In addition to TEM, energy dispersive x-ray spectroscopy (EDS) and selected area electron diffraction (SAED) analyses were also performed.

*Table 3.9: Tecnai G<sup>2</sup> F20 operating conditions*

Parameter	Unit	Value
High tension (HT)	kV	200
Magnification	-	40k-400k
Resolution	nm	0.16
EDS: solid angle	sr	0.30

### 3.2.2.7 HYSPLIT modelling

The HYSPLIT model is an open computer model used for atmospheric trajectory and dispersion calculations (Stein et al. 2015). Backward (or archive) trajectory analysis was used for air mass origins and long-range transport cluster determinations (for detailed information on the HYSPLIT model, how it works and its applications see section 2.3.1).

#### 3.2.2.7.1 Equipment and materials

Backward trajectory analyses were performed using the HYSPLIT-WEB model (internet-based), version 4.9, in accordance with the *HYSPLIT user guide* (available at [www.arl.noaa.gov/documents/reports/hysplit\\_user\\_guide.pdf](http://www.arl.noaa.gov/documents/reports/hysplit_user_guide.pdf)). The model was driven by the NCEP/NCAR (National Centres for Environmental Prediction/National Centre for Atmospheric Research) Global Reanalysis Meteorological Data at the web server of the National Oceanic and Atmospheric Administration Air Resources Laboratory (NOAA ARL).

#### 3.2.2.7.2 Backward trajectory analysis

A total of 121 backward trajectories were generated for the study period (one for each sample collected). Trajectories were categorised into six primary transport routes (see Fig 4.20, page 118). User-specific settings used for single backward trajectories are shown in Table 3.10.

**Table 3.10:** *HYSPLIT user settings for single backward trajectory plots*

<b>Parameter</b>	<b>Setting</b>
Meteorology data model	GDAS-1
Vertical motion	Model vertical velocity
Level 1 height (elevation)	500 m
Total run time	24 hours
Trajectory intervals	1 hour
Plot projection	Default
Zoom factor	50-70 %
Latitude	-33.842900
Longitude	18.702600

Since a single backward trajectory has a large uncertainty and is of limited significance, an assembly of trajectories (or clusters) with 500 m starting height and a fixed offset grid factor

of 250 m was used in this study (i.e. 250 m and 750 m also used) as done in other studies (Molnár et al., 2017). The daily average trajectories were calculated backwards for 72 hours and used for cluster analysis. The clustering algorithm coupled in HYSPLIT was based on the distance between a trajectory endpoint and the corresponding cluster mean endpoint. Cluster analyses were performed seasonally (autumn, winter, spring and summer) due to the limitation of using very large sample sizes in the clustering function of the HYSPLIT software, as performed in other studies (Molnár et al., 2017). Autumn included the following days: 18 April – 31 May 2017, and 1 March – 16 April 2018, winter (1 June – 31 August 2017), spring (1 September – 30 November 2017), and summer (1 December 2017 – 28 February 2018). Between three and four transport clusters were categorised according to their mean pathways in the four seasons (see Fig. 4.22, page 114). User-specific settings used for cluster plots are shown in Table 3.11. See Appendix 12 for trajectory clusters and corresponding sampling dates.

**Table 3.11:** HYSPLIT user settings for backward trajectory cluster plots

Parameter	Setting
Meteorology data model	CDC-1
Vertical motion	Model vertical velocity
Level 1, 2, 3 heights (elevation)	250, 500, 750 m
Total run time	72 hours
Trajectory intervals	6 hours
Plot projection	Default
Zoom factor	30 %
Latitude	-33.842900
Longitude	18.702600

Seasonal trajectory frequency plots (see Fig. 4.23 and Fig. 4.24, pages 115 and 116) were also generated with swathes of red (> 90 %), orange, yellow, green, blue and purple (< 10 %) representing the number of times trajectories passed through each square grid as a percentage of total trajectories for the specified time period. Seasonal trajectory frequency plots were generated using the same parameter settings used to generate single trajectories (see Table 3.10, page 87).



### 3.3 Air pollution data collected by the City of Cape Town

Daily air pollution data from six AAQM stations was requested from the City of Cape Town (CoCT) for the study period (see Appendix 13). The stations were chosen based on their locations (Fig. 3.20) (distance from sampling site: 3-37 km, distribution: NNW-ESE, coverage: 180-210°). Stations chosen were:

- Atlantis ( 37 km NNW of site)
- Somerset-West (29 km SSE of site)
- City Hall (27 km WSW of site)
- Tableview (18 km WNW of site)
- Goodwood (14 km WSW of site)
- Wallacedene (3 km SE of site)

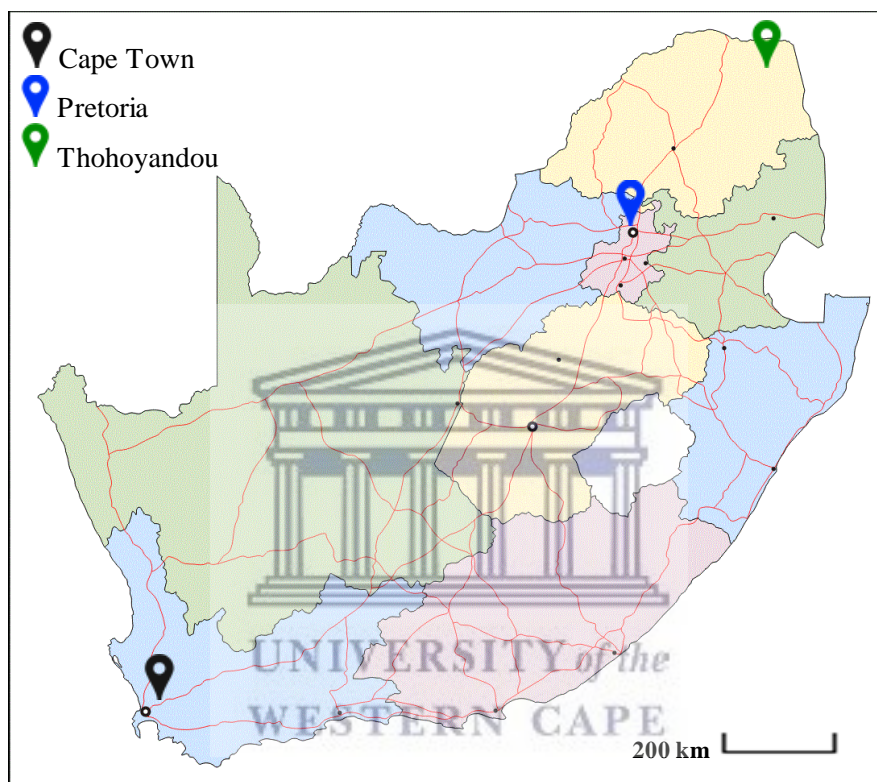


*Fig. 3.20: Locations of the six AAQM stations whose data was used for correlation purposes*

Study data was compared with air pollution data collected by the CoCT and correlation analyses performed, not only to determine the extent of air mass transport in Cape Town and the region, but also to check air pollution levels at different locations throughout Cape Town and if air pollution data from any one AAQM stations could be used to determine air pollution levels at another location.

### 3.4 Air pollution data for Pretoria and Thohoyandou

Ambient air sampling was performed in Pretoria (sample site coordinates: -25.7317, 28.2003) and Thohoyandou (sample site coordinates: -22.9761, 30.4443) by researchers from the University of Pretoria (UP) and the University of Venda (UniVen). The location of each sampling site is shown in Fig. 3.21.



Distance (km)	Cape Town	Pretoria	Thohoyandou
Cape Town	-	1,285	1,675
Pretoria	1,285	-	390
Thohoyandou	1,675	390	-

**Fig. 3.21:** Locations of the Cape Town, Pretoria and Thohoyandou sampling sites

This study formed part of a larger project investigating the health effects, air mass transport and concentrations of ambient APM in South Africa. Study data was compared to air pollution data for Pretoria and Thohoyandou to determine the effects of meteorological conditions and geographical location on air pollution levels for each region.

### 3.5 Statistical analysis

This section provides an overview of the statistical methodologies used for this study. Statistical analyses were performed using Microsoft Excel (Office 2010), *Essential Statistics* (Rees, 2000) handbook and other literature.

#### 3.5.1 Study data

For calendar samples (section 4.1), graphical plots are of single data points despite some sampling days (25 in total) having duplicate samples. Data points were selected based on the following criteria:

- Difference between primary and duplicate PM<sub>2.5</sub> concentrations or absorption coefficient values > 2 % (highest value used)
- Difference between primary and duplicate PM<sub>2.5</sub> concentrations or absorption coefficient values ≤ 2 % (mean value used)

##### 3.5.1.1 Data management

PM<sub>2.5</sub> concentrations and absorption coefficients for calendar samples were sorted into two groups - seasonal and weekday/weekend day data sets. These data sets were tested for linear normality, correlation and significance. Composite samples (section 4.5) were collected during September 2017 and January 2018 and the significance of certain chemical constituents for weekday and corresponding weekend day samples tested.

##### 3.5.1.2 Determination of outliers in data sets

Outliers are observations in data sets that differ from the majority. Robust scores were calculated with univariate location estimation equation 14 (Rousseeuw et al., 2011) that were used to detect outliers (robust score > 2.5).

$$\text{Robust score} = [x_i - \text{median}(x_j)]/\text{MAD} \quad (14)$$

Where *MAD* is the median of the absolute deviation of  $x_i$  from the median.

### 3.5.1.3 Normality analysis

Shapiro-Wilks' Normality Tests were performed to determine normality and symmetry of data. When  $p < \alpha$ , reject null hypothesis. When  $p \geq \alpha$ , do not reject null hypothesis (null hypothesis = data has normal distribution).

### 3.5.1.4 Correlation and significance analyses

Correlation coefficient is a measure of the strength of a relationship between two variables (Samuels et al., 2014). Pearson Product-Moment Correlation (PPMC, parametric) was used for normally distributed data sets. Pearson coefficient ( $r$ ) was calculated with equation 15.

$$r = \frac{n(\sum xy) - (\sum x)^2(\sum y)^2}{\sqrt{[n\sum x^2 - (\sum x)^2][n\sum y^2 - (\sum y)^2]}} \quad (15)$$

Where  $n$  is sample size. Spearman Rank-Order Correlation (SROC, non-parametric) was used for non-normally distributed data sets. Because all non-normally distributed data sets did not have tied (or equal) values, Spearman coefficient ( $\rho$ ) was calculated with equation 16.

$$\rho = 1 - \frac{6\sum d^2}{n(n^2-1)} \quad (16)$$

Where  $d$  is difference in paired ranks and  $n$  is number of pairs. Kruskal-Wallis H-Test (or Significance Test) was conducted to determine whether the medians of data sets were different (null hypothesis = medians are equal). The test statistic used in the test was the H-statistic and was calculated with equation 17.

$$H = \left( \frac{12}{n(n+1)} \sum_{j=1}^c \frac{T_j^2}{n_j} \right) - 3(n+1) \quad (17)$$

Where  $n$  is the sum of sample sizes for all data sets,  $c$  is the number of samples,  $T_j$  is the sum of ranks in  $j^{\text{th}}$  sample and  $n_j$  is size of  $j^{\text{th}}$  sample. For composites samples, Student's T-test was used to check data similarity between composite samples for September 2017 and January 2018. The t-statistic was calculated with equation 18 (page 93):

$$t = \frac{(\sum D)/N}{\sqrt{\frac{\sum D^2 - \frac{(\sum D)^2}{N}}{(N-1)(N)}}} \quad (18)$$

Where  $D$  is the difference between data points of data sets and  $N$  is number of data pairs.

### 3.5.2 Air pollution data collected by the CoCT

#### 3.5.2.1 Normality analyses

Shapiro-Wilks Normality Test was used to determine whether air pollution data (collected by the CoCT) had normality.

#### 3.5.2.2 Correlation and significance analyses

Spearman Rank-Order Correlation was used to determine the correlation (strength of association) between study data (PM<sub>2.5</sub> concentrations and absorption coefficients) and data collected by the CoCT.



## CHAPTER 4: RESULTS

This chapter is divided into five main sections, sections 4.1-4.5. Sections 4.1-4.4 present data and information for calendar samples and section 4.5 presents data for composite samples.

### 4.1 Calendar samples

Data obtained from analytical methodology and statistical information pertaining to PM<sub>2.5</sub> concentrations and absorption coefficients for calendar samples are presented in this section. Meteorological and air mass transport information is also presented.

#### 4.1.1 PM<sub>2.5</sub> mass concentrations

Over 1,000 mass measurements were performed across 14 measurement sessions. Primary control filter checks were performed during each session that had to comply with specific requirements of the working procedure and SOP 3.0. Quality control information is shown in Table 4.1 (see Appendix 6B and 6C).

*Table 4.1: Quality control information for gravimetric analyses*

<b>Working procedure requirement</b>	<b>Actual (%)</b>	<b>Limit (%)</b>	<b>Compliance</b>
Percentage difference between minimum/maximum mass and mean mass	5.42x10 <sup>-5</sup> - 7.57x10 <sup>-4</sup>	< 1.00x10 <sup>-3</sup>	Yes
<b>SOP 3.0 requirements</b>	<b>Actual (µg)</b>	<b>Limit (µg)</b>	<b>Compliance</b>
Absolute mass difference of replicates	0-5	5	Yes
Mean mass change (m <sub>r</sub> ) of control filter (before and after measurement sessions)	-10.4 to 14	± 15	Yes

PM<sub>2.5</sub> concentration was calculated as the dividend of PM<sub>2.5</sub> mass and volume of air sampled.

Total volume of air sampled over 24 hours was calculated with equations 25 and 26:

$$Q_{AVE}(\text{L} \cdot \text{min}^{-1}) = \frac{\text{flow rate}(\text{before}) + \text{flow rate}(\text{after})}{2} \quad (19)$$

$$V(\text{m}_3) = \frac{Q_{AVE} \times 24 \times 60}{1,000} = 1.44(Q_{AVE}) \quad (20)$$

Daily PM<sub>2.5</sub> concentrations for the study period are shown in Fig. 4.1 (page 95) and Fig. 4.2 (page 96). See Appendix 6A for daily PM<sub>2.5</sub> concentrations.

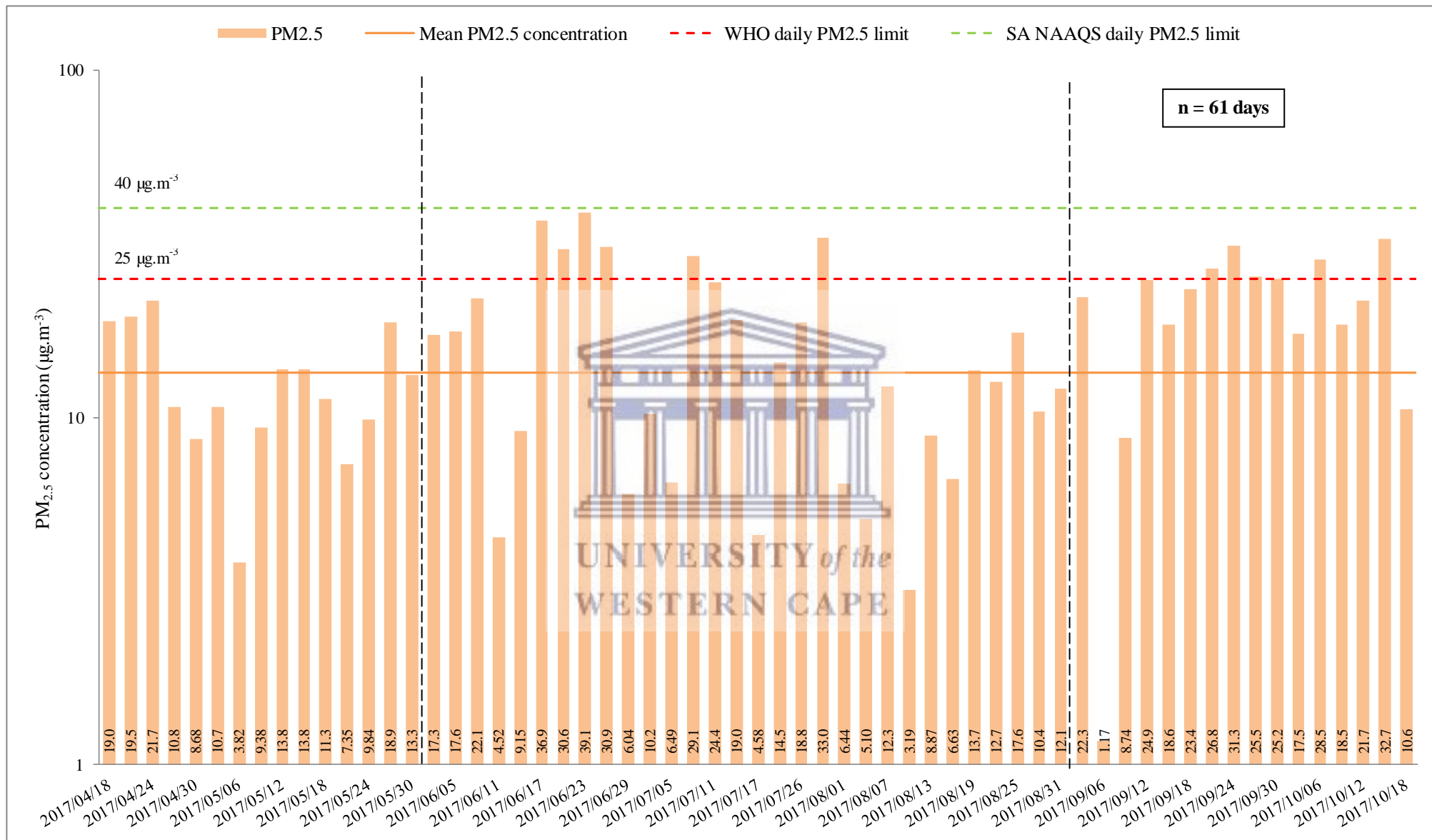


Fig. 4.1: PM<sub>2.5</sub> concentrations for period 2017/04/18 to 2017/10/18. Broken black lines indicate the start of a new season.

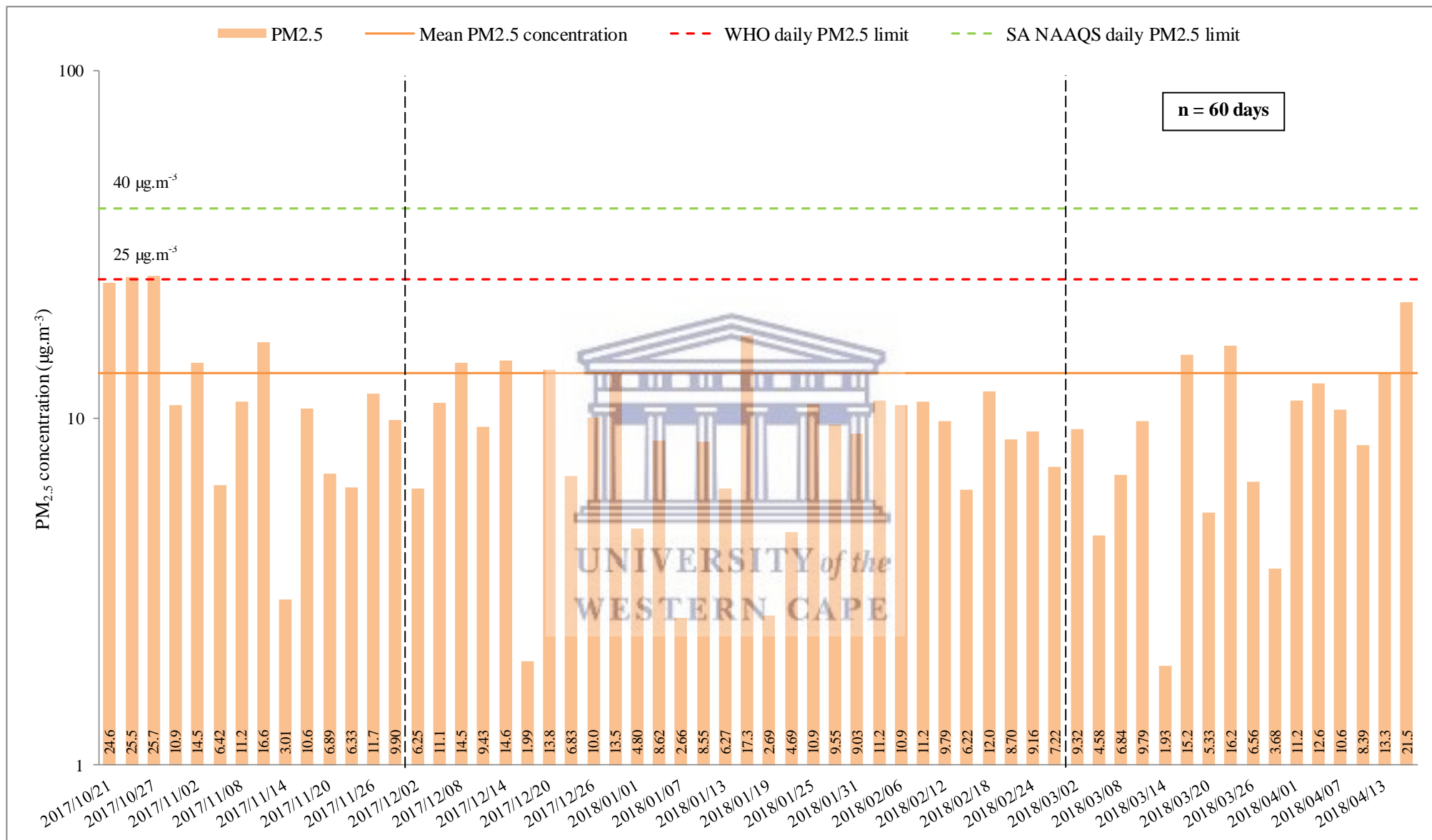
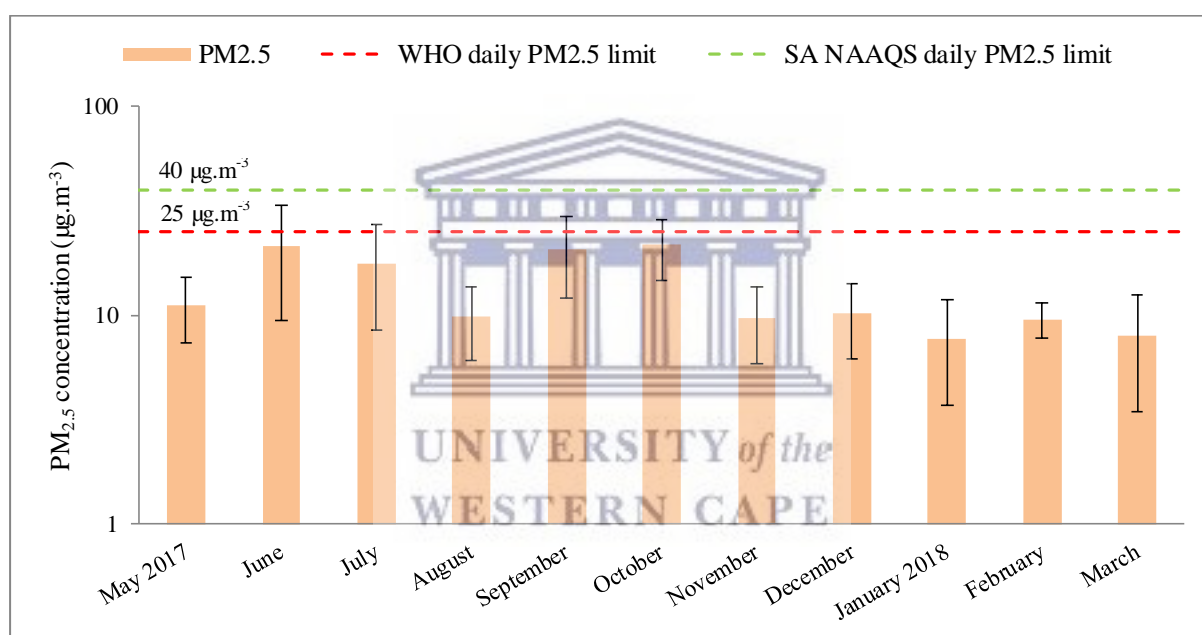


Fig. 4.2: PM<sub>2.5</sub> concentrations for period 2017/10/21 to 2018/04/16. Broken black lines indicate the start of a new season.



Mean PM<sub>2.5</sub> concentration for the study period was  $13.4 \pm 8.1 \mu\text{g}\cdot\text{m}^{-3}$  which was below the WHO and SA NAAQS (2015) daily PM<sub>2.5</sub> limits of  $25 \mu\text{g}\cdot\text{m}^{-3}$  and  $40 \mu\text{g}\cdot\text{m}^{-3}$  respectively. The WHO daily limit was exceeded 14 times during the study period. Spring (September–November) had the most number of exceedances with eight. Highest ( $39.1 \mu\text{g}\cdot\text{m}^{-3}$ ) and lowest ( $1.17 \mu\text{g}\cdot\text{m}^{-3}$ ) PM<sub>2.5</sub> concentrations were recorded on 23 June 2017 and 6 September 2017, respectively. Mean monthly PM<sub>2.5</sub> concentrations are shown in Fig. 4.3. *April 2017 (n = 5) and April 2018 (n = 6) were omitted because sample size (n) was insufficient to be considered representative (n must be  $\geq 7$ ).*



**Fig. 4.3:** Monthly PM<sub>2.5</sub> concentrations

October and January had the highest and lowest concentrations with  $21.6 \pm 6.9 \mu\text{g}\cdot\text{m}^{-3}$  and  $7.74 \pm 4.04 \mu\text{g}\cdot\text{m}^{-3}$  respectively. Data for June ( $\sigma = 12.0 \mu\text{g}\cdot\text{m}^{-3}$ ) had the most variability and February ( $\sigma = 1.84 \mu\text{g}\cdot\text{m}^{-3}$ ) the least. There were similarities between seasonal concentrations. Concentrations for winter ( $16.1 \pm 10.2 \mu\text{g}\cdot\text{m}^{-3}$ ) and spring ( $17.4 \pm 8.5 \mu\text{g}\cdot\text{m}^{-3}$ ) were similar as were the concentrations for autumn ( $11.3 \pm 5.2 \mu\text{g}\cdot\text{m}^{-3}$ ) and summer ( $9.11 \pm 3.66 \mu\text{g}\cdot\text{m}^{-3}$ ). Mean seasonal PM<sub>2.5</sub> concentrations are shown in Fig. 4.4 (page 98). See Appendix 1B for seasonal sampling day information (useful for interpreting seasonal data

from this point forth).

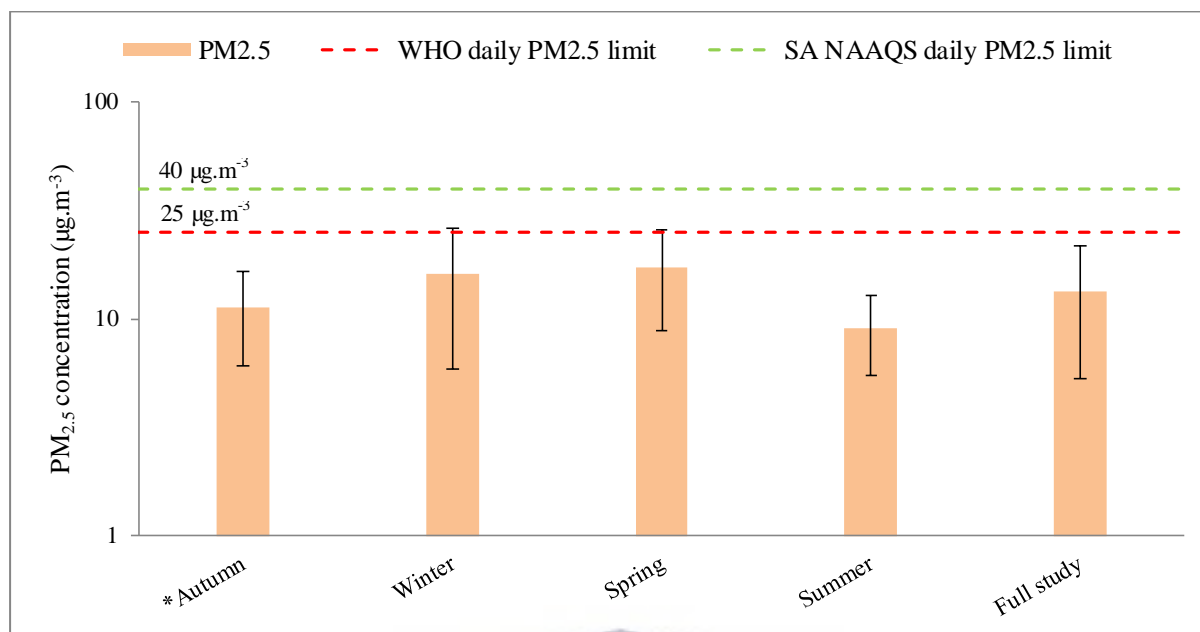


**Fig. 4.4:** Seasonal PM<sub>2.5</sub> concentrations (\*includes data for April 2017/18)

#### 4.1.2 Absorption coefficient values and soot concentrations

900 reflectance measurements were performed across six measurement sessions. Quality control checks were performed at various stages during each session that had to comply with the specific requirements of SOP 4.0. Quality control information is shown in Table 4.2 (see Appendix 7B and 7C).

**Table 4.2:** Quality control information for reflectometric analyses

	Actual (%)	Limit (%)	Compliance
Primary control filter absorbance	99-101.4	98-102	Yes
Percentage difference (primary control filter, before and after measurement session)	-1.38 to 0.70	± 3	Yes
Percentage difference (original and duplicate R <sub>s</sub> )	-2.51 to 0.88	± 3	Yes

Absorption coefficient was calculated using equation 13 (section 3.2.2.2.2). Absorption coefficient values for the study period are shown in Fig. 4.5 (page 99) and Fig. 4.6 (page 100). See Appendix 7A for daily absorption coefficient values.

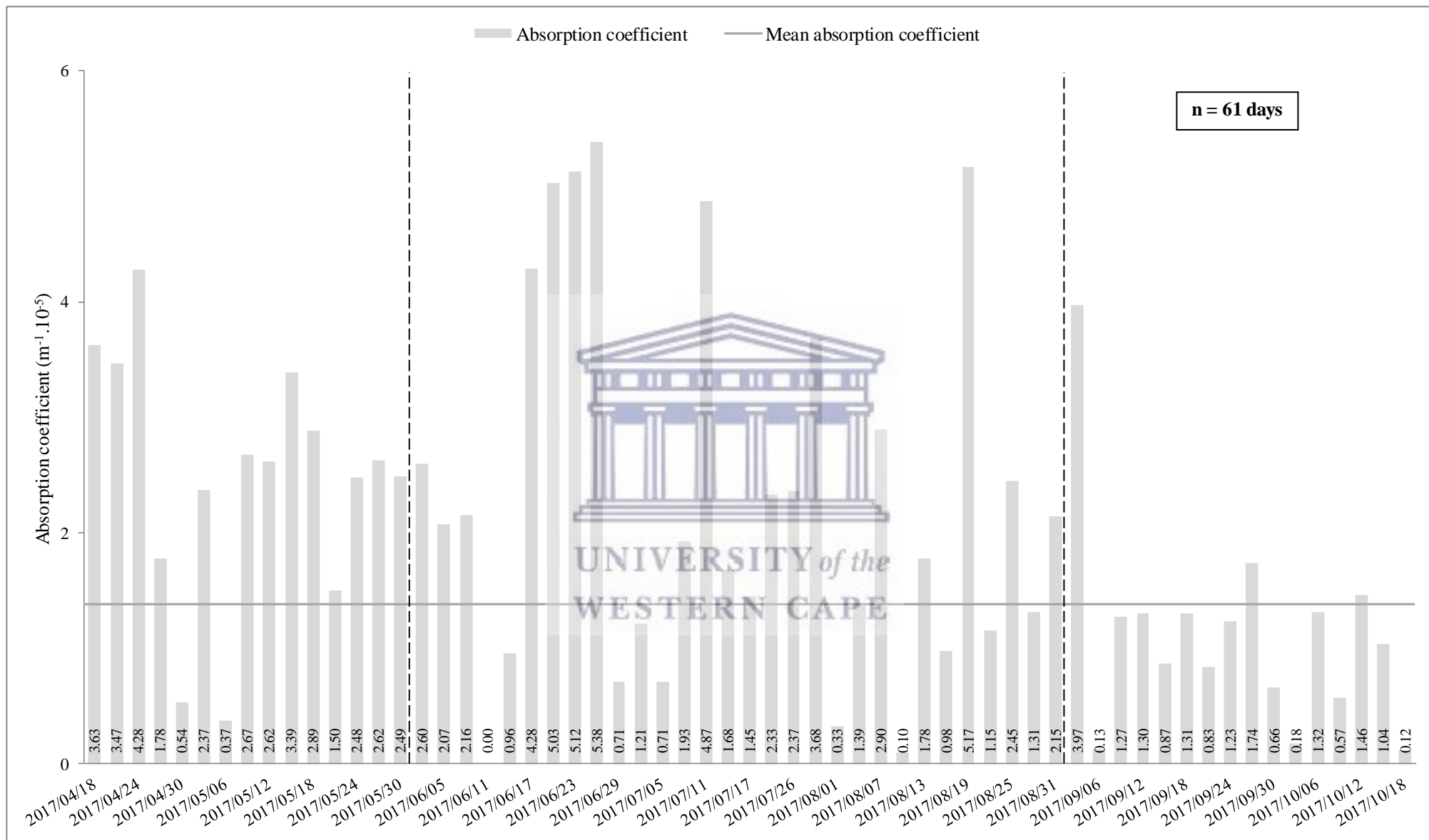


Fig. 4.5: Absorption coefficients for period 2017/04/18 to 2017/10/18. Broken black lines indicate the start of a new season.

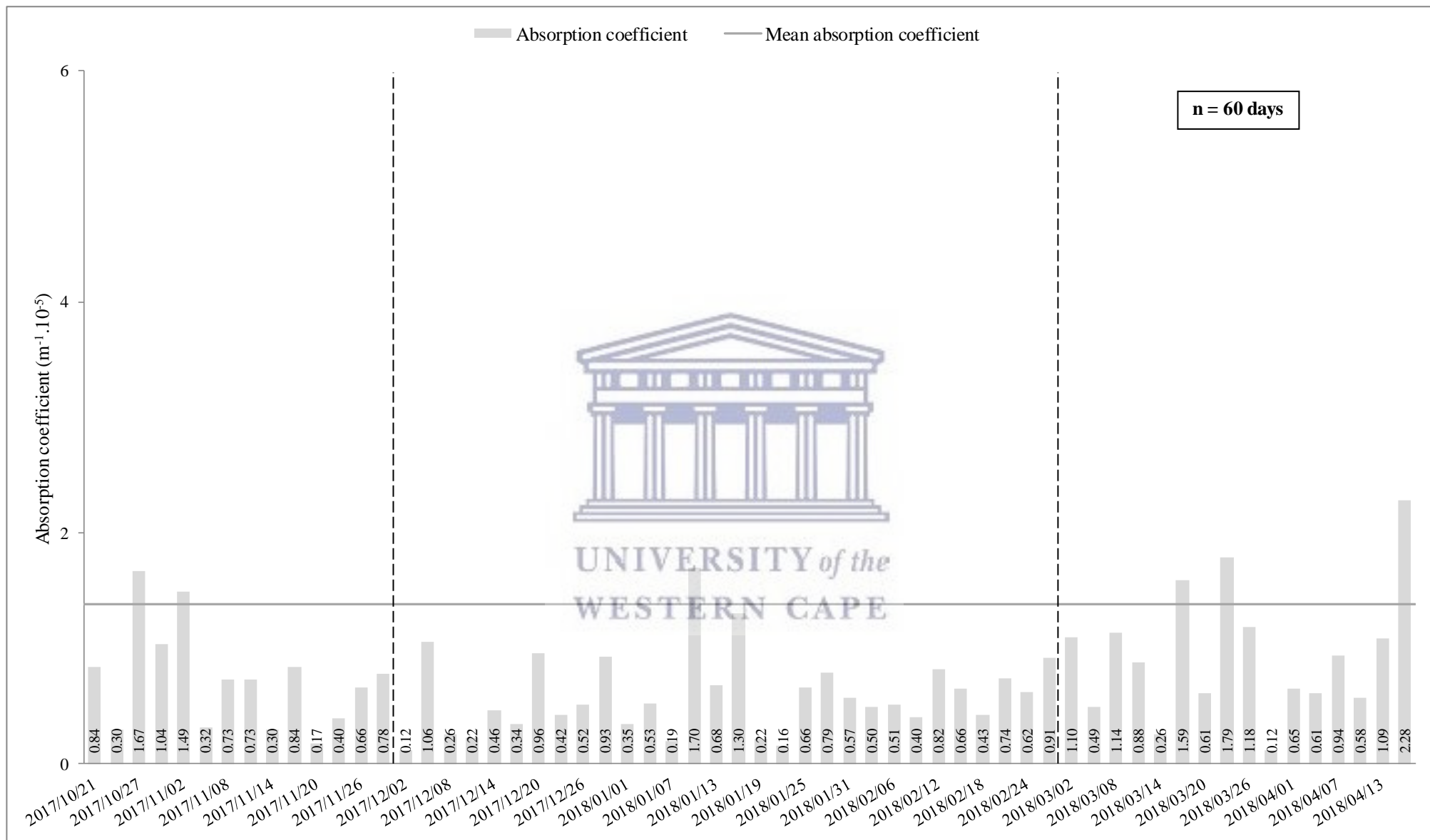
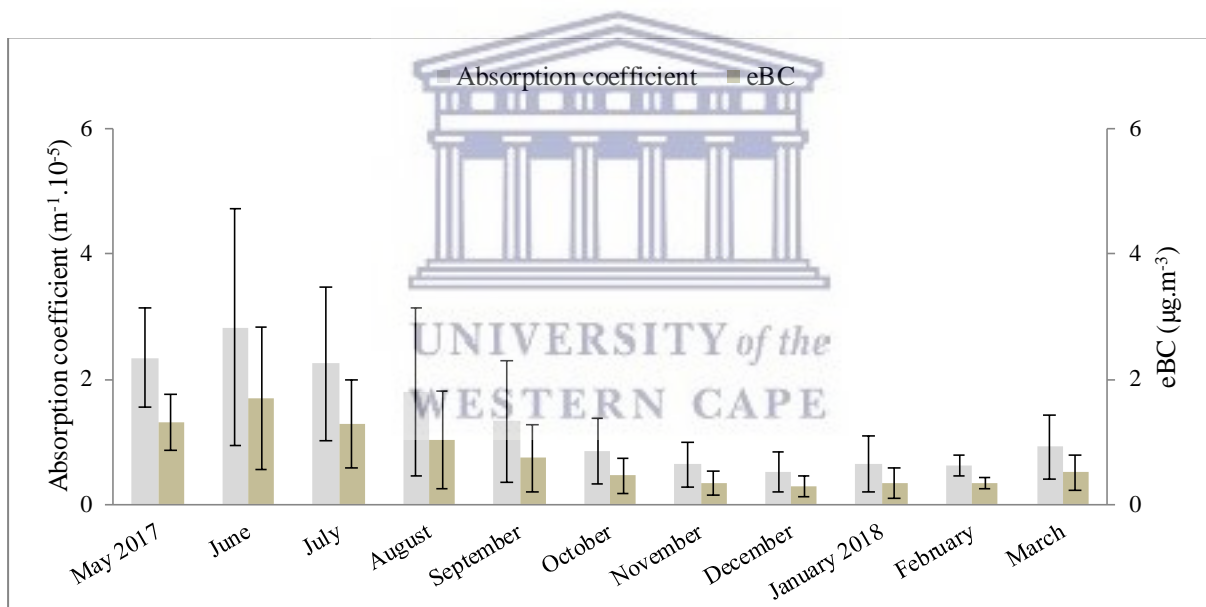


Fig. 4.6: Absorption coefficients for period 2017/10/21 to 2018/04/16. Broken black lines indicate the start of a new season.

Mean absorption coefficient value for the study period was  $1.38 \pm 1.23 \text{ m}^{-1} \cdot 10^{-5}$  with the largest ( $5.38 \text{ m}^{-1} \cdot 10^{-5}$ ) and smallest ( $0.00 \text{ m}^{-1}$ ) values recorded on 26 June 2017 and on 11 June 2017, respectively. Soot concentration (eBC) was calculated with equation 21 (simplification of equation 13, page 71).

$$\text{eBC } (\mu\text{g} \cdot \text{m}^{-3}) = \frac{855}{39V} \times R(1 + 0.3R) \quad (21)$$

Where  $R$  is reflectance and  $V$  is volume of air sampled. Monthly absorption coefficient and equivalent black carbon (eBC) values are shown in Fig. 4.7. April 2017 ( $n = 5$ ) and April 2018 ( $n = 6$ ) were omitted because sample size ( $n$ ) was insufficient to be considered representative ( $n$  must be  $\geq 7$ ).



**Fig. 4.7:** Monthly absorption coefficient and eBC values

June and January had the largest and smallest absorption coefficient values with  $2.83 \pm 1.89 \text{ m}^{-1} \cdot 10^{-5}$  and  $0.53 \pm 0.32 \text{ m}^{-1} \cdot 10^{-5}$  respectively. Data for June ( $\sigma = 1.89$ ) had the most variability and February ( $\sigma = 0.17$ ) the least. Absorption coefficient values had a consistent downward trend over a six month period (June-December). Winter and summer had the highest and lowest eBC values with  $1.34 \pm 0.88 \mu\text{g} \cdot \text{m}^{-3}$  and  $0.32 \pm 0.19 \mu\text{g} \cdot \text{m}^{-3}$  respectively. Mean eBC ( $0.28\text{-}1.70 \mu\text{g} \cdot \text{m}^{-3}$ ) for the study period was well below the WHO limit of 20

$\mu\text{g}\cdot\text{m}^{-3}$ . Mean seasonal absorption coefficient and eBC values are shown in Fig. 4.8.

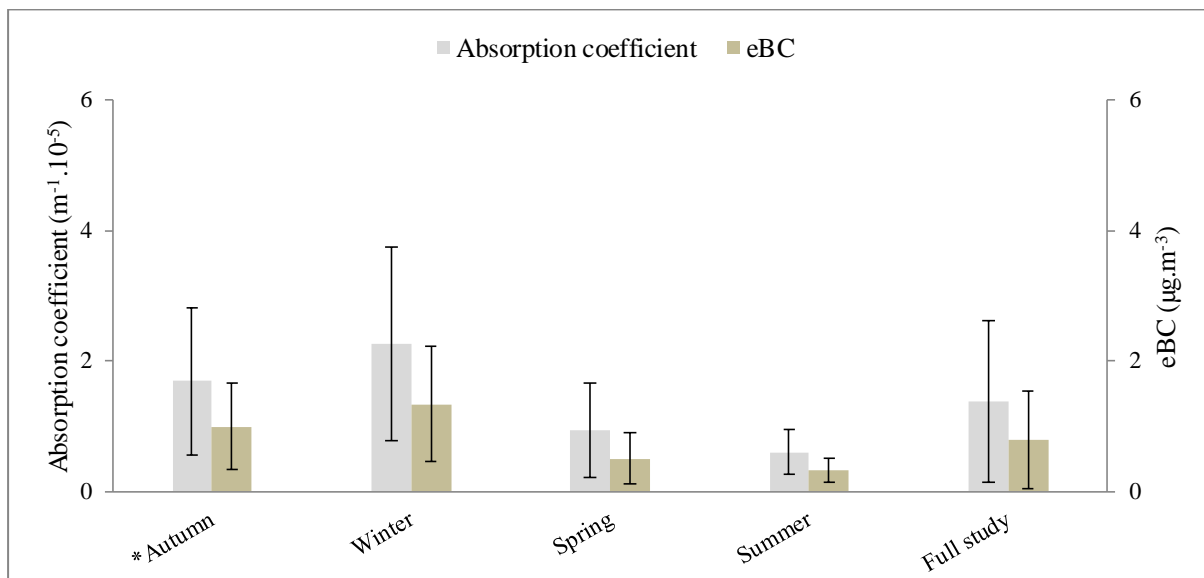


**Fig. 4.8:** Seasonal absorption coefficient and eBC values (\*includes data for April 2017/18)

#### 4.1.3 Statistical analysis

##### 4.1.3.1 Descriptive statistics and normality analysis

$\text{PM}_{2.5}$  concentrations and absorption coefficient values for the study period yielded negative trend lines and coefficients of determination ( $R^2$ ) values of 0.10 (negligible) and 0.30 (weak) respectively.  $\text{PM}_{2.5}$  concentrations and absorption coefficients values are shown in Fig. 4.9 (page 103).

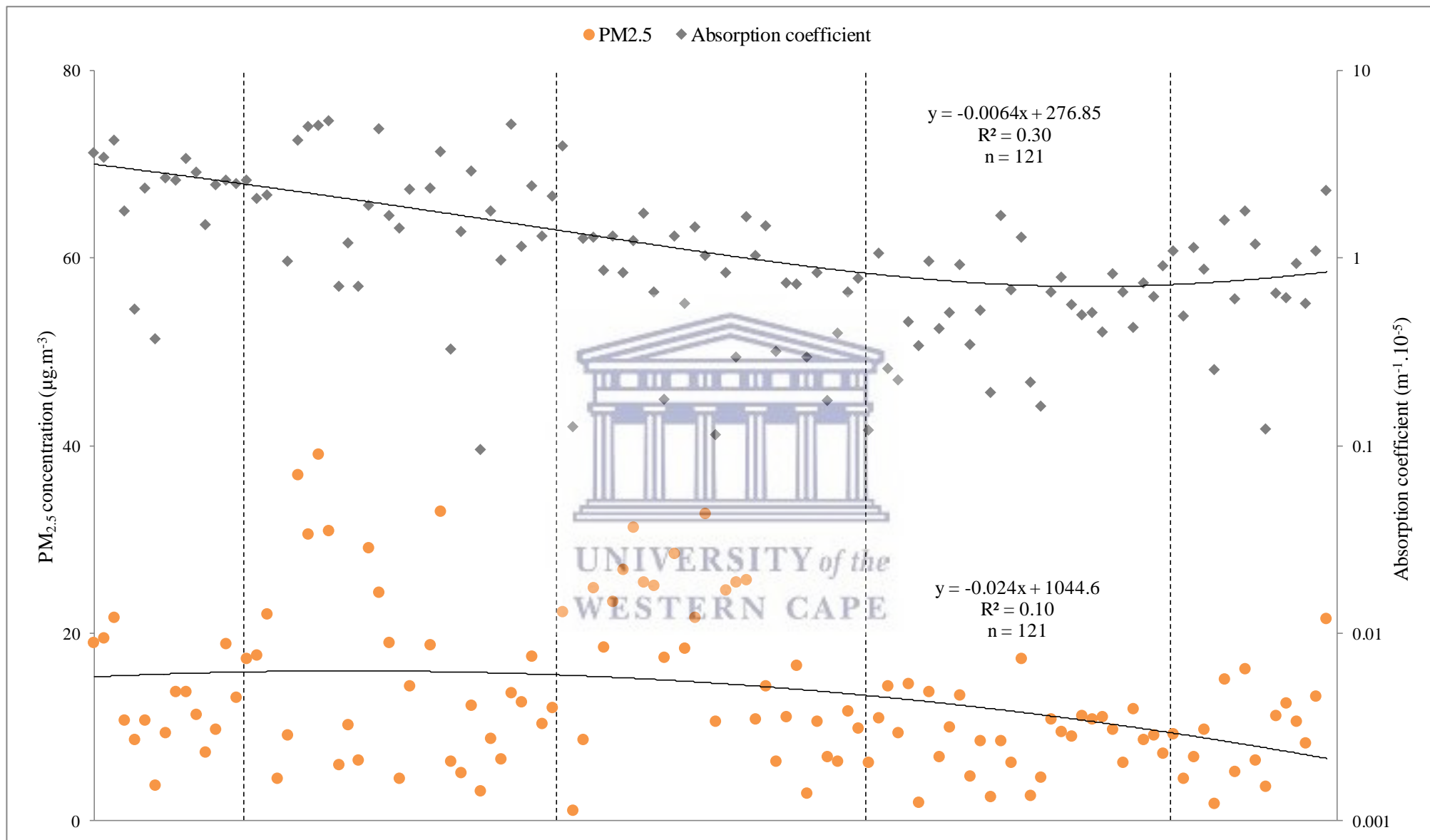


Fig. 4.9: PM<sub>2.5</sub> concentrations and absorption coefficients for the study period. Black broken lines indicate the start of a new season.

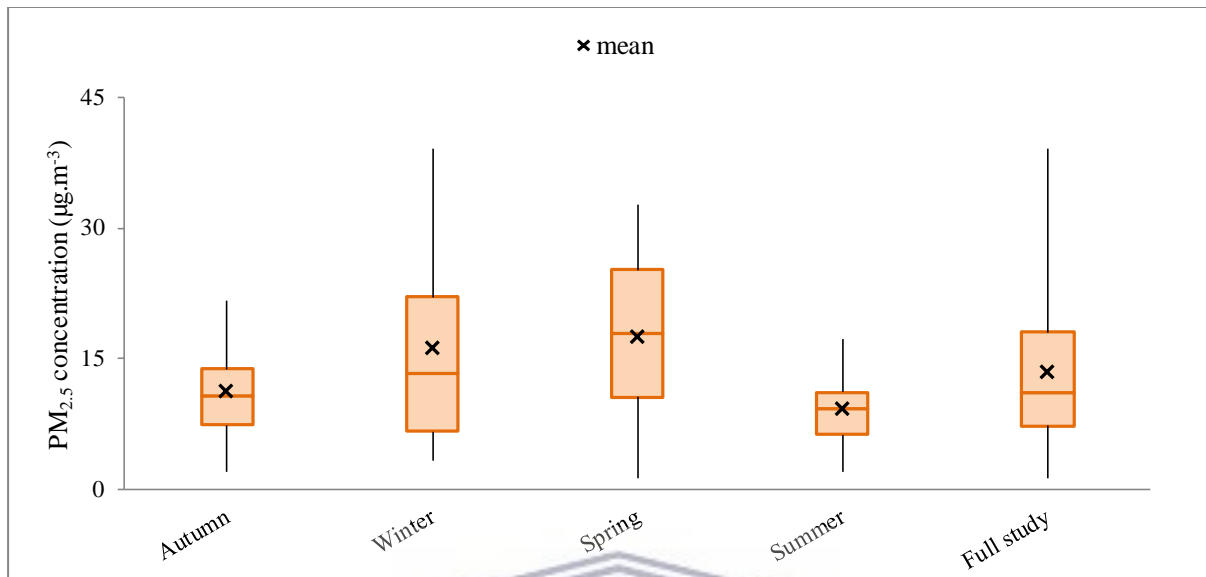
There were nine (7.44 %) and 12 (9.92 %) outliers in the data sets of PM<sub>2.5</sub> concentration and absorption coefficient values respectively (see Appendix 8). Outliers omitted, R<sup>2</sup> for both parameters did not improve thus all data points were considered for statistical calculations. The descriptive statistics for seasonal PM<sub>2.5</sub> concentration and absorption coefficient data are shown in Table 4.3 (see Appendices 9 and 10 for monthly and weekday/weekend day descriptive statistics).

**Table 4.3:** Descriptive statistics of seasonal PM<sub>2.5</sub> concentration and absorption coefficient data (concentrations in  $\mu\text{g.m}^{-3}$  and coefficient values in  $\text{m}^{-1} \cdot 10^{-5}$ )

Sample size (n)	31	30	30	30	121
Weekdays (%)	22 (71)	23 (77)	21 (70)	19 (63)	85 (70)
Weekend + public holidays (%)	9 (29)	7 (23)	9 (30)	11 (37)	36 (30)
<b>PM<sub>2.5</sub> concentration</b>	<b>Autumn</b>	<b>Winter</b>	<b>Spring</b>	<b>Summer</b>	<b>Full study</b>
Mean	11.3	16.1	17.4	9.11	13.4
Median	10.7	13.2	18.0	9.29	11.1
Variance	26.7	104	75.3	13.4	66.1
Standard deviation	5.17	10.2	8.68	3.66	8.13
R.S.D (%)	45.6	63.4	49.9	40.2	60.7
Standard error	0.93	1.86	1.58	0.67	0.74
95 % confidence limit (lower)	9.48	12.5	14.3	7.80	11.9
95 % confidence limit (upper)	13.1	19.7	20.5	10.4	14.9
Range	1.93-21.7	3.19-39.1	1.17-32.1	1.99-17.3	1.17-39.1
WHO exceedances	0	6	8	0	14
SA NAAQS exceedances	0	0	0	0	0
<b>Absorption coefficient</b>					
Mean	1.76	2.29	0.94	0.60	1.38
Median	1.50	2.00	0.84	0.52	0.96
Variance	1.25	2.22	0.53	0.12	1.51
Standard deviation	1.12	1.49	0.73	0.35	1.23
R.S.D (%)	63.6	65.1	77.7	58.5	89.1
Standard error	0.20	0.27	0.13	0.06	0.11
95 % confidence limit (lower)	1.37	1.76	0.69	0.48	1.16
95 % confidence limit (upper)	2.15	2.82	1.19	0.72	1.60
Range	0.12-4.28	0.00-5.38	0.12-3.97	0.12-1.70	0.00-5.38

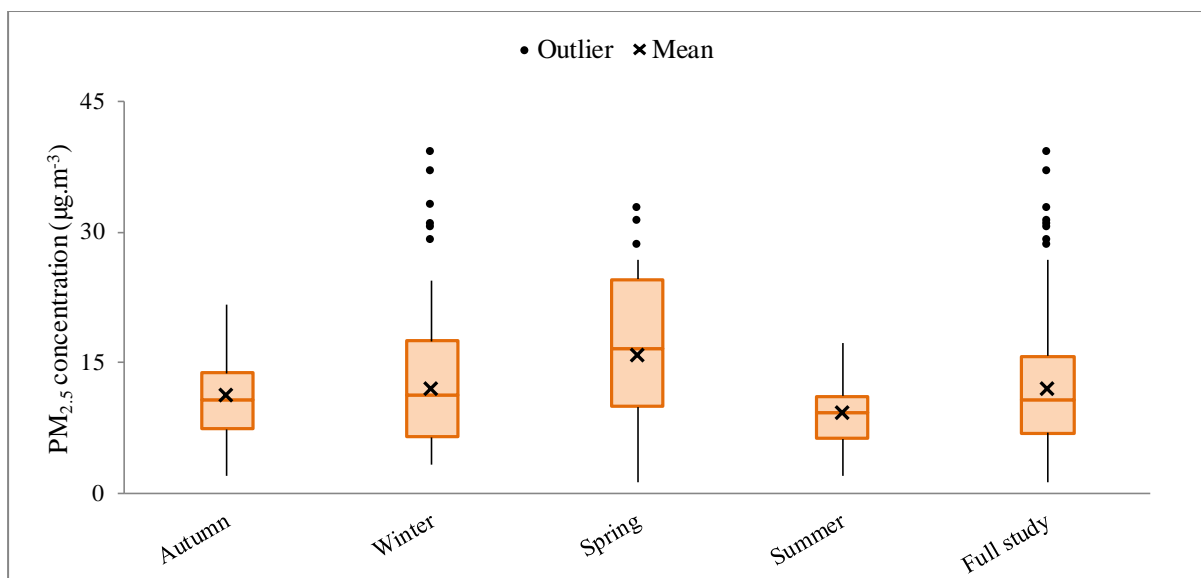


Box and whisker (BW) plots show data distribution, median values and variability. The distribution of seasonal  $PM_{2.5}$  concentration data is shown in Fig. 4.10.



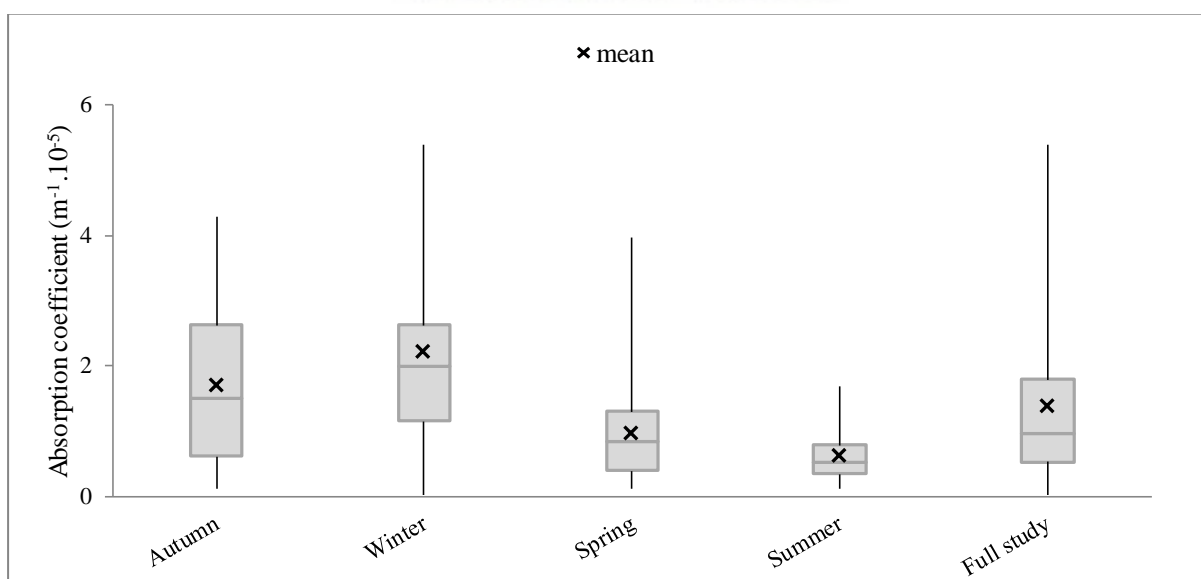
**Fig. 4.10:** BW plots of seasonal  $PM_{2.5}$  concentration data

Autumn ( $p = 0.456$ ), spring ( $p = 0.243$ ) and summer ( $p = 0.800$ ) had normal Gaussian distribution while winter ( $p = 0.015$ ) had non-normal distribution ( $\alpha = 0.05$ ). Data distribution for autumn was the most symmetrical of all seasons (winter, spring, summer and full study were all unsymmetrical). Data for winter ( $\sigma = 10.2$ ) had the most variability and summer ( $\sigma = 3.66$ ) the least. Winter and full study ( $p = 4.219 \times 10^{-6}$ ) showed significant departures from normality. Outliers omitted, distribution for autumn, summer and full study remained unchanged while winter ( $p = 0.320$ , previously 0.015) became normal. Symmetries of winter and full study improved but spring deteriorated [distribution became non-normal ( $p = 0.045$ , previously 0.243)]. The distribution of seasonal  $PM_{2.5}$  concentration data (outliers omitted) is shown in Fig. 4.11 (page 106).



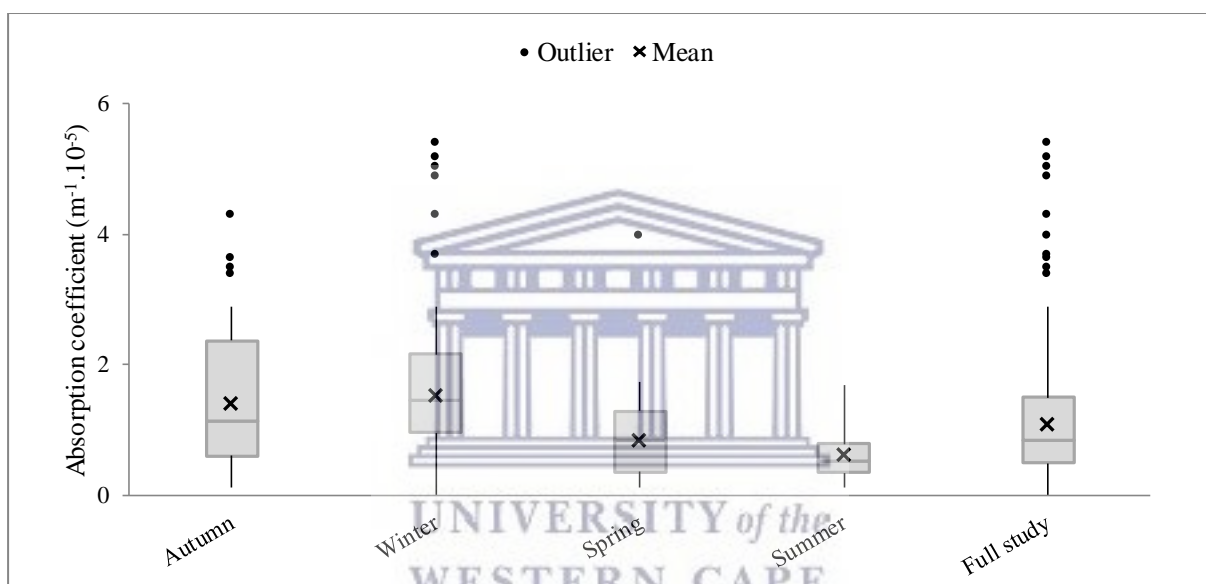
**Fig. 4.11:** BW plots of seasonal  $PM_{2.5}$  concentration data (outliers omitted)

Shapiro-Wilks' tests were conducted on absorption coefficient data. Autumn ( $p = 0.055$ ) was the only season with normal distribution ( $\alpha = 0.05$ ). Winter ( $p = 0.026$ ), spring ( $p = 0.010$ ), summer ( $p = 0.042$ ) and full study ( $p = 8.783 \times 10^{-10}$ ) showed significant departures from normality. Absorption coefficient data for autumn was the most symmetrical while winter was the least symmetrical. Winter ( $\sigma = 1.49$ ) had the most variability and summer ( $\sigma = 0.35$ ) the least. The distribution of seasonal absorption coefficient data is shown in Fig. 4.12.



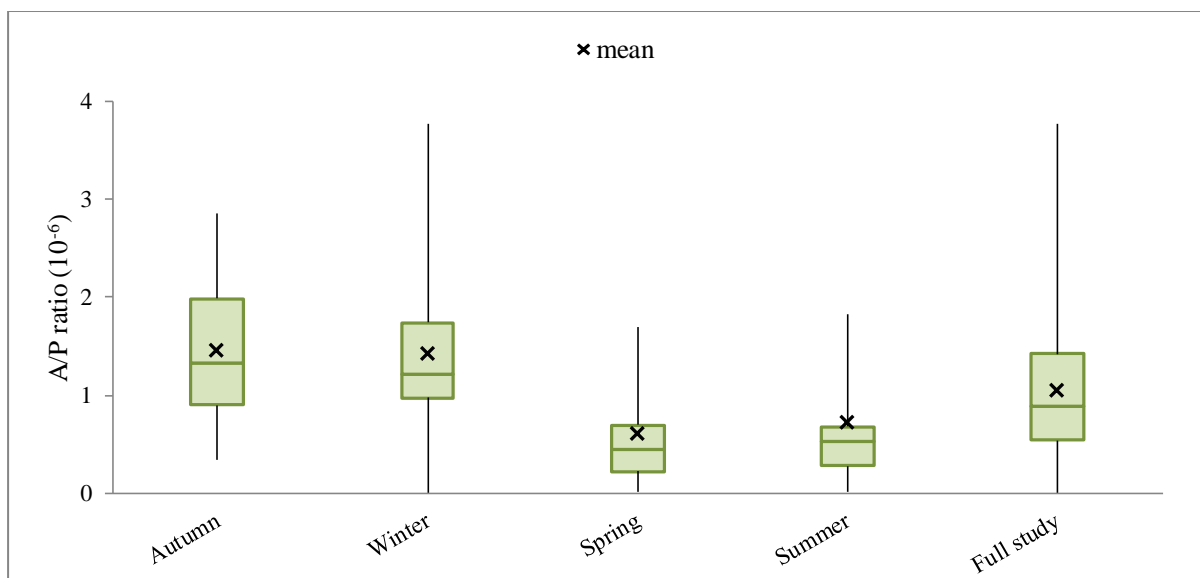
**Fig. 4.12:** BW plots of seasonal absorption coefficient data

Outliers omitted, summer remained unchanged with the p-value of the full study changing only slightly. Winter and spring, that previously had non-normal distributions now had normal distributions with  $p = 0.522$  (previously 0.026) and  $p = 0.252$  (previously 0.010) respectively. Autumn, that previously had normal distribution now had non-normal distribution ( $p = 0.025$ , previously 0.055). Symmetries of winter, spring and full study all improved while autumn deteriorated. Seasonal absorption coefficient data (outliers omitted) is shown in Fig. 4.13.



**Fig. 4.13:** BW plots of seasonal absorption coefficient data (outliers omitted)

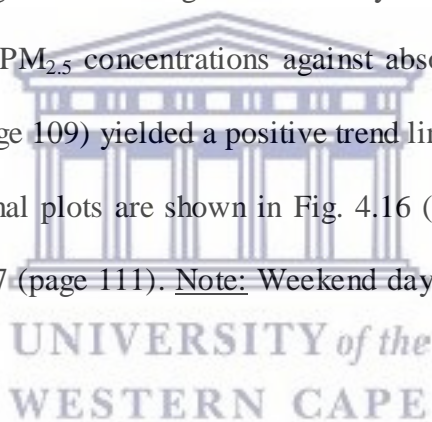
Finally, Shapiro-Wilks' tests were conducted on absorption coefficient/PM<sub>2.5</sub> ratios (A/P ratios). A/P ratios for autumn ( $p = 0.367$ ) and winter ( $p = 0.050$ ) had normal distribution of data. Distribution for autumn was the most symmetrical while summer was the least symmetrical (highest variability). Spring ( $p = 0.016$ ), summer ( $p = 0.010$ ), and full study ( $p = 1.92 \times 10^{-6}$ ) all showed significant departures from normality. A/P ratios are shown in Fig. 4.14 (page 108).



**Fig. 4.14:** BW plots of A/P ratios

#### 4.1.3.2 Correlation, linear regression and significance analyses

Linear regression analysis of  $PM_{2.5}$  concentrations against absorption coefficient values for the study period (Fig. 4.15, page 109) yielded a positive trend line ( $R^2 = 0.36$ ) and strong data association ( $\rho = 0.61$ ). Seasonal plots are shown in Fig. 4.16 (page 110), and weekday and weekend day plots in Fig. 4.17 (page 111). Note: Weekend day data includes data for public holidays.



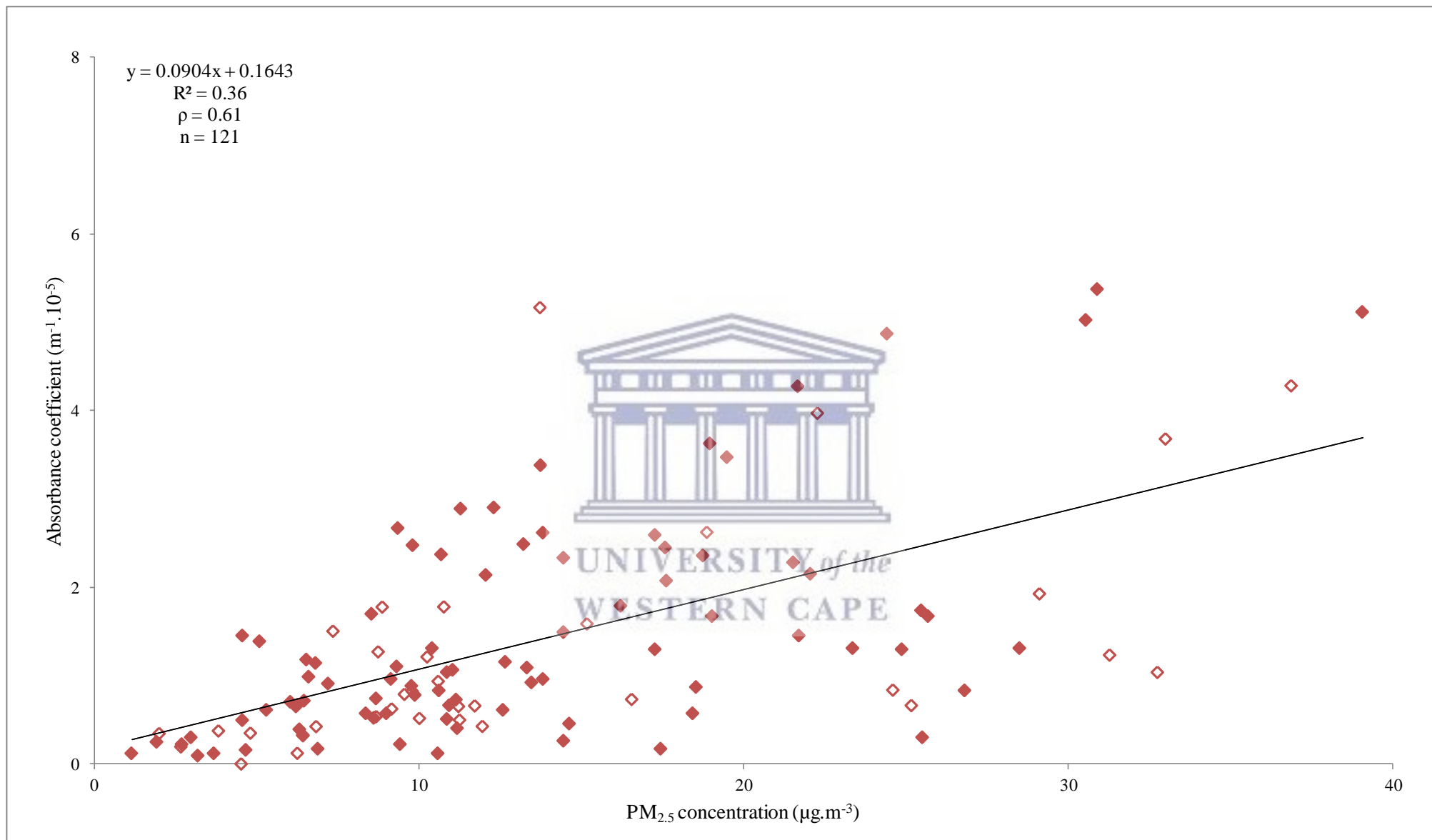


**Fig. 4.15:** PM<sub>2.5</sub> concentrations v. absorption coefficients for the study period. Weekdays are represented by purple diamonds and weekend days by clear diamonds

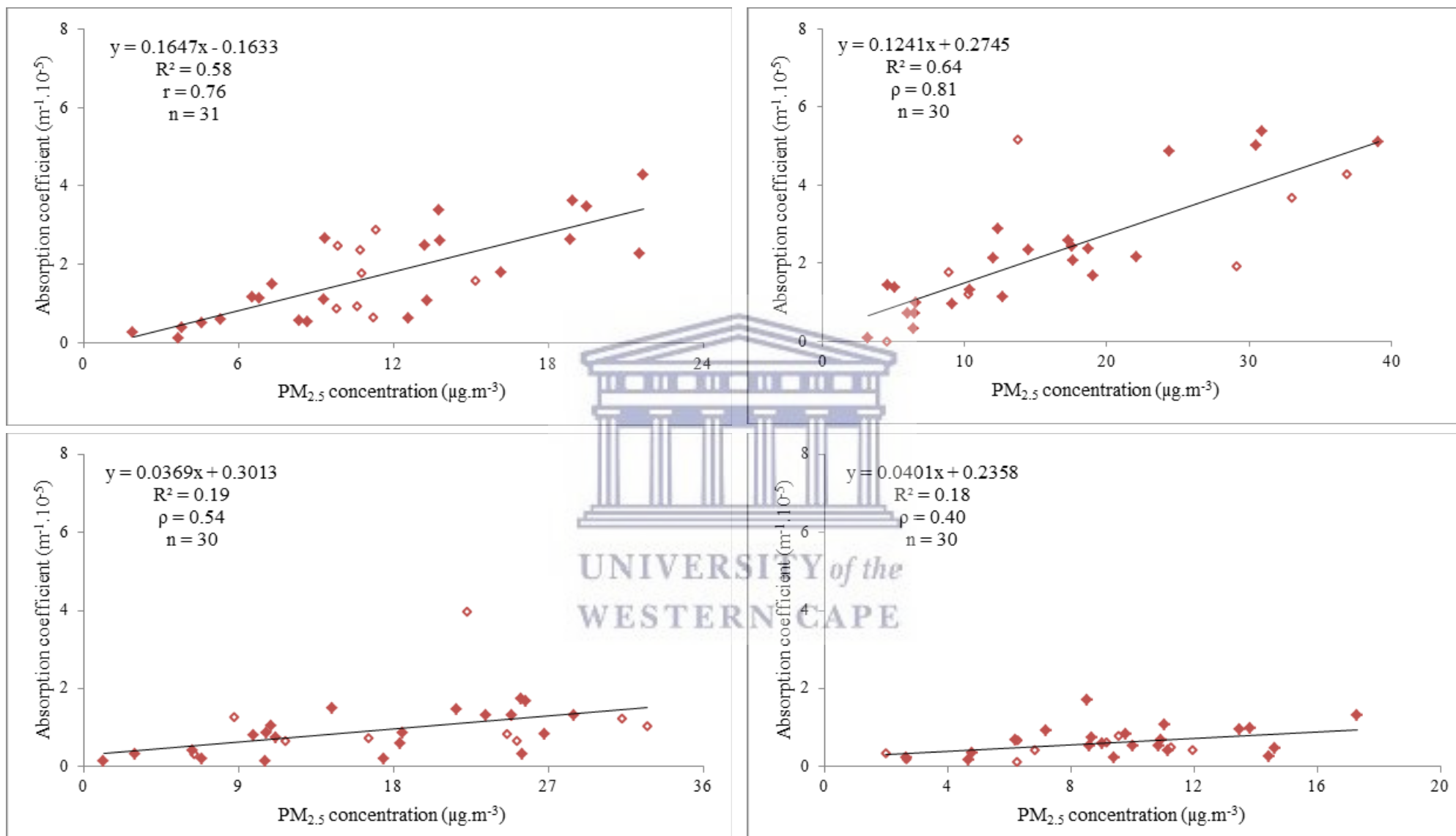


**Fig. 4.16:** PM<sub>2.5</sub> concentrations v. absorption coefficients for, clockwise from top left, autumn, winter, summer and spring. Weekdays are represented by purple diamonds and weekend days by clear diamonds

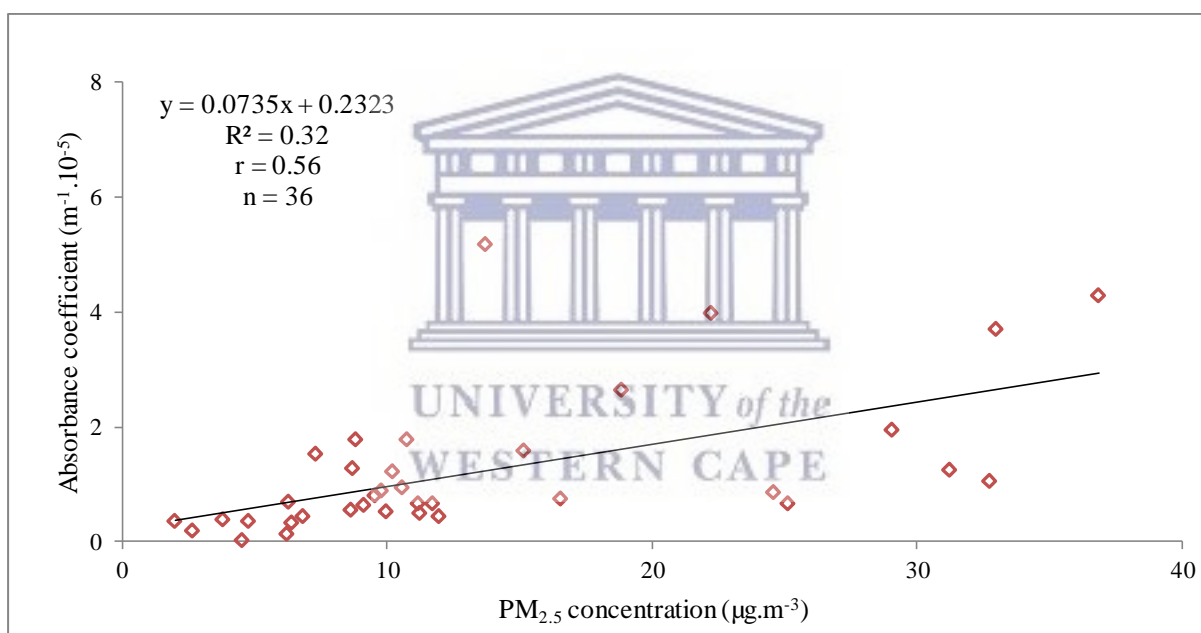
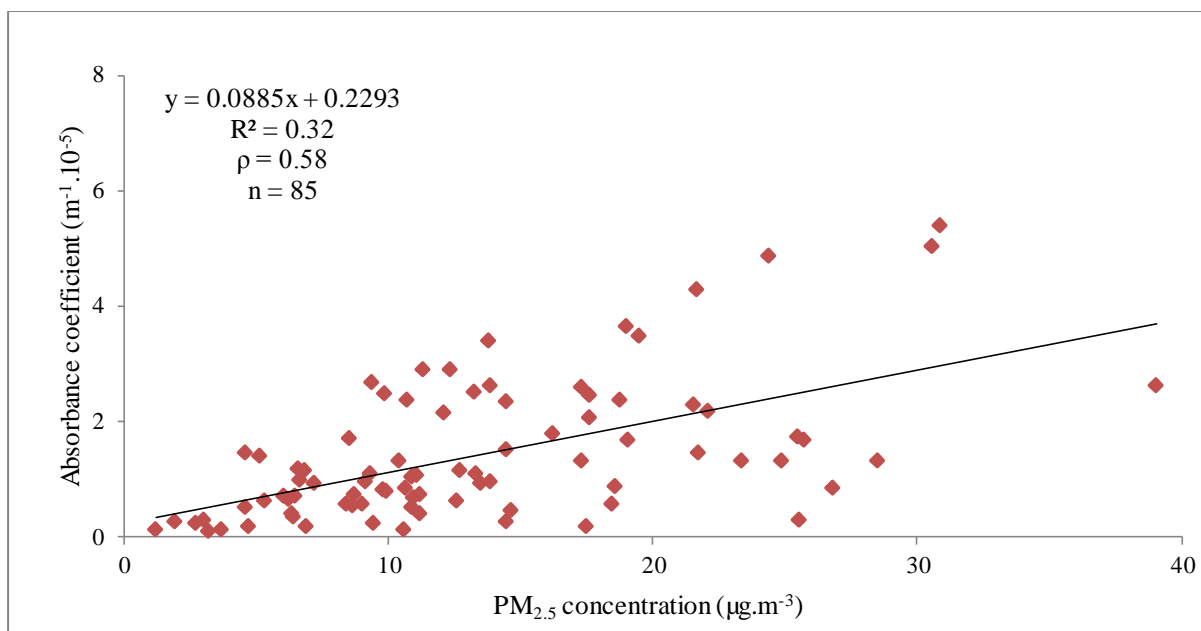


**Fig. 4.17:**  $PM_{2.5}$  concentrations v. absorption coefficients for, from top to bottom, weekday and weekend day data

Correlation between  $PM_{2.5}$  concentration and absorption coefficient values decreased winter through summer but increased sharply in autumn (omission of outliers only affected the strengths of association minimally). Correlation coefficients for weekday and weekend day data were near identical despite  $PM_{2.5}$  concentration and absorption coefficient data having non-normal and normal distribution respectively. Correlation coefficients, strengths of association and linear relationships are shown in Table 4.4 (page 112).

**Table 4.4:** Correlation information

	<b>Normality Test passed?</b>	<b>r</b>	<b><math>\rho</math></b>	<b>R<sup>2</sup></b>	<b>Strength of Association</b>	<b>Strength of linear relationship</b>
Autumn	Yes	0.76	-	0.58	Large	Very strong
Winter	No	-	0.81	0.64	Large	Very strong
Spring	No	-	0.54	0.19	Large	Moderate
Summer	No	-	0.40	0.18	Medium	Moderate
Full study	No	-	0.61	0.36	Large	Strong
Weekday	No	-	0.58	0.32	Large	Strong
Weekend day	Yes	0.56	-	0.32	Large	Strong

In section 4.1.1 it was shown that mean PM<sub>2.5</sub> concentrations for autumn and summer were similar and so were the concentrations for winter and spring. Mean absorption coefficient values, however, varied from season-to-season (no similarities). Data for autumn/summer, winter/spring, and weekday/weekend day samples were tested for significance using the Kruskal-Wallis Test. H-statistics are shown in Table 4.5.

**Table 4.5:** Significance information

	<b>n</b>	<b>H-statistic PM<sub>2.5</sub> concentration</b>	<b>Absorption coefficient</b>
Autumn/Summer	61	613	673
Winter/Spring	60	655	701
Full study	121	14.4	29.0
Weekday/Weekend day	121	0.17	4.94

H-statistic values for autumn/summer and winter/spring were greater than the critical chi-square value (43.7,  $\alpha = 0.05$ ) for sample sizes  $> 31$  thus the null hypothesis was rejected (i.e. medians were unequal). Despite autumn/summer and winter/spring being significantly different, H-statistic values for full study data showed significance between PM<sub>2.5</sub> concentration (14.4) and absorption coefficient values (29.0). Like the full study data, H-statistic values for weekdays/weekend days were  $< 43.7$  thus the null hypothesis was not



rejected (i.e. medians were equal). There was also not enough evidence to suggest that mean values were unequal thus there was no significant differences between filter samples collected on weekdays and weekend days.

#### 4.2 Meteorological conditions for Cape Town

Cape Town has a traditionally Mediterranean climate (see section 2.4.2). Meteorological conditions for the study period did not deviate far from historical trends despite the on-going drought. Meteorological data, supplied by the SAWS station at the South African Astronomical Observatory (SAAO, 23 km SE of the sampling site), is shown in Fig. 4.18.

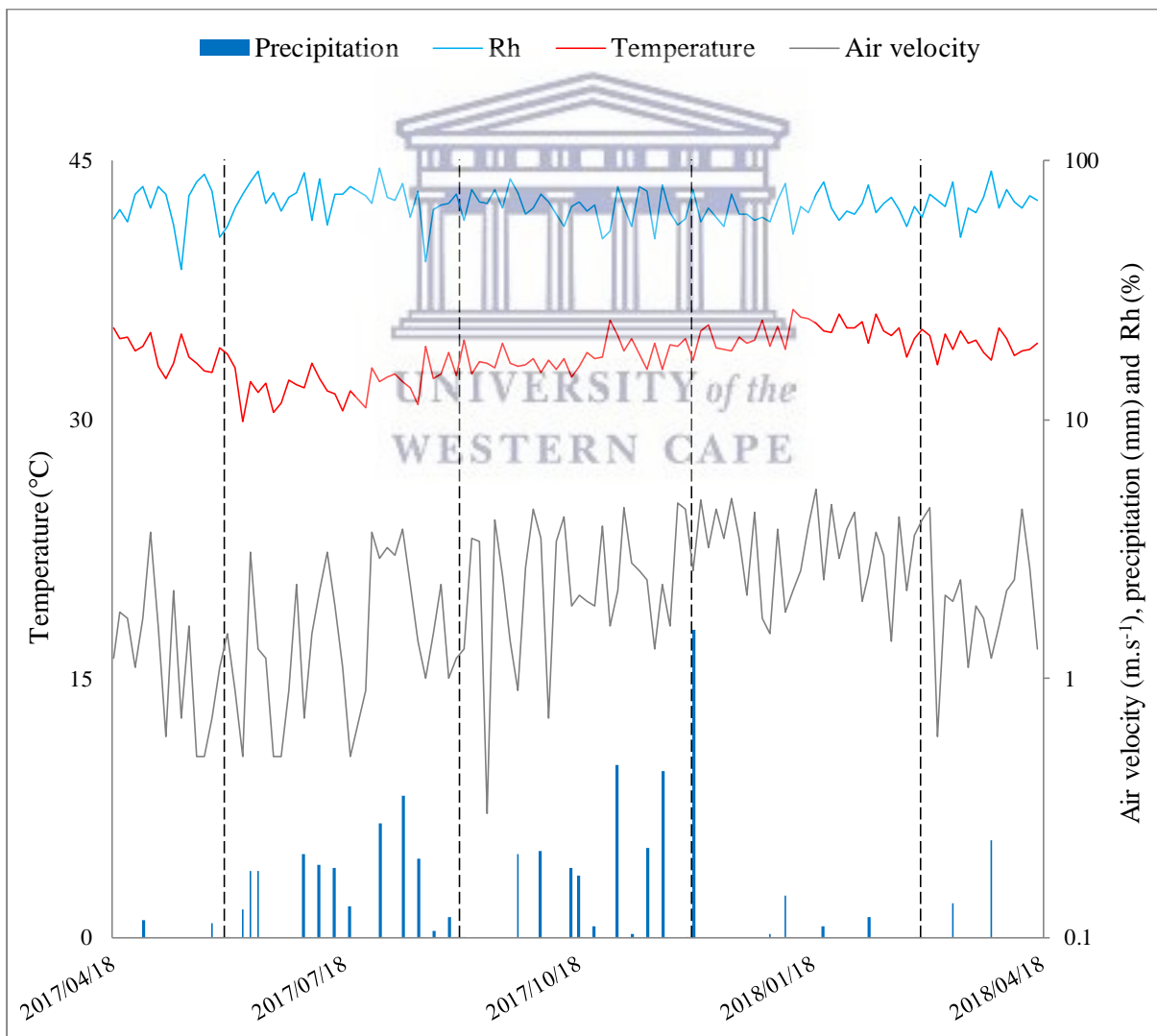


**Fig. 4.18:** Meteorological data for Cape Town for the study period. Broken black lines indicate the start of a new season.

Three meteorological parameters are considered to have the greatest impact on ambient APM dispersion and atmospheric residence times: Rh, temperature and wind. Mean temperature and air velocity were highest for summer with 21.7 °C and 3.2 m.s<sup>-1</sup> respectively. Winter had the lowest mean temperature and air velocity with 14.0 °C and 1.7 m.s<sup>-1</sup> respectively. As expected, winter had the most number of days with rainfall (12) while autumn, surprisingly, had the least number of days with rainfall (4). Meteorological information for the study period is shown in Table 4.6.

**Table 4.6:** Mean temperature, air velocity, Rh and precipitation for the study period

	<b>Autumn</b>	<b>Winter</b>	<b>Spring</b>	<b>Summer</b>	<b>Full study</b>
Mean temperature (°C)	19.1	14.0	17.9	21.7	18.2
Mean min. temperature (°C)	15.0	10.9	14.4	18.5	14.7
Mean max. temperature (°C)	25.7	18.6	23.0	27.1	23.6
Mean air velocity (m.s <sup>-1</sup> )	1.8	1.7	2.6	3.2	2.4
Mean max. air velocity (m.s <sup>-1</sup> )	9.5	8.9	12.2	13.6	11.0
Mean Rh (%)	69	72	67	66	69
Mean min. Rh (%)	47	53	47	48	49
Mean max. Rh (%)	86	89	84	80	85
Precipitation (mm)	9.4	45.0	43.0	22.2	120
Number of days with rainfall	4	12	9	5	30

Of the aforementioned parameters none had a greater effect on air pollution than wind. While wind can reduce pollution levels, a good example being the south-easterly wind (nicknamed “Cape Doctor”) that blows in Cape Town harmful air pollutants from the area, wind can also contribute to pollution levels, moving pollutants from one area to another. In section 2.4.2 it was shown that south-easterly and north-westerly wind directions dominated the region in 2016, with 21 % and 13 % respectively. For the study period, three wind directions dominated: northerly (N, 17.5 %), south-south easterly (SSE, 16.5 %) and north-westerly (NW, 15 %). The frequencies for southerly- and northerly directions were near identical with 44.0 % and 43.9 % respectively (combined, easterly and westerly directions totalled 12.1 %). Monthly and seasonal wind direction information for the study period is shown in Table 4.7 (page 115) and seasonal frequencies in Fig. 4.19 (page 116) and Fig. 4.20 (page 117).

**Table 4.7: Monthly and seasonal wind direction information**

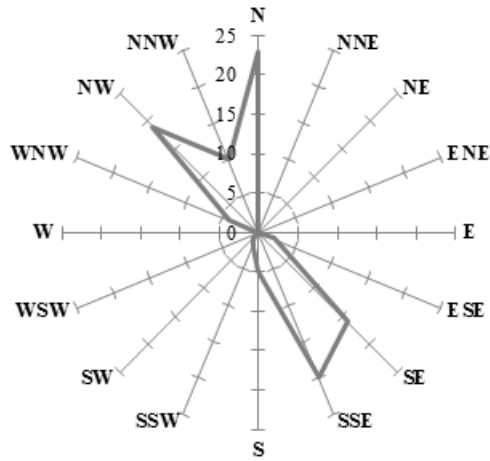
**MONTHLY DATA**

Wind direction																											
Month	Wind direction																Total occurrences	Northerly directions	Southerly directions	% N	% S	% other directions	Sample days	% Weekdays	Weekend +PH	% Weekend +PH	
	N	NNE	NE	ENE	E	ESE	SE	SSE	S	SSW	SW	WSW	W	WNW	NW	NNW											
April 2017	3	0	0	0	0	0	3	5	0	0	0	0	0	2	1	14	6	8	42.9	57.1	0.0	5	3	60	2	40	
May	7	0	0	0	0	1	2	4	2	1	1	0	0	3	8	3	32	18	10	56.3	31.3	12.5	10	7	70	3	30
June	9	0	0	1	1	1	2	3	3	3	1	1	1	2	7	4	39	20	12	51.3	30.8	17.9	10	8	80	2	20
July	8	0	0	0	1	0	4	3	1	0	0	0	0	5	6	7	35	21	8	60.0	22.9	17.1	9	6	67	3	33
August	4	0	0	0	0	2	4	5	5	0	1	1	0	1	5	5	33	14	15	42.4	45.5	12.1	11	9	82	2	18
September	6	0	0	0	1	4	2	7	5	0	0	0	0	6	2	33	14	14	42.4	42.4	15.2	10	6	60	4	40	
October	6	0	0	0	0	2	5	5	2	0	0	1	1	3	7	4	36	17	12	47.2	33.3	19.4	10	8	80	2	20
November	5	0	0	0	1	1	7	5	2	0	0	0	0	5	3	1	30	9	14	30.0	46.7	23.3	10	7	70	3	30
December	1	0	0	1	0	2	9	9	0	0	0	0	0	2	3	3	30	7	18	23.3	60.0	16.7	10	6	60	4	40
January 2018	5	0	0	0	0	4	5	4	4	6	2	0	0	1	1	2	34	8	21	23.5	61.8	14.7	11	7	64	4	36
February	3	0	0	0	0	0	5	5	3	3	1	0	0	2	3	2	27	8	17	29.6	63.0	7.4	9	6	67	3	33
March	8	0	0	0	0	0	6	6	3	1	0	0	0	1	5	3	33	16	16	48.5	48.5	3.0	10	8	80	2	20
April	5	0	0	0	0	1	5	5	0	0	0	0	0	0	4	3	23	12	10	52.2	43.5	4.3	6	4	67	2	33
Mean	5.4	0.0	0.0	0.2	0.3	1.4	4.5	5.1	2.3	1.1	0.5	0.2	0.2	1.9	4.6	3.1	30.7	13.1	13.5	42.3	45.1	12.6	9.3	6.5	69.7	2.8	30.3

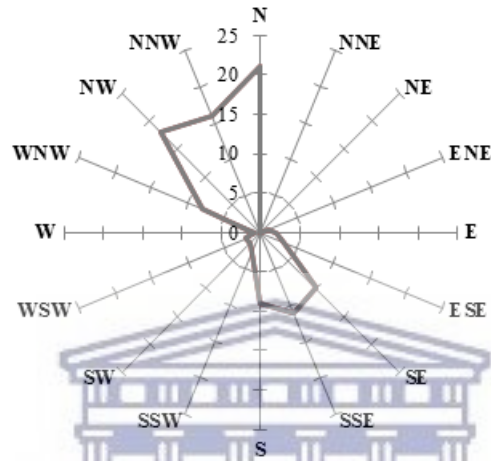
**SEASONAL DATA**

Wind direction																											
Month	Wind direction																Total occurrences	Northerly directions	Southerly directions	% N	% S	% other directions	Sample days	% Weekdays	Weekend +PH	% Weekend +PH	
	N	NNE	NE	ENE	E	ESE	SE	SSE	S	SSW	SW	WSW	W	WNW	NW	NNW											
Autumn 2017	10	0	0	0	0	1	5	9	2	1	1	0	0	3	10	4	46	24	18	52.2	39.1	8.7	15	10	67	5	33
Winter	21	0	0	1	2	3	10	11	9	3	2	2	1	8	18	16	107	55	35	51.4	32.7	15.9	30	23	77	7	23
Spring	17	0	0	0	2	7	14	17	9	0	0	1	1	8	16	7	99	40	40	40.4	40.4	19.2	30	21	70	9	30
Summer	9	0	0	1	0	6	19	18	7	9	3	0	0	5	7	7	91	23	56	25.3	61.5	13.2	30	19	63	11	37
Autumn 2018	13	0	0	0	0	1	11	11	3	1	0	0	0	1	9	6	56	28	26	50.0	46.4	3.6	16	12	75	4	25
Mean	14.0	0.0	0.0	0.4	0.8	3.6	11.8	13.2	6.0	2.8	1.2	0.6	0.4	5.0	12.0	8.0	79.8	34.0	35.0	43.9	44.0	12.1	24.2	17.0	70.3	7.2	29.7

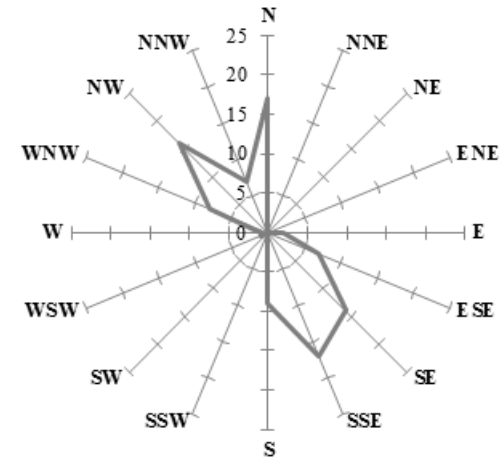
**AUTUMN**



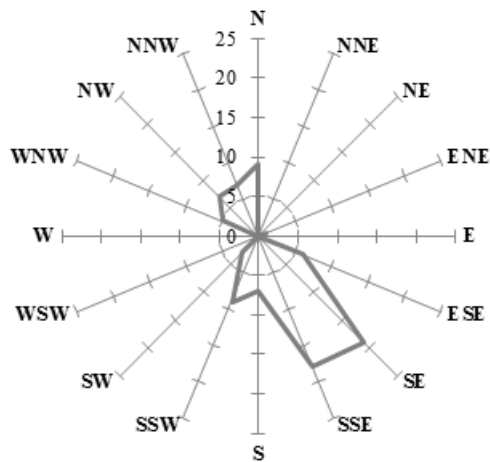
**WINTER**



**SPRING**



**SUMMER**



**PRIMARY WIND DIRECTIONS**

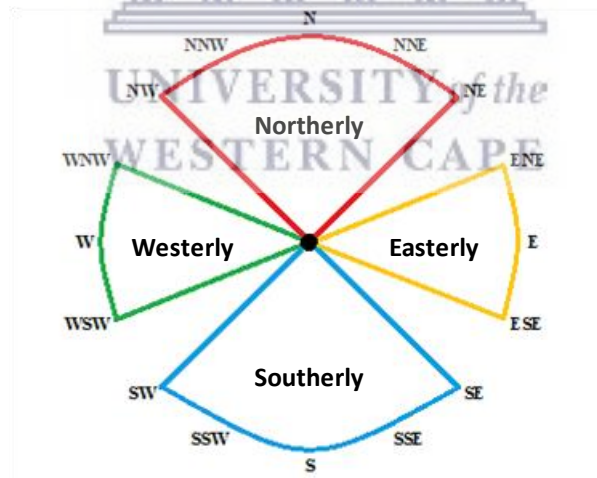


*Fig. 4.19: Seasonal wind direction frequencies.*

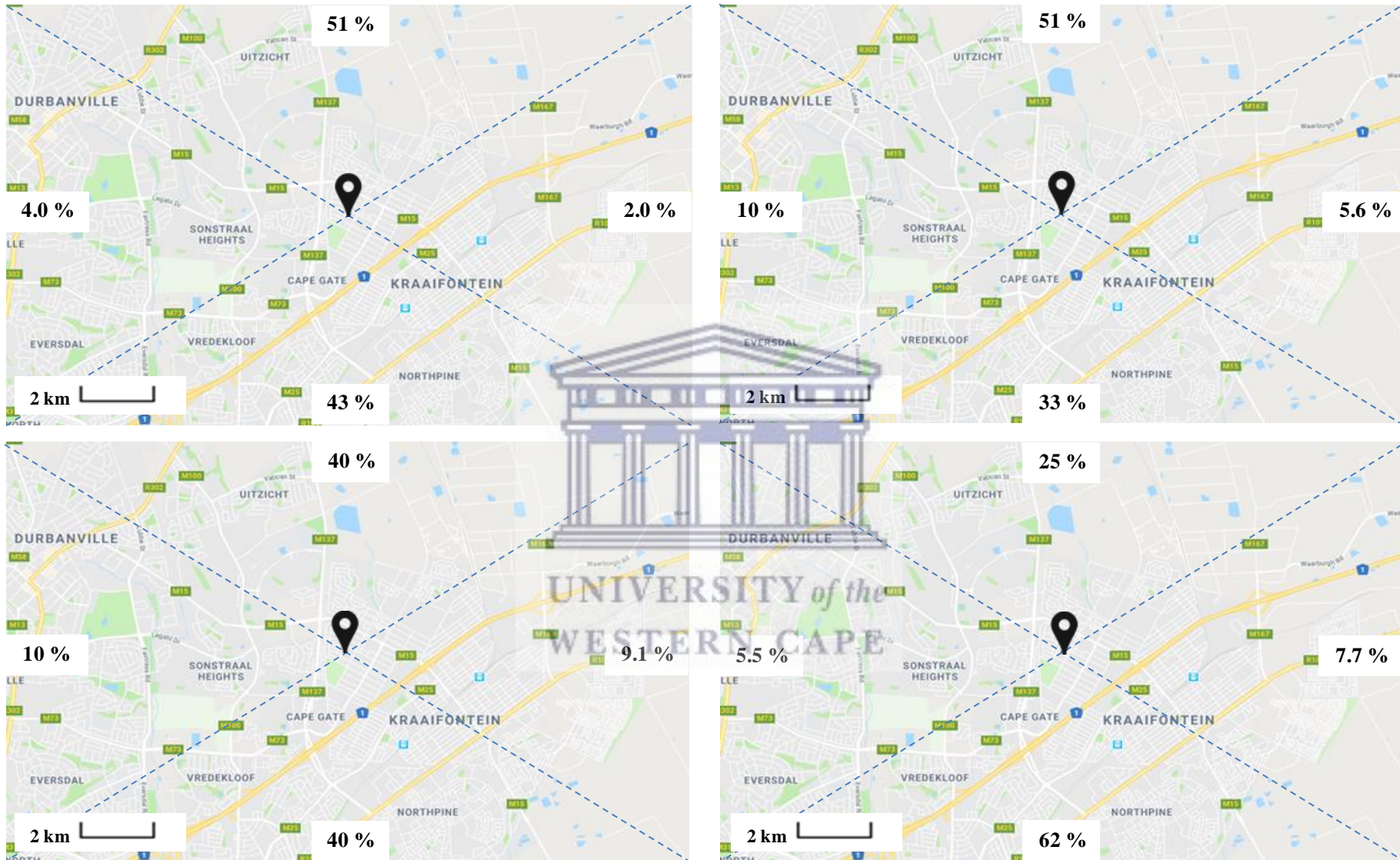


**Fig. 4.20:** Seasonal wind direction frequencies (continued). Percentage frequency of the four primary wind directions (North, East, South and West) for, clockwise from top-left, autumn, winter, summer and spring. *Note:* Wind directions indicate which direction wind was blowing from and black markers show the location of the sampling site.

Seasonal frequencies for northerly and southerly wind directions were remarkably similar. Radar plots of seasonal wind directions (Fig. 4.19, page 116) showed that northerly directions dominated in autumn (51.0 %) and winter (51.4 %) while southerly directions dominated in summer (61.5 %). Frequencies for northerly and southerly directions were identical for spring (40.4 %). Wind information for the study period showed that south-easterly (SE, SSE) frequency increased from 21 % (in 2016) to 31.3 % (an increase of 48 % year-on-year) and north-westerly (NNW, NW) frequency increased from 13 % (in 2016) to 25.1 % (an increase of 93 % year-on-year). Changes in PM<sub>2.5</sub> concentrations and absorption coefficients with temperature are shown in Table 4.8 which is immediately followed by changes in seasonal PM<sub>2.5</sub> concentrations and absorption coefficients shown in Fig. 4.21.

**Table 4.8:** Mean PM<sub>2.5</sub> concentration and absorption coefficient values for three temperature ranges. Concentrations are in  $\mu\text{g}\cdot\text{m}^{-3}$  and absorption coefficients in  $\text{m}^{-1}\cdot 10^{-5}$ .

Temperature (°C)	< 16	16-20	> 20
PM <sub>2.5</sub> concentration	15.9	13.1	11.5
Absorption coefficient	1.94	1.08	1.25
Number of samples	36	47	38

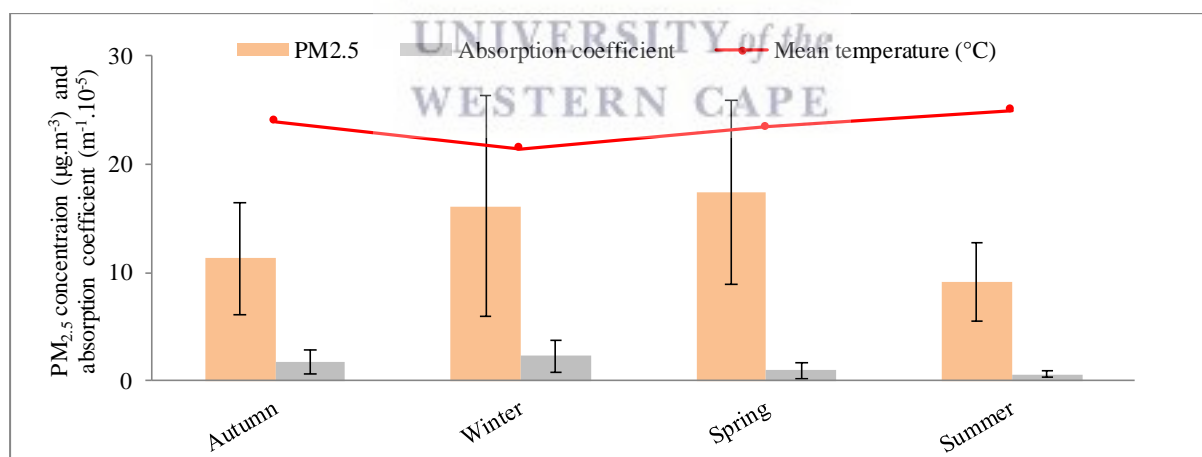


**Fig. 4.21:** Seasonal ambient APM concentrations v. temperature

Changes in ambient APM concentrations with temperature are discussed in section 5.1.2.2. Changes in PM<sub>2.5</sub> concentrations and absorption coefficients with Rh and precipitation are shown in Table 4.9 (page 119) which is immediately followed by changes in seasonal PM<sub>2.5</sub> concentrations and absorption coefficients are shown in Fig. 4.22.

**Table 4.9:** Mean  $PM_{2.5}$  concentration and absorption coefficient values for three Rh and precipitation ranges. Concentrations are in  $\mu g.m^{-3}$  and absorption coefficients in  $m^{-1}.10^{-5}$ .

Rh (%)	< 65	65-75	> 75
$PM_{2.5}$ concentration	14.4	14.1	10.3
Absorption coefficient	1.64	1.44	0.97
Number of samples	41	50	30
Precipitation (mm)	0	0.1-3	> 3
$PM_{2.5}$ concentration	13.9	11.5	12.6
Absorption coefficient	1.57	0.96	0.73
Number of samples	91	13	17

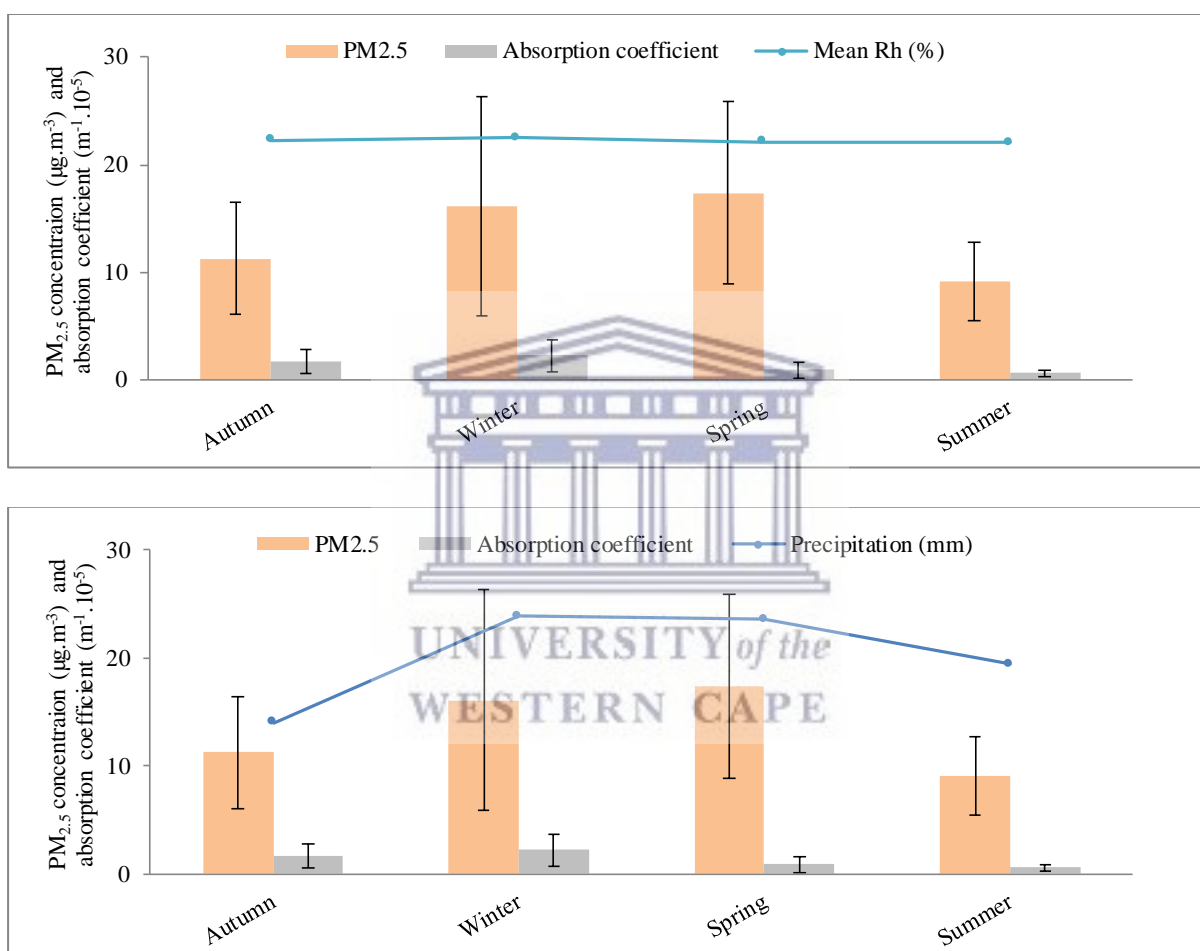


**Fig. 4.22:** Seasonal ambient APM concentrations v. Rh and precipitation

Changes in ambient APM concentrations with Rh and precipitation are discussed in section 5.1.2.3. Changes in  $PM_{2.5}$  concentrations and absorption coefficients with air velocity are shown in Table 4.10 (page 120) which is immediately followed by changes in seasonal  $PM_{2.5}$  concentrations and absorption coefficients shown in Fig. 4.23.

**Table 4.10:** Mean  $PM_{2.5}$  concentration and absorption coefficient values for three air velocity ranges. Concentrations are in  $\mu g.m^{-3}$  and absorption coefficients in  $m^{-1}.10^{-5}$ .

Air velocity ( $m.s^{-1}$ )	< 1.5	1.5-2.5	> 2.5
$PM_{2.5}$ concentration	16.9	12.5	11.8
Absorption coefficient	2.26	1.17	0.94
Number of samples	34	41	46

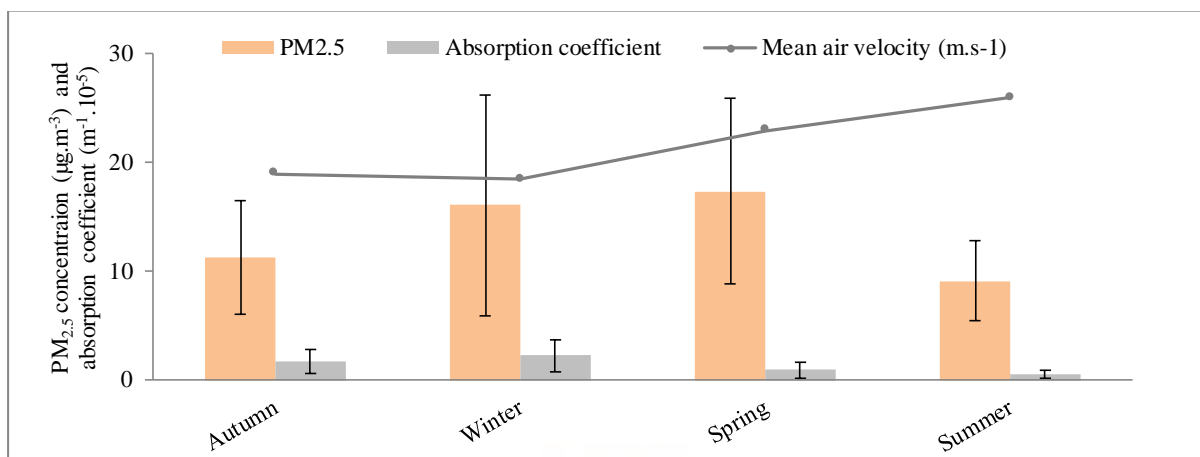


**Fig. 4.23:** Seasonal ambient APM concentrations v. air velocity

Changes in ambient APM concentrations with air velocity are discussed in section 5.1.2.4.

Changes in  $PM_{2.5}$  concentrations and absorption coefficients with wind direction are shown in

Fig. 4.24

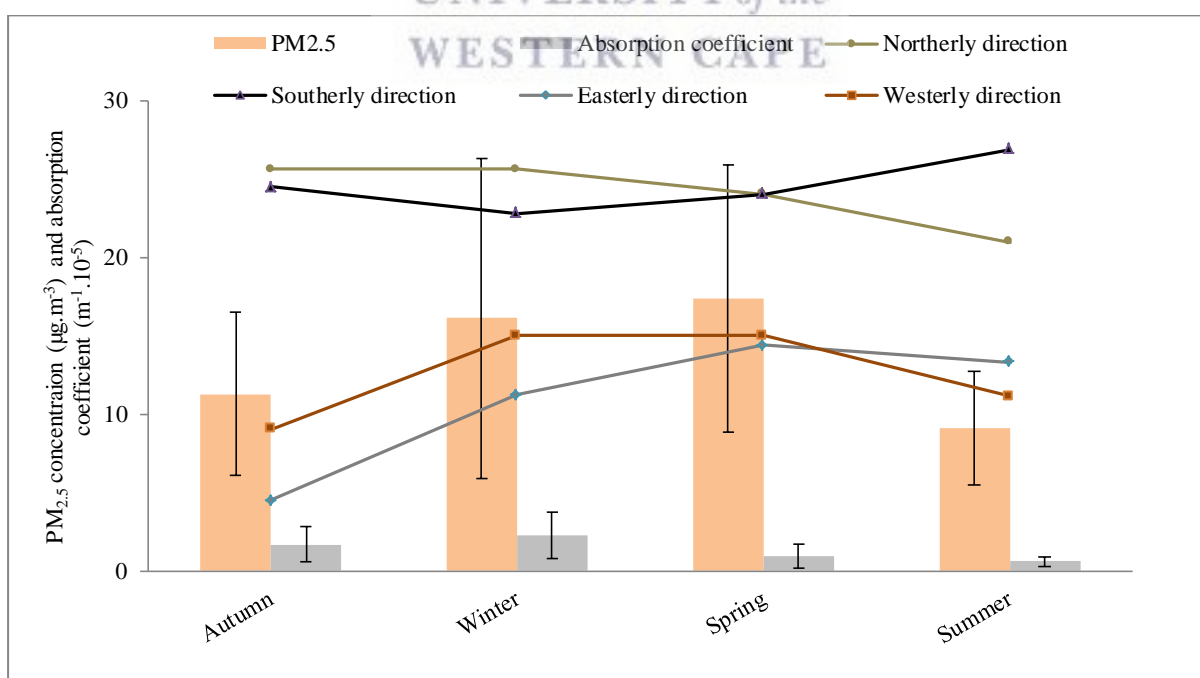


**Fig. 4.24:** Seasonal ambient APM concentrations v. wind direction



Changes in ambient APM concentrations with wind direction are discussed in section 5.1.3.

Changes in  $PM_{2.5}$  concentrations and absorption coefficients with percentage clear skies (UV exposure) are shown in Fig. 4.25.

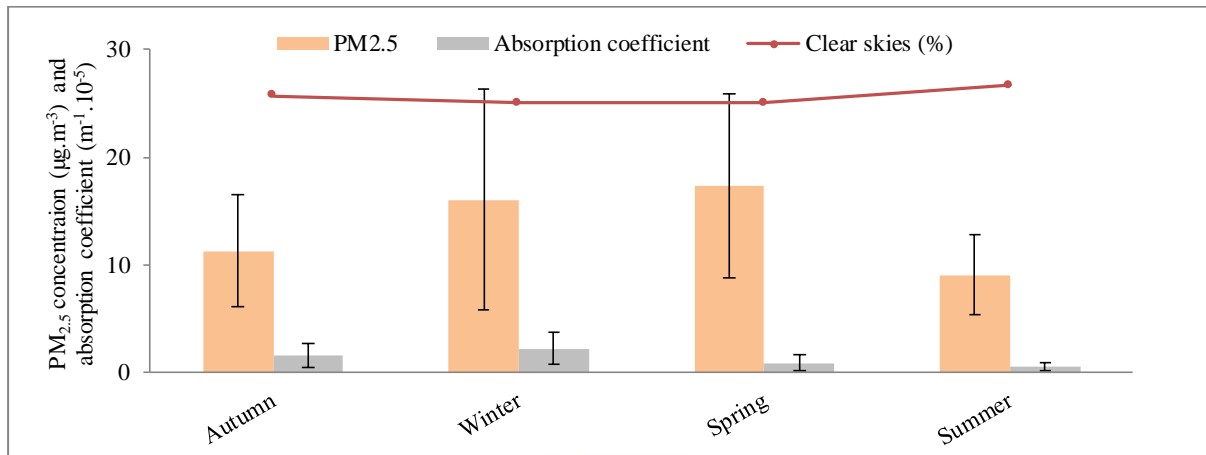


**Fig. 4.25:** Seasonal ambient APM concentrations v. percentage clear skies. Maximum UV exposure was had when skies were clear

Changes in ambient APM concentrations with UV exposure are discussed in section 5.1.2.4.

The effects of meteorological conditions on ambient APM concentrations varied considerably. In some instances there were significant differences in seasonal concentrations while meteorological conditions were similar while in others, seasonal concentrations were similar when meteorological conditions varied considerably. Some meteorological parameters had greater impact on ambient APM concentrations than others (e.g. air velocity) but ultimately changes in ambient APM concentrations cannot solely be explained by changes in meteorological conditions. The impacts of meteorological parameters  $PM_{2.5}$  concentrations and absorption coefficients are discussed in section 5.2.

### 4.3 Origins and trajectories of air masses in Cape Town

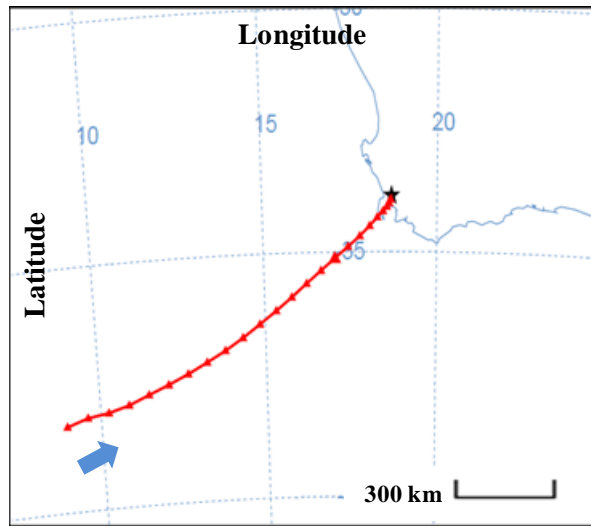
#### 4.3.1 Trajectories

Trajectories are visual representations of air mass transport routes for a particular geographical area over a specific time period. A total of 121, 24-hour backward trajectories (09:00 a.m. to 09:00 a.m.) were generated for the sample period using the HYSPLIT-WEB model. Six trajectories predominated (Fig. 4.26, page 123). These were:

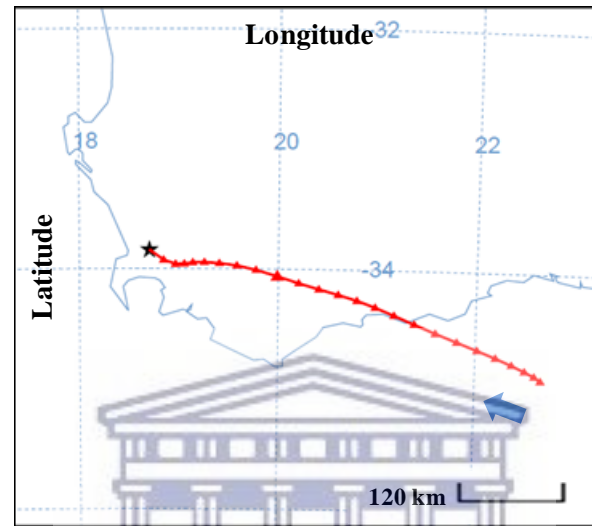
- Atlantic-Ocean
- Indian-Ocean
- Regional
- Saldanha
- National
- Transboundary

The trajectory *Atlantic-Ocean* was characterised by air masses emanating from the most southerly and south-easterly parts of the Atlantic Ocean; *Indian-Ocean* by air masses emanating from the most south-westerly parts of the Indian Ocean (from False Bay to Mossel Bay); *Regional* by air masses emanating from within the Western Cape; *Saldanha* by air masses emanating from the Atlantic Ocean passing over the town of Saldanha; *National* by air masses emanating from the Eastern and Northern Cape Provinces and *Transboundary* by air masses emanating from neighbouring countries Botswana and Namibia.

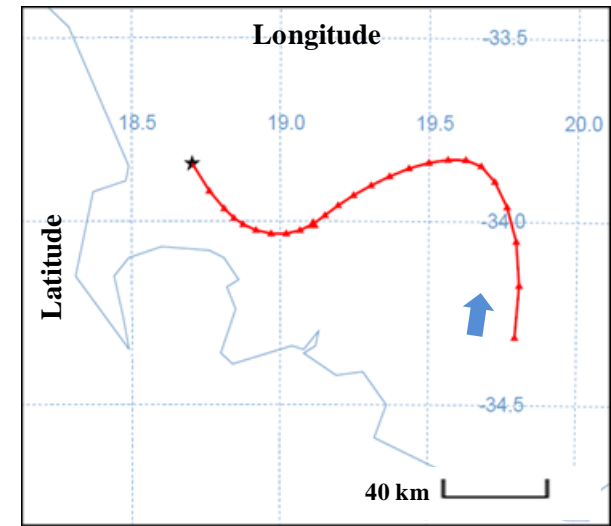
Atlantic-Ocean



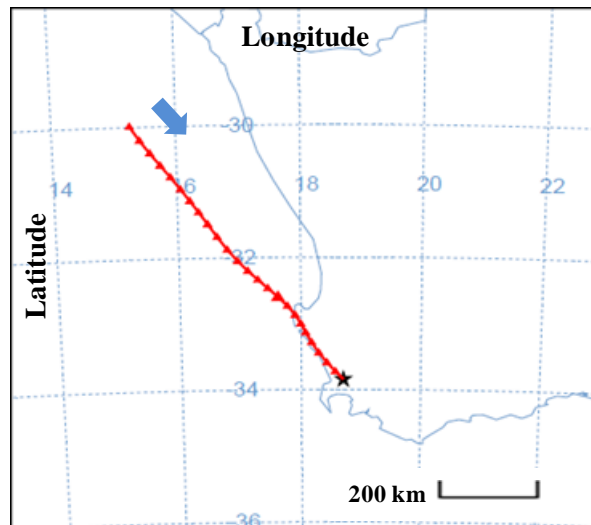
Indian-Ocean



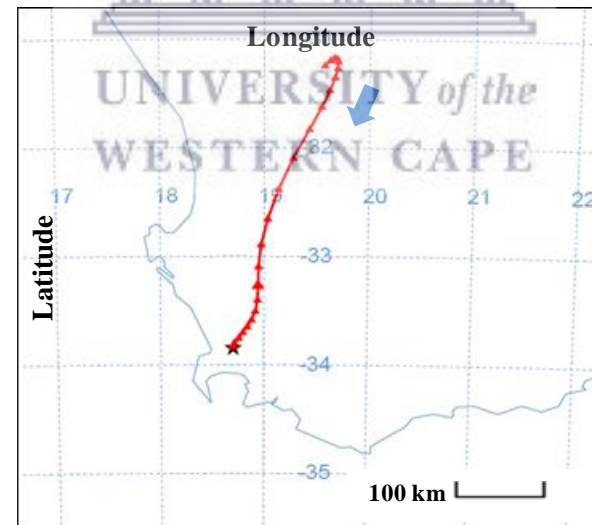
Regional



Saldanha



National



Transboundary

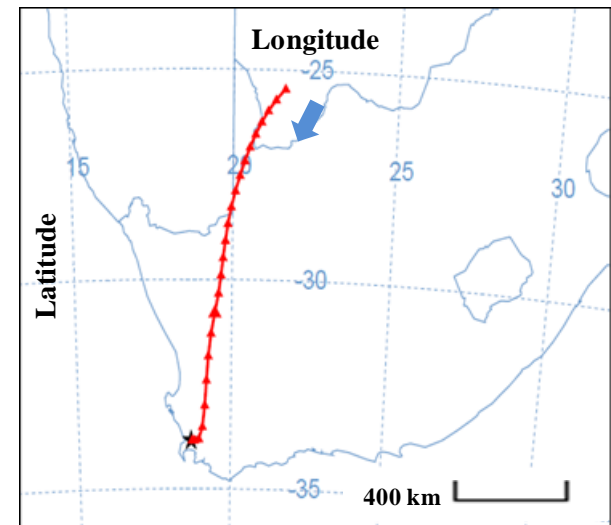


**Fig. 4.26:** Dominating trajectories derived from the HYSPLIT model. Trajectories plot the movement of air masses from their origins to the sampling site (star) over a period of 24 hours with one hour markers (triangles). Single 24 hour trajectories, like above, have an error of 30 %.

### 4.3.2 Trajectory frequencies

Annual frequencies of the six predominating trajectories were *Atlantic-Ocean* (38.8 %), *Indian-Ocean* (26.4 %), *Regional* (16.5 %), *Saldanha* (12.4 %), *National* (4.96 %) and *Transboundary* (0.83 %). Seasonality of trajectories showed that trajectory *Atlantic-Ocean* was the most frequent in autumn, winter and spring (32.3-46.7 %). Trajectory *Indian-Ocean* was most frequent in summer with 13 occurrences (43.3 %). Autumn had the highest occurrences of cluster *Regional* (10, 29.0 %) while the highest occurrences of *Saldanha*, *National* and *Transboundary* trajectories were in winter (7, 23.3 %), summer (3, 10.0 %), and autumn (1, 3.23 %) respectively. Seasonal trajectory frequencies are shown in Fig. 4.27.

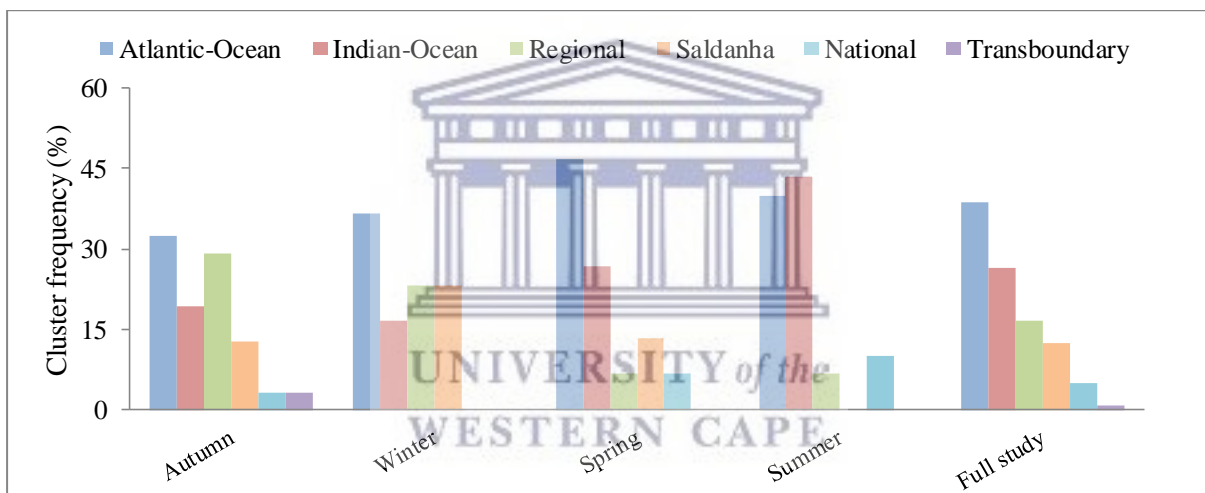


**Fig. 4.27:** Single trajectory frequencies

Trajectories *Atlantic-Ocean* and *Regional* predominated in autumn with frequencies of 32.3 % and 29.0 % respectively. In winter, three trajectories predominated; *Atlantic-Ocean* with 36.7 % followed by *Saldanha* and *Regional* both with 23.3 %. *Atlantic-Ocean* was most frequent in spring (46.7 %) with *Indian-Ocean* (26.7 %) and *Saldanha* (13.3 %) in second and third places. Trajectory *Indian-Ocean* (43.3 %) was most frequent in spring followed closely by cluster *Atlantic-Ocean* with 40.0 %. Seasonal trajectory clusters are shown in Fig. 4.28 (page 125) and plots of trajectory frequencies in Fig. 4.29 (page 126) and Fig. 4.30 (page 127).

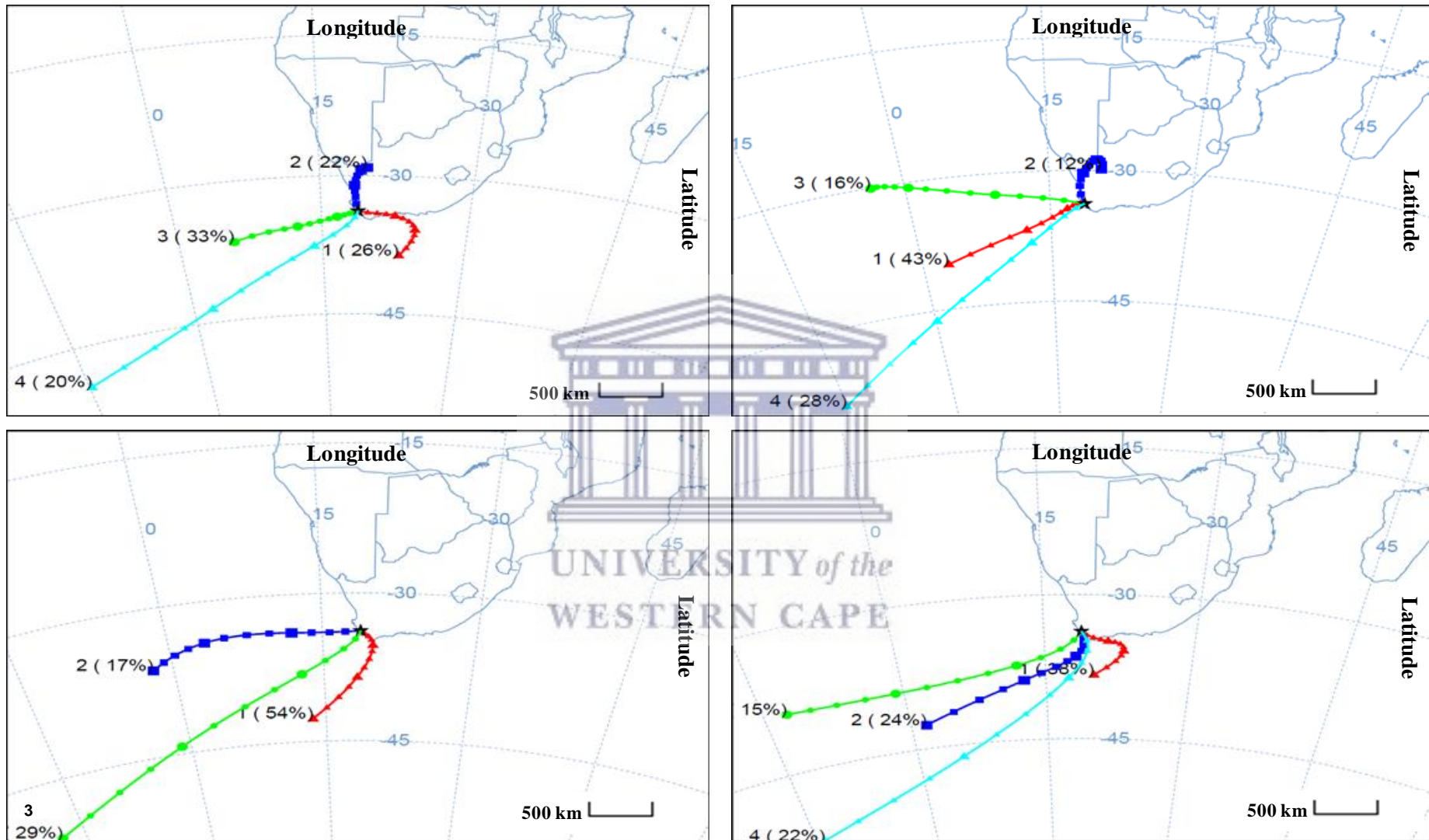
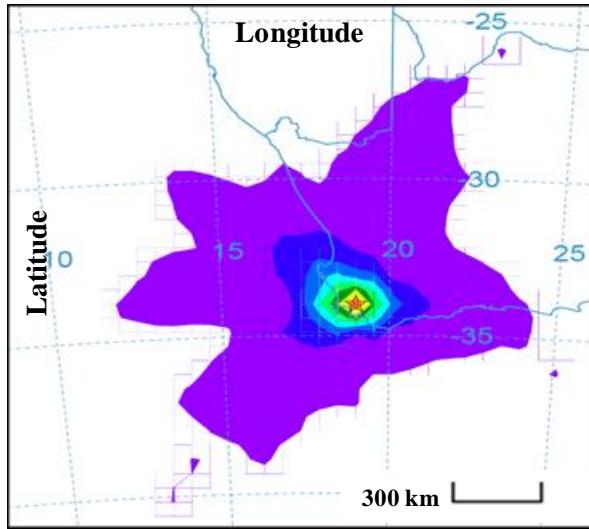
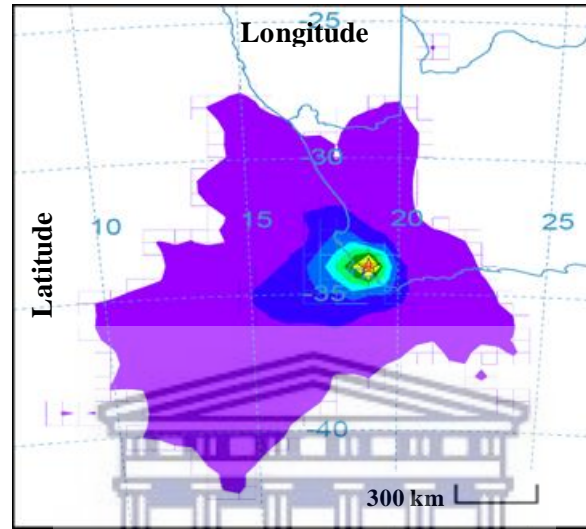


*Fig. 4.28: Seasonal cluster plots. Clusters are “mean” values of the most prevalent trajectories for each season. Clusters for, clockwise from top-left, autumn, winter, summer and spring are shown above.*

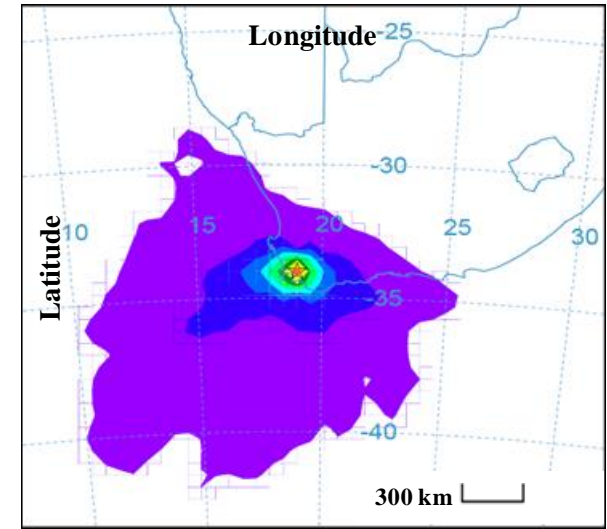
Autumn (18 April – May 2017)



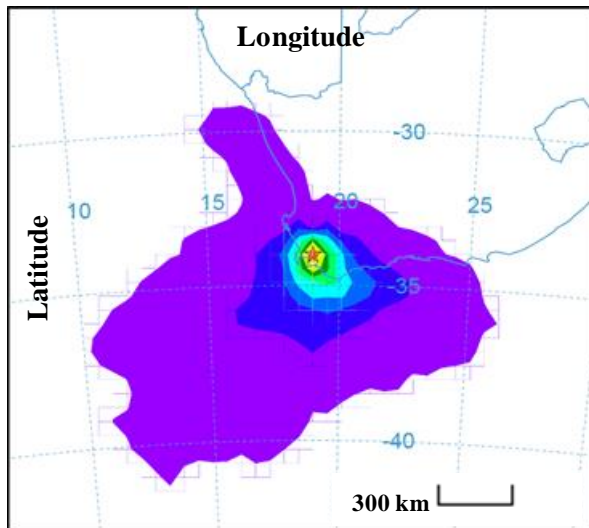
Winter (June – August 2017)



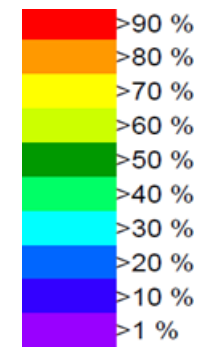
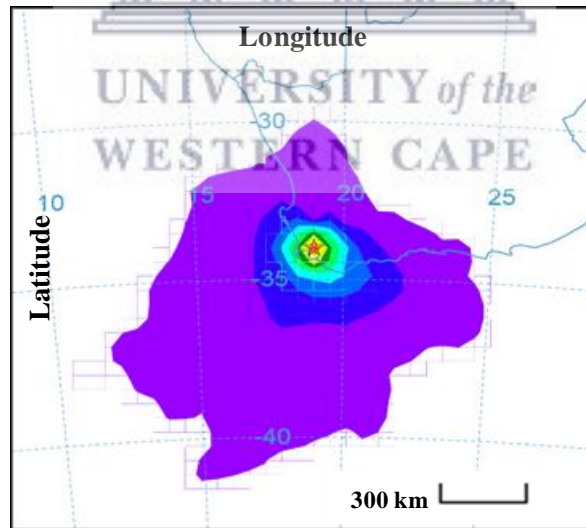
Spring (September – November 2017)



Summer (December 2017 – February 2018)



Autumn (March – 16 April 2018)

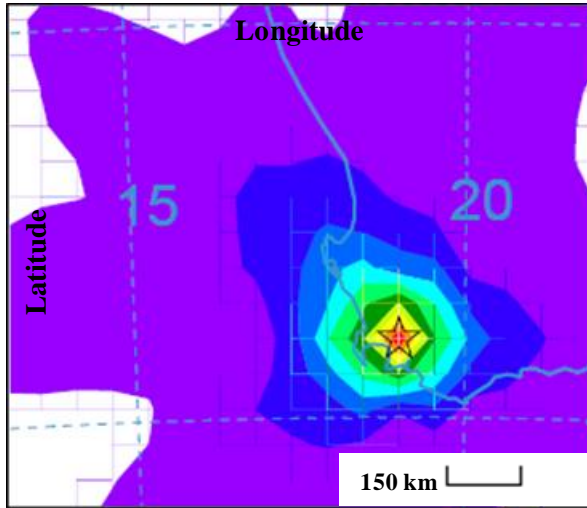


**Frequency scale**

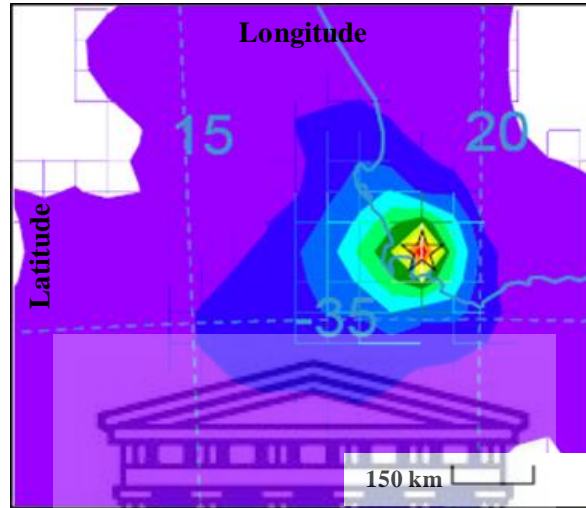
(Number of trajectories passing through square grid divided by number of trajectories) multiplied by 100

**Fig. 4.29:** Seasonal trajectory frequency plots (with the star representing the sampling site). The origins of air masses differed considerably season-to-season. A commonality amongst frequency, cluster and single plots was that a large percentage of trajectories originated from the Atlantic and Indian oceans.

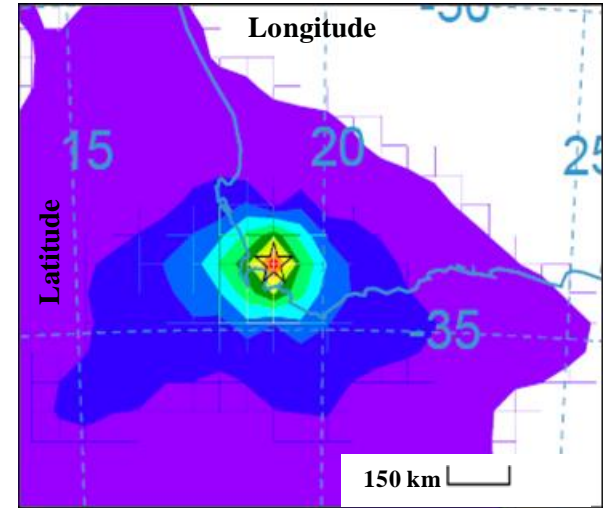
Autumn (18 April – May 2017)



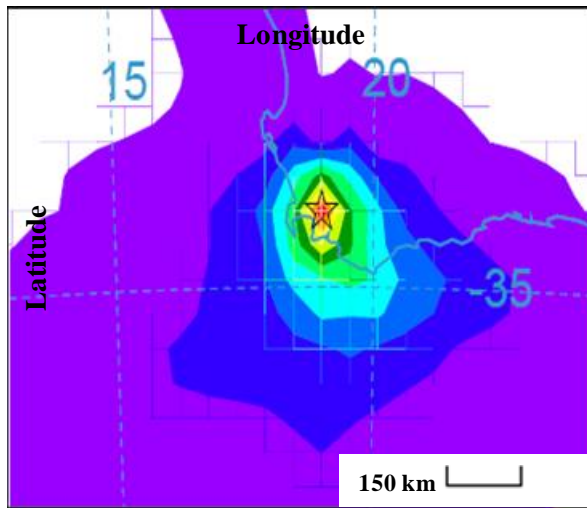
Winter (June – August 2017)



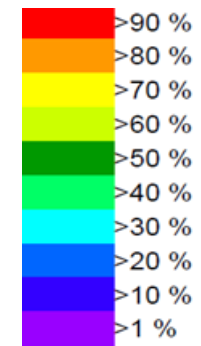
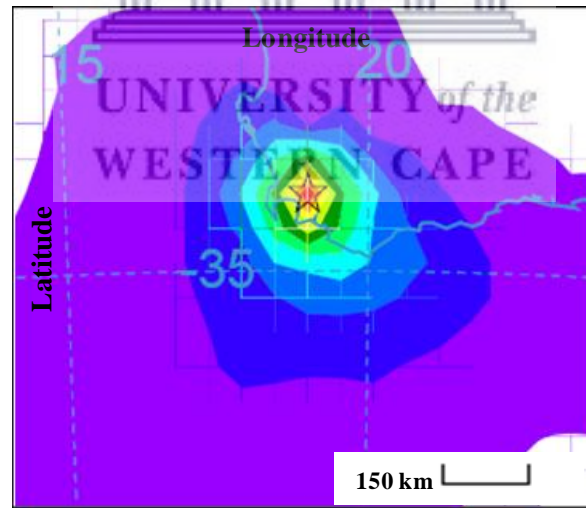
Spring (September – November 2017)



Summer (December 2017 – February 2018)



Autumn (March – 16 April 2018)



**Frequency scale**

(Number of trajectories passing through square grid divided by number of trajectories) multiplied by 100

Fig. 4.30: Seasonal trajectory frequency plots (Zoom factor: 2)

Seasonal air mass clusters (Fig. 4.28, page 125) were plots of mean transport routes of air masses for each season during the study period. Three clusters dominated: clusters Atlantic-Ocean, Indian-Ocean and Inland. Mean cluster frequencies are shown in Table 4.11.

**Table 4.11:** Cluster frequencies (%) for each season and full study period

	<b>Autumn</b>	<b>Winter</b>	<b>Spring</b>	<b>Summer</b>	<b>Full study (mean)</b>
Atlantic-Ocean	53	87	46	61	61.8
Indian-Ocean	26	-	54	38	29.5
Inland	22	12	-	-	8.50
Total	101	99	100	99	99.8

Air masses emanating from Atlantic Ocean dominated for autumn, winter, summer and the full study period. Mean frequency for cluster Atlantic-Ocean was 61.8 % (nearly two-thirds of all trajectories passing over Cape Town emanated from the Atlantic Ocean). Air masses emanating from the Indian Ocean dominated for spring. Mean frequency for cluster Indian-Ocean was 29.5 % (nearly one-third of all trajectories passing over Cape Town emanated from the Indian Ocean). Combined, air mass clusters emanating from oceanic areas accounted for 91.3 % of all trajectories passing over Cape Town. Chemical compositions of PM in composite samples (see section 4.5.4), particularly chloride (27-31 wt. %), was evidence of this. Air masses emanating from inland and regional areas were the least frequent with a mean frequency of 8.50 %.

#### 4.4 Correlation between study data and air pollution data collected by the CoCT

##### 4.4.1 Seasonal air pollution data

Availability of AAQM stations was a major issue as all stations experienced periods of down time (ranging from an hour to several months) during which no data was recorded (overall station availability index: 41-87 %). Table 4.12 (page 129) shows seasonal air pollution data. Mean seasonal concentrations were calculated from mean monthly concentrations (see Appendix 14). Representative sample sizes were calculated using Yamane (1967) formula.



**Table 4.12:** Mean seasonal concentrations for six AAQM stations in Cape Town (concentrations of NO<sub>2</sub>/SO<sub>2</sub>/O<sub>3</sub>/PM<sub>10</sub> in µg.m<sup>-3</sup>, CO in mg.m<sup>-3</sup>)

	Atlantis	City Hall	Goodwood	Somerset-West	Tableview	Wallacedene
Coordinates (latitude/longitude)	-33.5623, 18.4805	-33.9251, 18.4237	-33.9024, 18.5651	-34.0774, 18.8318	-33.8196, 18.5143	-33.8570, 18.7259
Distance from sampling site (km)	37	27	14	29	18	3
Station availability (%)	73	63	41	81	87	74
Number of parameters monitored	2	3	4	1	2	4
<b>AUTUMN (Yamane sample size (n) = 14 days, e = 0.05)</b>						
Carbon monoxide (CO)	-	2.14	*	-	-	-
Nitrogen dioxide (NO <sub>2</sub> )	-	22.5	*	-	11.9	20.5
Ozone (O <sub>3</sub> )	45.4	-	24.1	-	-	27.8
Sulfur dioxide (SO <sub>2</sub> )	2.61	6.52	6.96	2.74	7.49	5.11
Particulate matter (PM <sub>10</sub> )	-	-	-	-	-	33.2
<b>WINTER (Yamane sample size (n) = 14 days, e = 0.05)</b>						
Carbon monoxide (CO)	-	2.64	1.06	-	-	-
Nitrogen dioxide (NO <sub>2</sub> )	-	31.3	27.1	-	13.7	*
Ozone (O <sub>3</sub> )	50.6	-	28.9	-	-	27.5
Sulfur dioxide (SO <sub>2</sub> )	3.66	1.81	12.5	3.14	5.43	5.09
Particulate matter (PM <sub>10</sub> )	-	-	-	-	-	39.2
<b>SPRING (Yamane sample size (n) = 14 days, e = 0.05)</b>						
Carbon monoxide (CO)	-	0.24	*	-	-	-
Nitrogen dioxide (NO <sub>2</sub> )	-	27.1	25.2	-	10.4	*
Ozone (O <sub>3</sub> )	53.8	-	*	-	-	37.3
Sulfur dioxide (SO <sub>2</sub> )	3.17	2.37	*	2.48	7.62	6.80
Particulate matter (PM <sub>10</sub> )	-	-	-	-	-	33.4
<b>SUMMER (Yamane sample size (n) = 14 days, e = 0.05)</b>						
Carbon monoxide (CO)	-	*	*	-	-	-
Nitrogen dioxide (NO <sub>2</sub> )	-	24.5	21.9	-	6.97	*
Ozone (O <sub>3</sub> )	47.8	-	25.3	-	-	35.0
Sulfur dioxide (SO <sub>2</sub> )	2.89	4.26	*	2.86	5.89	6.43
Particulate matter (PM <sub>10</sub> )	-	-	-	-	-	37.3

\* No data (number of data points < n), - Parameter not monitored

#### 4.4.2 Statistical analyses

##### 4.4.2.1 Normality analyses

A total of 90 data sets were tested, none of which had normal Gaussian distribution ( $\alpha = 0.05$ ).

##### 4.4.2.2 Correlation and significance analyses

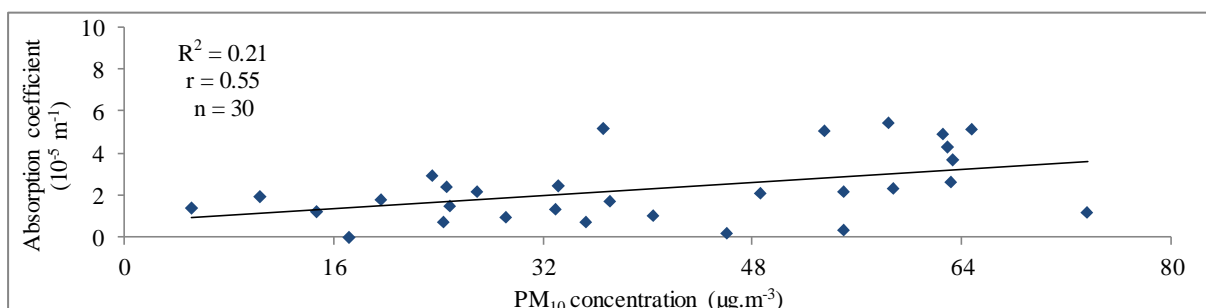
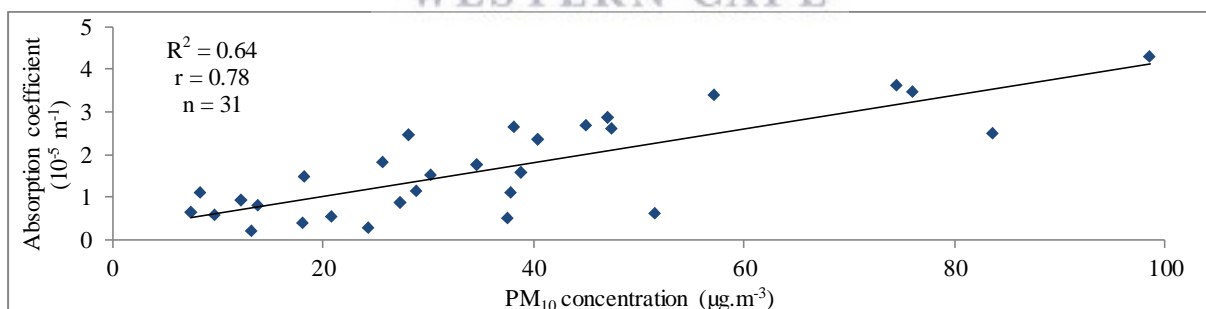
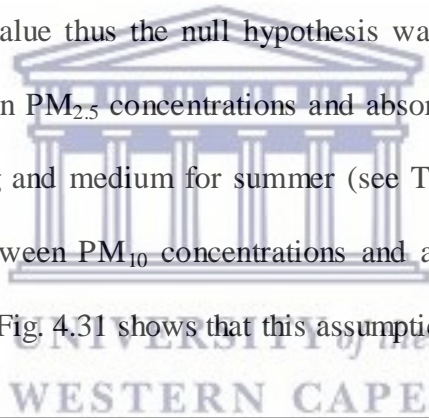
Table 4.13 shows the Spearman correlation coefficients ( $\rho$ ) for each season. Correlation between study data and data from AAQM stations at Atlantis and Tableview were weak, with the exceptions of O<sub>3</sub> data for Atlantis for autumn ( $\rho = 0.51$ - $0.56$ ) and NO<sub>2</sub> data for Tableview for winter ( $\rho = 0.29$ - $0.38$ ). Data for City Hall, Somerset-West and Wallacedene showed the largest associations with study data, particularly for autumn and winter, and was most useful for discussing the relationships between study and CoCT data.

**Table 4.13:** Spearman correlation coefficients ( $\rho$ )

	PM <sub>2.5</sub>				Absorption coefficient			
	AUT	WIN	SPR	SUM	AUT	WIN	SPR	SUM
<b>Wallacedene (3 km ESE)</b>								
NO <sub>2</sub>	0.51	*	*	*	0.46	*	*	*
O <sub>3</sub>	-0.19	-0.23	-0.13	-0.03	-0.46	-0.03	-0.28	-0.41
PM <sub>10</sub>	0.47	0.55	0.09	-0.33	0.75	0.41	0.05	-0.33
SO <sub>2</sub>	0.12	0.28	-0.22	-0.32	0.52	0.18	-0.26	-0.28
<b>Goodwood (14 km WSW)</b>								
NO <sub>2</sub>	*	0.51	*	-0.40	*	0.38	*	-0.43
O <sub>3</sub>	*	-0.53	*	*	*	-0.40	*	*
SO <sub>2</sub>	*	0.62	*	*	*	0.33	*	*
<b>Tableview (18 km WNW)</b>								
NO <sub>2</sub>	0.28	0.29	0.20	-0.33	0.23	0.38	0.15	-0.31
SO <sub>2</sub>	-0.15	0.25	0.04	-0.42	0.05	0.26	-0.01	-0.30
<b>City Hall (27 km WSW)</b>								
NO <sub>2</sub>	0.41	0.17	-0.09	-0.40	0.70	0.14	-0.22	-0.36
SO <sub>2</sub>	0.49	0.72	-0.24	-0.24	0.71	0.74	-0.33	-0.14
<b>Somerset-West (29 km SSE)</b>								
NO <sub>2</sub>	0.34	-0.12	0.48	0.17	0.60	0.09	0.54	-0.04
<b>Atlantis (37 km NNW)</b>								
O <sub>3</sub>	0.51	-0.27	0.02	0.13	0.56	-0.10	-0.09	-0.11
SO <sub>2</sub>	0.02	0.17	0.02	0.08	0.23	0.29	-0.22	-0.24

\* No data (number of data points < n)

Correlation between study data and CoCT data was strongest for autumn and winter and weakest for spring and summer. The only correlation of significance for spring was between the study data and NO<sub>2</sub> data for Somerset-West ( $\rho = 0.48-0.54$ ). Correlation between study data and pollutant PM<sub>10</sub> at Wallacedene varied from moderate to strong for autumn and winter ( $\rho = 0.41-0.75$ ) but was negligible to weak for spring and summer (0.00-0.09). Correlation between study data and the pollutant O<sub>3</sub> varied from strongly negative to strongly positive. Kruskal-Wallis Test was used to determine if the medians of PM<sub>2.5</sub> (study data) and PM<sub>10</sub> (for Wallacedene) concentrations were different. H-statistics for autumn (27.2), winter (23.2) and spring (23.7) were below the chi-squared value of 42.6 ( $\alpha = 0.05$ ) thus the null hypothesis was accepted (i.e. medians were equal). The H-statistic for summer (43.1) was higher than the chi-squared value thus the null hypothesis was rejected (i.e. medians were unequal). Correlations between PM<sub>2.5</sub> concentrations and absorption coefficients were large for autumn, winter and spring and medium for summer (see Table 4.4, page 112) so it was expected that correlations between PM<sub>10</sub> concentrations and absorption coefficients would have exhibited similar trends. Fig. 4.31 shows that this assumption was not true.



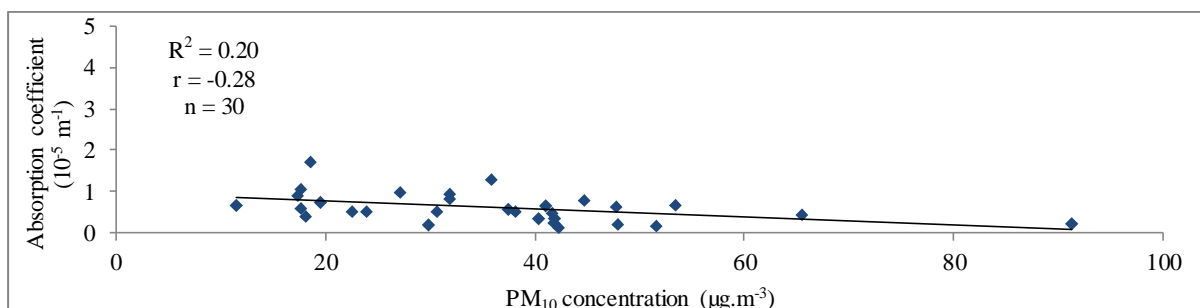
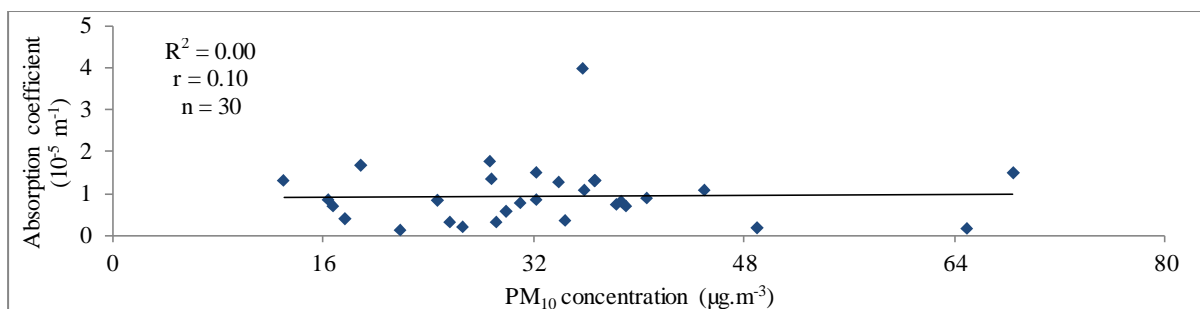


**Fig. 4.31:**  $PM_{10}$  concentrations v. absorption coefficients. Seasonal  $PM_{10}$  concentrations (Wallacedene) plotted against absorption coefficient values for, from top to bottom, autumn, winter, spring and summer.

The correlations between  $PM_{10}$  concentrations and absorption coefficients for autumn ( $r = 0.78$ ) and winter ( $r = 0.55$ ) were strong. Spring ( $r = 0.10$ ) and summer ( $r = -0.28$ ), however, exhibited negligible and weak negative correlations respectively. Table 4.14 shows the spearman correlation coefficients between study data and data collected by the CoCT at different distances from the sampling site. The correlation between study data and data collected by the CoCT is further discussed in section 5.1.4.

**Table 4.14:** Spearman correlation coefficients ( $\rho$ ) for pollutants  $NO_2$ ,  $SO_2$  and  $PM_{10}$ . Where applicable, mean values were calculated based on distance and direction from sampling site

$NO_2$	0-10 km				11-20 km				21-30 km			
	N	E	S	W	N	E	S	W	N	E	S	W
$PM_{2.5}$ concentration												
Autumn	#	0.51	#	#	#	#	#	0.28	#	#	0.34	0.41
Winter	#	*	#	#	#	#	#	0.40	#	#	-0.12	0.17
Spring	#	*	#	#	#	#	#	0.20	#	#	0.48	-0.09
Summer	#	*	#	#	#	#	#	-0.37	#	#	0.17	-0.40
Absorption coefficient												
Autumn	#	0.46	#	#	#	#	#	0.23	#	#	0.60	0.70
Winter	#	*	#	#	#	#	#	0.38	#	#	0.09	0.22
Spring	#	*	#	#	#	#	#	0.15	#	#	0.54	-0.22
Summer	#	*	#	#	#	#	#	-0.37	#	#	-0.04	-0.36

SO <sub>2</sub>	0-10 km				11-20 km				21-30 km			
	N	E	S	W	N	E	S	W	N	E	S	W
PM <sub>2.5</sub> concentration												
Autumn	#	0.12	#	#	#	#	#	-0.15	#	#	*	0.49
Winter	#	0.28	#	#	#	#	#	0.43	#	#	*	0.72
Spring	#	-0.22	#	#	#	#	#	0.04	#	#	*	-0.24
Summer	#	-0.32	#	#	#	#	#	-0.42	#	#	*	-0.24
Absorption coefficient												
Autumn	#	0.52	#	#	#	#	#	0.05	#	#	*	0.71
Winter	#	0.18	#	#	#	#	#	0.30	#	#	*	0.74
Spring	#	-0.22	#	#	#	#	#	-0.01	#	#	*	-0.33
Summer	#	-0.26	#	#	#	#	#	-0.30	#	#	*	-0.14
PM <sub>10</sub>	0-10 km				11-20 km				21-30 km			
	N	E	S	W	N	E	S	W	N	E	S	W
PM <sub>2.5</sub> concentration												
Autumn	#	0.47	#	#	#	#	#	#	#	#	#	#
Winter	#	0.55	#	#	#	#	#	#	#	#	#	#
Spring	#	0.09	#	#	#	#	#	#	#	#	#	#
Summer	#	-0.33	#	#	#	#	#	#	#	#	#	#
Absorption coefficient												
Autumn	#	0.75	#	#	#	#	#	#	#	#	#	#
Winter	#	0.41	#	#	#	#	#	#	#	#	#	#
Spring	#	0.05	#	#	#	#	#	#	#	#	#	#
Summer	#	-0.33	#	#	#	#	#	#	#	#	#	#

# No data for correlation, \* No data collected by AAQM stations

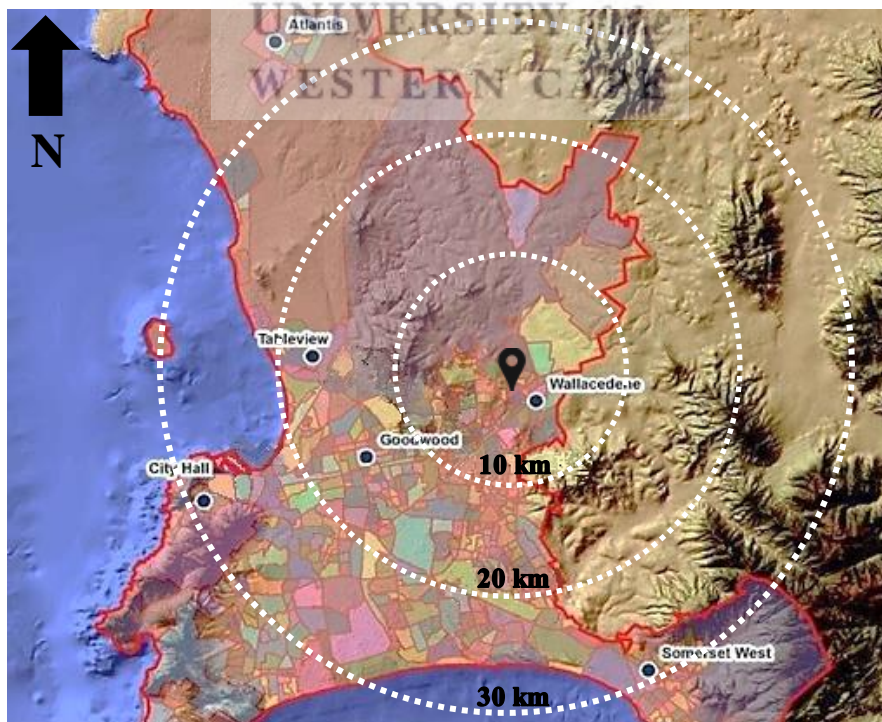


Fig. 4.32: Locations of AAQM stations. Concentric rings (10 km radii increments) were added to show the locations of AAQM stations relative to the sampling site (black marker)

Seasonal data correlation at equidistant intervals from the sampling site (see Table 4.14, page 134) was preferred over individual scatter plots of study data against air pollution data supplied by the CoCT (SO<sub>2</sub> and NO<sub>2</sub>) for the entire study period simply because seasonal correlation coefficients holistically showed the effects that distance from sampling site, direction from sampling site, and meteorological parameters (different for each season) had on APM concentrations in samples. See Appendices 13 A-F (mean daily pollutant concentrations) and 14 A-C (mean daily pollutant concentrations) for data supplied by the CoCT.

#### 4.4.3 Air pollution data for Pretoria and Thohoyandou

In addition to sampling in Cape Town, ambient PM samples were also collected in Pretoria (1,285 km NNE) and Thohoyandou (1,675 km NNE). Sampling dates were synchronised to the sampling calendar (see Appendix 1A) albeit deviations for Cape Town due to human error (sampling times and intervals were identical). Descriptive statistics for PM<sub>2.5</sub> concentration and absorption coefficient data for Pretoria and Thohoyandou are shown in Table 4.15 (page 135). The correlation, similarities and differences between ambient APM concentrations from all three sites are discussed in section 5.1.5.

**Table 4.15:** Descriptive statistics of seasonal PM<sub>2.5</sub> concentration and absorption coefficient data for Pretoria and Thohoyandou (concentrations in  $\mu\text{g.m}^{-3}$  and coefficient values in  $\text{m}^{-1}.10^{-5}$ )

<b>Pretoria (coordinates: -25.7317, 28.2003)</b>					
	<b>Autumn</b>	<b>Winter</b>	<b>Spring</b>	<b>Summer</b>	<b>Full study</b>
Sample size (n)	31	31	30	30	122
Weekdays (%)	22 (71)	23 (74)	21 (70)	19 (63)	85 (70)
Weekend + public holidays (%)	9 (29)	8 (26)	9 (30)	11 (37)	37 (30)
<b>PM<sub>2.5</sub> concentration</b>					
Mean	23.4	35.5	14.3	10.7	21.1
Variance	246	202	66.9	21.5	225
Standard deviation	15.7	14.2	8.18	4.64	15.0
Range	3.40-57.9	14.6-66.8	1.35-35.4	0.69-21.6	0.69-66.8
<b>Absorption coefficient</b>					
Mean	2.69	4.33	1.30	0.96	2.34
Variance	3.76	4.70	1.17	0.24	4.20
Standard deviation	1.94	2.17	1.08	0.49	2.05
Range	0.46-8.21	0.94-8.62	0.35-5.58	0.08-1.66	0.08-8.62
<b>Thohoyandou (coordinates: -22.9761, 30.4443)</b>					
	<b>Autumn</b>	<b>Winter</b>	<b>Spring</b>	<b>Summer</b>	<b>Full study</b>
Sample size (n)	31	30	30	29	120
Weekdays (%)	22 (71)	22 (73)	21 (70)	18 (62)	83 (69)
Weekend + public holidays (%)	9 (29)	8 (27)	9 (30)	11 (38)	37 (31)
<b>PM<sub>2.5</sub> concentration</b>					
Mean	10.4	9.83	14.7	8.64	10.9
Variance	51.4	65.6	90.8	52.1	68.7
Standard deviation	7.17	8.10	9.53	7.22	8.29
Range	1.35-33.6	1.18-37.5	1.06-31.3	1.83-34.3	1.06-37.5
<b>Absorption coefficient</b>					
Mean	0.60	0.78	0.76	0.63	0.69
Variance	0.24	0.44	0.49	0.12	0.32
Standard deviation	0.49	0.66	0.70	0.34	0.57
Range	0.03-1.50	0.14-2.40	0.05-2.79	0.12-1.47	0.03-2.79

#### 4.5 Composite samples

Data obtained from analytical methodology and statistical information pertaining to composite samples is presented in the section. Unlike calendar samples (exposure time: 24 hours), composite samples were collected for four weeks (total exposure time: 96 hours) during September 2017 and January 2018 (see Appendix 1C for sampling information).

##### 4.5.1 Anion profiling

The anion concentrations in PM were determined by ion chromatography (IC) (see section 3.2.2.4.7). A  $2.00 \text{ mg.kg}^{-1}$ , multi-anion control solution (Table 4.16) was analysed before and after sample analyses. Table 4.16 is immediately followed by percentage recovery for each anion shown in Fig. 4.33 (see Appendices 17 and 18 for information).

**Table 4.16:** Anion concentrations in control solution (concentrations in  $\text{mg.kg}^{-1}$ )

	Target	Pre-sample analysis	Post-sample analysis
Chloride	2.00	2.02	1.99
Nitrate	2.00	2.01	2.04
Sulfate	2.00	2.04	2.05
Bromide	2.00	1.90	1.91
Fluoride	2.00	1.85	1.94
Nitrite	2.00	1.96	2.00
Phosphate	2.00	2.06	2.03

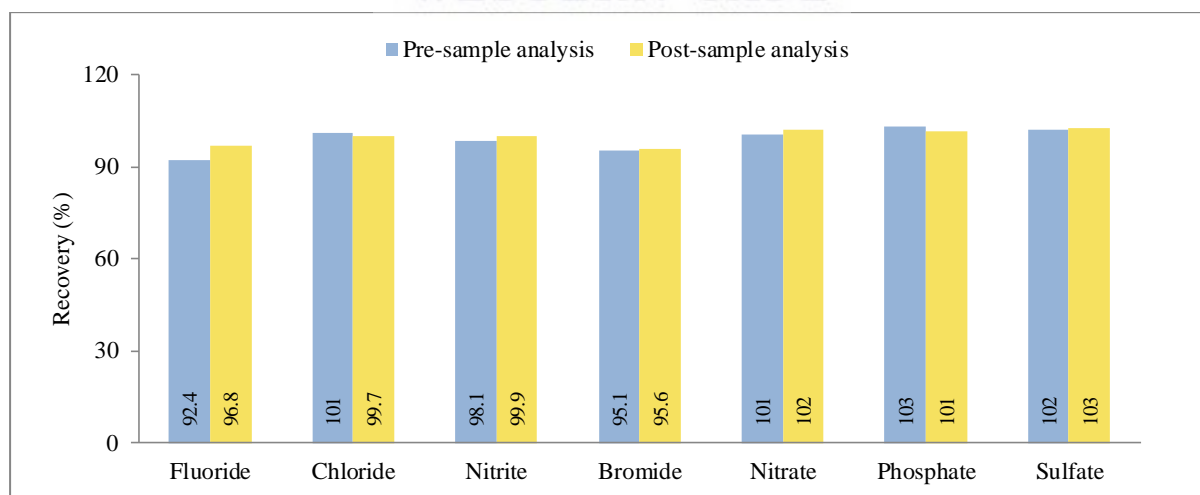


**Fig. 4.33:** Percentage recovery for anions in control solution

Relative standard deviation (limit:  $\leq 3.00 \%$ ), concentration (limit:  $2.00 \pm 0.60 \text{ mg.kg}^{-1}$ ) and percentage recovery (limit:  $100 \pm 30 \%$ ) met analytical requirements. Experimental data and



anion masses for sub-samples (1.00 cm<sup>2</sup>) are shown in Table 4.17 that is immediately followed by anion masses in composite samples shown in Fig. 4.34.

**Table 4.17:** Experimental data and anion masses for 1 cm<sup>2</sup> sub-samples (ND = not detected)

Concentration in sample solution (mg.kg <sup>-1</sup> )	September 2017		January 2018	
	Weekday	Weekend	Weekday	Weekend
Chloride	0.62	0.67	0.72	0.71
Nitrate	0.11	0.11	0.28	0.20
Sulfate	0.15	0.18	0.27	0.35
Bromide	ND	ND	ND	ND
Fluoride	ND	ND	ND	ND
Nitrite	ND	ND	ND	ND
Phosphate	ND	ND	ND	ND
Mass in 1.00 cm <sup>2</sup> sub-sample (µg)				
Chloride	9.33	9.99	10.9	10.7
Nitrate	1.71	1.67	4.19	2.98
Sulfate	2.28	2.70	4.10	5.17

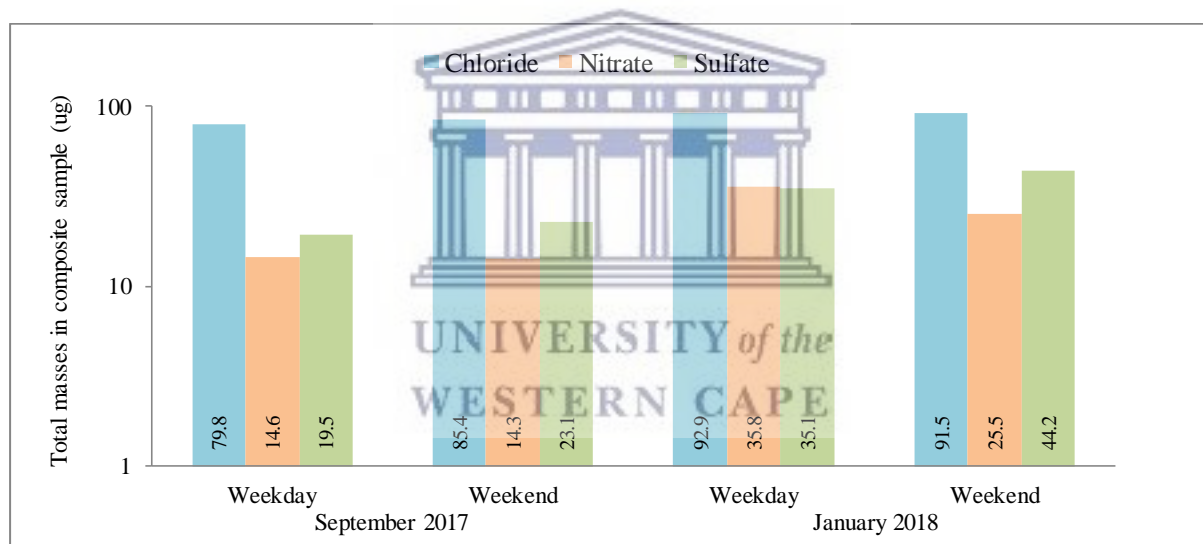


**Fig. 4.34:** Total anion masses in composite samples. See Table 4.21 for wt. %

T-test results indicated that weekday and weekend day data for September 2017 (t-value = 1.712,  $p > \alpha = 0.05$ ) had similarity as did weekday and weekend day data for January 2018 (t-value = 0.155,  $p > \alpha = 0.05$ ). When weekday and weekend day data for September was compared to the corresponding data for January, T-test results for weekday data (t-value = 6.946,  $p < \alpha = 0.05$ ) showed no similarity while weekend day data (t-value = 2.907,  $p > \alpha = 0.05$ ) showed similarity. Weight percentages of anionic species in composite samples are shown in Table 4.21 (page 142).

#### 4.5.2 Elemental profiling

The elemental concentrations in PM were determined by inductively coupled plasma-optical emission spectrometry (ICP-OES) (see section 3.2.2.3.6). A multi-concentration, multi-element control solution (Table 4.18) was analysed before and after sample analyses. Table 4.18 is immediately followed by the percentage recovery for each metal shown in Fig. 4.35 (see Appendix 16 for standardisation information).

**Table 4.18:** Metals concentrations in control solution (concentrations in  $\text{mg}\cdot\text{kg}^{-1}$ )

	Target	Pre-sample analysis	Post-sample analysis
Zinc	2.00	1.98	2.01
Iron	2.00	1.87	1.84
Magnesium	2.00	1.89	2.05
Aluminium	2.00	1.99	2.02
Calcium	10.0	8.46	8.71
Sodium	10.0	7.46	7.75

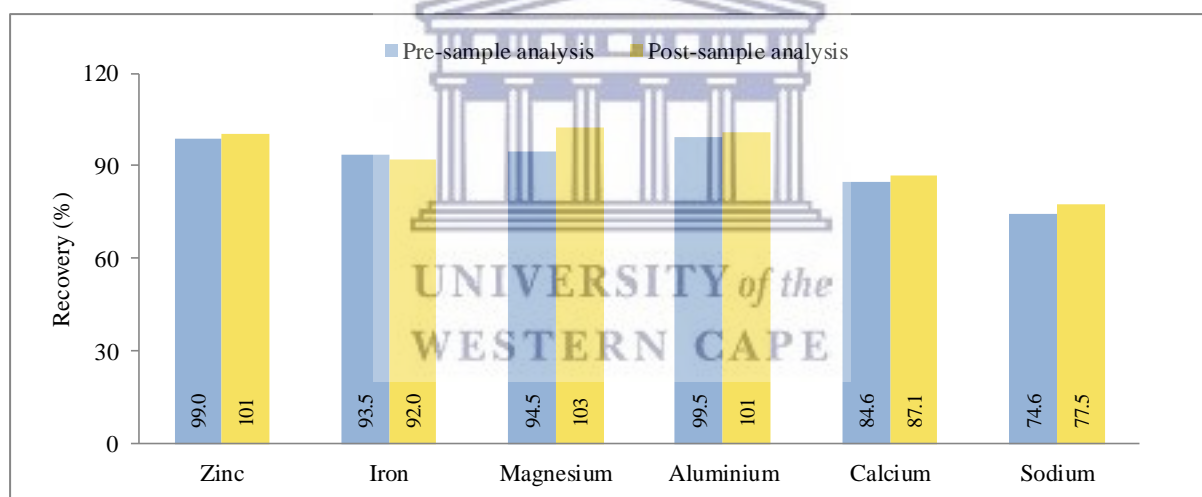


**Fig. 4.35:** Percentage recovery for metals in control solution

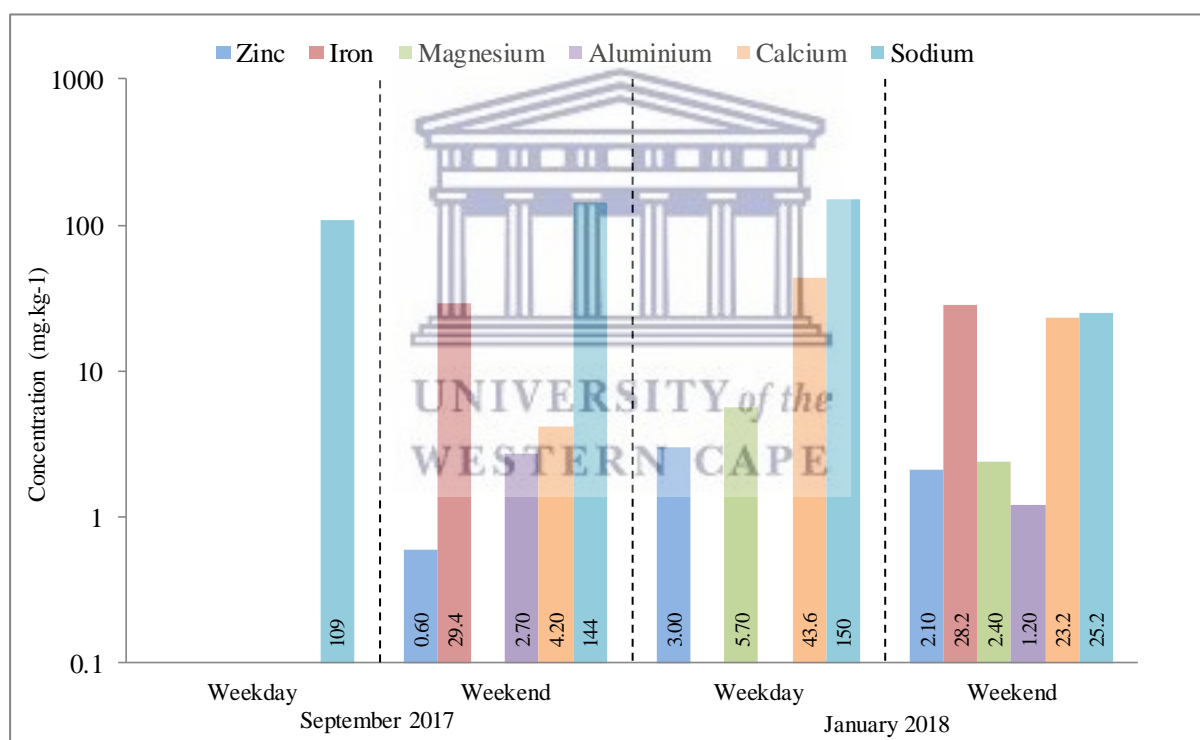
Relative standard deviation (limit:  $\leq 3.00\%$ ), concentration (limits:  $2.00 \pm 0.60$  and  $10.0 \pm 3.0 \text{ mg}\cdot\text{kg}^{-1}$ ) and percentage recovery (limit:  $100 \pm 30\%$ ) met analytical requirements. Of the 23 elements tested for, only six had concentrations greater than the minimum detection limit of  $1.00 \mu\text{g}\cdot\text{kg}^{-1}$ . Experimental data and metals masses for sub-samples ( $4.28 \text{ cm}^2$ ) are shown in Table 4.19 (page 139) that is immediately followed by metals masses in composite samples shown in Fig. 4.36.

**Table 4.19:** Experimental data and metal masses for 4.28 cm<sup>2</sup> sub-samples

Concentration in sample solution (mg.kg <sup>-1</sup> )	September 2017		January 2018	
	Weekday	Weekend	Weekday	Weekend
Sodium	3.63	4.79	5.01	0.84
Iron	< 0.01	0.98	< 0.01	0.94
Aluminium	< 0.01	0.09	< 0.01	0.04
Magnesium	< 0.01	< 0.01	0.19	0.08
Calcium	< 0.01	0.14	1.45	0.77
Zinc	< 0.01	0.02	0.10	0.07

Mass in 4.28 cm <sup>2</sup> sub-sample (µg)	Weekday	Weekend	Weekday	Weekend
Sodium	54.5	71.9	75.2	12.6
Iron	< 0.02	14.7	< 0.02	14.1
Aluminium	< 0.02	1.35	< 0.02	0.60
Magnesium	< 0.02	< 0.02	2.85	1.20
Calcium	< 0.02	2.10	21.8	11.6
Zinc	< 0.02	0.30	1.50	1.05



**Fig. 4.36:** Total metals masses in composite samples. See Table 4.21 for wt. %

Weekday and weekend day data for September 2017 and January 2018 showed some similarities. Sodium was detected in all samples and the aluminium and iron contents for weekend day samples were similar. Each sample had its own unique metallic composition. Weight percentages of metallic species in composite samples are shown in Table 4.21 (page 142).

### 4.5.3 Inorganic carbon content

The absorption coefficient values of samples were determined by smoke stain reflectometry (SSR) (see section 3.2.2.2.2). Absorption coefficients were used to calculate soot content (soot accounted for all inorganic carbon content in samples). Experimental data and inorganic carbon concentrations are shown in Table 4.20 that is immediately followed by the inorganic carbon mass in PM of composite samples shown in Fig. 4.37. Unlike calendar samples (five replicates), the mean of three replicates was used (filter sizes were not sufficient for five replicates).

**Table 4.20:** Experimental data and inorganic carbon concentrations in composite samples

	September 2017		January 2018	
	Weekday	Weekend	Weekday	Weekend
R <sub>s</sub> (%)	25.5	22.1	37.8	33.2
R <sub>0</sub> (%)	101	101	101	101
R	1.38	1.52	0.98	1.11
Absorption coefficient (m <sup>-1</sup> .10 <sup>-5</sup> )	2.56	2.83	1.82	2.05
Inorganic carbon concentration (µg.m <sup>-3</sup> )	1.85	2.11	1.44	1.41

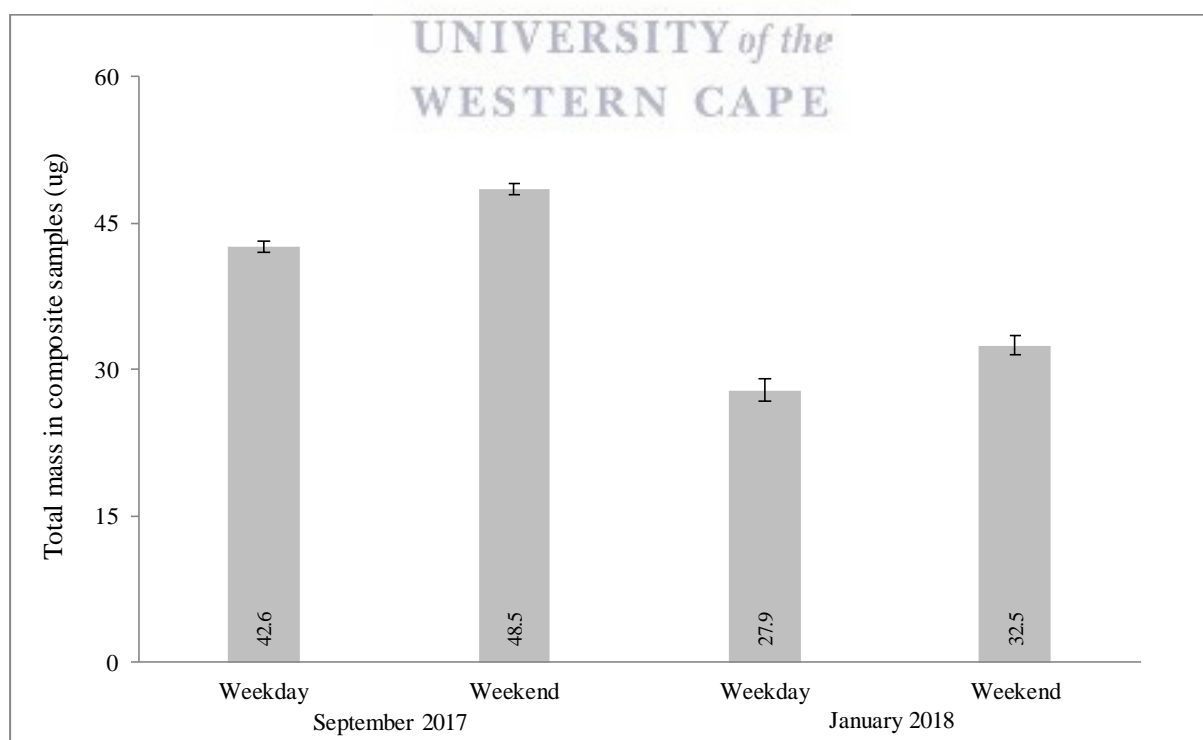


**Fig. 4.37:** Total inorganic carbon mass in composite samples. See Table 4.21 for wt. %

On physical inspection, weekday and weekend day composite samples for September 2017 were considerably darker than the corresponding samples for January. Mean inorganic carbon content in composite samples for September (45.6  $\mu\text{g}$ ) was 51.0 % higher than the mean content for January samples (30.2  $\mu\text{g}$ ). The difference in inorganic carbon content for weekday samples for September (42.6  $\mu\text{g}$ ) and January (27.9  $\mu\text{g}$ ) was 14.7  $\mu\text{g}$ , very similar to the difference between corresponding weekend day samples (16.0  $\mu\text{g}$ ). Weight percentage of inorganic carbon in composite samples is shown in Table 4.21 (page 142).

#### 4.5.4 Chemical composition of PM in composite samples

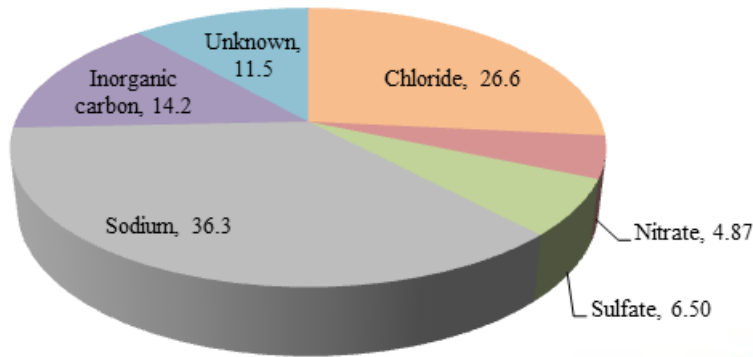
PM is a complex mixture of various chemical constituents. Collectively, anionic species (chloride, nitrate and sulfate) represented the largest proportion of PM mass (38-54 wt. %). Inorganic carbon was the second most abundant species in composite samples (9.30-16.2 wt. %). Inorganic carbon (or soot) content for weekday and weekend day samples were similar but corresponding samples for September 2017 and January 2018 showed no correlation. Soot content for weekend day samples were higher than the corresponding weekday samples. Metals content (0.67-20.6 wt. %) fluctuated from weekday-to-weekend and from month-to-month without any correlation. The only exception to this was the iron content of PM in weekend day samples that were near identical for September (10.7 wt. %) and January (10.4 wt. %). Student's T-test was applied to the data. T-test results indicated that weekday and weekend day data for September ( $t\text{-value} = 2.334, p > \alpha = 0.05$ ) had similarity as did weekday and weekend day data for January ( $t\text{-value} = 2.232, p > \alpha = 0.05$ ). When weekday and weekend day data for September were compared to the corresponding data for January, T-test results for weekday data ( $t\text{-value} = 3.334, p < \alpha = 0.05$ ) showed no similarity while weekend day data ( $t\text{-value} = 2.843, p > \alpha = 0.05$ ) showed similarity. Compositional data for weekday and weekend day composite samples is shown in Table 4.21 (page 142) that is immediately followed by graphical representations in Fig. 4.38 (page 143).

**Table 4.21:** Chemical compositions of weekday and weekend day composite samples. Mass measurements were performed with a Mettler-Toledo ML 204 Microbalance (readability: 100 µg)

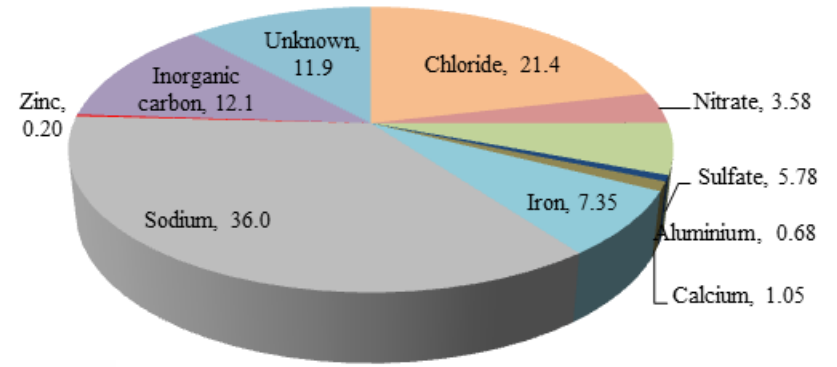
	September 2017				January 2018			
	Weekday		Weekend		Weekday		Weekend	
Pre-sampling filter mass (µg)	192,400		183,200		169,100		192,000	
Post-sampling filter mass (µg)	192,700		183,600		169,500		192,300	
PM mass (µg)	300		400		400		300	
	Mass (µg)	Wt. (%)	Mass (µg)	Wt. (%)	Mass (µg)	Wt. (%)	Mass (µg)	Wt. (%)
<b>Anions</b>	<b>113.9</b>	<b>38.0</b>	<b>122.8</b>	<b>30.7</b>	<b>163.8</b>	<b>41.0</b>	<b>161.2</b>	<b>53.7</b>
Chloride	79.8	26.6	85.4	21.4	92.9	23.2	91.5	30.5
Nitrate	14.6	4.87	14.3	3.58	35.8	8.95	25.5	8.50
Sulfate	19.5	6.50	23.1	5.78	35.1	8.78	44.2	14.7
<b>Metals</b>	<b>109</b>	<b>36.3</b>	<b>181</b>	<b>45.2</b>	<b>202</b>	<b>50.5</b>	<b>82.3</b>	<b>27.4</b>
Aluminium	-	-	2.70	0.68	-	-	1.20	0.40
Calcium	-	-	4.20	1.05	43.6	10.9	23.2	7.73
Iron	-	-	29.4	7.35	-	-	28.2	9.40
Magnesium	-	-	-	-	5.70	1.43	2.40	0.80
Sodium	109	36.3	144	36.0	150	37.5	25.2	8.30
Zinc	-	-	0.60	0.15	3.00	0.75	2.10	0.70
<b>Inorganic carbon</b>	<b>42.6</b>	<b>14.2</b>	<b>48.5</b>	<b>12.1</b>	<b>27.9</b>	<b>6.98</b>	<b>32.5</b>	<b>10.8</b>
<b>Unknown</b>	<b>34.5</b>	<b>11.5</b>	<b>47.7</b>	<b>11.9</b>	<b>6.30</b>	<b>1.58</b>	<b>24.0</b>	<b>8.00</b>

Weight percentage (Wt. %) was calculated by taking the mass (experimental data) and dividing it by the total PM mass (in this instance 300 µg) and multiplying by 100. Mean weight percentage of “unknown” was 11.7 wt. % and 4.79 wt. % for September 2017 and January 2018 respectively. Due to the limited sensitivity of the ML204 microbalance, water content could not be determined. The “unknown” proportion of ambient PM collected in samples was possibly water (differences in wt. % for September and January, January had higher mean temperature and lower mean Rh and precipitation than September), ammonium (a major cation formed when gaseous NH<sub>3</sub> neutralises gaseous H<sub>2</sub>SO<sub>4</sub> and HNO<sub>3</sub> in the atmosphere), and organic carbon (including VOCs from vehicular emissions and combustion of biomass and fossil fuels for domestic purposes). Silica (SiO<sub>2</sub>) was eliminated as a potential constituent because silicon concentration was < 1.00 µg.kg<sup>-1</sup> for all samples.

**SEPTEMBER (Weekday)**



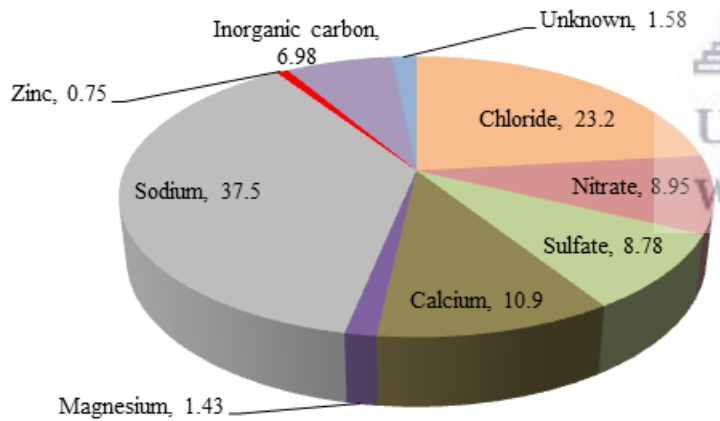
**SEPTEMBER (Weekend)**



Chloride Nitrate Sulfate Zinc Inorganic carbon Unknown

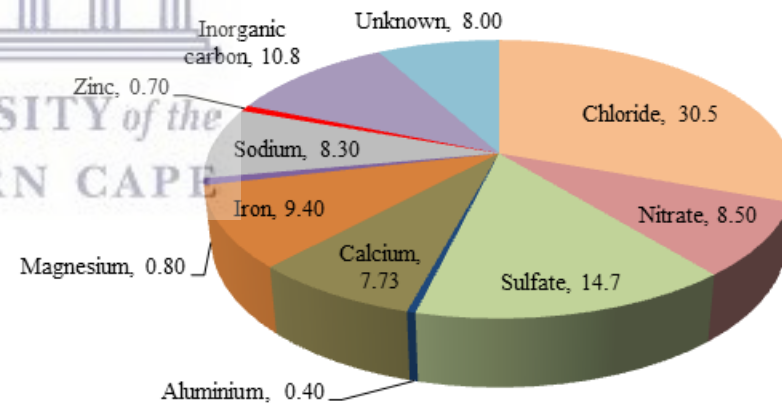
Chloride Nitrate Sulfate Aluminium  
Calcium Iron Sodium Zinc

**JANUARY (Weekday)**



Chloride Nitrate Sulfate  
Calcium Magnesium Sodium  
Zinc Inorganic carbon Unknown

**JANUARY (Weekend)**



Chloride Nitrate Sulfate Aluminium  
Calcium Iron Magnesium Sodium  
Zinc Inorganic carbon Unknown

**Fig. 4.38:** Chemical make-up of PM in composite samples (amounts are in wt. %).

#### 4.5.5 Microscopic information

##### 4.5.5.1 Coagulated and agglomerate particulates

Coagulated and agglomerate particulates on the surfaces of composite samples were photomicrographed at 10,000-80,000x normal magnifications by scanning electron microscopy (SEM). Photomicrographs of the surface of the weekday composite sample for September 2017 are shown in Fig. 4.39.

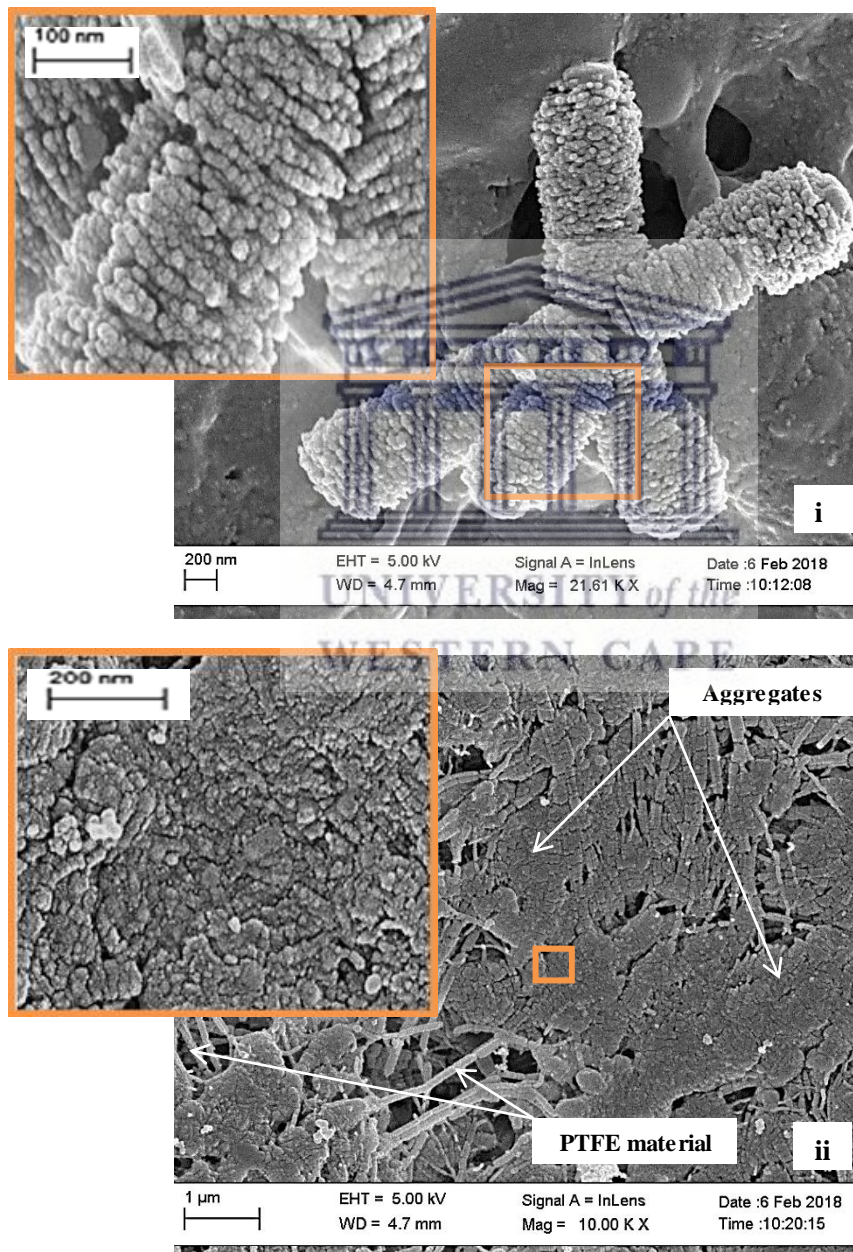


**Fig. 4.39:** SEM photomicrographs of weekday composite samples for September 2017 (Images: EMU).



Photomicrograph (i) shows a star-like agglomerate particulate with five projections. When zooming in for a closer look, it was discovered that each projection consisted of thousands of tinier particulates with diameters in the sub 10 nm range. The formation of agglomerate particulates was expected because of the highly diffusive nature of particulates in the sub 100 nm range and high Rh (mean Rh for study period: 69 %) in Cape Town during the study period. Photomicrograph (ii) shows smaller particulates coagulated into larger aggregates. PM was easily distinguishable from the PTFE filter material. When zooming in for a closer look, it was discovered that the surfaces of aggregates consisted of tiny particulates of various shapes (circular, cubical, spherical) and sizes (10-100 nm).

#### 4.5.5.2 Particulate morphology

Mesh grids were photomicrographed at 40,000-400,000x normal magnification by transmission electron microscopy (TEM). TEM operates on the principal of electron beam transmission and was the preferred magnification technique for examining the morphologies of specimens (in the 10-100 nm range), and determining what they are made of (chemical constituents). Photomicrographs of mesh grid 1 (onto which a concentrated extraction solution of PM collected during weekend days in January was pipetted) did not show individual particulates, only large, indistinguishable black masses. Photomicrographs of mesh grid 2 (onto which a diluted extraction solution of PM collected during weekend days in January was pipetted) clearly showed individual particulates. Photomicrographs of PM collected on weekend days during January are shown in Fig. 4.40 (page 146). Particulates varied in shape and size. Some were angular (hexagonal, heptagonal) while others were spherical, but mostly occurred as conglomerates. In TEM photomicrographs, soot can appear as individual spherical particulates or grape-like conglomerates (Soot Testing Lab, 2013).

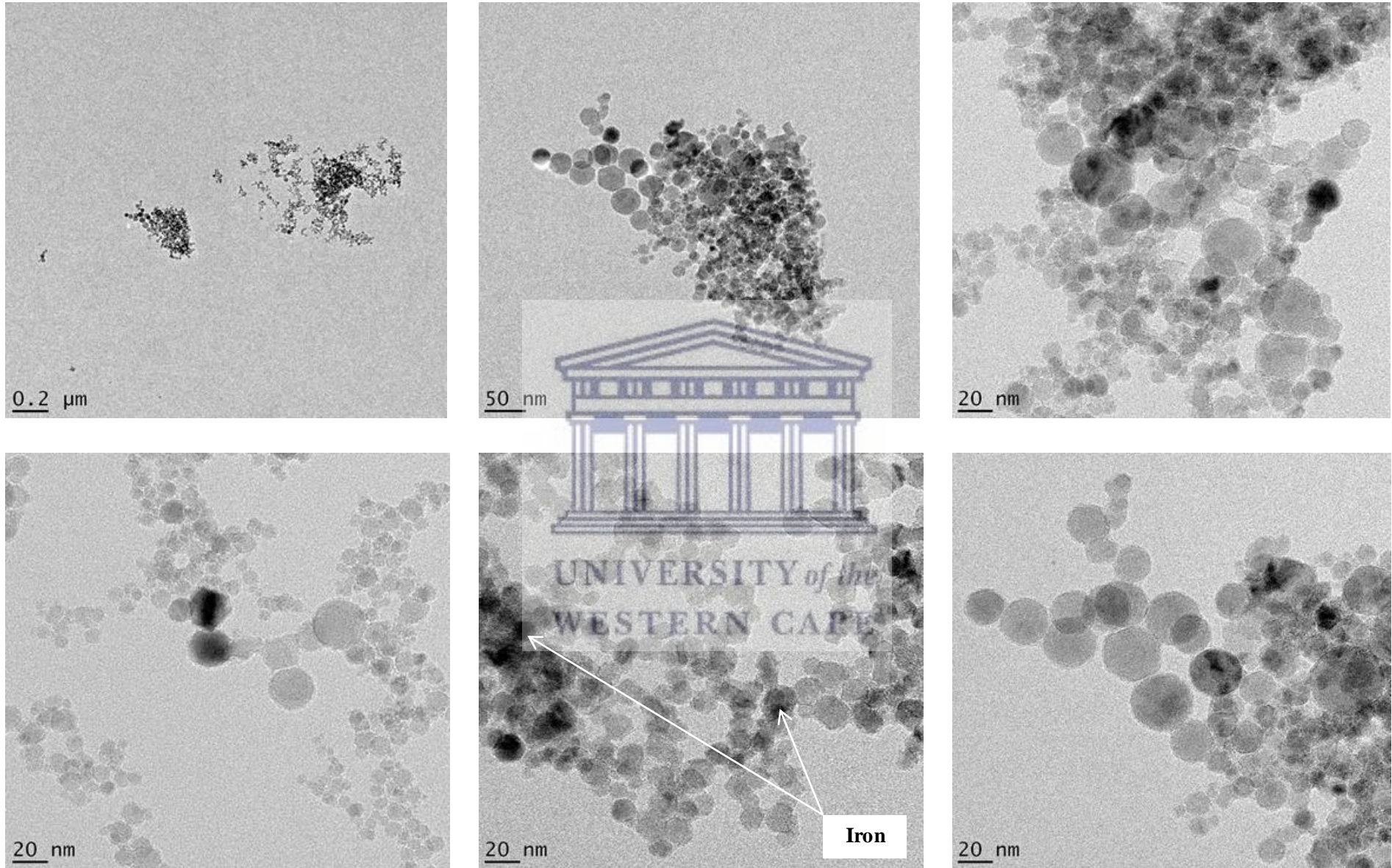


*Fig. 4.40: TEM photomicrographs of PM collected on weekend days during January 2018 (Images: EMU).*

Particulate opacity varied considerably. The opacity (or transparency) of particulates is density-dependent (the denser the particulate the darker it will appear). The particulates photomicrographed had black areas indicating the presence of a dense substance. Photomicrographs were of the January weekend day composite sample which had high iron content (10.4  $\mu\text{g}$ ) that could explained the black colouration. SAED was performed to determine the crystallographic properties of the sample. SAED produced a ring pattern (Fig. 4.41). Rings were diffuse indicating that some particulates were amorphous (or non-crystalline). Bright white spots indicated that some particulates were crystalline in nature. There were small spots making up two rings, A ( $d = 0.15$ ) and B ( $d = 0.22$  nm), which indicated that some particulates were nano-polycrystalline (solids composed of many crystallites of varying size). Crystallites were possibly ionic salts of chloride, nitrates and sulfates (53.7 wt. % of PM collected). The elemental composition of January weekend day composite sample is shown in the EDS spectrum (Fig. 4.42) on page 148.

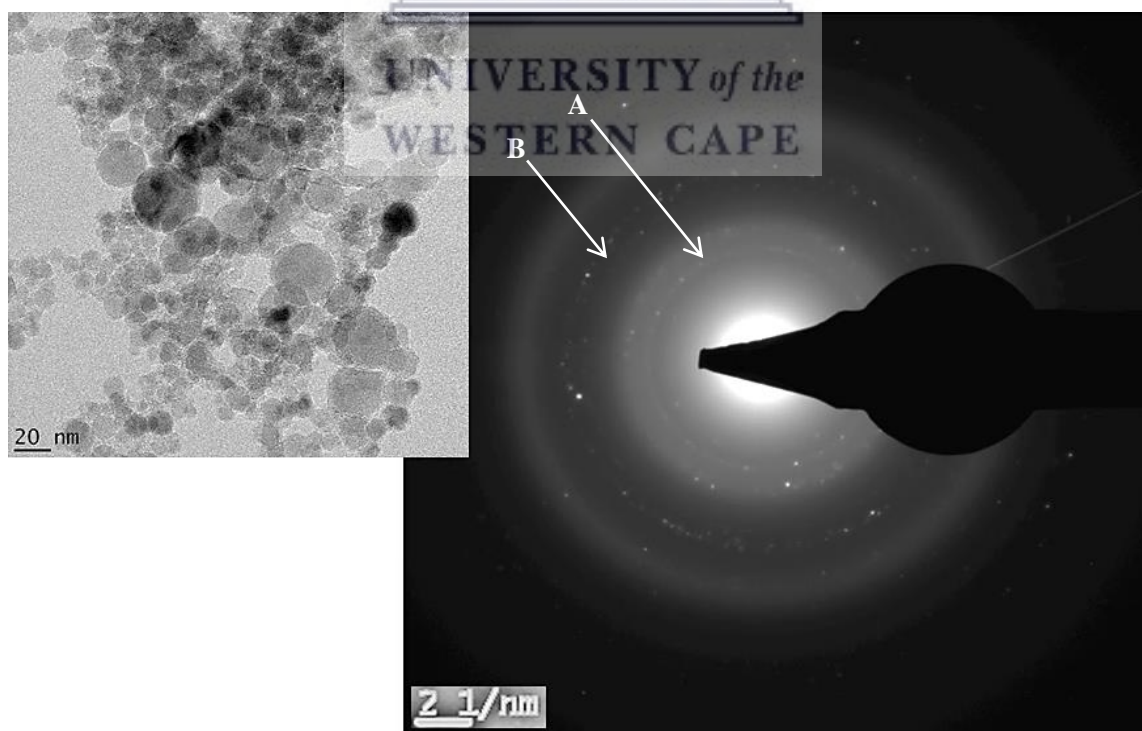


**Fig. 4.41:** TEM and SAED. Photomicrograph (left) and SAED pattern (right) of the weekend day composite sample for January 2018 (Images: EMU).

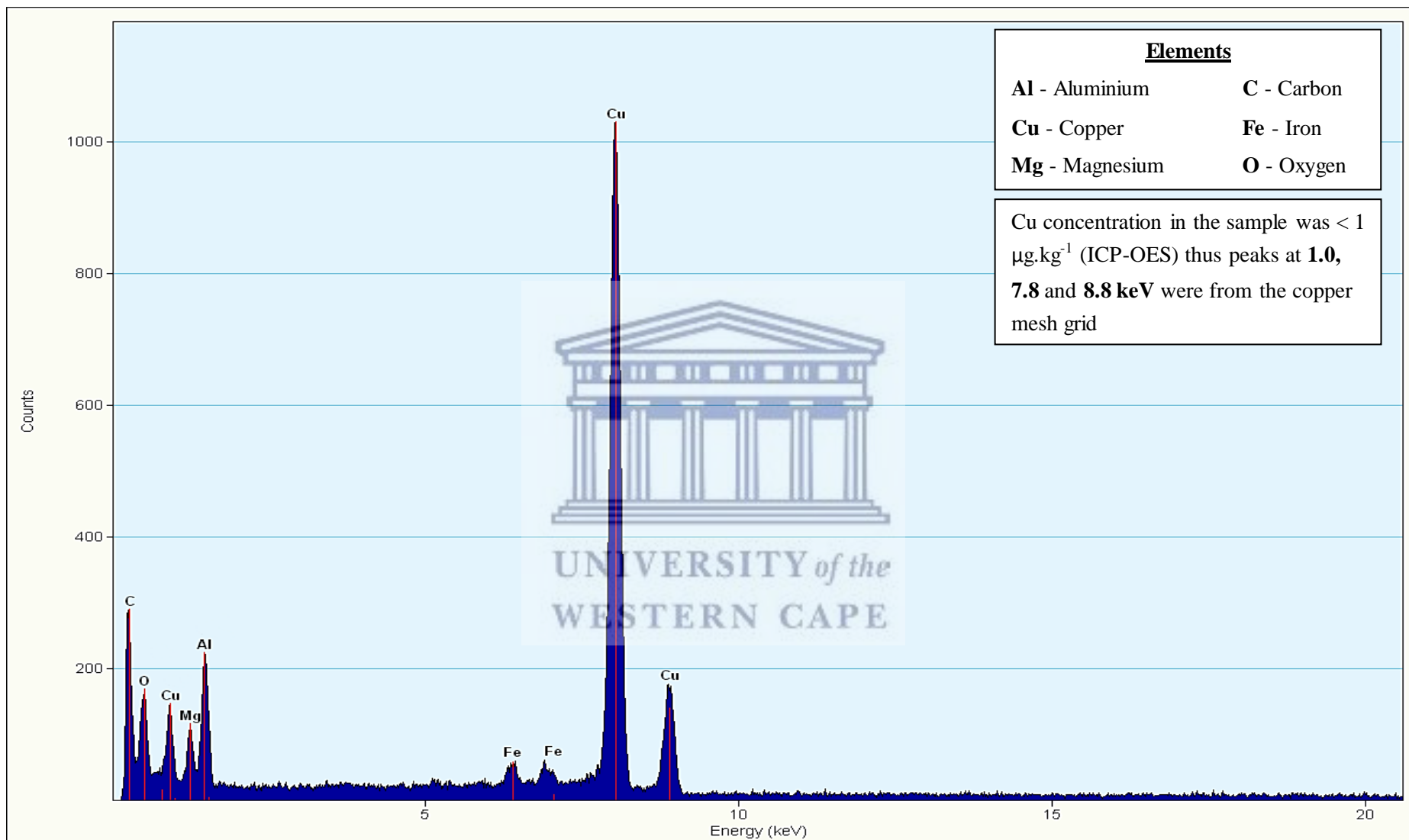


*Fig. 4.42: EDS spectrum of the weekend day composite sample for January 2018. Compositional information is comparable with data produced by analytical techniques ICP-OES and SSR (Source: EMU).*

## **CHAPTER 5: DISCUSSION**

This chapter is divided into two main sections, section 5.1 and section 5.2. Section 5.1 discusses data and information obtained for calendar samples (samples collected at three day intervals for the full study period) while section 5.2 discusses data and information obtained for composite samples (samples collected at seven day intervals during September 2017 and January 2018).

### 5.1 Calendar samples

Experimental data and statistical information for calendar samples are discussed in this section. This section also discusses the relationships, similarities and differences between  $PM_{2.5}$  and absorption coefficient data, not only for study data but between study data and data collected by the CoCT and sampling sites in Pretoria and Thohoyandou, while assessing the effects of meteorological parameters and air mass transport on ambient APM concentrations.

#### 5.1.1 Relationship between $PM_{2.5}$ concentrations and absorption coefficients

In section 4.1.3 scatter plots of  $PM_{2.5}$  concentration and absorption coefficient data for the study period yielded trend lines that were contradictory of one another (see Fig. 4.9, page 103).  $PM_{2.5}$  concentrations showed a slight increase (starting mid-April until mid-July, 2017) before trending downwards steadily until the end of the study period (mid-April, 2018). A coefficient of determination ( $R^2$ ) value of 0.1 (negligible) indicated that there was no definitive correlation between  $PM_{2.5}$  concentrations and time of year. The trend for absorption coefficients (soot content) was the complete opposite. Absorption coefficient values decreased steadily (starting mid-April, 2017, until mid-February, 2018) before increasing until the end of the study period. A  $R^2$  value of 0.3 (weak), although three times larger than  $R^2$  for  $PM_{2.5}$  data, indicated no definitive correlation between absorption coefficients and time of year. Mean  $PM_{2.5}$  concentration and absorption coefficient was 13.4

$\pm 8.1 \mu\text{g.m}^{-3}$  and  $1.38 \pm 1.24 \text{ m}^{-1} \cdot 10^{-5}$  respectively. Both parameters did not exceed any safety limits. The highest ( $39.1 \mu\text{g.m}^{-3}$ ) and lowest ( $1.17 \mu\text{g.m}^{-3}$ )  $\text{PM}_{2.5}$  concentrations were recorded on 23 June 2017 and 6 September 2017 respectively. The  $\text{PM}_{2.5}$  concentration recorded on 23 June 2017 can be explained. On this day, mean air velocity was  $0.5 \text{ m.s}^{-1}$  (mean seasonal value:  $1.7 \text{ m.s}^{-1}$ ). Maximum air velocity was  $4.5 \text{ m.s}^{-1}$  which was the lowest recorded maximum air velocity for the study period. Below average air velocity and lowest maximum air velocity did not promote dispersion of air pollution from the sampling area leading to elevated APM concentrations. Furthermore, mean Rh was 64 % (mean seasonal value: 72 %). Below average Rh meant air pollutants remained aloft for longer periods meaning APM concentrations in ambient air were higher. The  $\text{PM}_{2.5}$  concentration recorded on 6 September 2017 can only be explained with mean Rh information. On this day, mean air velocity was  $3.5 \text{ m.s}^{-1}$  (mean seasonal value:  $2.6 \text{ m.s}^{-1}$ ). Maximum air velocity was  $11.8 \text{ m.s}^{-1}$  which was not the highest recorded maximum air velocity for the study period (highest maximum air velocity for the study period was  $19.0 \text{ m.s}^{-1}$ ) thus air velocity information cannot be used to explain the low  $\text{PM}_{2.5}$  concentration recorded on this day. On 6 September 2017, however, mean Rh was 78 % (mean seasonal value: 67 %). Above average Rh meant that fine APM fractions were deposited more rapidly (decreasing their atmospheric lifetimes) which decreased APM concentrations in ambient air. The highest ( $5.38 \mu\text{g.m}^{-3}$ ) and lowest ( $0.00 \mu\text{g.m}^{-3}$ ) absorption coefficient values were recorded on 26 June 2017 and 11 June 2017 respectively. The absorption coefficient of 26 June 2017 can be explained. Braaiing (recreational activity) is a large source of soot in the Kraaifontein area, if not the largest. On this day (Saturday), mean air velocity ( $0.9 \text{ m.s}^{-1}$ ) was low and mean Rh (72 %) moderate. Favourable weather conditions and the day of week (weekend day) suggest that soot from braaiing was responsible for an elevated absorption coefficient. The absence of soot ( $0.00 \text{ m}^{-1}$ ) on 11 June 2017 was due to rainfall (3.8 mm) and above average mean Rh (83 %).

Descriptive statistics (see Table 4.3, page 104) for seasonal PM<sub>2.5</sub> concentrations showed that autumn ( $11.3 \pm 5.2 \mu\text{g.m}^{-3}$ ) and summer ( $9.11 \pm 3.66 \mu\text{g.m}^{-3}$ ) had similar mean PM<sub>2.5</sub> concentrations as did winter ( $16.1 \pm 10.2 \mu\text{g.m}^{-3}$ ) and spring ( $17.4 \pm 8.7 \mu\text{g.m}^{-3}$ ). Absorption coefficients, however, did not show the same trends. Autumn ( $1.76 \pm 1.12 \text{ m}^{-1} \cdot 10^{-5}$ ) and winter ( $2.29 \pm 1.49 \text{ m}^{-1} \cdot 10^{-5}$ ) had similar mean absorption coefficient values as did spring ( $0.94 \pm 0.73 \text{ m}^{-1} \cdot 10^{-5}$ ) and summer ( $0.60 \pm 0.35 \text{ m}^{-1} \cdot 10^{-5}$ ). Winter (R.S.D = 63.4 %) and spring (R.S.D = 77.7 %) had the greatest variation in PM<sub>2.5</sub> and absorption coefficient data respectively while summer had the lowest variations (for both parameters). Despite having low R<sup>2</sup> values (0.1 and 0.3), statistical analyses showed moderate to strong linear relationships when full study and seasonal PM<sub>2.5</sub> concentration and absorption coefficient data were plotted against each other (see Fig. 4.15, page 109, and Fig. 4.16, page 110). PPMC and SROC tests revealed large seasonal associations with the exception of summer that had medium association (see Table 4.4, page 112). The strengths of association for autumn, winter, spring and summer were 0.76, 0.81, 0.54 and 0.40 respectively. Shapiro-Wilks normality tests showed that PM<sub>2.5</sub> data for autumn ( $p = 0.456$ ), spring ( $p = 0.243$ ) and summer ( $p = 0.800$ ) had normal Gaussian distribution while winter had non-Gaussian distribution. Normality testing of absorption coefficients showed that only data for autumn had Gaussian distribution ( $p = 0.055$ ) while winter, spring and summer all had non-Gaussian distributions ( $\alpha = 0.05$ ). When seasonal PM<sub>2.5</sub> and absorption coefficient data underwent Kruskal-Wallis significance tests, no significance was found (i.e. median values were different) (see Table 4.5, page 112). This was expected considering that meteorological conditions (which have a dramatic effect on ambient APM concentrations) for Cape Town changed from season-to-season. There was, however, significance between full study PM<sub>2.5</sub> ( $H = 14.4$ ) and absorption coefficient ( $H = 29.0$ ) data. Similarities between weekday ( $H = 0.17$ ) and weekend day ( $H = 4.94$ ) data were also significant while strengths of association

were near identical with 0.58 and 0.56 respectively. Section 5.1.2 and section 5.1.3 investigate the effects of meteorological parameters and air mass transport on ambient APM concentrations.

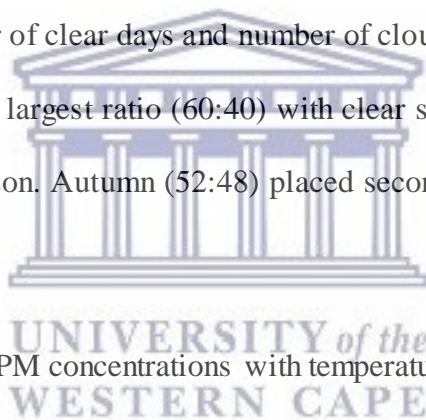
#### 5.1.2 The effects of meteorological conditions on ambient APM concentrations

The effects of meteorological parameters and inversion phenomena on ambient APM dispersion and atmospheric residence times were shown in section 2.2.5. According to the U.S. EPA, three meteorological parameters have the greatest impact on ambient APM concentrations - relative humidity (Rh), temperature and wind. The amount of sunshine (catalyst for chemical transformations) and rain (wash-out of water soluble pollutants) can also affect the levels of air pollution (Waikato Regional Council, 2018). Ambient APM concentrations are directly proportional to ambient air temperatures. Areas with low temperatures and high Rh generally have low ambient APM concentrations. These conditions are conducive for fine and ultrafine particulate coagulation processes into larger aggregates. Larger particulates do not have long residence times and are readily deposited through a process called sedimentation (see Fig. 2.8, page 20). Conversely, areas with high temperatures and low Rh are prone to high levels of particulate pollution (particularly fine fractions). Warm air currents and low moisture content allow tiny particulates to stay aloft for prolonged periods of time. Of the aforementioned parameters, none affect pollution levels more than wind. Wind carries pollutants away from their sources causing them to disperse. The higher the air velocity, the more pollutants are dispersed and the lower their concentrations. It is not a single meteorological parameter but rather by a combination of parameters that impacts air pollution levels in an area or region (Waikato Regional Council, 2018). Studies of this type are rare in South Africa hence correlations between study data and meteorological parameters were compared to the findings of Wang at al., 2015 and Zhang et al., 2018 who conducted studies in Nagasaki, Japan and Chang-Zhu-Tan, China respectively.



### 5.1.2.1 Meteorological conditions for Cape Town

Cape Town's climate is described as Mediterranean in nature with warm, dry summers and cold, wet winters (see section 2.4.2). Weather conditions for the study period were similar (see section 4.2). The highest temperature was recorded in January (33.4 °C) and the lowest in June (5.1 °C). As expected, mean relative humidity (Rh) was highest for winter (72 %) and lowest for summer (66 %). Despite experiencing its worst drought in 100 years, precipitation for Cape Town amounted to 120 mm with winter having the most rainfall (45 mm, 38 %) and autumn the least (9.4 mm, 7.8 %). Northerly (44 %) and southerly (44 %) wind directions dominated with summer having the highest mean air velocity (3.2 m.s<sup>-1</sup>) and winter the lowest (1.7 m.s<sup>-1</sup>). The amount of sunshine (UV exposure), per season, was calculated as a percentage ratio of the number of clear days and number of cloudy and/or partly cloudy days. Summer, as expected, had the largest ratio (60:40) with clear skies for the majority of 18 of 30 sampling days for that season. Autumn (52:48) placed second with winter and spring tied for third (47:53).



### 5.1.2.2 Change in ambient APM concentrations with temperature

Ambient APM concentrations may have negative or positive correlations with air temperature (Wang et al, 2015 and Zhang et al., 2018). Correlations can either be negative or positive depending on geographical location, meteorological mean variables and other factors. Mean temperature for summer (21.7 °C) was the highest of all four seasons yet summer had the lowest PM<sub>2.5</sub> concentration (9.11 ± 3.66 µg.m<sup>-3</sup>) and smallest absorption coefficient (0.60 ± 0.35 m<sup>-1</sup>.10<sup>-5</sup>). Mean temperature for winter (14.0 °C) was the lowest of all four seasons yet PM<sub>2.5</sub> concentration (16.1 ± 10.2 µg.m<sup>-3</sup>) and absorption coefficient (2.27 ± 1.49 m<sup>-1</sup>.10<sup>-5</sup>) were 7.0 µg.m<sup>-3</sup> (77 %) and 1.67 m<sup>-1</sup>.10<sup>-5</sup> (278 %) higher than the corresponding values for summer. The same phenomenon was seen when comparing PM<sub>2.5</sub> data for autumn and spring. Mean temperatures for autumn (19.1°C) and spring (17.9 °C) were very similar thus it was

expected that  $PM_{2.5}$  concentrations would be very similar.  $PM_{2.5}$  concentration for spring was  $6.1 \mu\text{g}\cdot\text{m}^{-3}$  (54 %) higher than autumn despite autumn having the higher mean temperature. Absorption coefficient for spring ( $0.94 \text{ m}^{-1}\cdot 10^{-5}$ ) was lower than the corresponding value for autumn (expected because the mean temperature of autumn was higher than spring), however, when compared with summer ( $3.8 \text{ }^\circ\text{C}$  higher than spring), absorption coefficient was  $0.34 \text{ m}^{-1}\cdot 10^{-5}$  (57 %) higher for spring. Data was sorted into three temperature ranges (see Table 4.8, page 118). Mean values were calculated to determine if deviation from literature was exclusively for seasonal data. Mean  $PM_{2.5}$  concentration was highest when temperature was below  $16 \text{ }^\circ\text{C}$  and lowest when temperature exceeded  $20 \text{ }^\circ\text{C}$ . Mean absorption coefficient was highest when temperature was low. A comparison of mean seasonal data and data in Table 4.8 showed that ambient APM concentration had low positive correlation with ambient air temperature for the study period.

#### 5.1.2.3 Change in ambient APM concentrations with Rh and precipitation

Ambient APM concentrations have largely positive correlations with Rh and precipitation (or rainfall) (Wang et al., 2015 and Zhang et al., 2018). As Rh and precipitation increases so do APM concentrations. Again, correlations between APM concentrations, Rh and precipitation are dependent on geographical location, meteorological mean variables and other factors. Seasonal humidity (66-72 %) was consistent for the study period but variations in  $PM_{2.5}$  and absorption coefficient data fluctuated by as much as  $8.3 \mu\text{g}\cdot\text{m}^{-3}$  (91 %) and  $1.67 \text{ m}^{-1}\cdot 10^{-5}$  (278%) respectively. When investigating the effects of rain on ambient APM concentrations (see Fig. 4.22, page 119), only  $PM_{2.5}$  and absorption coefficient data for autumn and summer showed alignment to literature.  $PM_{2.5}$  concentration and absorption coefficient for autumn (precipitation: 9.4 mm) were higher than that for summer (precipitation: 22.2 mm). There was no further alignment to literature.  $PM_{2.5}$  and absorption coefficient data for winter (precipitation: 45 mm) and spring (precipitation: 43 mm) were expected to be lower than the

corresponding values for autumn and summer but were not. Despite winter and spring having, on average, 21-36 mm more rainfall than autumn and summer, mean  $PM_{2.5}$  concentrations were 4.8-8.3  $\mu\text{g}\cdot\text{m}^{-3}$  higher. Data was sorted into three Rh and precipitation ranges (see Table 4.9, page 119). Mean values were calculated to determine if deviation from literature was exclusively for seasonal data. Mean  $PM_{2.5}$  concentration was highest when Rh was below 65 % and precipitation was low (0 mm), and lowest when Rh exceeded 75 % and precipitation was high (above 3 mm). Mean absorption coefficient was highest when Rh and precipitation values were low. High Rh facilitates coagulation processes in the atmosphere while rain “washes-out” water-soluble constituents of ambient APM, decreasing particulate pollution levels (UK-AIR, 2005). A comparison of mean seasonal data and data in Table 4.9 showed that ambient APM concentration had very low positive to no correlation whatsoever with Rh but high positive correlations with precipitation for the study period. Study findings differed from the findings of Wang et al. (2015) and Zhang et al. (2018) who showed a high positive correlation between ambient APM concentration and Rh. Correlations between study data and precipitation, however, were positive like the findings of Wang et al. and Zhang et al. Like temperature, Rh and precipitation could not solely explain the variations in mean seasonal ambient APM concentrations.

#### 5.1.2.4 Change of ambient APM concentrations with air velocity and UV exposure

Ambient APM concentration has largely positive correlation with air velocity (Wang et al., 2015 and Zhang et al., 2018). The faster wind blows, the more pollutants are dispersed and the lower their concentrations. Air velocity had the greatest effect on ambient APM concentrations. The idea that ambient APM concentration decreased as air velocity increased was true for autumn, winter and summer (see Fig. 4.23, page 120). Summer had the highest mean air velocity ( $3.2 \text{ m}\cdot\text{s}^{-1}$ ) and lowest mean  $PM_{2.5}$  concentration for the study period. Winter had the lowest mean air velocity ( $1.7 \text{ m}\cdot\text{s}^{-1}$ ) and although its mean  $PM_{2.5}$

concentration was not the highest, spring was higher, it was  $7.0 \mu\text{g}\cdot\text{m}^{-3}$  (77 %) higher than summer. The mean air velocity for autumn was  $1.8 \text{ m}\cdot\text{s}^{-1}$  ( $0.1 \text{ m}\cdot\text{s}^{-1}$  quicker than winter), its mean  $\text{PM}_{2.5}$  concentration was  $4.8 \mu\text{g}\cdot\text{m}^{-3}$  (42 %) lower than winter. Spring was anomalous. With a mean air velocity of  $2.6 \text{ m}\cdot\text{s}^{-1}$ , spring's  $\text{PM}_{2.5}$  concentration should have been lower than autumn but it was  $6.1 \mu\text{g}\cdot\text{m}^{-3}$  (54 %) higher. Data was sorted into three air velocity ranges (Table 4.10, page 120). Mean values were calculated to determine if agreement with literature was exclusively for seasonal data. Mean  $\text{PM}_{2.5}$  concentration was highest when air velocity was below  $1.5 \text{ m}\cdot\text{s}^{-1}$  and lowest when air velocity was above  $2.5 \text{ m}\cdot\text{s}^{-1}$ . Mean absorption coefficient was highest when air velocity was low. High correlation between mean seasonal data and data in Table 5.3, and alignment between study data and findings by Wang et al. (2015) and Zhang et al. (2018) showed that air velocity had the lowest positive correlation with ambient APM concentration of all meteorological parameters. Wind directions were important for determining the origins and transport routes of pollutants. The effects of wind directions on ambient APM concentration are investigated in section 5.1.3. Sunlight is another factor affecting ambient APM concentration. Sunlight (or UV) catalyses atmospheric transformations of primary pollutants into secondary pollutants (see section 2.1.4) thus ambient APM concentration is directly proportional to amount of sunlight. Summer had the lowest  $\text{PM}_{2.5}$  concentration of all four season despite having the highest percentage clear skies (60 %) while spring had the highest  $\text{PM}_{2.5}$  concentration despite having the lowest percentage clear skies (47 %, tied with winter) (see Fig. 4.25, page 121). From findings it was deduced that the amount of sunlight did not affect  $\text{PM}_{2.5}$  concentrations nearly as much as the meteorological parameters previously discussed. Wang et al. and Zhang et al. had no correlation data for UV exposure so direct comparisons could not be drawn.

#### 5.1.2.5 Summary

In summary, the effects of five meteorological parameters (including UV exposure) on  $\text{PM}_{2.5}$

concentrations and absorption coefficients were investigated. Air velocity had the greatest impact on ambient APM concentration. Cape Town is often windy (mean air velocity: 0.3-5.4 m.s<sup>-1</sup>, mean air velocity  $\geq 2.0$  m.s<sup>-1</sup> on more than 40 % of sampling days) so the pronounced impact (very low correlation between APM concentrations and mean air velocity) was expected. Temperature and precipitation also had low correlations with ambient APM concentrations but were contradictory to literature. High temperatures result in low Rh which leads to elevated ambient APM concentrations while precipitation “washes-away” water-soluble PM. Theoretically, ambient APM concentration should increase as temperature increases and decrease as precipitation increases. The complete opposite was observed. Ambient APM concentrations decreased with temperature increased and decreased as precipitation increased. High PM<sub>2.5</sub> and absorption coefficient values for low temperature days and/or days with precipitation may have resulted from increased combustion of fossil fuel and biomass for heating (warming of households) and travel (more people opt to travel by vehicle during cold, wet conditions). Because seasonal Rh was fairly consistent and mean PM<sub>2.5</sub> concentration (Rh: 65-75 %) was 0.3 ug. m<sup>-3</sup> lower than the mean concentration when Rh < 65 %, Rh was disregarded as factor influencing ambient APM concentration. Like Rh, UV exposure had negligible impact on ambient APM concentration. The formation of secondary pollutants in the vicinity of the sampling site was a given (urban-industrial area near freeway) but the rate of pollutant dispersion by wind was greater than the rate of secondary pollutant formation. A study by Zhang et al. (2018), conducted in the Chang-Tzu-Tan area of China during 2013, ranked the correlation between meteorological parameters and ambient APM concentrations, from high to low, as Rh > temperature > air velocity > rainfall. A study by Wang et al. (2015), also conducted during 2013 but in Nagasaki, Japan, had similar findings. For this study the correlation between meteorological parameters and ambient APM concentration was ranked, from high to low, as rainfall > temperature >>> air

velocity (Rh and UV exposure excluded because of their negligible effects).

### 5.1.3 The effects of air mass transport on ambient APM concentrations

In the previous section, it was shown that three meteorological parameters affected ambient APM concentrations, some more than others. Air velocity had the greatest effect on ambient APM concentrations but did wind direction and long-range transport (LRT) have similar effects on ambient APM concentrations? Northerly (25-51 % of the time) and southerly (33-62 % of the time) wind directions dominated during the study period (see Fig. 4.20, page 117, and Fig. 4.24, page 120). In section 2.4.2 it was discussed that south-easterly winds (nicknamed the “Cape Doctor”) helped rid Cape Town and the region of air pollutants. Mean  $PM_{2.5}$  concentrations and absorption coefficients were lowest for summer when southerly directions dominated (62 % of the time) and northerly directions were at their lowest (25 % of the time). Conversely, winter had the lowest frequency of southerly directions (33 % of the time) and joint highest frequency of northerly directions (51 % of the time), its mean  $PM_{2.5}$  concentration was  $7.0 \mu\text{g}\cdot\text{m}^{-3}$  higher than summer. Winter also recorded the highest mean absorption coefficient value ( $2.27 \text{ m}^{-1}\cdot 10^{-5}$ ). The “neutralising” effect on air pollution by southerly directions is shown by the differences in ambient APM concentrations for winter and summer (as much as 77 % and 278 % for mean  $PM_{2.5}$  concentration and absorption coefficient respectively). Despite dominating, southerly and northerly directions could not solely explain the fluctuations in ambient APM concentrations. The less frequent easterly and westerly wind directions also impacted PM collected in samples. Changes in ambient APM concentration from season-to-season were in-line with changes in easterly and westerly direction frequencies, particularly westerly directions (as frequencies increased so too did  $PM_{2.5}$  concentrations). This phenomenon can be explained by the geographical location of the sampling site. Four of the eight major air pollution sources: Clara Anna Fontein construction site (Durbanville), Portland quarry (Durbanville), Cape Town harbour (Foreshore) and

Chevron refinery (Tableview) were located to the west of the sampling site. The only large air pollution source to the east of the sampling site was the N1 freeway but freeway pollution could have originated from a southerly or westerly direction since the freeway stretches across all three directions. Overall ambient APM concentration and wind direction frequency trends showed that pollution sources to the west of the sampling site greatly impacted PM collected in filter samples but southerly directions had the greatest effect on ambient APM concentrations in the area. Seasonal air mass cluster information (see Fig. 4.28, page 125) supported this claim. Cluster Atlantic-Ocean dominated in autumn, winter and spring, and placed second (behind cluster Indian-Ocean) in summer. Mean  $PM_{2.5}$  concentrations and absorption coefficients were highest when trajectory Atlantic-Ocean dominated. Trajectory Atlantic-Ocean emanated from the most southerly parts of the Atlantic Ocean and as it “migrated” inland, it passed over the five large sources of pollution, including the Cape Town Central Business District (CBD), carrying APM to the sampling site. Ore refineries in Saldanha (166 km NNW of the sampling site) were large sources of ambient APM in the region. The sum of percentage frequencies of trajectories Atlantic-Ocean and Saldanha explained the mean  $PM_{2.5}$  concentration trends shown in Fig. 5.5 (page 153). Mean seasonal  $PM_{2.5}$  concentrations were very similar (within the uncertainties). Mean seasonal  $PM_{2.5}$  concentrations ranked in descending order were spring ( $17.4 \pm 8.7 \mu\text{g}\cdot\text{m}^{-3}$ ) > winter ( $16.1 \pm 10.2 \mu\text{g}\cdot\text{m}^{-3}$ ) > autumn ( $11.3 \pm 5.7 \mu\text{g}\cdot\text{m}^{-3}$ ) > summer ( $9.11 \pm 3.22 \mu\text{g}\cdot\text{m}^{-3}$ ) which corresponded with the sum of percentage frequencies for each season that were, in descending order, spring (60 %), winter (59%), autumn (45 %) and summer (40 %). Summer had the highest frequency of trajectory Indian-Ocean (43 %), nearly identical to trajectory Atlantic-Ocean (40 %), which demonstrated the dispersion effect of southerly wind directions in the region. A combination of north-westerly and westerly wind directions and, air mass transport saw winter and spring record the highest mean ambient APM concentrations for the

study period while strong southerly winds (mean velocity:  $3.8 \text{ m}\cdot\text{s}^{-1}$ ) led to greater air pollutant dispersion and ultimately lower ambient APM concentrations for summer.

#### 5.1.4 Correlation between study data and air pollution data from the CoCT

Correlation between study data and data collected by ambient air quality monitoring (AAQM) stations was important for determining the effects of LRT on PM collected in filter samples. Air quality information was used to determine potential sources of ambient APM in the region. Stations were selected to provide “complete coverage” around the sampling site. The station at Atlantis provided data for the north, stations at City Hall, Goodwood, and Tableview for the west, station at Somerset-West for the south, and station at Wallacedene for the east. The station at Atlantis (37 km NNW of the sampling site) monitored for two air pollutants, ozone ( $\text{O}_3$ ) and sulfur dioxide ( $\text{SO}_2$ ).  $\text{O}_3$  is an atmospheric gas and strong oxidising agent but the pollutant of interest was  $\text{SO}_2$ .  $\text{O}_3$  is regarded as the most important indicator of photochemical air pollution but because  $\text{O}_3$  data had fluctuated considerably and, as discussed in section 5.1.4, to determine the impact of sources N-NW of the sampling site stability of data was important hence  $\text{SO}_2$  was selected for correlation purposes. Besides being the most abundant air pollutant (see Table 2.1, page 13),  $\text{SO}_2$  data was far more stable than that of  $\text{O}_3$ .  $\text{SO}_2$  is a known by-product of refining processes. Because Atlantis was situated between the sampling site and Saldanha, correlation between study data and data collected by this station would have given an indication of overall contribution by ore refineries to PM collected in filter samples. Correlations between  $\text{SO}_2$  concentrations and seasonal  $\text{PM}_{2.5}$  concentration (0.02-0.17) and absorption coefficient (-0.24 to 0.29) were very weak and weak for the study period respectively. This indicated that contribution to PM mass in samples was negligible to none by LRT from sources, more specifically refineries in Saldanha, N-NW of the sampling site. The five remaining stations were all within a 30 km radius of the sampling site thus any correlation with data collected by these stations was



considered “local” source contribution.  $O_3$  is a strong oxidising agent that oxidises air pollutants nitrogen dioxide ( $NO_2$ ) and  $SO_2$  into nitrates ( $NO_3^-$ ) and sulfates ( $SO_4^{2-}$ ), two major chemical constituents of ambient APM. These chemical reactions deplete  $O_3$  in the atmosphere thus correlations between itself and  $PM_{2.5}$  concentrations and absorption coefficients should be negative. Correlations between study data and  $O_3$  data from Atlantis fluctuated considerably. Seasonal correlation coefficient values were -0.27 to 0.51 and -0.11 to 0.56 for  $PM_{2.5}$  concentration and absorption coefficient respectively. The same correlations for Wallacedene had seasonal correlation coefficients of -0.23 to -0.03 and -0.46 to -0.03 for  $PM_{2.5}$  concentration and absorption coefficient data respectively. Weak correlation between study data and  $SO_2$  data, and the fluctuations in correlation coefficient values for study data and  $O_3$  data from Atlantis showed that contributions by local sources to PM collected in samples far exceeded that of LRT, if any at all. Correlation between  $NO_2$  data (recorded 21-30 km, west of sampling site) and mean  $PM_{2.5}$  concentration and absorption coefficient data was moderate to high for autumn (0.41 and 0.70) while correlation between  $SO_2$  data and mean  $PM_{2.5}$  concentration and absorption coefficient data was moderate to high for autumn (0.49 and 0.71) and high for winter (0.72 and 0.74). As  $NO_2$  and  $SO_2$  concentrations had increased (at a distance of 21-30 km, west of the sampling site), so did mean ambient APM concentrations in filter samples. From the correlation values above it can be deduced that there was a high possibility that secondary pollutants,  $NO_3^-$  and  $SO_4^{2-}$  (originating 21-30 km, south and west of the sampling site), contributed to overall PM mass in samples during autumn and winter. Correlation between  $NO_2$  data (recorded 11-20 km, west of sampling site) and mean  $PM_{2.5}$  concentration and absorption coefficient data was moderate for autumn (0.23 and 0.28) and winter (0.38 to 0.40) while correlation between  $SO_2$  data and mean  $PM_{2.5}$  concentration and absorption coefficient data was moderate for winter (0.30 and 0.43). From the correlation values above it can be deduced that there was a high possibility that secondary

pollutants,  $\text{NO}_3^-$  and  $\text{SO}_4^{2-}$  (originating 11-20 km, west of the sampling site), contributed to overall PM mass in samples during autumn and winter, especially winter. Correlation between study data and AAQM data (within 10 km of the sampling site) meant a direct comparison between study data and air quality data from Wallacedene (3 km ESE). Correlation between  $\text{NO}_2$  data and mean  $\text{PM}_{2.5}$  concentration and absorption coefficient data was moderate to high for autumn (0.46 and 0.51). Unfortunately there was no data for the winter, spring and summer (AAQM station unavailability). Correlation between  $\text{SO}_2$  data and mean  $\text{PM}_{2.5}$  concentration was moderate for winter (0.28) while correlation between  $\text{SO}_2$  data and absorption coefficient data was high for autumn (0.52). The AAQM station at Wallacedene was the only station that monitored  $\text{PM}_{10}$  concentrations. Correlation between  $\text{PM}_{10}$  data and mean  $\text{PM}_{2.5}$  concentration and absorption coefficient data was moderate to high correlation for autumn (0.47 and 0.75) and winter (0.41 and 0.55). Because of Wallacedene's proximity to the sample site it could be argued that air pollution data for the area would be directly proportional to the ambient APM concentrations in samples. This claim was rejected because correlation between  $\text{PM}_{10}$  and  $\text{SO}_2$  data, and mean  $\text{PM}_{2.5}$  concentration for spring was low to negligible. In summary, Spearman Rank-Order Correlation (SROC) testing was performed on study data and data collected by the City of Cape Town (CoCT). Correlation coefficients were moderate to high for AAQM stations to the south and west of the sampling site (within 40 km), particularly for autumn and winter. Favourable correlation with these stations, along with the findings from section 5.1.3, indicated that pollution sources to the west and south of the site had contributed to PM mass collected in filter samples during autumn and winter. Correlation coefficients were mostly weak and negative for spring and summer (for mean  $\text{PM}_{2.5}$  concentration and absorption coefficient data). This indicated that PM collected during spring and summer was emitted by local sources within 3 km of the sampling site.

### 5.1.5 Correlation between air pollution data for Cape Town, Pretoria and Thohoyandou

This study formed part of a larger project investigating air quality in South Africa. The contents herein are from the sampling site in Cape Town but how did the city fare against Pretoria and Thohoyandou? According to the Western Cape Government, Cape Town is the second largest city in South Africa, only behind Johannesburg (Gauteng Province). The Johannesburg/Pretoria mega city is home to some 10 million inhabitants, six million (150 %) more than in Cape Town. Thohoyandou finds itself on the opposite end of the population scale. Thohoyandou, regarded as a resort town in the Limpopo Province, is home to approximately 70,000 inhabitants with little to no industrial activity. Geographically, elevations of the three sites were considerably different. Cape Town has an elevation of 20-50 m while the mega city and Thohoyandou are situated 1350-1750 m and 700-750 m above sea level respectively. Differences in elevation meant that air was thinner in the mega city and Thohoyandou making these regions more conducive for LRT and the geographical locations of both the mega city and Thohoyandou made them more susceptible to elevated ambient APM concentrations than Cape Town. All of South Africa's 18 coal power stations are located in Gauteng and neighbouring provinces - Free State, Limpopo and Mpumalanga. Combined, coal stations emit an estimated 100-110 kt of APM annually. Did emissions from coal stations impact air quality in the mega city and Thohoyandou during the study period? See Table 4.3 (page 104) and Table 4.15 (page 135) for descriptive statistics for each site. Mean  $PM_{2.5}$  concentrations and absorption coefficients were similar for the three locations (within the uncertainties). Pretoria had the highest mean  $PM_{2.5}$  concentration for the study period ( $21.1 \pm 15.0 \mu\text{g}\cdot\text{m}^{-3}$ ) followed by Cape Town ( $13.4 \pm 8.1 \mu\text{g}\cdot\text{m}^{-3}$ ) and Thohoyandou ( $10.9 \pm 8.3 \mu\text{g}\cdot\text{m}^{-3}$ ). Pretoria also had the highest mean  $PM_{2.5}$  concentrations for autumn, winter, and summer. This information was expected considering the demand for energy and resources by the city's inhabitants, and that eight coal power stations are located within

200 km of the sampling site. This claim was further substantiated by mean absorption coefficient data. Pretoria had the highest mean absorption coefficient for the study period ( $2.34 \pm 2.05 \text{ m}^{-1} \cdot 10^{-5}$ ) followed by Cape Town ( $1.38 \pm 1.23 \text{ m}^{-1} \cdot 10^{-5}$ ) and Thohoyandou ( $0.69 \pm 0.57 \text{ m}^{-1} \cdot 10^{-5}$ ). Pretoria, surprisingly, recorded the lowest  $\text{PM}_{2.5}$  concentration ( $14.3 \pm 8.2 \text{ } \mu\text{g} \cdot \text{m}^{-3}$ ) for spring while the corresponding values for Cape Town ( $17.4 \pm 8.7 \text{ } \mu\text{g} \cdot \text{m}^{-3}$ ) and Thohoyandou ( $14.7 \pm 9.5 \text{ } \mu\text{g} \cdot \text{m}^{-3}$ ) were the highest for the study period. This anomaly was attributed to meteorological conditions for the mega city during the months of September-November 2017 or a substantial decrease in LRT from distant sources for that period. A commonality amongst air quality data for all three sites was high relative standard deviation (R.S.D). R.S.D values for mean  $\text{PM}_{2.5}$  concentration and absorption coefficient data were > 60 % and 80 % respectively. In summary, ambient APM concentrations had high correlation with population size and geographical location. Ambient APM concentrations of two of the country's largest cities, Johannesburg/Pretoria mega city and Cape Town, exceeded that of Thohoyandou for most of the study period. Despite having little to no industrial activity, Thohoyandou's air quality information clearly showed the effects of LRT (from distant sources) on the rural area. There was high correlation between time of year and ambient APM concentrations for Pretoria and Thohoyandou. Highest mean seasonal  $\text{PM}_{2.5}$  concentration and absorption coefficient values for the two areas, ranked in descending order, were for winter > autumn > spring > summer. Mean absorption coefficient data for Cape Town showed the same correlation, however, mean  $\text{PM}_{2.5}$  concentration was highest for spring.

## 5.2 Composite samples

Experimental data for composite samples is discussed in this section. This section discusses the chemical compositions of composite samples (see Table 4.21, page 142) and possible sources of pollution that may have contributed to the ambient PM collected in each sample.

The effects of meteorological parameters and air mass transport will also be discussed. Composite samples were collected over four week periods (sampling time: 24 hours, sampling interval: seven days) on weekdays and weekend days during the months of September 2017 (spring) and January 2018 (summer). See Appendix 1C for composite samples sampling information.

### 5.2.1 The effects of meteorological conditions on composite samples

In section 5.1.2 it was shown that mean seasonal meteorological conditions for spring and summer were rather different with the only similarity being parameter Rh. Were the same differences between spring and summer found for September 2017 and January 2018? Apart from percentage clear skies (UV exposure) and some similarities in wind direction frequencies, meteorological conditions for September and January, like spring and summer, were unique. Mean temperatures for September (17 °C) and January (23 °C) differed by 6 °C. On average, weekend days were slightly warmer than weekdays. In section 5.1.2.2, it was shown that air temperature had moderate correlation with ambient APM concentrations. For composite samples, however, correlation was high, particularly for inorganic carbon content. Mean inorganic carbon (or soot) content differed by as much as 4 wt. % for September (13 wt. %) and January (8.9 wt. %). Cooler temperatures in September could have explained the difference in inorganic carbon content (as more people opted to burn biomass and fossil fuels for heating purposes) but ultimately it was the holiday period (during December-January) that affected inorganic carbon content the most. Around this time every year businesses close for the annual Christmas holidays from mid-December up until mid-January. Fewer business activities equates to fewer emissions. The number of cars travelling on the N1 freeway also decreases during this time, lowering exhaust emissions in the area. A counter theory would be that since more people are on leave in January, more people will “braai” (recreational activity for cooking meat over an open-flame) more often. “Braaiing” is a national past time in South

Africa and more people tend to braai outdoors when the weather is good but cooler temperatures would not reduce the number of households that braai drastically since many households are equipped with indoor braai facilities. The location of the sampling station is surrounded by six neighbour properties, all of which had occupants that “braaiied” at least 1-2 times per week (exact frequency unknown). Precipitation is another factor that affected the chemical compositions of composite samples. In section 5.1.2.3 it was shown that precipitation had low correlations with ambient APM concentrations. For composite samples, correlations were moderate to high. Weight percentage of water-soluble species chloride  $\text{Cl}^-$ ,  $\text{NO}_3^-$  and  $\text{SO}_4^{2-}$  were, on average, 12 %, 107 % and 91 % higher for January (mean precipitation: 0.2 mm) than September (mean precipitation: 0.6 mm). The effects of air velocity were not as pronounced for composite samples as they were for calendar samples (see section 5.1.2.4). In fact, weight percentages of all but two chemical constituents, inorganic carbon and iron (weekend day samples only), were higher for January (mean air velocity:  $3.4 \text{ m.s}^{-1}$ ) than for September (mean air velocity:  $2.9 \text{ m.s}^{-1}$ ). This finding contradicted the claim made in section 5.1.2.4 that correlation between ambient APM concentration and air velocity was very low. One explanation for this could have been the composite (or accumulative) sampling method used but a more plausible explanation would have been that despite January having a higher mean air velocity, the concentrations of chemical species in the atmosphere during January far exceeded the concentrations of these species for September. The metallic content of each composite sample was unique (irrespective of month sampled), however, there was a strange observation for weekend day samples in particular. Weekend day composite samples were the only samples that contained aluminium (0.4-0.7 wt. %) and iron (7.4-9.4 wt. %). The property adjacent to the location of the sampling station was the scene of metal works over weekends (the owner of the property worked during the week and performed “private” metal works over weekends). This is the

only explanation for elevated aluminium and iron concentration in weekend day composite samples.

### 5.2.2 The effects of air mass transport on composite samples

Air mass transport had a pronounced effect on ambient APM concentrations for calendar samples (see section 5.1.3). Like calendar samples, composite samples were also affected by air mass transport.  $\text{Na}^+$  (8.3-38 wt. %) and  $\text{Cl}^-$  (21-31 wt. %) were the largest components of PM in all composite samples. Trajectories Atlantic-Ocean (40-47 %) and Indian-Ocean (27-43 %) dominated during September 2017 and January 2018. Using this information it was determined that the Atlantic (20 km W) and Indian (25 km S) oceans were the most probable source of  $\text{Na}^+$  and  $\text{Cl}^-$  in PM. Correlations between study data (calendar samples) and  $\text{SO}_2$  and  $\text{PM}_{10}$  data for Wallacedene for spring and summer were very low to moderately negative respectively. This indicated that contributions to overall PM mass from sources at Wallacedene (or sources within 3 km east of the sampling site) were negligible to nothing. A commonality between calendar and composite samples was that contributions to PM collected in samples were attributed primarily to sources in a southerly and/or westerly direction from the sampling site.

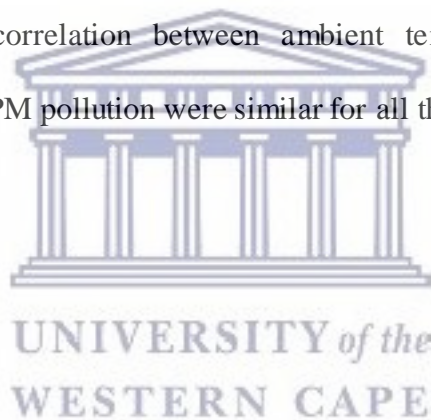
### 5.2.3 Summary

T-test results indicated that weekday and weekend day data for September 2017 had similarity as did weekday and weekend day data for January 2018. Anionic and metallic species represented the largest proportions of ambient PM collected in composite samples with 31-54 wt. % and 27-51 wt. % respectively. Inorganic carbon (or soot) was the third most abundant species in the samples (7.0-14 wt. %). Mean soot content for September (13 wt. %) was 48 % higher than January (8.9 wt. %) which could be explained by the reduction of traffic and shutdown of business for the Christmas holidays (mid-December to mid-January).

Mean anion content for September (34 wt. %) was 38 % lower than January (47 wt. %) which could be explained by the increase in mean temperature (5.9 °C) and decrease in mean Rh (4 %) and mean precipitation (0.4 mm) for January over September which meant ambient APM remained airborne for longer periods and could travel greater distances (no difference cluster information, clusters Atlantic-Ocean and Indian-Ocean were equally dominant during these periods). Anions, metals and soot accounted for the majority of ambient PM collected (88-98 wt. %). The mean weight percentages of unidentified species (or unknown species) for September and January composite samples were 12 wt. % and 4.8 wt. % respectively. Based on the meteorological conditions (see Appendix 15), the largest constituent of “unknown” was likely water. When weekday and weekend day data for September were compared to the corresponding data for January, T-test results for weekday data showed no similarity while weekend day data showed similarity. Iron content of ambient PM in weekend day samples of September (7.4 wt. %) and January (9.4 wt. %) were anomalous and emanated from metal works performed at the neighbouring property. Unknown (or unidentified) constituents of composite samples (1.6-12 wt. %) are believed to have been primarily water (unable to accurately quantitate water content post-drying due to the readability limitations of the Mettler-Toledo ML204 microbalance), ammonium, and organic carbon (including VOCs adsorbed to PM). Cluster information and correlation coefficients for calendar samples (see Table 4.14, page 132) showed that although constituents like chloride were transported from oceanic areas to the sampling site, other constituents like sulfates (oxidation of SO<sub>2</sub> in the atmosphere), nitrates (oxidation of NO<sub>2</sub> in the atmosphere) and soot in ambient PM collected in composite samples largely emanated from sources within 3 km of the sampling site, the most probable source being the N1 freeway (two millions vehicles per day) and the combustion of biomass and fossil fuels (for recreational and heating purposes). Overall, PM<sub>2.5</sub> and soot data for the study period showed largely positive correlations for all seasons as did



the correlations between APM concentrations and meteorological parameters. Mean monthly and seasonal  $PM_{2.5}$  and absorption coefficient data were similar within uncertainties (see section 5.1.1). When study data was compared to air pollution data for Pretoria and Thohoyandou they were similar (within uncertainties) but it was Pretoria, because of its geographical location and close proximity to coal power stations, that had the highest mean  $PM_{2.5}$  and absorption coefficient values. Because of the rarity of these studies in South Africa and the entire African as a whole, correlation data was compared to data from two studies conducted in two East Asian cities namely Chang-Zhu-Tan (China) and Nagasaki (Japan) during 2013. Both of these cities are situated in the Northern Hemisphere as opposed to Cape Town that is situated in the Southern Hemisphere. Despite the differences in geography and seasonal meteorology, the correlation between ambient temperature, precipitation, air velocity and Rh and ambient PM pollution were similar for all three studies.



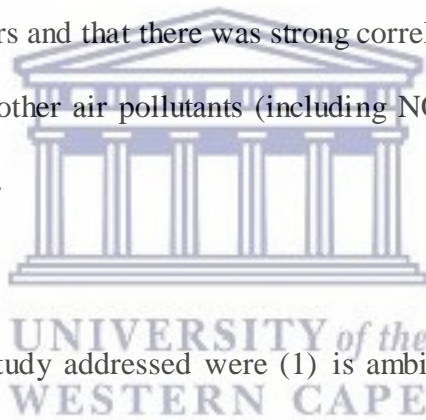
## **CHAPTER 6: CONCLUSION**

### 6.1 Outcomes of study

The intent of this study was to determine the concentrations of hazardous air pollutants PM<sub>2.5</sub> and soot in Cape Town and the region. From 18 April 2017 to 16 April 2018, 146 filters samples were collected from a fixed sampling site in the residential suburb of Kraaifontein (27 km ENE of the City Centre). The intent of sampling was to determine ambient PM<sub>2.5</sub> and soot concentrations in the area as part of a larger project investigating ambient APM concentrations across South Africa. South Africa is a developing nation and the second largest economy in Africa. This growth has seen an increase in emissions, more specifically PM<sub>2.5</sub> and soot. These pollutants (fourth and fifth most abundant in our atmosphere) penetrate lung tissue deeply to enter the cardiovascular system. Because of their complex chemistries, PM<sub>2.5</sub> and soot are hazardous to human health and thus it is imperative that detailed ambient APM studies be conducted to determine particulate pollution trends. Detailed ambient APM studies are important for determining (1) ambient APM concentrations in an area/region, (2) how external factors affect pollutant mobility and transport and (3) the largest sources of ambient APM in an area/region, information useful for calculating particulate pollution trends in an area/region for a specified time period. Ambient APM was collected using the PTFE filter/vacuum pump technique, a common methodology amongst both air quality and atmospheric sciences communities. This technique was selected because of its relatively low operating costs, ease of use and popularity. PM<sub>2.5</sub> and soot concentrations were determined using accredited methodologies used in studies conducted abroad. Mean PM<sub>2.5</sub> concentration ( $13.8 \pm 8.1 \mu\text{g}\cdot\text{m}^{-3}$ ) for the study period was below the SA NAAQS limit but exceeded the WHO annual limit. Mean absorption coefficient ( $1.38 \pm 1.23 \text{ m}^{-1}\cdot 10^{-5}$ ) did not exceed any limits for the study period. Two observations were made from study data - statistically, there were no differences between PM concentrations in samples collected on weekday and

weekend days and strengths of association between  $PM_{2.5}$  concentration and absorption coefficient data (for weekday and weekend days) were mostly large while corresponding linear relationships were strong. Meteorological conditions had affected study data with some meteorological parameters affecting PM concentrations more than others. Air velocity had the greatest impact, by far, followed by temperature and rainfall (Rh and UV exposure were discarded due because of their negligible effect on ambient APM concentrations). Air mass transport was another factor that affected ambient PM concentrations in filter samples, particularly from westerly and southerly directions of the sampling site. The lack of significant polluters to the north of the sampling site and poor correlation with air pollution data for the town of Atlantis (37 km NNE) indicated that air mass transport (including LRT) of ambient APM from the north was minimal to nothing. Another deduction that was made was that air quality in the area was not impacted by LRT. Study, meteorological and trajectory data indicated that PM collected in filter samples were from sources located to the east, but mostly west and south of the sampling site. Trajectory data was based on single, 24 hour plots of air current movement with an error of 30%. The greater the distance from the sampling site along the generated plot, the greater the deviation to the left or right of the plot (e.g. if a plot passes over a potential source that is situated 20 km from the sampling site, deviation is 6 km to the left or right of the source's location). Cluster analysis would resolve this problem but due to limited resources, that options could not be pursued. In addition to 146 calendar sample, four composite samples were taken during the months of September 2017 and January 2018. The aim was to determine the chemical compositions of PM in these samples. The single largest component was chloride (27-31 %) that travelled inland from the Atlantic and Indian Oceans. Inorganic carbon content was another prominent component of PM. Concentrations varied from 15-16 wt. % and 10-11 wt. % for September and January respectively. An analysis of chemical composition data for composite samples indicated

ambient APM from the combustion of biomass (wood) and fossil fuels (petrol, diesel, and liquid petroleum gas) for domestic purposes and transportation, and air mass transport from the Atlantic Ocean (west of sampling site) and Indian Ocean (south of sampling site) were the largest contributors to overall ambient PM mass collected in samples. The intent of this study was to determine the concentrations of hazardous air pollutants  $PM_{2.5}$  and soot in Cape Town and was the first of its kind for the region. The study investigated the effects of meteorological conditions and air mass transport on ambient APM while correlation analyses were performed, not only between seasonal data sets, but between study data and air pollution data from six AAQM stations ranging from 3 km to 37 km from the sampling site with a total coverage of 200°. Study data showed that some meteorological parameters impacted APM concentrations more than others and that there was strong correlation between  $PM_{2.5}$  and soot and between  $PM_{2.5}$ , soot and other air pollutants (including  $NO_2$ , PM and  $SO_2$ ) within a 10 km radius of the sampling site.



## 6.2 Research questions

The research questions this study addressed were (1) is ambient  $PM_{2.5}$  and soot (or black carbon) data, collected at a fixed sampling site, representative of an entire area or region? Correlation analyses between study data and air pollution data from the CoCT showed mostly positive and stable correlation within a 10 km radius of the sampling site thus ambient APM data from a single sampling site is not representative of an entire area or region. (2) What are the probable sources of ambient  $PM_{2.5}$  and soot in Cape Town? Several analytical methodologies were used to analyse daily and composite samples in attempts to determine their chemical make-ups. The two most probable sources of  $PM_{2.5}$  and soot collected in samples were identified as vehicular and residential emissions (including braaiing) and sea salt blown in from the Atlantic and Indian Oceans. (3) Are there associations between ambient  $PM_{2.5}$  and soot concentrations for monthly and seasonal data sets and why are there

differences between monthly and seasonal associations? Correlation analyses showed strong positive correlation between  $PM_{2.5}$  and soot for monthly and seasonal data sets, however, associations between seasons were low to moderately positive. This could be explained by the changes of meteorological conditions and demand for energy (cooking, heating and travel to name only a few).

(4) Are there associations between study data and air pollution data produced by the CoCT? Why do associations between study data and data from individual AAQM stations differ with direction and distance of these stations from the sampling site? As discussed earlier, positive associations between study data and air pollution data from the CoCT were stable up to a radius of 10 km after which, the farther one moved beyond 10 km, positive association began to diminish. Ambient APM concentrations are dependent on several factors. The topographical and geographical properties of Cape Town might have had an impact of air mass transport from distant sources thus the weak associations between study data and data from AAQM stations located farther than 10 km. Further studies are required to determine the specific factors responsible the fluctuations in correlation between data sets.

(5) Do ambient  $PM_{2.5}$  and soot concentrations for the study period fall below or exceed WHO and SA NAAQS limits? Why do APM concentrations in Cape Town differ from concentrations in Pretoria and Thohoyandou? Mean annual  $PM_{2.5}$  concentration for the samples exceeded the WHO limit of  $10 \mu\text{g}\cdot\text{m}^{-3}$  but fell below the SA NAAQS limit of  $20 \mu\text{g}\cdot\text{m}^{-3}$  for the study period. Soot concentrations did not exceed any limits for the study period. Differences in ambient APM concentrations for Cape Town, Pretoria and Thohoyandou are mainly because of geographical location and differences in seasonal meteorological conditions. Pretoria is situated within 200 km of eight coal power stations hence it is expected that Pretoria will have higher  $PM_{2.5}$  and soot levels, on average, than Cape Town, which it did. Ambient APM levels for Cape Town and Thohoyandou were quite similar.

(6) Is HYSPLIT an effective tool for determining air mass origins? Why was it used

or trajectory and cluster analyses? NOAA ARL's HYSPLIT model is used by many researchers for trajectory and cluster analysis. v. Roosbroeck et al. (2006), Wang et al. (2015), Molnár et al. (2017) and Zhang et al. (2018), to name only a few, used the HYSPLIT model to generate back trajectories in their respective studies. HYSPLIT proved to be an important tool for this study. HYSPLIT was used for this study because of its popularity amongst fellow air quality researchers. (7) Do meteorological parameters impact ambient APM concentrations? Why do some meteorological parameters affect APM concentrations more than others? Seasonal data sets clearly showed that meteorological condition did have an impact on APM levels. Air velocity had a pronounced effect on concentrations, some parameters (like rainfall and temperature) impacted concentration somewhat while other parameters like Rh and UV exposure had negligible effects on PM concentrations in samples. (8) Is air quality in Cape Town impacted by LRT? Is the impact of LRT on air pollution levels in the city significant? Long range transport (from sources farther than 40 km from the sampling site) did not impact the PM concentrations in the samples whatsoever. The biggest sources of APM (located more than 10 km from the sampling site) were the Atlantic and Indian Oceans (20-25 km from the sampling site).

### 6.3 Research delimitations and limitations

Research delimitations were investigating the effects of meteorological conditions and air mass transport on pollutant levels, and correlation between study data and air pollution data collected by the CoCT. Meteorological data (supplied by SAWS), trajectory cluster information (generated from the HYSPLIT model) and air pollution data (supplied by the CoCT) indicated that PM collected in filters samples were transported from local sources (within 40 km of the sampling site) with the largest sources of ambient APM identified as the Atlantic and Indian Oceans, N1 freeway and dwellings within a 3 km radius of the sampling site. Research limitations were determining the percentage contribution by each of the

sources of ambient APM using source apportionment (factor analysis and receptor modelling) and identifying the “unknown” (or unidentified) constituents in composite samples for a complete qualitative and quantitative breakdown of the chemical make-up of PM in samples (unable to quantify due to the limitations of laboratory instrumentation).

#### 6.4 Recommendations

Recommendations for future studies is to investigate source apportionment in Cape Town to determine the exact contributions by individual APM sources to overall ambient APM concentrations in the region. The extent of plastic and microplastic pollution should also be explored. Speaking at the “Science for Ocean Action” conference in Norway (November 2018), Dr. B. Grøsvik, marine chemist at the Institute of Marine Research, indicated that plastics and microplastics derived from automotive tyres (through abrasion with tarmac) is the single largest contributor to plastics pollution in the oceans. The concern is that, before microplastics are deposited into the oceans, these species become airborne where they are transported by air currents to the coast. Microplastic particulates are tiny (less than 25 µm in diameter) making them inhalable. Microplastics, like most APM, have adverse health outcomes on human beings therefore a study investigating concentrations and transportation of airborne microplastics in Cape Town is recommended. The effects of LRT on PM concentrations were negligible so a final recommendation would be to perform a comparative study between Cape Town and its international counterparts (cities with similar demographics, industrial outputs and meteorological conditions) to determine the extent of LRT on ambient APM concentrations based on the geographical location of the study area.

## **BIBLIOGRAPHY**

1. Aeroqual, 2017. *Aeroqual AQM 65: Ambient Air Quality Monitoring station*. URL: [aeroqual.com/product/aqm-65-air-quality-monitoring-station](http://aeroqual.com/product/aqm-65-air-quality-monitoring-station)
2. Aerosol Science and Engineering program, University of Florida and University of Washington (in St. Louis), 2017. *Atmospheric aerosol*. URL: [aerosol.ees.ufl.edu/atmos\\_aerosol/section04.html](http://aerosol.ees.ufl.edu/atmos_aerosol/section04.html)
3. Alitieri, K. & Keen, S., 2016. *The cost of air pollution in South Africa*. URL: [theigc.org/blog/the-cost-of-air-pollution-in-south-africa/](http://theigc.org/blog/the-cost-of-air-pollution-in-south-africa/)
4. Amaral, S., Carvalho, J., Costa, M. & Pinheiro, C., 2015. *An overview of particulate matter measurement instruments*. *Atmosphere*, Vol. 6, pp. 1327-1345
5. APPA (Atmospheric Pollution Prevention Act), 1965. URL: [up.ac.za/media/shared/600/LAS%20Legislation/air-pollution-prevention-act\\_17-april-1965.zp53523.pdf](http://up.ac.za/media/shared/600/LAS%20Legislation/air-pollution-prevention-act_17-april-1965.zp53523.pdf)
6. Australian Department of the Environment and Energy, 2005. *National standards for criteria air pollutants 1 in Australia*. URL: [environment.gov.au/protection/publications/factsheet-national-standards-criteria-air-pollutants-australia](http://environment.gov.au/protection/publications/factsheet-national-standards-criteria-air-pollutants-australia)
7. Bèrubè, K., Jones, T., Williamson, B., Winters, C., Morgan, A. & Richards, R., 1999. *Physiochemical characterisation of diesel exhaust particles: factors for assessing biological activity*. *Atmospheric Environment*, Vol. 33 pp. 1599-1614
8. Beta Attenuation (Thermo Scientific), 2017. URL: [thermofisher.com/za/en/home/industrial/environmental/environmental-learning-center/air-quality-analysis-information/beta-attenuation-technology-particulate-matter-measurement.html](http://thermofisher.com/za/en/home/industrial/environmental/environmental-learning-center/air-quality-analysis-information/beta-attenuation-technology-particulate-matter-measurement.html)
9. BP Statistical Review of World Energy, 2013. URL: [large.stanford.edu/courses/2013/ph240/lim1/docs/bpreview.pdf](http://large.stanford.edu/courses/2013/ph240/lim1/docs/bpreview.pdf)



10. Business Tech. report, 2016. *Nigeria overtakes South Africa as Africa's biggest economy*. URL: [businesstech.co.za/news/finance/140681/nigeria-overtakes-south-africa-as-africas-biggest-economy/](http://businesstech.co.za/news/finance/140681/nigeria-overtakes-south-africa-as-africas-biggest-economy/)
11. Calkins, D., 1998. *Global Partnerships: A Collaborative Effort to Improve Air Quality in Developing Countries*. 98-TA42.01. URL: [epa.gov/ttnamti1/archive/files/ambient/gems/gpem101.pdf](http://epa.gov/ttnamti1/archive/files/ambient/gems/gpem101.pdf)
12. Cashins and Associates Ltd., 2013. *Industrial Hygiene - What is Soot and why is it dangerous*. URL: [blog.cashins.com/blog-0/bid/191511/Industrial-Hygiene-What-is-Soot-and-Why-is-it-Dangerous](http://blog.cashins.com/blog-0/bid/191511/Industrial-Hygiene-What-is-Soot-and-Why-is-it-Dangerous)
13. Claxton, L., Matthews, P. & Warren, S., 2004. *The genotoxicity of ambient outdoor air, a review: Salmonella mutagenicity*. *Mutat. Res.* Vol. 567, pp. 347-399
14. CNN (Central News Network) report by van Dam, D., 2017. *Cape Town contends with the worst drought in over a century*. URL: [edition.cnn.com/2017/05/31/africa/cape-town-drought/index.html](http://edition.cnn.com/2017/05/31/africa/cape-town-drought/index.html)
15. Constitution of South Africa, 1996. URL: [justice.gov.za/legislation/constitution/saconstitution-web-eng.pdf](http://justice.gov.za/legislation/constitution/saconstitution-web-eng.pdf)
16. CTIA (Cape Town International Airport), 2017. URL: [capetown-airport.com/](http://capetown-airport.com/)
17. Davy, P., Tremper, A., Nicolosi, E., Quincey, P. & Fuller, G., 2017. *Estimating particulate black carbon concentrations using two offline light absorption methods applied to four types of filter media*. *Atmospheric Environment*, Vol. 152, pp. 24-33
18. DEA (Department of Environmental Affairs), 2000. *Integrated Pollution and Waste Management Policy*. URL: [environment.gov.za/sites/default/files/legislations/integrated\\_pollutionand\\_wastemanagement\\_0.pdf](http://environment.gov.za/sites/default/files/legislations/integrated_pollutionand_wastemanagement_0.pdf)
19. DEA (Department of Environmental Affairs), 2001. *Air Quality Bill*. URL: [environment.gov.za/sites/default/files/legislations/nem\\_air\\_quality62b.pdf](http://environment.gov.za/sites/default/files/legislations/nem_air_quality62b.pdf)

20. DEA (Department of Environmental Affairs), 2016. NEMAQA (National Environmental Management: Air Quality Act). URL: [environment.gov.za/sites/default/files/legislations/nema\\_amendment\\_act39.pdf](http://environment.gov.za/sites/default/files/legislations/nema_amendment_act39.pdf)
21. DEA (Department of Environmental Affairs), 2017. National Framework for Air Quality Management in the Republic of South Africa. URL: [saaqis.environment.gov.za/pagesfiles/draft%202017%20national%20framework.pdf](http://saaqis.environment.gov.za/pagesfiles/draft%202017%20national%20framework.pdf)
22. DEA (Department of Environmental Affairs), 2017. NEMAQA: National Ambient Air Quality Standards. URL: [environment.gov.za/sites/default/files/legislations/nemaqa\\_airquality\\_g32816gon1210.pdf](http://environment.gov.za/sites/default/files/legislations/nemaqa_airquality_g32816gon1210.pdf)
23. DEA (Department of Environmental Affairs), 2017. *State of Air Chapter. 3: Air Quality Standards and Objectives*. URL: [environment.gov.za/sites/default/files/docs/stateofair\\_executive\\_iaiquality\\_standardsonjectives.pdf](http://environment.gov.za/sites/default/files/docs/stateofair_executive_iaiquality_standardsonjectives.pdf)
24. Desert Research Institute, 2002. *Use of LiDAR (Light Detection and Ranging) for detection of BC (black carbon) from automobiles in Las Vegas, NV (Nevada)*. URL: [epa.gov/ttnemc01/meetnw/2002op/epa\\_hans.pdf](http://epa.gov/ttnemc01/meetnw/2002op/epa_hans.pdf)
25. Dockery, D., Pope, C., Xu, X., Spengler, J., Ware, J., Fay, M., Ferris Jr., B. & Speizer, F., 1993. *An Association between Air Pollution and Mortality in Six U.S. Cities*. N Engl. J Med. Vol.329, pp. 1753-1759
26. Draxler, R. & Hess, D., 1998. *An overview of the HYSPLIT\_4 modelling system of trajectories, dispersion and deposition*. Aust. Meteor. Mag., Vol. 47, pp. 295-308
27. Duan, J., Tan, J., Yang, L., Wu, S. & Hao, J, 2008. *Concentration, sources and ozone formation potential of volatile organic compounds (VOCs) during ozone episode in Beijing*. Atmos. Res., Vol. 88, pp. 25-35

28. Electronic National administration Transport Information System (eNaTIS), 2017.  
URL: [enatis.com/index.php/statistics/14-new-vehicle-registrations/622-new-vehicle-registrations-for-december-2017](http://enatis.com/index.php/statistics/14-new-vehicle-registrations/622-new-vehicle-registrations-for-december-2017)
29. Encyclopedia Britannica, 2017. *Air Pollution*. URL: [britannica.com/science/air-pollution](http://britannica.com/science/air-pollution)
30. Eskom Holdings Ltd., 2017. URL: [eskom.co.za/AboutElectricity/ElectricityTechnologies/Pages/Coal\\_Power.aspx](http://eskom.co.za/AboutElectricity/ElectricityTechnologies/Pages/Coal_Power.aspx)
31. Falcon-Rodriquez, C., Vargas, A., Sada-Ovalle, I. & Segura-Medina, P., 2016. *Aeroparticles, Composition, and Lung Diseases*. *Frontiers in Immunology*. Vol. 7
32. Fleming, Z., Monks, P. & Manning, A., 2012. *Review: Untangling the influence of air-mass history in interpreting observed atmospheric composition*. *Atmospheric Research*, Vol. 104-105, pp. 1-39
33. Gábelová, A., Valovicová, Z., Horváthová, E., Slamenová, D., Binková, B. Štám, R. & Farmer, P., 2004. *Genotoxicity of environmental air pollution in three European cities: Prague, Kosice and Sofia*. *Mutat. Res.* Vol. 563, pp. 49-59
34. Gaudio, P., 2015. *Detection and monitoring of pollutant sources with Lidar/Dial techniques*. *J. Phys.: Conf. Ser.*, Vol. 658
35. Gramsch, E., Caceres, D., Oyola, P. & Sánchez, G., 2014. *Influence of surface and subsidence thermal inversion on PM<sub>2.5</sub> and black carbon concentration*. *Atmospheric Environment*, Vol. 98, pp. 290-298
36. Guarieiro, L. & Guarieiro, A., 2015. *Impact of the Biofuels Burning on Particle Emissions from the Vehicular Exhaust*. DOI: 10.5772/60110

37. Gutiérrez-Castillo, M., Roubicek, D., Cebrián-García, M., Vizcaya-Ruíz, A., Sordo-Cedeño, M. & Ostrosky-Wegman, P., 2006. *Effect of chemical composition on the induction of DNA damage by urban airborne particulate matter*. Environmental and Molecular Mutagenesis. Vol. 47, pp. 199-211
38. Hallquist, M., Munthe, J., Hu, M., Wang, T., Chan, C., Gao, J., Boman, J., Guo, S., Hallquist, Å., Mellqvist, J., 2016. *Photochemical smog in China: scientific challenges and implications for air-quality policies*. National Science Review. Vol. 3, pp. 401-403
39. Healey, K., Lingard, J., Tomlin, A. Hughes, A., White, K., Wild, C. & Routledge, M., 2005. *Genotoxicity of size-fractionated samples of urban particulate matter*. Environmental and Molecular Mutagenesis. Vol. 45, pp. 380-387
40. Helfand, W. Lazarus, J. & Theerman, P., 2001. *Donora, Pennsylvania: an environmental disaster of the 20<sup>th</sup> century*. Am. J. Pub. Health, Vol. 91, pp. 55
41. Hinds, W., 1999. *Aerosol Technology: Properties, Behaviours, and Measurements of Airborne Particles*. Wiley and Sons, second edition, pp. 75-107. ISBN: 978-0-471-19410-1
42. Hunter, D., Salzman, J. and Zaelke, D., 2002. *International Environmental Law and Policy*. Foundation Press, second edition
43. Kittelson, D. & Kraft, M., 2014. *Particle Formation and Models*. Encyclopedia of Automotive Engineering, pp. 1-23. DOI: 10.1002/9781118354179.auto161
44. Koenig, J., 2000. *Health Effects of Ambient Air Pollution*. Springer, First edition. ISBN: 978-1-4615-4569-9
45. Landrigan, P., 2017. *Air pollution and health*. The Lancet Public Health, Vol. 2, No. 1, e4-e5

46. Lin, J., Gerbig, C., Wofsy, S., Andrews, A., Daube, B., Davis, K. & Grainger, C., 2003. *A near-field tool for simulating the upstream influence of atmospheric observations: The Stochastic Time-Inverted Lagrangian Transport (STILT) model*. *J. Geophys. Res.*, Vol. 108. DOI: 10.1029/2002JD003161
47. Mail & Guardian report, 2015. *South Africa's air quality is improving - DEA (Department of Environmental Affairs)*. URL: [mg.co.za/article/2015-10-29-south-africas-air-quality-is-improving-dea](http://mg.co.za/article/2015-10-29-south-africas-air-quality-is-improving-dea)
48. Martinelli, N., Olivieri, O. & Girelli, D., 2013. *Air particulate matter and cardiovascular disease: a narrative review*. *Eur. J. Intern. Med.* Vol. 24, pp. 295-302
49. Molnár, P., Tang, L., Sjöberg, K. & Wichmann, J (2017). *Long-range transport clusters and positive matrix factorisation source apportionment for investigating transboundary PM<sub>2.5</sub> in Gothenburg, Sweden*. *Environ. Sci. Processes Impacts*, Vol. 19, pp. 1270-1277
50. Mondy, L., Graham, A., Stroeve, P. & Majumdar, A., 1987. *Effects of particle surface roughness on particle interactions in concentrated suspensions*. *AIChE Journal*. Vol. 33, pp. 862-866
51. Myllyvitra, L., 2014. *Health impacts and social costs of Eskom's proposed non-compliance with South Africa's air emission standards*. Greenpeace International
52. National Research Council, 2002. *Estimating the Public Health Benefits of Proposed Air Pollution Regulations*. The National Academies Press. DOI: 10.17226/10511
53. NIOSH (National Institute for Occupational Safety and Health), 1973. *The industrial environment - its evaluation and control, 3rd edition*. Department of Health, Education, and Welfare, Public Health Service, Centers for Disease Control, Publication No. 74-117, pp. 101-122

54. Omidvarborna, H., Kumar, A. & Dong-Shik, K., 2015. *NO<sub>x</sub> emissions from low-temperature combustion of biodiesel made of various feedstocks and blends*. Fuel Processing Technology. Vol. 140, pp. 113-118
55. Pope, C., Burnett, R., Thun, M., Calle, E., Krewski, D., Ito, K., 2002. *Lung cancer, cardiopulmonary mortality, and long-term exposure to fine particulate air pollution*. JAMA. Vol. 287, pp. 1132-1141
56. Queensland Department of Environment and Heritage Protection, 2017. *Air monitoring*. URL: [qld.gov.au/environment/pollution/monitoring/air-monitoring](http://qld.gov.au/environment/pollution/monitoring/air-monitoring)
57. R'Mili, B., Dutouquet, C., Sirven, J. & Frejafon, E., 2011. *Detection of airborne micrometric-sized CNT (Carbon Nanotubes) bundles using TEM (Transmission Electron Microscopy) samplers and LIBS (Laser-Induced Breakdown Spectroscopy)*. J. Nanopart. Res. DOI: 10.1007/s11051-010-0050-z
58. Romanian Space Agency (ROSA), 2017. *LiDAR (Light Detection and Ranging) applications*. URL: [rosa.ro/index.php/en/rosa-home?catid=0&id=14&start=222](http://rosa.ro/index.php/en/rosa-home?catid=0&id=14&start=222)
59. Rousseeuw, P. & Hubert, M., 2011. *Robust statistics for outlier detection*. WIREs data mining and knowledge discovery, Vol.1, pp. 73-79
60. SAAQIS (South African Air Quality Information System), 2014. National Environmental Management: Air Quality Act (Act 39 of 2004): Standards and Regulations, 2014. URL: [saaqis.org.za/documents/NEM-AQA%20Booklet\\_2014.pdf](http://saaqis.org.za/documents/NEM-AQA%20Booklet_2014.pdf)
61. SAAQIS (South Africa Ambient Air Quality Information System), 2017. URL: [saaqis.org.za/NAAQM.aspx](http://saaqis.org.za/NAAQM.aspx)
62. Samuels, P. & Gilchrist, M., 2014. *Pearson correlation*. Technical report, report number: step-gilchristsamuels-3, Birmingham City University
63. SAWS (South African Weather Services), 2017. URL: [weathersa.co.za/climate/historical-rain-maps](http://weathersa.co.za/climate/historical-rain-maps)

64. Schwela, D., 2004. *Air Quality Management: Sustainable Transport: A Sourcebook for Policy Makers in Developing Cities: Module 5*
65. Soot Testing Lab, 2013. *What you should know about soot (black carbon)*. URL: [soottestinglab.com/index-1.html](http://soottestinglab.com/index-1.html)
66. South Africa Growth Rate Indicators, 2017. URL: [tradingeconomics.com/south-africa/indicators](http://tradingeconomics.com/south-africa/indicators)
67. South Africa population (worldometers.com), 2017. URL: [worldometers.info/world-population/south-africa-population/](http://worldometers.info/world-population/south-africa-population/)
68. Spengler, J., Levy, J., Houseman, E., Loh, P. & Ryan, L., 2001. *Fine particulate matter and polycyclic aromatic hydrocarbon concentration patterns in Roxbury, Massachusetts: a community-based GIS analysis*. Environ. Health Perspect. Vol. 109, pp. 341-347
69. Stein, A., Draxler, R., Rolph, G., Stunder, B., Cohen, M. & Ngan, F., 2015. *NOAA's HYSPLIT Atmospheric Transport and Dispersion Modeling System*. DOI: 10.1175/BAMS-D-14-00110.2
70. Stephens, E., 1965. *Temperature Inversions and the Trapping of Air Pollutants*. Weatherwise, Vol. 18, pp. 172-175
71. The Guardian article, 2017. *Pant by numbers: the cities with the most dangerous air – listed*. URL: [theguardian.com/cities/datablog/2017/feb/13/most-polluted-cities-world-listed-region?CMP=share\\_btn\\_link](http://theguardian.com/cities/datablog/2017/feb/13/most-polluted-cities-world-listed-region?CMP=share_btn_link)
72. Topography of Cape Town (topographic-map.com), 2017. URL: [en-za.topographic-map.com/places/Cape-Town-6699134/](http://en-za.topographic-map.com/places/Cape-Town-6699134/)
73. UK-AIR (United Kingdom Air Information Resource), 2005. *Particulate Matter in the United Kingdom*. Crown copyright. ISBN: 0-85521-144-X

74. UN (United Nations), 2016. *UN health agency warns of rise in urban air pollution*. URL: [un.org/sustainabledevelopment/blog/2016/05/un-health-agency-warns-of-rise-in-urban-air-pollution-with-poorest-cities-most-at-risk/](http://un.org/sustainabledevelopment/blog/2016/05/un-health-agency-warns-of-rise-in-urban-air-pollution-with-poorest-cities-most-at-risk/)
75. UN (United Nations) report, 2016. *Vast majority of world - 6.76 billion people - living with excessive air pollution*. URL: [un.org/sustainabledevelopment/blog/2016/09/vast-majority-of-world-6-76-billion-people-living-with-excessive-air-pollution-un-report/](http://un.org/sustainabledevelopment/blog/2016/09/vast-majority-of-world-6-76-billion-people-living-with-excessive-air-pollution-un-report/)
76. UN (United Nations), 2017. *Sustainable Development Goals*. URL: [un.org/sustainabledevelopment/health/](http://un.org/sustainabledevelopment/health/)
77. United States Department of Commerce, 2016. *Pollution Control Equipment*. URL: [export.gov/article?id=South-Africa-pollution-control](http://export.gov/article?id=South-Africa-pollution-control)
78. U.S. EPA (United States Environmental Protection Agency), 2012. Ambient Monitoring Technology Information Centre (AMTIC): PM<sub>2.5</sub>. URL: [epa.gov/ttnamti1/amticpm.html](http://epa.gov/ttnamti1/amticpm.html)
79. U.S. EPA (United States Environmental Protection Agency), 2012. *Thermo Scientific FDMS & Beta Attenuation Instrumentation - an overview and recommendations to maximize operational performance*. URL: [epa.gov/ttnamti1/files/2012conference/1B02Thermo.pdf](http://epa.gov/ttnamti1/files/2012conference/1B02Thermo.pdf)
80. U.S. EPA (United States Environmental Protection Agency), 2015. *Particulate Matter Emissions*. URL: [cfpub.epa.gov/roe/indicator\\_pdf.cfm?i=1](http://cfpub.epa.gov/roe/indicator_pdf.cfm?i=1)
81. U.S. EPA (United States Environmental Protection Agency), 2017. *Criteria Air Pollutants*. URL: [epa.gov/criteria-air-pollutants](http://epa.gov/criteria-air-pollutants)
82. U.S. EPA (United States Environmental Protection Agency), 2017. *Health and Environmental Effects of Particulate Matter (PM)*. URL: [epa.gov/pm-pollution/health-and-environmental-effects-particulate-matter-pm](http://epa.gov/pm-pollution/health-and-environmental-effects-particulate-matter-pm)
83. U.S. EPA (United States Environmental Protection Agency), 2017. *History of Air Pollution*. URL: [epa.gov/air-research/history-air-pollution](http://epa.gov/air-research/history-air-pollution)



84. U.S. EPA (United States Environmental Protection Agency), 2017. *List of Designated Reference and Equivalent Methods*. URL: [epa.gov/sites/production/files/2018-01/documents/amtic\\_list\\_dec\\_2017\\_update\\_1-20-2018\\_0.pdf](http://epa.gov/sites/production/files/2018-01/documents/amtic_list_dec_2017_update_1-20-2018_0.pdf)
85. U.S. EPA (United States Environmental Protection Agency), 2017. *Managing Air Quality – Ambient Air Monitoring*. URL: [epa.gov/air-quality-management-process/managing-air-quality-ambient-air-monitoring#overview](http://epa.gov/air-quality-management-process/managing-air-quality-ambient-air-monitoring#overview)
86. U.S. EPA (United States Environmental Protection Agency), 2017. *Particulate Pollution and Cardiovascular Effects*. URL: [epa.gov/pmcourse/particle-pollution-and-cardiovascular-effects](http://epa.gov/pmcourse/particle-pollution-and-cardiovascular-effects)
87. Valavanidis, A., Fiotakis, T. & Vlachogianni, T., 2008. *Airborne particulate matter and human health: toxicological assessment and importance of size and composition of particles for oxidative damage and carcinogenic mechanisms*. J. Environ. Sci. Health. Vol. 26, pp. 339-362
88. Vallius, M., Ruuskanen, J., Mirme, A. & Pekkanen, J., 2000. *Concentration and estimated soot content of PM<sub>1</sub>, PM<sub>2.5</sub> and PM<sub>10</sub> in a subarctic urban atmosphere*. Environ. Sci. Technol., Vol. 34, pp. 1919-1925
89. van Roosbroeck, S., Wichmann, J., Janssen, N., Hoek, G., v. Wijnen, J., Lebret, E. & Brunekreef, B., 2006. *Long-term personal exposure to traffic-related air pollution among school children, a validation study*. Science of the Total Environment, Vol. 368, pp. 565-573
90. Waikato Regional Council, 2017. *Air Quality: Discharges and Pollutants*. URL: [waikatoregion.govt.nz/environment/natural-resources/air/discharges-and-pollutants/](http://waikatoregion.govt.nz/environment/natural-resources/air/discharges-and-pollutants/)
91. Wang, J and Ogawa, S., 2015. *Effects of Meteorological Conditions on PM<sub>2.5</sub> concentrations in Nagasaki, Japan*. Int. J. Environ. Res. Public Health, Vol.12 pp 9089-9101

92. Western Cape Government, 2017. URL: [westerncape.gov.za/your\\_gov/70](http://westerncape.gov.za/your_gov/70)
93. Weather history of Cape Town ([worldweatheronline.com](http://worldweatheronline.com)), 2017. URL: [worldweatheronline.com/cape-town-weather-history/western-cape/za.aspx](http://worldweatheronline.com/cape-town-weather-history/western-cape/za.aspx)
94. WHO (World Health Organization), 2003. *Health Risks of Persistent Organic Pollutants from Long-Range Transboundary Air Pollution*
95. WHO (World Health Organisation), 2013. *Health Effects of Particulate Matter*. ISBN: 978 92 890 0001 7
96. Wichmann, J., Molnár, P., Petrik, L., Gitari, W., Williams, J., Novela, R. & Adeyemi, A., 2017. *PM<sub>2.5</sub>, soot, source apportionment, geographical origin of air masses and health effects thereof in Cape Town, Pretoria and Thohoyandou*. Project description, URL: [researchgate.net/project/PM25-soot-source-apportionment-geographical-origin-of-air-masses-and-health-effects-thereof-in-Cape-Town-Pretoria-and-Thohoyandou](http://researchgate.net/project/PM25-soot-source-apportionment-geographical-origin-of-air-masses-and-health-effects-thereof-in-Cape-Town-Pretoria-and-Thohoyandou)
97. Willeke, K & Baron, P., 1993. *Aerosol measurement: principles, techniques and applications*. Wiley, first edition, pp. 8-40
98. Wind information for Cape Town ([windfinder.com](http://windfinder.com)), 2017. URL: [windfinder.com/forecast/cape\\_town\\_airport](http://windfinder.com/forecast/cape_town_airport)
99. World Air Quality website, 2017. URL: [aqicn.org/map/southafrica/](http://aqicn.org/map/southafrica/)
100. World Economic Forum, 2016. *92% of us are breathing unsafe air. This map shows just how bad the problem is*. URL: [weforum.org/agenda/2016/09/92-of-the-world-s-population-lives-in-areas-with-unsafe-air-pollution-levels-this-interactive-map-shows-just-how-bad-the-problem-is/](http://weforum.org/agenda/2016/09/92-of-the-world-s-population-lives-in-areas-with-unsafe-air-pollution-levels-this-interactive-map-shows-just-how-bad-the-problem-is/)
101. Yamane, T., 1967. *Statistics, An Introductory Analysis*, 2<sup>nd</sup> ed. New York: Harper and Row.
102. Zhang, Y. & Jiang, W., 2018. *Pollution characteristics and influencing factors of atmospheric particulate matter (PM<sub>2.5</sub>) in Chang-Zhu-Tan area*. IOP Conf. Ser.: Earth Environ. Sci., Vol. 108. DOI: 10.1088/1755-1315/108/4/042047

**APPENDIX 1A - SAMPLING INFORMATION (CALENDAR SAMPLES)**

Date	Day, Sample	Date	Day, Sample	Date	Day, Sample	Date	Day, Sample	Date	Day, Sample
2017/04/18	D1, C1+C2	2017/07/02	D26, C31+C32	2017/09/15	D51, C63	2017/11/29	D76, C94	2018/02/12	D101, C124
2017/04/21	D2, C3	2017/07/05	D27, C33	2017/09/18	D52, C64	2017/12/02	D77, C95	2018/02/15	D102, C125
2017/04/24	D3, C4	2017/07/08	D28, C34	2017/09/21	D53, C65	2017/12/05	D78, C96	2018/02/18	D103, C126
2017/04/27	D4, C5	2017/07/11	D29, C35	2017/09/24	D54, C66	2017/12/08	D79, C97	2018/02/21	D104, C127
2017/04/30	D5, C6	2017/07/14	D30, C36	2017/09/27	D55, C67+C68	2017/12/11	D80, C98+C99	2018/02/24	D105, C128+C129
2017/05/03	D6, C7+C8	2017/07/17	D31, C37+C38	2017/09/30	D56, C69	2017/12/14	D81, C100	2018/02/27	D106, C130
2017/05/06	D7, C9	2017/07/20	D32, C39	2017/10/03	D57, C70	2017/12/17	D82, C101	2018/03/02	D107, C131
2017/05/09	D8, C10	2017/07/23	D33, C40	2017/10/06	D58, C71	2017/12/20	D83, C102	2018/03/05	D108, C132
2017/05/12	D9, C11	2017/07/26	D34, C41	2017/10/09	D59, C72	2017/12/23	D84, C103	2018/03/08	D109, C133
2017/05/15	D10, C12	2017/07/29	D35, C42	2017/10/12	D60, C73+C74	2017/12/26	D85, C104+C105	2018/03/11	D110, C134+C135
2017/05/18	D11, C13+C14	2017/08/01	D36, C43+C44	2017/10/15	D61, C75	2017/12/29	D86, C106	2018/03/14	D111, C136
2017/05/21	D12, C15	2017/08/04	D37, C45	2017/10/18	D62, C76	2018/01/01	D87, C107	2018/03/17	D112, C137
2017/05/24	D13, C16	2017/08/07	D38, C46	2017/10/21	D63, C77	2018/01/04	D88, C108	2018/03/20	D113, C138
2017/05/27	D14, C17	2017/08/10	D39, C47	2017/10/24	D64, C78	2018/01/07	D89, C109	2018/03/23	D114, C139
2017/05/30	D15, C18	2017/08/13	D40, C48	2017/10/27	D65, C79+C80	2018/01/10	D90, C110+C111	2018/03/26	D115, C140+C141
2017/06/02	D16, C19+C20	2017/08/16	D41, C49+C50	2017/10/30	D66, C82	2018/01/13	D91, C112	2018/03/29	D116, C142
2017/06/05	D17, C21	2017/08/19	D42, C51	2017/11/02	D67, C83	2018/01/16	D92, C113	2018/04/01	D117, C143
2017/06/08	D18, C22	2017/08/22	D43, C52	2017/11/05	D68, C84	2018/01/19	D93, C114	2018/04/04	D118, C144
2017/06/11	D19, C23	2017/08/25	D44, C53	2017/11/08	D69, C85	2018/01/22	D94, C115	2018/04/07	D119, C145
2017/06/14	D20, C24	2017/08/28	D45, C54	2017/11/11	D70, C86+C87	2018/01/25	D95, C116+C117	2018/04/10	D120, C146+C147
2017/06/17	D21, C25+C26	2017/08/31	D46, C55	2017/11/14	D71, C88	2018/01/28	D96, C118	2018/04/13	D121, C148
2017/06/20	D22, C27	2017/09/03	D47, C57+C58	2017/11/17	D72, C89	2018/01/31	D97, C119	2018/04/16	D122, C149
2017/06/23	D23, C28	2017/09/06	D48, C59	2017/11/20	D73, C90	2018/02/03	D98, C120		
2017/06/26	D24, C29	2017/09/09	D49, C60	2017/11/23	D74, C91	2018/02/06	D99, C121		
2017/06/29	D25, C30	2017/09/12	D50, C61+C62	2017/11/26	D75, C92+C93	2018/02/09	D100, C122+C123		

□ Duplicate sampling days (initial)

■ Duplicate sampling days (adjusted)

**NOTE:** 2017/08/31, filter C56 not shipped to Cape Town (duplicate sampling performed on 2017/09/03)

2017/10/21, filter C77 not shipped to Cape Town (filter C81 used as replacement)

2017/10/30, filter C82 replaced C81

2018/04/13 and 2018/04/16, filters C148 and C149 added to sampling calendar

## APPENDIX 1B - SEASONAL SAMPLING INFORMATION

Date	Season	n	Date	Season	n	Date	Season	n
2017/04/18	Autumn	15	2017/08/22	Spring	30	2017/12/23	Summer	30
2017/04/21			2017/08/25			2017/12/26		
2017/04/24			2017/08/28			2017/12/29		
2017/04/27			2017/08/31			2018/01/01		
2017/04/30			2017/09/03			2018/01/04		
2017/05/03			2017/09/06			2018/01/07		
2017/05/06			2017/09/09			2018/01/10		
2017/05/09			2017/09/12			2018/01/13		
2017/05/12			2017/09/15			2018/01/16		
2017/05/15			2017/09/18			2018/01/19		
2017/05/18			2017/09/21			2018/01/22		
2017/05/21			2017/09/24			2018/01/25		
2017/05/24			2017/09/27			2018/01/28		
2017/05/27			2017/09/30			2018/01/31		
2017/05/30			2017/10/03			2018/02/03		
2017/06/02	2017/10/06	2018/02/06						
2017/06/05	2017/10/09	2018/02/09						
2017/06/08	2017/10/12	2018/02/12						
2017/06/11	2017/10/15	2018/02/15						
2017/06/14	2017/10/18	2018/02/18						
2017/06/17	2017/10/21	2018/02/21						
2017/06/20	2017/10/24	2018/02/24						
2017/06/23	2017/10/27	2018/02/27						
2017/06/26	2017/10/30	2018/03/02						
2017/06/29	2017/11/02	2018/03/05						
2017/07/02	2017/11/05	2018/03/08						
2017/07/05	2017/11/08	2018/03/11						
2017/07/08	2017/11/11	2018/03/14						
2017/07/11	2017/11/14	2018/03/17						
2017/07/14	2017/11/17	2018/03/20						
2017/07/17	2017/11/20	2018/03/23						
2017/07/20	2017/11/23	2018/03/26						
2017/07/26	2017/11/26	2018/03/29						
2017/07/29	2017/11/29	2018/04/01						
2017/08/01	2017/12/02	2018/04/04						
2017/08/04	2017/12/05	2018/04/07						
2017/08/07	2017/12/08	2018/04/10						
2017/08/10	2017/12/11	2018/04/13						
2017/08/13	2017/12/14	2018/04/16						
2017/08/16	2017/12/17							
2017/08/19	2017/12/20							

Where  $n$  is the number of sampling days. The number of sampling days for winter, spring and summer were the same ( $n = 30$ ). Autumn (2018/04/18 to 2017/05/30 and 2018/03/02 to 2018/04/16) had 31 sampling days and was the only “non-consecutive” season with sampling days in 2017 and 2018.

**APPENDIX 1C - SAMPLING INFORMATION (COMPOSITE SAMPLES)**

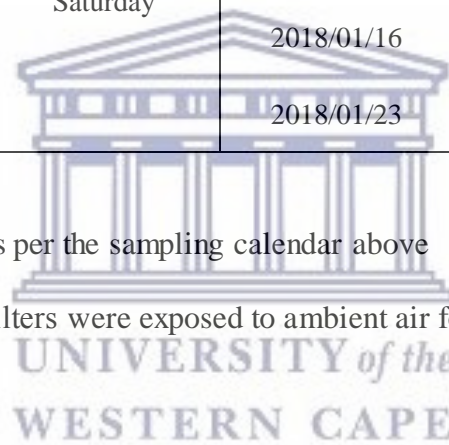
<b>September 2017</b>				<b>January 2018</b>			
<b>Weekday</b>		<b>Weekend</b>		<b>Weekday</b>		<b>Weekend</b>	
<b>Date</b>	<b>Day</b>	<b>Date</b>	<b>Day</b>	<b>Date</b>	<b>Day</b>	<b>Date</b>	<b>Day</b>
2017/09/07		2017/09/09		2018/01/02		2018/01/06	
2017/09/14	Thursday	2017/09/16	Saturday	2018/01/09	Tuesday	2018/01/13	Saturday
2017/09/21		2017/09/23		2018/01/16		2018/01/20	
2017/09/28		2017/09/30		2018/01/23		2018/01/27	

Composite (or accumulative) samples were collected as per the sampling calendar above

Unlike “calendar” samples (see Appendix 1A) where filters were exposed to ambient air for 24 hours, total exposure time for composite samples was 96 hours

Sampling time: 24 hours (09:00 a.m. to 09:00 a.m.)

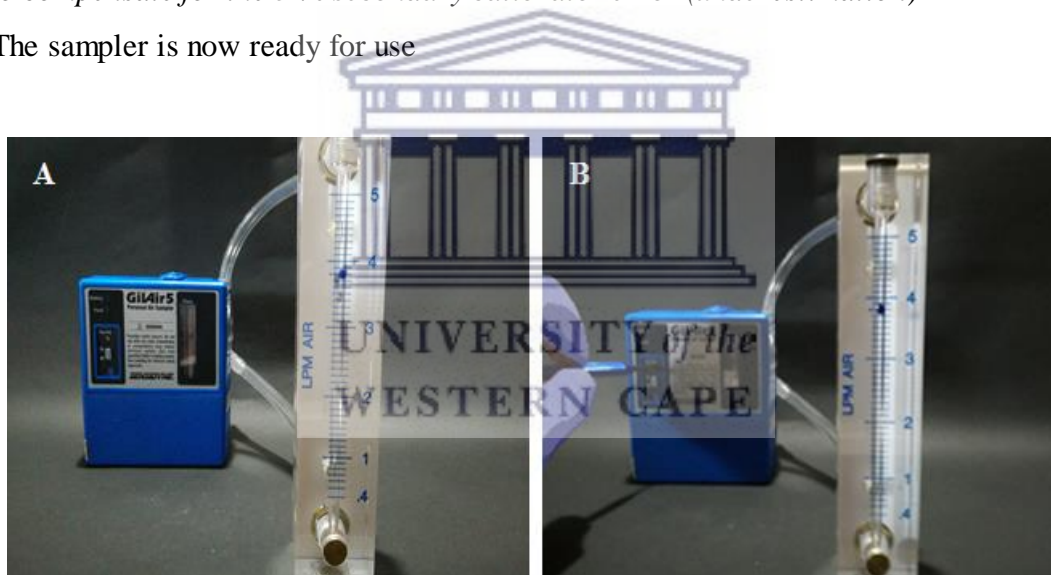
Sampling interval: seven days



## APPENDIX 2 - AMBIENT APM SAMPLING INSTRUCTIONS

### I. Calibrating the GilAir-5 air sampler

1. Switch the sampler on and check battery level. **Note:** *If battery charge indicator is red – charge battery before use. If it is green – proceed with calibration*
2. Switch sampler off
3. Insert plastic fitting into inlet tube of the field calibrator. Connect outlet tube of field calibrator to inlet of sampler (outlet tube should not have a plastic fitting). **Note:** *Calibrate field calibrator with a primary calibrator (primary standard) before use.*
4. Switch sampler on
5. Check flow rate (A)
6. Adjust flow rate using a small flat screwdriver (B). **Note:** *To increase flow rate – turn flow adjuster clockwise, to decrease flow rate – turn it anti-clockwise*
7. Adjust flow rate to  $4.0 \text{ L}\cdot\text{min}^{-1}$ . **Note:** *Sampler was adjusted to  $3.8 \text{ L}\cdot\text{min}^{-1}$  (blue marker) to compensate for the 5 % secondary calibrator error (underestimation)*
8. The sampler is now ready for use

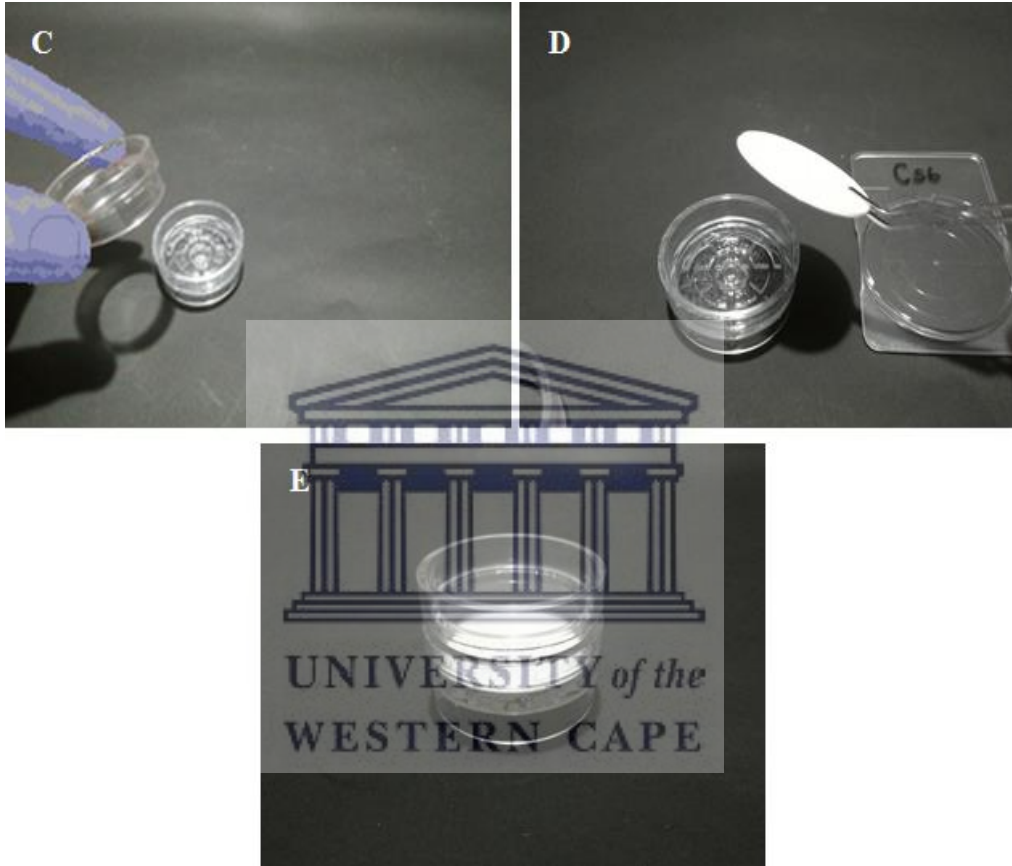


### II. Assembling the air sampling cassette

1. Separate the air sampling cassette into its individual parts **I. Note:** *If this cannot be done by hand, use flat screwdriver to pry apart the inner ring and cassette outlet*
2. Carefully remove filter and support pad from the petri slide using a flat-nosed tweezers **(D). Note:** *Do not contaminate clean filter nor apply excessive pressure when handling it*
3. Separate the air sampling cassette into its individual parts **I. Note:** *If this cannot be done by hand, use flat screwdriver to pry apart the inner ring and cassette outlet*

## APPENDIX 2 - AMBIENT APM SAMPLING INSTRUCTIONS

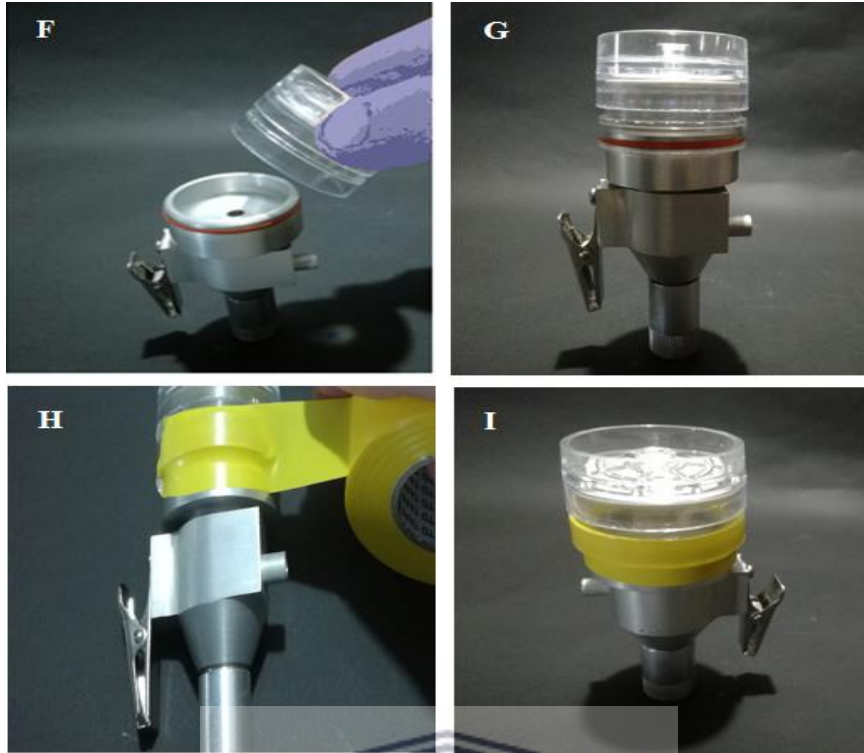
- Carefully remove filter and support pad from the petri slide using a tweezers (**D**). **Note:** *Do not contaminate clean filter nor apply excessive pressure when handling it*
- Place filter and support pad into cassette outlet. **Note:** *Ensure filter orientation is correct. The coarse side must face inner ring*
- Insert inner ring into cassette outlet by applying firm downward pressure to secure filter and support pad (**E**)



### III. Attaching air sampling cassette to the cyclone

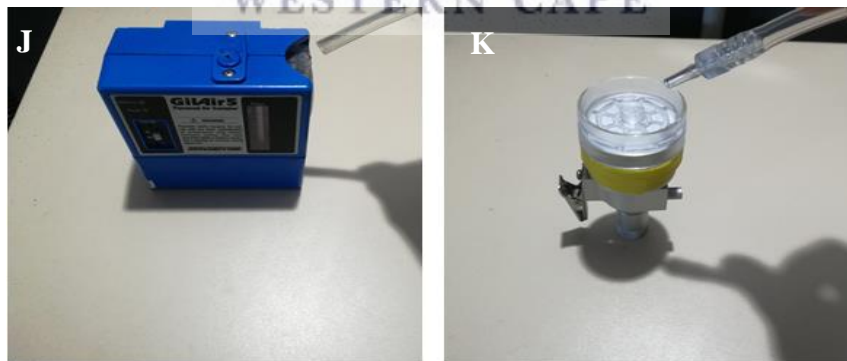
- Attach cassette to the cyclone by applying firm downward pressure until inner ring clears the orange o-ring by 3-5 mm (**F**) + (**G**)
- Tape cassette to cyclone with insulation tape (**H**). This will ensure that cassette-cyclone assembly is airtight. **Note:** *For duplicate sampling, mark one cyclone so that it is easily distinguishable from the other*
- The cassette-cyclone assembly can now be connected to the sampler (**I**)

## APPENDIX 2 - AMBIENT APM SAMPLING INSTRUCTIONS



### IV. Connecting the cassette-cyclone assembly to sampler

1. Connect end of connecting tube (without fitting) to inlet of sampler (**J**)
2. Connect opposite end (with fitting) to the outlet of cassette-cyclone assembly (**K**)
3. Pump and cassette-cyclone assembly are now connected (**L**). Proceed with sampling

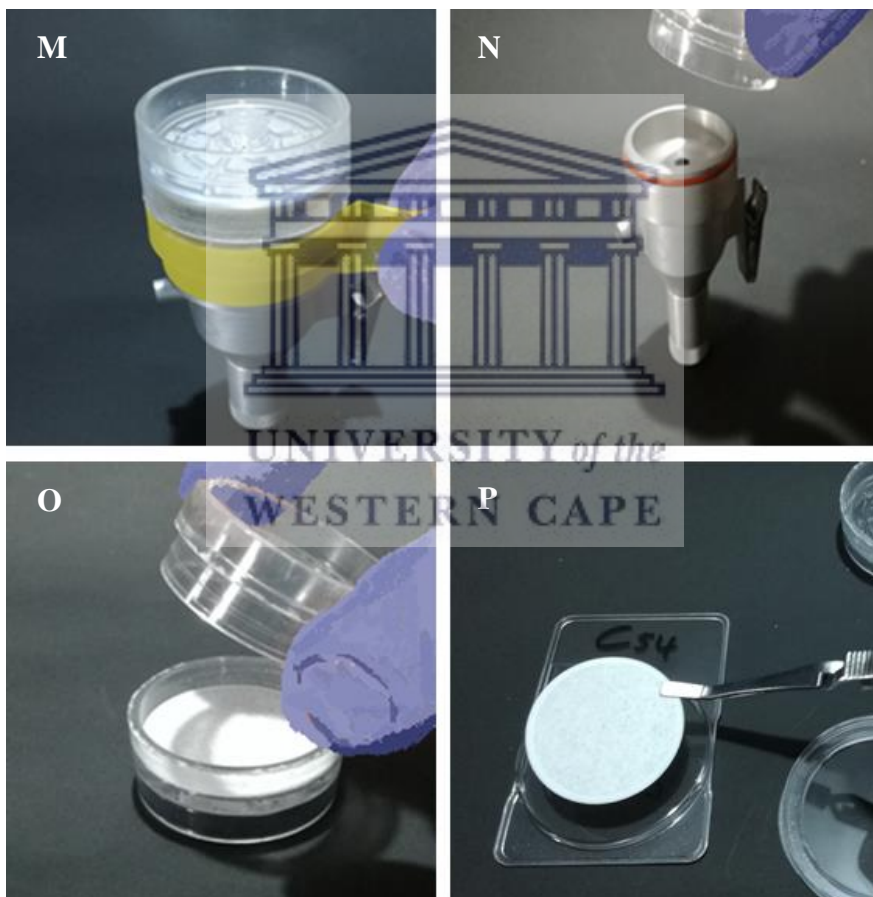




## APPENDIX 2 - AMBIENT APM SAMPLING INSTRUCTIONS

### V. Retrieval of filter sample

1. Switch sampler off
2. Disconnect cassette-cyclone assembly from sampler and remove insulation tape (M).
3. Detach cassette from cyclone (N)
4. Pry apart inner ring and cassette outlet (O). **Note:** Use screwdriver if this cannot be done by hand
5. Remove filter sample and support pad with a tweezers and store in a clean, labelled petri slide (P). **Note:** Do not contaminate the sample
6. Refrigerate sample



### APPENDIX 3 - CHRONOLOGY OF ANALYSES

<b>UNIVERSITY OF PRETORIA</b>	
Activity/Analysis	Gravimetric analysis
Start date	6 April 2017
End date	19 April 2018
Reason for activity/analysis	Determination of PM <sub>2,5</sub> mass concentrations
Activity/Analysis	SSR
Start date	30 August 2017
End date	21 April 2018
Reason for activity/analysis	Determination of absorption coefficients
Activity/Analysis	HYSPLIT backward trajectory analysis
Start date	23 April 2018
End date	24 April 2018
Reason for activity/analysis	Determination of origins and trajectories of air masses
<b>UNIVERSITY OF THE WESTERN CAPE</b>	
Activity/Analysis	ICP-OES
Start date	8 February 2018
End date	8 February 2018
Reason for activity/analysis	Determination of select metals concentrations
Activity/Analysis	SEM
Start date	14 February 2018
End date	14 February 2018
Reason for activity/analysis	Particulate morphology
Activity/Analysis	IC
Start date	7 March 2018
End date	7 March 2018
Reason for activity/analysis	Determination of selected anions concentrations
Activity/Analysis	TEM, EDS and SAED
Start date	23 July 2018
End date	23 July 2018
Reason for activity/analysis	Particulate morphology and compositional information

## APPENDIX 4 - FILTER WEIGHING PROCEDURE

**Mettler-Toledo ultra-microbalance weighing procedure: Reference (control) and sample filters (Note: Weigh filters in shortest time period possible)**

1. Capture data from laboratory environmental monitor
2. Check if environmental conditions in the laboratory were maintained for the previous 24 hours within prescribed limits
  - Dry air temperature:  $21 \pm 1.0$  °C
  - Relative humidity:  $50 \pm 5$  %
3. Capture environmental conditions immediately prior to weighing reference (control) filters
4. Ensure balance is level
5. Tare balance
6. Weigh a 2 gram weight (certified weight set) repeatedly until repeatability is reached. Repeatability is when the min. and max. readings of three (3) consecutive measurements do not differ from the mean by more than one (1) percent
7. When repeatability is reached, remove weight
8. Close weighing chamber door and tare balance
9. Open balance and place three (3) reference filters on the weighing grid.
10. Close balance and start 30 second countdown timer. Allow 30 seconds for balance to stabilise. Note: Record reading on balance immediately when settling time is reached
11. Record three (3) consecutive readings for the reference filters
12. Remove reference filters from the weighing chamber and hold it next to the chamber with a flat-nosed tweezers. Note: Do not breathe over the filters
13. Close weighing chamber door and wait for balance to return to zero (0)
14. If balance does not return to zero (0), do the following:
  - Reject all prior mass measurements
  - Inspect balance pan for dust or any other obstacles
  - Reweigh filters
15. Repeat steps 9-14 for 10 individual sample filters. Note: Reference filters are reweighed after every 10 samples
16. Record environmental conditions immediately after the final reference filters are weighed. Note: If min. and max. readings of reference filters differ by  $> 10^{-3}$  (0.001) percent from the mean – reject all readings preceding it and reweigh samples
17. Place weighed filter samples on clearly labelled support pads in clean petri slides

## APPENDIX 5 - REFLECTOMETRY PROCEDURE

### Determination of Absorption Coefficient using Reflectometric Method (SOP 4.0)

1. Clean the measuring head, mask and standard plate with an alcohol swab.
2. Connect measuring head to the reflectometer and switch it on. **Note:** Allow lamp to warm up for 30 minutes
3. After 30 minutes, disconnect measuring head and adjust reading to 0.0 using the zero knob
4. Tightly attach the mask to the measuring head and reconnect it to the reflectometer
5. Place measuring head over white standard of standard plate and adjust reading to 100.0 using the coarse and fine knobs.
6. Once completed, move the measuring head to the grey standard (for the EEL model 43 D it should read  $33.5 \pm 1.5$ ). Repeat Step.5 if out-of-limits
7. Perform reflectance measurements on five (5) reference (control) filters. Each filter is measured in quintuplicate (5x) using the five-point method. **Note:** Do not readjust the reflectometer between filters
8. Calculate the mean ( $\mu$ ) of each reference filter. The filter with the median mean (M) is selected as the primary control filter. **Note:** This step is only performed in the first measurement session. The primary control filter must be stored safely and used to adjust the reflectometer to 100.0 in subsequent sessions
9. Proceed with filter sample measurements
10. Using a flat-nosed tweezers, remove the sample from petri slide and place it centrally over the white standard of standard plate
11. Carefully place the measuring head on the sample and record reading. Repeat measurements using five-point method and record readings
12. Repeat reflectometer calibration using the primary control filter after every 25 sample measurements. Record reading of control filter before making adjustments (if required). **Note:** Control filter should read 98-102
13. Clean mask, standard plate and tweezers after every 25 samples (with recalibration)
14. At the end of each measurement session, repeat the measurement of 10 % of the samples. **Note:** If the mean of the replicate measurements deviates by more than  $\pm$  three (3) percent from the original readings, all samples in measured during the corresponding session must be measured again
15. If new boxes of filters are opened and used, record lot numbers and check reflectance of blank filter. **Note:** The mean of the blank filter must be within  $\pm$  two (2) units of the primary control filter. If not, a separate mean needs to be calculated

**APPENDIX 6A - GRAVIMETRIC ANALYSIS DATA**

Sample ID	Sample date	Pump ID	Pre/Post-sampling	Replicates (µg)			s (µg)	µ (µg)	Δµ (µg)	Flow rate (L.min <sup>-1</sup> )	Normalised flow rate (L.min <sup>-1</sup> )
				R1	R2	R3					
C1	2017/04/18	UP23	Pre	181283	181281	181283	0.94	181282.3		3.8	4.0
			Post	181394	181395	181395	0.47	181394.7	112	3.8	4.0
C2*	2017/04/18	UP26	Pre	173722	173722	173721	0.47	173721.7		3.8	4.0
			Post	173815	173819	173815	1.89	173816.3	94.7	3.9	4.1
C3	2017/04/21	UP23	Pre	188067	188064	188062	2.05	188064.3		3.8	4.0
			Post	188180	188179	188180	0.47	188179.7	115	3.8	4.0
C4	2017/04/24	UP23	Pre	157674	157673	157673	0.47	157673.3		3.8	4.0
			Post	157802	157801	157801	0.47	157801.3	128	3.8	4.0
C5	2017/04/27	UP23	Pre	180963	180962	180960	1.25	180961.7		3.8	4.0
			Post	181028	181027	181025	1.25	181026.7	65.0	3.8	4.0
C6	2017/04/30	UP23	Pre	185656	185654	185655	0.82	185655		3.8	4.0
			Post	185708	185708	185708	0.00	185708	53.0	3.8	4.0
C7	2017/05/03	UP23	Pre	181864	181864	181864	0.00	181864		3.8	4.0
			Post	181929	181928	181929	0.47	181928.7	64.7	3.8	4.0
C8*	2017/05/03	UP26	Pre	185264	185261	185262	1.25	185262.3		3.8	4.0
			Post	185312	185313	185312	0.47	185312.3	50.0	3.7	3.9
C9	2017/05/06	UP23	Pre	169788	169788	169789	0.47	169788.3		3.8	4.0
			Post	169813	169814	169813	0.47	169813.3	25.0	3.8	4.0
C10	2017/05/09	UP23	Pre	161162	161160	161161	0.82	161161		3.8	4.0
			Post	161218	161218	161218	0.00	161218	57.0	3.8	4.0
C11	2017/05/12	UP23	Pre	163071	163068	163070	1.25	163069.7		3.8	4.0
			Post	163153	163152	163152	0.47	163152.3	82.7	3.8	4.0
C12	2017/05/15	UP23	Pre	171057	171057	171058	0.47	171057.3		3.8	4.0
			Post	171141	171139	171139	0.94	171139.7	82.3	3.8	4.0
C13	2017/05/18	UP23	Pre	167691	167690	167691	0.47	167690.7		3.8	4.0
			Post	167760	167757	167757	1.41	167758	67.3	3.7	3.9
C14*	2017/05/18	UP26	Pre	171107	171106	171106	0.47	171106.3		3.8	4.0
			Post	171155	171157	171156	0.82	171156	49.7	3.8	4.0
C15	2017/05/21	UP23	Pre	175781	175781	175782	0.47	175781.3		3.8	4.0
			Post	175828	175828	175824	1.89	175826.7	45.3	3.8	4.0

\* Duplicate sample

## APPENDIX 6A - GRAVIMETRIC ANALYSIS DATA

Sample ID	Sample date	Pump ID	Pre/Post-sampling	Replicates ( $\mu\text{g}$ )			s ( $\mu\text{g}$ )	$\mu$ ( $\mu\text{g}$ )	$\Delta\mu$ ( $\mu\text{g}$ )	Flow rate ( $\text{L}\cdot\text{min}^{-1}$ )	Normalised flow rate ( $\text{L}\cdot\text{min}^{-1}$ )
				R1	R2	R3					
C16	2017/05/24	UP23	Pre	164215	164219	164217	1.63	164217	59.7	3.8	4.0
			Post	164277	164276	164277	0.47	164276.7			
C17	2017/05/27	UP23	Pre	163700	163699	163695	2.16	163698	112	3.8	4.0
			Post	163810	163810	163809	0.47	163809.7			
C18	2017/05/30	UP23	Pre	183699	183698	183698	0.47	183698.3	79.3	3.8	4.0
			Post	183775	183779	183779	1.89	183777.7			
C19	2017/06/02	UP23	Pre	177443	177444	177442	0.82	177443	103	3.8	4.0
			Post	177547	177544	177546	1.25	177545.7			
C20*	2017/06/02	UP26	Pre	182073	182072	182074	0.82	182073	78.3	3.8	4.0
			Post	182151	182152	182151	0.47	182151.3			
C21	2017/06/05	UP26	Pre	157143	157140	157141	1.25	157141.3	106	3.8	4.0
			Post	157248	157246	157247	0.82	157247			
C22	2017/06/08	UP26	Pre	180385	180381	180382	1.70	180382.7	131	3.8	4.0
			Post	180514	180514	180513	0.47	180513.7			
C23	2017/06/11	UP26	Pre	203727	203722	203722	2.36	203723.7	31.3	3.8	4.0
			Post	203754	203756	203755	0.82	203755			
C24	2017/06/14	UP26	Pre	175736	175736	175736	0.00	175736	58.0	3.8	4.0
			Post	175794	175794	175794	0.00	175794			
C25	2017/06/17	UP26	Pre	188620	188620	188616	1.89	188618.7	218	3.8	4.0
			Post	188836	188837	188836	0.47	188836.3			
C26*	2017/06/17	UP23	Pre	160056	160054	160053	1.25	160054.3	220	3.8	4.0
			Post	160275	160274	160274	0.47	160274.3			
C27	2017/06/20	UP26	Pre	183219	183222	183220	1.25	183220.3	181	3.8	4.0
			Post	183401	183401	183403	0.94	183401.7			
C28	2017/06/23	UP26	Pre	164709	164709	164709	0.00	164709	230	3.8	4.0
			Post	164939	164941	164938	1.25	164939.3			
C29	2017/06/26	UP26	Pre	158711	158706	158706	2.36	158707.7	183	3.8	4.0
			Post	158891	158891	158891	0.00	158891			
C30	2017/06/29	UP26	Pre	164975	164971	164970	2.16	164972	39.7	3.8	4.0
			Post	165011	165010	165014	1.70	165011.7			

\* Duplicate sample

**APPENDIX 6A - GRAVIMETRIC ANALYSIS DATA**

Sample ID	Sample date	Pump ID	Pre/Post-sampling	Replicates ( $\mu\text{g}$ )			s ( $\mu\text{g}$ )	$\mu$ ( $\mu\text{g}$ )	$\Delta\mu$ ( $\mu\text{g}$ )	Flow rate ( $\text{L}\cdot\text{min}^{-1}$ )	Normalised flow rate ( $\text{L}\cdot\text{min}^{-1}$ )
				R1	R2	R3					
C31	2017/07/02	UP26	Pre	200962	200962	200959	1.41	200961	52.0	3.8	4.0
			Post	201013	201014	201012	0.82	201013		3.7	3.9
C32*	2017/07/02	UP23	Pre	170778	170777	170776	0.82	170777	64.3	3.8	4.0
			Post	170841	170841	170842	0.47	170841.3		3.8	4.0
C33	2017/07/05	UP26	Pre	155910	155908	155910	0.94	155909.3	42.7	3.8	4.0
			Post	155952	155952	155952	0.00	155952		3.8	4.0
C34	08/07/2017	UP26	Pre	165677	165673	165673	1.89	165674.3	173	3.8	4.0
			Post	165847	165847	165848	0.47	165847.3		3.8	4.0
C35	2017/07/11	UP26	Pre	194375	194375	194372	1.41	194374	146	3.8	4.0
			Post	194522	194519	194519	1.41	194520		3.8	4.0
C36	2017/07/14	UP26	Pre	173738	173738	173737	0.47	173737.7	115	3.8	4.0
			Post	173852	173852	173854	0.94	173852.7		3.8	4.0
C37	2017/07/17	UP26	Pre	189423	189428	189425	2.05	189425.3	27.0	3.8	4.0
			Post	189452	189452	189453	0.47	189452.3		3.8	4.0
C38*	2017/07/17	UP23	Pre	153177	153179	153176	1.25	153177.3	31.7	3.8	4.0
			Post	153208	153208	153211	1.41	153209		3.7	3.9
C39	2017/07/20	UP26	Pre	192830	192833	192834	1.70	192832.3	88.7	3.8	4.0
			Post	192921	192921	192921	0.00	192921		3.8	4.0
C41	2017/07/26	UP23	Pre	164713	164714	164713	0.47	164713.3	118	3.8	4.0
			Post	164834	164829	164830	2.16	164831		3.8	4.0
C42	2017/07/29	UP23	Pre	159199	159197	159196	1.25	159197.3	200	3.8	4.0
			Post	159399	159396	159396	1.41	159397		3.8	4.0
C43	2017/08/01	UP23	Pre	159860	159858	159859	0.82	159859	46.7	3.8	4.0
			Post	159907	159906	159904	1.25	159905.7		3.8	4.0
C44*	2017/08/01	UP26	Pre	170657	170654	170653	1.70	170654.7	38.0	3.8	4.0
			Post	170694	170691	170693	1.25	170692.7		3.8	4.0
C45	2017/08/04	UP23	Pre	183494	183492	183490	1.63	183492	39.0	3.8	4.0
			Post	183530	183533	183530	1.41	183531		3.8	4.0
C46	2017/08/07	UP23	Pre	155466	155463	155463	1.41	155464	80.7	3.8	4.0
			Post	155546	155544	155544	0.94	155544.7		3.8	4.0

\* Duplicate sample

**APPENDIX 6A - GRAVIMETRIC ANALYSIS DATA**

Sample ID	Sample date	Pump ID	Pre/Post-sampling	Replicates ( $\mu\text{g}$ )			s ( $\mu\text{g}$ )	$\mu$ ( $\mu\text{g}$ )	$\Delta\mu$ ( $\mu\text{g}$ )	Flow rate ( $\text{L}\cdot\text{min}^{-1}$ )	Normalised flow rate ( $\text{L}\cdot\text{min}^{-1}$ )
				R1	R2	R3					
C47	2017/08/10	UP23	Pre	171535	171531	171532	1.70	171532.7	28.0	3.8	4.0
			Post	171559	171560	171563	1.70	171560.7			
C48	2017/08/13	UP23	Pre	167785	167785	167785	0.00	167785	60.7	3.8	4.0
			Post	167846	167844	167847	1.25	167845.7			
C49	2017/08/16	UP23	Pre	160344	160344	160343	0.47	160343.7	47.3	3.8	4.0
			Post	160391	160390	160392	0.82	160391			
C50*	2017/08/16	UP26	Pre	181366	181366	181367	0.47	181366.3	40.3	3.8	4.0
			Post	181408	181405	181407	1.25	181406.7			
C51	2017/08/19	UP23	Pre	181091	181094	181090	1.70	181091.7	88.7	3.8	4.0
			Post	181180	181181	181180	0.47	181180.3			
C52	2017/08/22	UP23	Pre	179938	179939	179938	0.47	179938.3	82.7	3.8	4.0
			Post	180020	180020	180023	1.41	180021			
C53	2017/08/25	UP23	Pre	184036	184034	184034	0.94	184034.7	111	3.8	4.0
			Post	184144	184146	184147	1.25	184145.7			
C54	2017/08/28	UP23	Pre	178673	178669	178670	1.70	178670.7	69.7	3.8	4.0
			Post	178741	178740	178740	0.47	178740.3			
C55	2017/08/31	UP23	Pre	183308	183307	183308	0.47	183307.7	78.3	3.8	4.0
			Post	183387	183386	183385	0.82	183386			
C57	2017/09/03	UP23	Pre	181007	181006	181004	1.25	181005.7	136	3.8	4.0
			Post	181141	181144	181141	1.41	181142			
C58*	2017/09/03	UP26	Pre	168115	168116	168120	2.16	168117	108	3.8	4.0
			Post	168227	168224	168223	1.70	168224.7			
C59	2017/09/06	UP23	Pre	168910	168912	168910	0.94	168910.7	16.3	3.8	4.0
			Post	168928	168927	168926	0.82	168927			
C60	2017/09/09	UP23	Pre	183146	183148	183146	0.94	183146.7	59.3	3.8	4.0
			Post	183206	183207	183205	0.82	183206			
C61	2017/09/12	UP26	Pre	158381	158382	158383	0.82	158382	110	3.8	4.0
			Post	158491	158491	158493	0.94	158491.7			
C62*	2017/09/12	UP23	Pre	205761	205759	205760	0.82	205760	147	3.8	4.4
			Post	205908	205908	205905	1.41	205907			

\* Duplicate sample



**APPENDIX 6A - GRAVIMETRIC ANALYSIS DATA**

Sample ID	Sample date	Pump ID	Pre/Post-sampling	Replicates (µg)			s (µg)	µ (µg)	Δµ (µg)	Flow rate (L.min <sup>-1</sup> )	Normalised flow rate (L.min <sup>-1</sup> )
				R1	R2	R3					
C63	2017/09/15	UP26	Pre	208434	208434	208433	0.47	208433.7		3.8	4.0
			Post	208544	208546	208543	1.25	208544.3	111	3.8	4.0
C64	2017/09/18	UP26	Pre	182092	182091	182092	0.47	182091.7		3.8	4.0
			Post	182230	182231	182234	1.70	182231.7	140	3.9	4.1
C65	2017/09/21	UP26	Pre	197253	197253	197256	1.41	197254		3.8	4.0
			Post	197409	197410	197412	1.25	197410.3	156	3.7	3.9
C66	2017/09/24	UP26	Pre	215524	215519	215521	2.05	215521.3		3.8	4.0
			Post	215705	215702	215702	1.41	215703	182	3.7	3.9
C67	2017/09/27	UP26	Pre	199452	199452	199452	0.00	199452		3.8	4.0
			Post	199603	199600	199599	1.70	199600.7	149	3.7	3.9
C68*	2017/09/27	UP23	Pre	199217	199212	199213	2.16	199214		3.8	4.0
			Post	199360	199359	199360	0.47	199359.7	146	3.7	3.9
C69	2017/09/30	UP26	Pre	199810	199808	199805	2.05	199807.7		3.8	4.0
			Post	199958	199956	199955	1.25	199956.3	149	3.8	4.0
C70	2017/10/03	UP26	Pre	184403	184399	184400	1.70	184400.7		3.8	4.0
			Post	184507	184505	184503	1.63	184505	104	3.8	4.0
C71	2017/10/06	UP26	Pre	213066	213063	213062	1.70	213063.7		3.8	4.0
			Post	213232	213232	213231	0.47	213231.7	168	3.8	4.0
C72	2017/10/09	UP26	Pre	190585	190583	190583	0.94	190583.7		3.8	4.0
			Post	190695	190695	190691	1.89	190693.7	110	3.8	4.0
C73	2017/10/12	UP26	Pre	185998	185995	185995	1.41	185996		3.8	4.0
			Post	186122	186124	186124	0.94	186123.3	127	3.7	3.9
C74*	2017/10/12	UP23	Pre	172694	172695	172694	0.47	172694.3		3.8	4.0
			Post	172822	172823	172819	1.70	172821.3	127	3.8	4.0
C75	2017/10/15	UP26	Pre	181744	181744	181749	2.36	181745.7		3.8	4.0
			Post	181938	181938	181938	0.00	181938	192	3.8	4.0
C76	2017/10/18	UP26	Pre	175738	175739	175736	1.25	175737.7		3.8	4.0
			Post	175801	175804	175800	1.70	175801.7	64.0	3.7	3.9
C77	2017/10/21	UP26	Pre	177506	177507	177506	0.47	177506.3		3.8	4.0
			Post	177648	177652	177650	1.63	177650	144	3.7	3.9

\* Duplicate sample

**APPENDIX 6A - GRAVIMETRIC ANALYSIS DATA**

Sample ID	Sample date	Pump ID	Pre/Post-sampling	Replicates ( $\mu\text{g}$ )			s ( $\mu\text{g}$ )	$\mu$ ( $\mu\text{g}$ )	$\Delta\mu$ ( $\mu\text{g}$ )	Flow rate ( $\text{L}\cdot\text{min}^{-1}$ )	Normalised flow rate ( $\text{L}\cdot\text{min}^{-1}$ )
				R1	R2	R3					
C78	2017/10/24	UP26	Pre	205454	205458	205458	1.89	205456.7		3.8	4.0
			Post	205604	205607	205606	1.25	205605.7	149	3.7	3.9
C79	2017/10/27	UP26	Pre	201610	201605	201610	2.36	201608.3		3.8	4.0
			Post	201758	201758	201757	0.47	201757.7	149	3.8	4.0
C80*	2017/10/27	UP23	Pre	174200	174200	174202	0.94	174200.7		3.8	4.0
			Post	174352	174350	174350	0.94	174350.7	150	3.7	3.9
C82	2017/10/30	UP23	Pre	182999	182998	182999	0.47	182998.7		3.8	4.0
			Post	183066	183063	183065	1.25	183064.7	66.0	3.7	3.9
C83	2017/11/02	UP23	Pre	158531	158531	158532	0.47	158531.3		3.8	4.0
			Post	158618	158619	158616	1.25	158617.7	86.3	3.7	3.9
C84	2017/11/05	UP23	Pre	172667	172668	172666	0.82	172667		3.8	4.0
			Post	172708	172708	172708	0.00	172708	41.0	3.8	4.0
C85	2017/11/08	UP23	Pre	163292	163292	163291	0.47	163291.7		3.8	4.0
			Post	163360	163360	163360	0.00	163360	68.3	3.8	4.0
C86	2017/11/11	UP23	Pre	171737	171737	171736	0.47	171736.7		3.8	4.0
			Post	171836	171833	171834	1.25	171834.3	97.7	3.8	4.0
C87*	2017/11/11	UP26	Pre	161703	161703	161702	0.47	161702.7		3.8	4.0
			Post	161801	161803	161802	0.82	161802	99.3	3.8	4.0
C88	2017/11/14	UP23	Pre	158150	158153	158152	1.25	158151.7		3.8	4.0
			Post	158173	158173	158173	0.00	158173	21.3	3.8	4.0
C89	2017/11/17	UP23	Pre	160807	160803	160806	1.70	160805.3		3.8	4.0
			Post	160873	160869	160870	1.70	160870.7	65.3	3.8	4.0
C90	2017/11/20	UP23	Pre	167945	167943	167947	1.63	167945		3.8	4.0
			Post	167989	167989	167988	0.47	167988.7	43.7	3.8	4.0
C91	2017/11/23	UP23	Pre	166370	166370	166371	0.47	166370.3		3.8	4.0
			Post	166412	166410	166409	1.25	166410.3	40.0	3.7	3.9
C92	2017/11/26	UP23	Pre	160812	160811	160810	0.82	160811		3.8	4.0
			Post	160880	160881	160880	0.47	160880.3	69.3	3.7	3.9
C93*	2017/11/26	UP26	Pre	153754	153751	153752	1.25	153752.3		3.8	4.0
			Post	153822	153824	153823	0.82	153823	70.7	3.7	3.9

\* Duplicate sample

**APPENDIX 6A - GRAVIMETRIC ANALYSIS DATA**

Sample ID	Sample date	Pump ID	Pre/Post-sampling	Replicates (µg)			s (µg)	µ (µg)	Δµ (µg)	Flow rate (L.min <sup>-1</sup> )	Normalised flow rate (L.min <sup>-1</sup> )
				R1	R2	R3					
C94	2017/11/29	UP23	Pre	156425	156423	156422	1.25	156423.3		3.8	4.0
			Post	156485	156482	156484	1.25	156483.7	60.3	3.7	3.9
C95	2017/12/02	UP23	Pre	161434	161434	161431	1.41	161433		3.8	4.0
			Post	161470	161474	161475	2.16	161473	40.0	3.8	4.0
C96	2017/12/05	UP23	Pre	157909	157908	157908	0.47	157908.3		3.8	4.0
			Post	157976	157976	157976	0.00	157976	67.7	3.8	4.0
C97	2017/12/08	UP23	Pre	172630	172630	172630	0.00	172630		3.8	4.0
			Post	172716	172718	172718	0.94	172717.3	87.3	3.8	4.0
C98	2017/12/11	UP23	Pre	178764	178766	178764	0.94	178764.7		3.8	4.0
			Post	178823	178823	178823	0.00	178823	58.3	3.8	4.0
C99*	2017/12/11	UP26	Pre	180116	180116	180117	0.47	180116.3		3.8	4.0
			Post	180168	180167	180167	0.47	180167.3	51.0	3.7	3.9
C100	2017/12/14	UP23	Pre	165892	165891	165892	0.47	165891.7		3.8	4.0
			Post	165980	165980	165980	0.00	165980	88.3	3.8	4.0
C101	2017/12/17	UP26	Pre	206286	206290	206286	1.89	206287.3		3.8	4.0
			Post	206310	206312	206313	1.25	206311.7	24.3	3.7	3.9
C102	2017/12/20	UP26	Pre	213539	213538	213538	0.47	213538.3		3.8	4.0
			Post	213630	213632	213631	0.82	213631	92.7	3.8	4.0
C103	2017/12/23	UP26	Pre	214115	214110	214111	2.16	214112		3.8	4.0
			Post	214166	214165	214162	1.70	214164.3	52.3	3.8	4.0
C104	2017/12/26	UP26	Pre	203034	203030	203031	1.70	203031.7		3.8	4.0
			Post	203089	203089	203089	0.00	203089	57.3	3.7	3.9
C105*	2017/12/26	UP23	Pre	187956	187958	187956	0.94	187956.7		3.8	4.0
			Post	188029	188026	188027	1.25	188027.3	70.7	3.8	4.0
C106	2017/12/29	UP26	Pre	177406	177407	177408	0.82	177407		3.8	4.0
			Post	177500	177496	177497	1.70	177497.7	90.7	3.8	4.0
C107	2018/01/01	UP26	Pre	155534	155535	155532	1.25	155533.7		3.8	4.0
			Post	155574	155574	155574	0.00	155574	40.3	3.7	3.9
C108	2018/01/04	UP26	Pre	172928	172928	172928	0.00	172928		3.8	4.0
			Post	172991	172989	172992	1.25	172990.7	62.7	3.8	4.0

\* Duplicate sample

**APPENDIX 6A - GRAVIMETRIC ANALYSIS DATA**

Sample ID	Sample date	Pump ID	Pre/Post-sampling	Replicates ( $\mu\text{g}$ )			s ( $\mu\text{g}$ )	$\mu$ ( $\mu\text{g}$ )	$\Delta\mu$ ( $\mu\text{g}$ )	Flow rate ( $\text{L}\cdot\text{min}^{-1}$ )	Normalised flow rate ( $\text{L}\cdot\text{min}^{-1}$ )
				R1	R2	R3					
C109	2018/01/07	UP26	Pre	160923	160921	160924	1.70	160922.7		3.8	4.0
			Post	160952	160950	160951	1.25	160951	28.3	3.8	4.0
C110	2018/01/10	UP26	Pre	200266	200265	200262	0.94	200264.3		3.8	4.0
			Post	200318	200315	200317	1.25	200316.7	52.4	3.7	3.9
C111*	2018/01/10	UP23	Pre	157962	157962	157960	0.82	157961.3		3.8	4.0
			Post	158023	158023	158023	1.25	158023	61.7	3.7	3.9
C112	2018/01/13	UP26	Pre	171200	171198	171199	0.94	171199		3.8	4.0
			Post	171249	171246	171248	0.47	171247.7	48.7	3.7	3.9
C113	2018/01/16	UP26	Pre	175316	175318	175316	1.63	175316.7		3.8	4.0
			Post	175430	175429	175429	0.94	175429.3	113	3.8	4.0
C114	2018/01/19	UP26	Pre	206139	206143	206141	1.25	206141		3.8	4.0
			Post	206170	206168	206170	0.47	206169.3	28.3	3.7	3.9
C115	2018/01/22	UP26	Pre	178014	178016	178017	0.47	178015.7		3.8	4.0
			Post	178006	178005	178006	0.82	178055.7	40.0	3.8	4.0
C116	2018/01/25	UP26	Pre	159058	159058	159058	0.00	159058		3.8	4.0
			Post	159133	159131	159132	0.82	159132	74.0	3.8	4.0
C117*	2018/01/25	UP23	Pre	204411	204413	204411	0.94	204411.7		3.8	4.0
			Post	204487	204488	204488	0.47	204487.7	76.0	3.8	4.0
C118	2018/01/28	UP26	Pre	191254	191255	191255	0.47	191254.7		3.8	4.0
			Post	191323	191322	191321	0.82	191322	67.3	3.7	3.9
C119	2018/01/31	UP26	Pre	167326	167328	167325	1.25	167326.3		3.8	4.0
			Post	167391	167391	167392	0.47	167391.3	65.0	3.8	4.0
C120	2018/02/03	UP26	Pre	218496	218499	218497	1.25	218497.3		3.8	4.0
			Post	218575	218575	218573	0.94	218574.3	77.0	3.7	3.9
C121	2018/02/06	UP23	Pre	180386	180386	180386	0.00	180386		3.8	4.0
			Post	180441	180442	180441	0.47	180441.3	55.3	3.8	4.0
C122	2018/02/09	UP23	Pre	170274	170275	170276	0.82	170275		3.8	4.0
			Post	170332	170333	170331	0.82	170332	58.0	3.8	4.0
C123*	2018/02/09	UP26	Pre	163399	163396	163396	1.41	163397		3.8	4.0
			Post	163447	163445	163445	0.94	163445.7	48.7	3.8	4.0

\* Duplicate sample

**APPENDIX 6A - GRAVIMETRIC ANALYSIS DATA**

Sample ID	Sample date	Pump ID	Pre/Post-sampling	Replicates ( $\mu\text{g}$ )			s ( $\mu\text{g}$ )	$\mu$ ( $\mu\text{g}$ )	$\Delta\mu$ ( $\mu\text{g}$ )	Flow rate ( $\text{L}\cdot\text{min}^{-1}$ )	Normalised flow rate ( $\text{L}\cdot\text{min}^{-1}$ )
				R1	R2	R3					
C124	2018/02/12	UP23	Pre	220865	220863	220862	1.25	220863.3		3.8	4.0
			Post	220914	220911	220912	1.25	220912.3	49.0	3.8	4.0
C125	2018/02/15	UP23	Pre	166604	166602	166604	0.94	166603.3		3.8	4.0
			Post	166633	166632	166630	1.25	166631.7	28.4	3.8	4.0
C126	2018/02/18	UP23	Pre	173738	173737	173735	1.25	173736.7		3.8	4.0
			Post	173799	173797	173796	1.25	173797.3	60.6	3.7	3.9
C127	2018/02/21	UP23	Pre	220023	220024	220025	0.82	220024		3.8	4.0
			Post	220065	220067	220068	1.25	220066.7	42.7	3.8	4.0
C128	2018/02/24	UP23	Pre	204750	204750	204750	0.00	204750		3.8	4.0
			Post	204796	204793	204795	1.25	204794.7	44.7	3.7	3.9
C129*	2018/02/24	UP26	Pre	178594	178595	178594	0.47	178594.3		3.8	4.0
			Post	178632	178633	178631	0.82	178632	37.7	3.7	3.9
C130	2018/02/27	UP23	Pre	173977	173976	173978	0.82	173977		3.8	4.0
			Post	174013	174012	174010	1.25	174011.7	34.7	3.9	4.1
C131	2018/03/02	UP23	Pre	233208	233208	233207	0.47	233207.7		3.8	4.0
			Post	233256	233254	233252	1.63	233254	46.3	3.8	4.0
C132	2018/03/05	UP23	Pre	219894	219891	219892	1.25	219892.3		3.8	4.0
			Post	219911	219912	219911	0.47	219911.3	190	3.8	4.0
C133	2018/03/08	UP23	Pre	213911	213911	213909	0.94	213910.3		3.8	4.0
			Post	213940	213944	213943	1.70	213942.3	32.0	3.8	4.0
C134	2018/03/11	UP23	Pre	165369	165365	165367	1.63	165367		3.8	4.0
			Post	165417	165417	165414	1.41	165416	49.0	3.8	4.0
C135*	2018/03/11	UP26	Pre	177634	177630	177633	1.70	177632.3		3.8	4.0
			Post	177670	177670	177669	0.47	177669.7	37.4	3.8	4.0
C136	2018/03/14	UP23	Pre	209256	209256	209257	0.47	209256.3		3.8	4.0
			Post	209261	209259	209260	0.82	209260	3.70	3.8	4.0
C137	2018/03/17	UP23	Pre	210553	210553	210553	0.00	210553		3.8	4.0
			Post	210635	210632	210632	1.41	210633	80.0	3.8	4.0
C138	2018/03/20	UP23	Pre	210225	210222	210224	1.25	210223.7		3.8	4.0
			Post	210250	210246	210245	2.16	210247	23.3	3.8	4.0

\* Duplicate sample

**APPENDIX 6A - GRAVIMETRIC ANALYSIS DATA**

Sample ID	Sample date	Pump ID	Pre/Post-sampling	Replicates ( $\mu\text{g}$ )			s ( $\mu\text{g}$ )	$\mu$ ( $\mu\text{g}$ )	$\Delta\mu$ ( $\mu\text{g}$ )	Flow rate ( $\text{L}\cdot\text{min}^{-1}$ )	Normalised flow rate ( $\text{L}\cdot\text{min}^{-1}$ )
				R1	R2	R3					
C139	2018/03/23	UP23	Pre	203345	203348	203347	1.25	203346.7	86	3.8	4.0
			Post	203435	203431	203432	1.70	203432.7			
C140	2018/03/26	UP23	Pre	195911	195913	195910	1.25	195911.3	30.4	3.8	4.0
			Post	195944	195941	195940	1.70	195941.7			
C141*	2018/03/26	UP26	Pre	193686	193683	193684	1.25	193684.3	21.7	3.8	4.0
			Post	193706	193705	193707	0.82	193706			
C142	2018/03/29	UP26	Pre	218576	218574	218574	0.94	218574.7	14.6	3.8	4.0
			Post	218591	218588	218589	1.25	218589.3			
C143	2018/04/01	UP26	Pre	204875	204875	204877	0.94	204875.7	58	3.8	4.0
			Post	204933	204933	204935	0.94	204933.7			
C144	2018/04/04	UP26	Pre	196409	196407	196410	1.25	196408.7	66	3.8	4.0
			Post	196477	196473	196474	1.70	196474.7			
C145	2018/04/07	UP26	Pre	212310	212313	212314	1.70	212312.3	54.4	3.8	4.0
			Post	212368	212365	212367	1.25	212366.7			
C146	2018/04/10	UP26	Pre	224437	224436	224437	0.47	224436.7	33.6	3.8	4.0
			Post	224472	224470	224469	1.25	224470.3			
C147*	2018/04/10	UP23	Pre	222565	222563	222564	0.82	222564	41.7	3.8	4.0
			Post	222605	222607	222605	0.94	222605.7			
C148	2018/04/13	UP26	Pre	183897	183898	183899	0.82	183898	69.3	3.8	4.0
			Post	183968	183968	183966	0.94	183967.3			
C149	2018/04/16	UP26	Pre	172547	172549	172550	1.25	172548.7	119	3.8	4.0
			Post	172668	172668	172667	0.47	172667.7			

\* Duplicate sample

**APPENDIX 6B - GRAVIMETRIC ANALYSIS QUALITY CONTROL DATA (PRE-SAMPLING)**

Session date	Filter series		Replicates (µg)			s (µg)	µ (µg)	Δµ (µg)	m <sub>r</sub> (µg)	Min. mass (µg)	% diff. min. and mean (10 <sup>-4</sup> )	Max. mass (µg)	% diff. max. and mean (10 <sup>-4</sup> )
			R1	R2	R3								
2017/04/06	C1-10	before	528298	528295	528296	1.25	528296.3			528295	2.46	528298	3.22
		after	528294	528295	528296	0.82	528295	-1.3		528294	1.89	528296	1.89
	C11-20	before	528287	528288	528288	0.47	528287.7			528287	1.33	528288	5.68
		after	528295	528293	528296	1.25	528294.7	7	-1.6	528293	3.22	528296	2.46
2017/05/12	C21-30	before	543268	543263	543266	2.05	543265.7			543263	4.97	543268	4.23
		after	543265	543267	543264	1.25	543265.3	-0.4		543264	2.39	543267	3.13
	C31-40	before	543259	543263	543260	1.70	543260.7			543259	3.13	543263	4.23
		after	543256	543254	543256	0.94	543255.3	-5.4	-10.4	543254	2.39	543256	1.29
2017/07/17	C41-50	before	544232	544233	544235	1.25	544233.3			544232	2.39	544235	3.12
		after	544236	544240	544239	1.70	544238.3	5		544236	4.23	544240	3.12
	C51-60	before	544234	544235	544236	0.82	544235			544234	1.84	544236	1.84
		after	544249	544247	544246	1.25	544247.3	12.3	14	544246	2.39	544249	3.12
2017/09/05	C61-70	before	522328	522323	522327	2.16	522326			522323	5.74	522328	3.83
		after	522325	522326	522330	2.16	522327	1		522325	3.83	522330	5.74
	C71-80	before	522319	522318	522315	1.70	522317.3			522315	4.40	522319	3.25
		after	522314	522314	522318	1.89	522315.3	-2	-9.7	522314	2.49	522318	5.17
2017/10/19	C81-90	before	548019	548017	548016	1.25	548017.3			548016	2.37	548019	3.10
		after	548021	548017	548021	1.89	548019.7	2.4		548017	4.93	548021	2.37
	C91-100	before	548027	548027	548025	0.94	548026.3			548025	2.37	548027	1.28
		after	548028	548028	548028	0.00	548028	1.7	10.7	548028	0.00	548028	0.00
2017/12/05	C101-110	before	553688	553683	553688	2.36	553686.3			553683	5.96	553688	3.07
		after	553689	553685	553685	1.89	553686.3	0		553685	2.35	553689	4.88
	C111-120	before	553686	553691	553688	2.05	553688.3			553686	4.15	553691	4.88
		after	553700	553699	553701	0.82	553700	1.7	13.7	553699	1.81	553701	1.81
2018/02/02	C121-130	before	528264	528265	528267	1.25	528265.3			528264	2.46	528267	3.22
		after	528267	528268	528267	0.47	528267.3	2		528267	5.68	528268	1.33
	C131-140	before	528269	528270	528273	1.70	528270.7			528269	3.22	528273	4.35
		after	528271	528272	528273	0.82	528272	1.3	6.7	528271	1.89	528273	1.89
2018/02/02	C141-149	before	528268	528269	528269	0.47	528268.7			528268	1.33	528269	5.68
		after	528274	528271	528273	1.25	528272.7	4	4	528271	3.22	528274	2.46

**APPENDIX 6C - GRAVIMETRIC ANALYSIS QUALITY CONTROL DATA (POST-SAMPLING)**

Session date	Filter series		Replicates ( $\mu\text{g}$ )			s ( $\mu\text{g}$ )	$\mu$ ( $\mu\text{g}$ )	$\Delta\mu$ ( $\mu\text{g}$ )	$m_r$ ( $\mu\text{g}$ )	Min. mass ( $\mu\text{g}$ )	% diff. min. and mean ( $10^{-5}$ )	Max. mass ( $\mu\text{g}$ )	% diff. max. and mean ( $10^{-5}$ )
			R1	R2	R3								
2017/06/02	C1-10	before	528236	528235	528239	1.70	528236.7			528235	32.2	528239	43.5
		after	528230	528235	528237	2.94	528234	-2.7		528230	75.7	528237	56.8
	C11-20	before	528238	528237	528236	0.82	528237			528236	18.9	528238	18.9
		after	528242	528238	528239	1.70	528239.7	2.7	3	528238	32.2	528242	43.5
2017/07/28	C21-30	before	543267	543267	543267	0.00	543267			543267	0.00	543267	0.00
		after	543269	543268	543267	0.82	543268	1		543267	18.4	543269	18.4
	C31-40	before	543271	543268	543271	1.41	543270			543268	36.8	543271	18.4
		after	543273	543271	543273	0.94	543272.3	2.6	5.3	543271	23.9	543273	12.9
2017/09/19	C41-50	before	544263	544259	544260	1.70	544260.7			544259	31.2	544263	42.3
		after	544271	544272	544274	1.25	544272.3	11.6		544271	23.9	544274	31.2
	C51-60	before	544262	544259	544262	1.41	544261			544259	36.7	544262	18.4
		after	544270	544270	544271	0.47	544270.3	9.3	9.6	544270	5.51	544271	12.9
2017/11/03	C61-70	before	522558	522563	522559	2.16	522560			522558	38.3	522563	57.4
		after	522561	522564	522562	1.25	522562.3	2.3		522561	24.9	522564	32.5
	C71-80	before	522564	522562	522564	0.94	522563.3			522562	24.9	522564	13.4
		after	522561	522565	522565	1.89	522563.7	0.4	3.7	522561	51.7	522565	24.9
2017/12/28	C81-90	before	548031	548031	548031	0.00	548031			548031	0.00	548031	0.00
		after	548034	548038	548036	1.63	548036	5		548034	36.5	548038	36.5
	C91-100	before	548034	548038	548038	1.89	548036.7			548034	49.3	548038	23.7
		after	548033	548036	548036	1.41	548035	-1.7	4	548033	36.5	548036	18.2
2017/02/07	C101-110	before	553681	553682	553683	0.82	553682			553681	18.1	553683	18.1
		after	553682	553682	553684	0.94	553682.7	0.7		553682	12.6	553684	23.5
	C111-120	before	553685	553686	553686	0.47	553685.7			553685	12.6	553686	5.42
		after	553694	553696	553695	0.82	553695	9.3	13	553694	18.1	553696	18.1
2018/04/19	C121-130	before	553743	553742	553740	1.25	553741.7			553740	30.7	553743	23.5
		after	553735	553734	553734	0.47	553734.3	-7.3		553734	5.42	553735	12.6
	C131-140	before	553738	553735	553736	1.25	553736.3			553735	23.5	553738	30.7
		after	553737	553732	553734	2.05	553734.3	-2	-7.4	553732	41.5	553737	48.8
C141-149	before	553736	553732	553735	1.70	553734.3			553732	41.5	553736	30.7	
	after	553729	553728	553726	1.25	553727.7	-6.6	-6.6	553726	30.7	553729	23.5	



**APPENDIX 7A - REFLECTOMETRIC DATA**

Sample ID	Sample date	Replicates (%)					s (%)	R <sub>s</sub> (%)	A/2V (10 <sup>-5</sup> m <sup>-1</sup> )	R	Absorption coefficient (10 <sup>-5</sup> m <sup>-1</sup> )
		R1	R2	R3	R4	R5					
C1	2017/04/18	56.2	62.2	62.1	64.8	61.8	2.82	61.4	7.42	0.487	3.62
C2*	2017/04/18	61.0	62.6	61.7	63.8	62.7	0.95	62.4	7.42	0.472	3.50
C3	2017/04/21	59.3	63.9	66.2	62.0	62.3	2.28	62.7	7.42	0.466	3.46
C4	2017/04/24	56.6	54.6	56.1	58.4	55.6	1.26	56.3	7.42	0.575	4.27
C5	2017/04/27	78.3	81.1	78.7	76.6	79.3	1.46	78.8	7.42	0.238	1.77
C6	2017/04/30	93.5	93.3	92.6	93.2	93.2	0.30	93.2	7.42	0.071	0.53
C7	2017/05/03	74.0	75.8	77.2	73.6	78.6	1.89	75.8	7.42	0.277	2.05
C8*	2017/05/03	72.8	73.0	74.0	72.8	72.5	0.52	73.0	7.51	0.314	2.36
C9	2017/05/06	95.6	95.3	95.3	95.1	94.8	0.26	95.2	7.42	0.049	0.36
C10	2017/05/09	68.0	69.5	70.1	71.4	70.3	1.11	69.9	7.42	0.359	2.66
C11	2017/05/12	68.9	70.2	70.4	69.5	72.8	1.33	70.4	7.42	0.352	2.61
C12	2017/05/15	60.6	62.8	66.0	64.3	63.6	1.78	63.5	7.42	0.455	3.38
C13	2017/05/18	65.6	67.8	70.3	69.8	67.5	1.70	68.2	7.51	0.383	2.88
C14*	2017/05/18	71.1	70.9	71.3	72.3	72.0	0.54	71.5	7.42	0.335	2.49
C15	2017/05/21	81.0	80.5	82.5	83.1	81.8	0.95	81.8	7.42	0.201	1.49
C16	2017/05/24	70.8	72.2	70.8	72.7	72.0	0.77	71.7	7.42	0.333	2.47
C17	2017/05/27	69.2	70.7	72.4	69.5	69.8	1.15	70.3	7.42	0.352	2.61
C18	2017/05/30	73.2	69.5	70.1	72.5	72.5	1.47	71.6	7.42	0.335	2.48
C19	2017/06/02	69.1	70.6	72.7	70.9	69.1	1.34	70.5	7.42	0.350	2.60
C20*	2017/06/02	72.4	72.9	72.7	69.8	74.2	1.44	72.4	7.42	0.323	2.40
C21	2017/06/05	74.4	76.2	77.1	75.9	75.8	0.87	75.9	7.51	0.277	2.08
C22	2017/06/08	74.2	75.5	74.8	75.8	74.8	0.57	75.0	7.51	0.288	2.17
C23	2017/06/11	99.8	100.4	99.4	100.6	100.8	0.52	100	7.42	0.000	0.00
C24	2017/06/14	88.4	87.3	87.7	88.6	87.4	0.53	87.9	7.42	0.130	0.97
C25	2017/06/17	57.6	55.1	56.9	57.6	53.5	1.61	56.1	7.42	0.578	4.29
C26*	2017/06/17	53.9	54.9	57.1	57.1	56.0	1.25	55.8	7.33	0.584	4.29
C27	2017/06/20	49.4	54.9	49.3	47.8	52.6	2.58	50.8	7.42	0.678	5.03
C28	2017/06/23	49.8	50.5	49.5	50.6	50.6	0.46	50.2	7.42	0.690	5.12
C29	2017/06/26	48.4	46.2	50.0	48.1	49.4	1.30	48.4	7.42	0.726	5.39
C30	2017/06/29	91.4	90.6	91.6	91.1	90.3	0.49	91.0	7.51	0.095	0.72

\* Duplicate sample

## APPENDIX 7A - REFLECTOMETRIC DATA

Sample ID	Sample date	Replicates (%)					s (%)	R <sub>s</sub> (%)	A/2V (10 <sup>-5</sup> m <sup>-1</sup> )	R	Absorption coefficient (10 <sup>-5</sup> m <sup>-1</sup> )
		R1	R2	R3	R4	R5					
C31	2017/07/02	89.5	92.3	91.1	90.7	91.6	0.94	91.0	7.42	0.095	0.71
C32*	2017/07/02	84.7	85.3	85.4	84.4	84.8	0.38	84.9	7.42	0.164	1.22
C33	2017/07/05	91.0	91.5	91.6	91.2	89.0	0.95	90.9	7.51	0.097	0.72
C34	2017/07/08	77.6	77.3	76.0	76.3	78.4	0.87	77.1	7.51	0.261	1.94
C35	2017/07/11	49.0	51.2	53.2	52.6	53.3	1.61	51.9	7.42	0.658	4.88
C36	2017/07/14	80.8	80.3	78.8	79.4	79.5	0.71	79.8	7.42	0.227	1.69
C37	2017/07/17	83.4	85.6	84.6	83.3	83.2	0.94	84.0	7.42	0.175	1.30
C38*	2017/07/17	81.7	83.0	81.1	82.3	83.2	0.79	82.3	7.42	0.196	1.46
C39	2017/07/20	75.4	72.5	71.4	73.0	72.8	1.31	73.0	7.42	0.315	2.34
C41	2017/07/26	73.1	72.6	73.5	73.2	71.0	0.89	72.7	7.42	0.319	2.37
C42	2017/07/29	60.8	60.6	61.7	62.7	58.6	1.36	60.9	7.42	0.496	3.68
C43	2017/08/01	96.0	96.7	96.4	95.9	95.8	0.34	96.2	7.42	0.039	0.29
C44*	2017/08/01	95.0	96.2	96.1	95.6	95.2	0.47	95.6	7.42	0.045	0.33
C45	2017/08/04	81.6	84.3	83.2	83.5	81.8	1.03	82.9	7.42	0.188	1.39
C46	2017/08/07	66.1	67.0	69.8	68.4	66.9	1.31	67.6	7.42	0.391	2.90
C47	2017/08/10	97.5	98.0	97.3	97.6	98.0	0.28	97.7	7.42	0.023	0.17
C48	2017/08/13	77.8	79.2	80.8	76.8	78.8	1.35	78.7	7.42	0.240	1.78
C49	2017/08/16	88.7	87.4	86.7	87.2	88.6	0.79	87.7	7.51	0.131	0.98
C50*	2017/08/16	89.9	91.2	88.2	87.4	87.2	1.54	88.8	7.42	0.119	0.88
C51	2017/08/19	48.9	53.6	47.2	50.2	49.2	2.12	49.8	7.42	0.697	5.17
C52	2017/08/22	85.4	86.6	83.6	85.5	86.7	1.12	85.6	7.42	0.156	1.16
C53	2017/08/25	70.9	72.7	68.6	77.2	70.1	2.96	71.9	7.42	0.330	2.45
C54	2017/08/28	83.0	85.3	85.4	82.8	82.4	1.30	83.8	7.42	0.177	1.31
C55	2017/08/31	74.5	76.3	73.0	76.9	74.9	1.38	75.1	7.51	0.286	2.15
C57	2017/09/03	57.0	60.5	64.0	58.5	57.9	2.49	59.6	7.51	0.518	3.89
C58*	2017/09/03	56.5	57.3	61.5	60.0	59.3	1.81	58.9	7.51	0.529	3.97
C59	2017/09/06	98.5	98.3	98.6	98.2	97.8	0.28	98.3	7.42	0.017	0.13
C60	2017/09/09	83.6	85.0	83.7	85.6	84.2	0.77	84.4	7.51	0.169	1.27
C61	2017/09/12	83.6	86.8	84.8	83.5	86.6	1.42	85.1	7.42	0.176	1.30
C62*	2017/09/12	89.6	92.0	92.6	98.2	91.0	2.94	92.7	7.42	0.090	0.67

\* Duplicate sample

## APPENDIX 7A - REFLECTOMETRIC DATA

Sample ID	Sample date	Replicates (%)					s (%)	R <sub>s</sub> (%)	A/2V (10 <sup>-5</sup> m <sup>-1</sup> )	R	Absorption coefficient (10 <sup>-5</sup> m <sup>-1</sup> )
		R1	R2	R3	R4	R5					
C63	2017/09/15	88.8	89.2	92.2	90.9	89.9	1.23	90.2	7.42	0.117	0.87
C64	2017/09/18	84.1	84.7	85.0	86.2	84.0	0.79	84.8	7.33	0.179	1.31
C65	2017/09/21	89.4	90.8	90.8	91.7	90.8	0.74	90.7	7.51	0.112	0.84
C66	2017/09/24	87.7	87.5	83.9	84.4	86.6	1.58	86.0	7.51	0.164	1.24
C67	2017/09/27	78.5	81.2	83.0	80.3	79.2	1.58	80.4	7.51	0.232	1.74
C68*	2017/09/27	79.4	81.6	81.7	79.3	80.5	1.03	80.5	7.51	0.231	1.73
C69	2017/09/30	93.0	93.8	92.6	92.6	91.6	0.71	92.7	7.42	0.089	0.66
C70	2017/10/03	98.8	98.8	98.5	99.2	99.6	0.38	99.0	7.42	0.024	0.18
C71	2017/10/06	84.0	85.7	83.4	85.3	86.0	1.01	84.9	7.42	0.178	1.32
C72	2017/10/09	94.7	94.3	93.6	93.4	93.3	0.55	93.9	7.42	0.077	0.57
C73	2017/10/12	88.6	89.3	88.7	88.0	88.5	0.42	88.6	7.51	0.135	1.01
C74*	2017/10/12	82.2	83.2	84.7	83.2	83.1	0.80	83.3	7.42	0.197	1.46
C75	2017/10/15	88.4	88.6	87.4	88.6	87.7	0.50	88.1	7.42	0.140	1.04
C76	2017/10/18	99.9	99.8	99.7	99.9	99.8	0.07	99.8	7.51	0.016	0.12
C77	2017/10/21	90.8	90.9	90.4	90.9	90.4	0.23	90.7	7.51	0.112	0.84
C78	2017/10/24	97.1	98.2	97.7	97.0	97.2	0.45	97.4	7.51	0.040	0.30
C79	2017/10/27	78.3	81.9	83.3	80.7	81.0	1.64	81.0	7.42	0.224	1.66
C80*	2017/10/27	81.0	82.6	81.6	81.4	79.2	1.11	81.2	7.51	0.223	1.67
C82	2017/10/30	86.2	89.4	85.3	87.4	87.0	1.37	87.1	7.51	0.139	1.04
C83	2017/11/02	81.7	82.1	83.2	81.6	81.3	0.66	82.0	7.51	0.199	1.49
C84	2017/11/05	94.8	95.4	95.9	95.8	97.0	0.72	95.8	7.42	0.043	0.32
C85	2017/11/08	90.6	89.6	90.6	92.6	89.5	1.11	90.6	7.42	0.099	0.73
C86	2017/11/11	91.1	91.3	90.6	89.6	90.5	0.59	90.6	7.42	0.098	0.73
C87*	2017/11/11	93.6	92.3	93.6	93.8	92.7	0.59	93.2	7.42	0.070	0.52
C88	2017/11/14	94.7	98.2	95.2	95.6	96.7	1.25	96.1	7.42	0.040	0.30
C89	2017/11/17	89.7	89.0	88.9	89.5	89.6	0.33	89.3	7.42	0.113	0.84
C90	2017/11/20	98.5	96.3	97.1	98.1	98.4	0.85	97.7	7.42	0.023	0.17
C91	2017/11/23	95.1	95.3	95.3	93.7	94.9	0.60	94.9	7.51	0.053	0.40
C92	2017/11/26	92.7	92.4	92.9	93.7	93.5	0.49	93.0	7.51	0.072	0.54
C93*	2017/11/26	89.5	91.4	92.5	91.8	92.9	1.18	91.6	7.51	0.088	0.66

\* Duplicate sample

**APPENDIX 7A - REFLECTOMETRIC DATA**

Sample ID	Sample date	Replicates (%)					s (%)	R <sub>s</sub> (%)	A/2V (10 <sup>-5</sup> m <sup>-1</sup> )	R	Absorption coefficient (10 <sup>-5</sup> m <sup>-1</sup> )
		R1	R2	R3	R4	R5					
C94	2017/11/29	89.9	90.0	90.1	90.3	89.9	0.19	90.1	7.51	0.104	0.78
C95	2017/12/02	99.4	97.8	98.0	97.8	99.4	0.65	98.4	7.42	0.016	0.12
C96	2017/12/05	86.1	87.2	87.4	85.5	86.1	0.75	86.7	7.42	0.143	1.06
C97	2017/12/08	96.6	97.2	96.0	97.2	96.6	0.54	96.6	7.42	0.035	0.26
C98	2017/12/11	97.9	96.6	95.9	96.6	97.9	0.84	97.0	7.42	0.030	0.22
C99*	2017/12/11	98.7	97.9	96.2	96.2	98.7	1.27	97.7	7.51	0.024	0.18
C100	2017/12/14	94.5	94.3	94.5	93.7	94.5	0.61	94.0	7.42	0.062	0.46
C101	2017/12/17	96.2	96.4	96.7	96.7	96.2	0.22	96.4	7.51	0.046	0.35
C102	2017/12/20	88.9	87.6	89.6	90.3	87.1	1.20	88.7	7.42	0.130	0.96
C103	2017/12/23	95.5	94.3	94.4	96.3	96.3	0.88	95.4	7.42	0.057	0.43
C104	2017/12/26	94.4	94.5	95.0	94.6	94.1	0.29	94.5	7.51	0.066	0.50
C105*	2017/12/26	94.0	93.8	95.3	94.4	93.4	0.65	94.2	7.42	0.070	0.52
C106	2017/12/29	89.0	88.7	88.6	89.3	89.8	0.44	89.1	7.42	0.126	0.93
C107	2018/01/01	96.5	96.4	96.0	96.3	96.7	0.23	96.4	7.51	0.047	0.35
C108	2018/01/04	93.7	94.0	95.3	93.7	93.5	0.65	94.0	7.42	0.071	0.53
C109	2018/01/07	98.6	98.6	97.9	98.0	98.7	0.34	98.4	7.42	0.026	0.20
C110	2018/01/10	85.1	87.2	85.0	85.5	85.9	0.80	85.7	7.51	0.164	1.23
C111*	2018/01/10	80.9	81.0	79.6	79.4	81.9	0.94	80.6	7.51	0.226	1.70
C112	2018/01/13	92.7	91.9	93.0	92.4	91.3	0.60	92.3	7.51	0.091	0.68
C113	2018/01/16	85.2	84.4	85.1	84.5	84.5	0.34	84.7	7.42	0.176	1.30
C114	2018/01/19	98.4	98.2	98.4	98.0	97.4	0.37	98.1	7.51	0.029	0.22
C115	2018/01/22	98.7	98.7	98.4	99.6	98.5	0.43	98.8	7.42	0.022	0.16
C116	2018/01/25	92.3	92.6	92.7	92.2	91.8	0.32	92.3	7.42	0.090	0.67
C117*	2018/01/25	95.1	94.8	94.6	95.2	95.0	0.22	94.9	7.42	0.062	0.46
C118	2018/01/28	90.3	91.2	89.7	91.7	91.6	0.78	90.9	7.51	0.105	0.79
C119	2018/01/31	93.1	93.7	94.6	92.6	93.5	0.67	93.5	7.42	0.077	0.57
C120	2018/02/03	93.8	93.8	95.1	94.9	94.9	0.58	94.5	7.51	0.067	0.50
C121	2018/02/06	93.4	94.1	94.4	92.9	93.1	0.58	93.6	7.42	0.069	0.51
C122	2018/02/09	96.9	96.1	95.6	95.6	95.8	0.49	96.0	7.42	0.044	0.33
C123*	2018/02/09	94.4	94.4	94.9	95.2	95.9	0.56	95.0	7.42	0.055	0.41

\* Duplicate sample

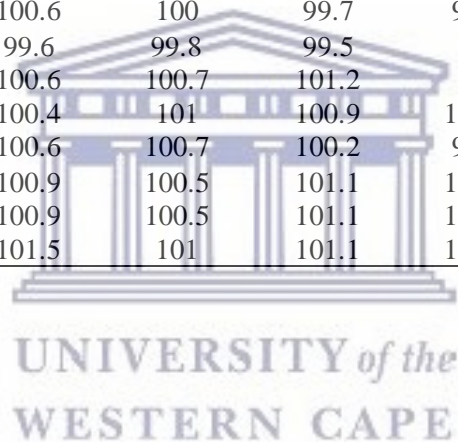
## APPENDIX 7A - REFLECTOMETRIC DATA

Sample ID	Sample date	Replicates (%)					s (%)	R <sub>s</sub> (%)	A/2V (10 <sup>-5</sup> m <sup>-1</sup> )	R	Absorption coefficient (10 <sup>-5</sup> m <sup>-1</sup> )
		R1	R2	R3	R4	R5					
C124	2018/02/12	90.6	89.1	90.7	89.3	89.1	0.73	89.8	7.42	0.111	0.82
C125	2018/02/15	91.2	91.7	92.2	91.9	92.0	0.34	91.8	7.42	0.089	0.66
C126	2018/02/18	93.2	92.1	93.3	92.4	92.8	0.46	92.8	7.51	0.078	0.58
C127	2018/02/21	90.9	90.2	90.9	91.4	90.5	0.41	90.8	7.42	0.100	0.74
C128	2018/02/24	92.4	92.9	92.0	91.7	92.5	0.41	92.3	7.51	0.083	0.62
C129*	2018/02/24	92.6	92.8	93.0	92.1	92.3	0.33	92.6	7.51	0.080	0.60
C130	2018/02/27	88.6	87.6	89.5	88.5	88.4	0.60	88.5	7.33	0.125	0.92
C131	2018/03/02	86.7	86.0	87.0	87.3	85.3	0.72	86.5	7.42	0.148	1.10
C132	2018/03/05	93.7	93.6	94.2	94.4	93.2	0.43	93.8	7.42	0.067	0.50
C133	2018/03/08	84.4	87.6	86.8	85.2	86.0	1.13	86.0	7.42	0.154	1.14
C134	2018/03/11	89.8	89.5	90.7	89.4	89.0	0.57	89.7	7.42	0.112	0.83
C135*	2018/03/11	88.6	89.5	88.9	89.8	88.6	0.49	89.1	7.42	0.119	0.88
C136	2018/03/14	96.7	96.6	96.6	97.4	97.1	0.32	96.9	7.42	0.035	0.26
C137	2018/03/17	79.8	80.6	81.5	81.7	81.3	0.70	81.0	7.42	0.214	1.59
C138	2018/03/20	93.2	91.7	93.1	92.5	91.5	0.70	92.4	7.42	0.082	0.61
C139	2018/03/23	78.2	78.2	78.6	79.2	79.8	0.62	78.8	7.42	0.241	1.79
C140	2018/03/26	83.2	82.1	82.3	81.8	81.2	0.66	82.1	7.42	0.200	1.48
C141*	2018/03/26	86.7	85.9	86.3	86.2	86.3	0.26	86.3	7.51	0.158	1.18
C142	2018/03/29	97.7	98.2	98.6	98.8	98.3	0.38	98.3	7.42	0.027	0.20
C143	2018/04/01	92.3	93.3	93.6	92.0	91.3	0.85	92.5	7.42	0.088	0.65
C144	2018/04/04	90.0	91.2	89.3	92.9	91.4	1.24	91.0	7.42	0.105	0.78
C145	2018/04/07	88.0	89.6	88.1	89.6	89.8	0.80	89.0	7.42	0.126	0.94
C146	2018/04/10	93.2	93.7	94.6	93.0	93.6	0.55	93.6	7.51	0.076	0.57
C147*	2018/04/10	93.4	94.1	92.7	93.1	93.9	0.51	93.4	7.42	0.078	0.58
C148	2018/04/13	87.1	87.9	86.6	88.2	87.0	0.60	87.4	7.51	0.145	1.09
C149	2018/04/16	73.0	73.7	74.0	74.2	74.9	0.62	74.0	7.33	0.312	2.28

\* Duplicate sample

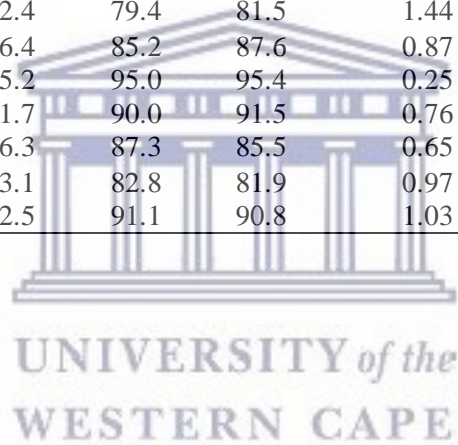
**APPENDIX 7B - REFLECTOMETRIC QUALITY CONTROL DATA (PRIMARY CONTROL FILTER)**

Session date	Sample series		Replicates (%)					s (%)	R <sub>0</sub> (%)	% difference before and after session
			R1	R2	R3	R4	R5			
2017/08/30	C1-20	before	100.4	99.9	100.2	100.1	100.1	0.16	100.1	
		after	100	100	99.5	98.9	98.8	0.52	99.4	-0.70
	C21-39	before	100.4	99.9	99.9	99.7	100	0.23	100	
		after	99.6	99.0	99.0	99.3	99.0	0.24	99.2	-0.80
2017/09/19	C41-60	before	100.4	99.9	99.8	100	99.7	0.24	100	
		after	99.4	99.2	98.6	98.8	98.8	0.29	99.0	-1.00
2017/11/03	C61-80	before	101.3	101.5	101.4	101.6	101	0.21	101.4	
		after	100	100.3	99.4	100.1	100	0.30	100	-1.38
2018/01/11	C82-C100	before	100.5	100.6	100	99.7	99.2	0.52	100	
		after	100.3	99.6	99.8	99.5	100	0.29	99.8	-0.16
2018/02/07	C101-120	before	101.3	100.6	100.7	101.2	101	0.27	101	
		after	100.5	100.4	101	100.9	100.8	0.23	100.7	-0.24
2018/04/21	C121-140	before	100.1	100.6	100.7	100.2	99.8	0.33	100.3	
		after	101.2	100.9	100.5	101.1	101.2	0.26	101	0.70
	C141-149	before	101.2	100.9	100.5	101.1	101.2	0.26	101	
		after	100.8	101.5	101	101.1	102.1	0.43	101.3	0.32



**APPENDIX 7C - REFLECTOMETRIC QUALITY CONTROL DATA (SAMPLES RECHECKED)**

Session date	Sample rechecked	Replicates (%)					s (%)	Duplicate R <sub>s</sub> (%)	Original R <sub>s</sub> (%)	% diff. original and duplicate R <sub>s</sub>
		R1	R2	R3	R4	R5				
2017/08/30	C6	92.9	93.0	92.4	92.2	92.8	0.31	92.7	93.2	-0.54
	C12	60.1	62.4	64.5	62.8	62.5	1.40	62.5	63.5	-1.58
	C26	52.1	54.5	57.6	54.0	53.8	1.79	54.4	55.8	-2.51
	C37	82.2	84.5	83.4	82.0	83.0	0.90	83.0	84.0	-1.19
2017/09/19	C43	95.0	95.0	95.3	93.8	94.3	0.55	94.7	96.2	-1.54
	C51	49.1	52.9	49.4	51.0	48.9	1.51	50.3	49.8	0.88
2017/11/03	C62	89.0	92.1	90.3	91.8	92.0	1.21	91.0	92.7	-1.77
	C74	82.7	82.0	84.7	84.5	84.0	1.05	83.6	83.3	0.36
2018/01/11	C83	83.1	83.4	82.4	79.4	81.5	1.44	82.0	82.0	-0.02
	C96	85.3	86.3	86.4	85.2	87.6	0.87	86.2	86.7	-0.60
2018/02/07	C104	95.3	94.7	95.2	95.0	95.4	0.25	95.1	94.5	0.63
	C118	90.3	91.8	91.7	90.0	91.5	0.76	91.1	90.9	0.18
2018/04/21	C131	86.6	85.7	86.3	87.3	85.5	0.65	86.3	86.5	-0.21
	C140	81.0	80.6	83.1	82.8	81.9	0.97	81.9	82.1	-0.29
	C143	91.7	89.4	92.5	91.1	90.8	1.03	91.1	92.5	-1.51



**APPENDIX 8 - OUTLIERS IN PM<sub>2.5</sub> CONCENTRATION AND ABSORPTION COEFFICIENT DATA SETS**

Sample date	Robust scores		Sample date	Robust scores		Sample date	Robust scores		Sample date	Robust scores	
	PM <sub>2.5</sub>	Abs. coeff		PM <sub>2.5</sub>	Abs. coeff		PM <sub>2.5</sub>	Abs. coeff		PM <sub>2.5</sub>	Abs. coeff
2017/04/18	1.17	3.30	2017/07/20	0.51	1.70	2017/10/24	2.14	0.82	2018/01/25	0.02	0.36
2017/04/21	1.25	3.10	2017/07/26	1.14	1.74	2017/10/27	2.16	0.88	2018/01/28	0.22	0.21
2017/04/24	1.57	4.10	2017/07/29	3.24	3.36	2017/10/30	0.02	0.10	2018/01/31	0.30	0.48
2017/04/27	0.04	1.01	2017/08/01	0.68	0.78	2017/11/02	0.50	0.66	2018/02/03	0.03	0.57
2017/04/30	0.35	0.52	2017/08/04	0.88	0.54	2017/11/05	0.68	0.79	2018/02/06	0.02	0.55
2017/05/03	0.05	1.75	2017/08/07	0.19	2.40	2017/11/08	0.02	0.28	2018/02/09	0.02	0.68
2017/05/06	1.07	0.72	2017/08/10	1.16	1.06	2017/11/11	0.81	0.28	2018/02/12	0.19	0.17
2017/05/09	0.25	2.12	2017/08/13	0.32	1.01	2017/11/14	1.19	0.82	2018/02/15	0.71	0.37
2017/05/12	0.41	2.05	2017/08/16	0.65	0.03	2017/11/17	0.06	0.15	2018/02/18	0.13	0.66
2017/05/15	0.40	3.00	2017/08/19	0.39	5.20	2017/11/20	0.62	0.97	2018/02/21	0.35	0.27
2017/05/18	0.04	2.38	2017/08/22	0.24	0.24	2017/11/23	0.70	0.69	2018/02/24	0.28	0.41
2017/05/21	0.55	0.67	2017/08/25	0.97	1.84	2017/11/26	0.10	0.37	2018/02/27	0.57	0.05
2017/05/24	0.18	1.88	2017/08/28	0.09	0.44	2017/11/29	0.17	0.22	2018/03/02	0.26	0.18
2017/05/27	1.15	2.06	2017/08/31	0.15	1.47	2017/12/02	0.71	1.03	2018/03/05	0.96	0.57
2017/05/30	0.32	1.90	2017/09/03	1.66	3.72	2017/12/05	0.00	0.13	2018/03/08	0.62	0.23
2017/06/02	0.92	2.03	2017/09/06	1.46	1.03	2017/12/08	0.50	0.87	2018/03/11	0.19	0.10
2017/06/05	0.97	1.38	2017/09/09	0.34	0.39	2017/12/11	0.24	0.91	2018/03/14	1.35	0.87
2017/06/08	1.63	1.48	2017/09/12	2.04	0.42	2017/12/14	0.53	0.61	2018/03/17	0.61	0.78
2017/06/11	0.96	1.18	2017/09/15	1.11	0.11	2017/12/17	1.34	0.76	2018/03/20	0.85	0.43
2017/06/14	0.28	0.00	2017/09/18	1.82	0.43	2017/12/20	0.41	0.00	2018/03/23	0.76	1.03
2017/06/17	3.81	4.11	2017/09/21	2.33	0.15	2017/12/23	0.62	0.66	2018/03/26	0.66	0.28
2017/06/20	2.88	5.03	2017/09/24	2.99	0.34	2017/12/26	0.15	0.55	2018/03/29	1.09	1.03
2017/06/23	4.14	5.15	2017/09/27	2.13	0.96	2017/12/29	0.36	0.03	2018/04/01	0.02	0.38
2017/06/26	2.93	5.47	2017/09/30	2.08	0.37	2018/01/01	0.92	0.75	2018/04/04	0.23	0.42
2017/06/29	0.74	0.31	2017/10/03	0.95	0.96	2018/01/04	0.36	0.53	2018/04/07	0.07	0.03
2017/07/02	0.12	0.31	2017/10/06	2.58	0.44	2018/01/07	1.24	0.94	2018/04/10	0.39	0.47
2017/07/05	0.67	0.31	2017/10/09	1.09	0.48	2018/01/10	0.37	0.91	2018/04/13	0.34	0.16
2017/07/08	2.67	1.20	2017/10/12	1.58	0.62	2018/01/13	0.71	0.35	2018/04/16	1.55	1.64
2017/07/11	1.98	4.84	2017/10/15	3.20	0.10	2018/01/16	0.92	0.42			
2017/07/14	1.18	0.89	2017/10/18	0.07	1.04	2018/01/19	1.23	0.91			
2017/07/17	0.96	0.61	2017/10/21	2.00	0.15	2018/01/22	0.94	0.98			

■ Outliers



**APPENDIX 9 - DESCRIPTIVE STATISTICS (MONTHLY DATA)**

	<b>May-17</b>	<b>Jun</b>	<b>Jul</b>	<b>Aug</b>	<b>Sept</b>	<b>Oct</b>	<b>Nov</b>	<b>Dec</b>	<b>Jan-18</b>	<b>Feb</b>	<b>Mar</b>
Sample size	10	10	9	11	10	10	10	10	11	9	10
Weekdays (%)	7 (70)	8 (80)	6 (68)	9 (82)	6 (60)	8 (80)	7 (70)	6 (60)	7 (64)	6 (67)	8 (80)
Weekend + public holidays (%)	3 (30)	2 (20)	3 (32)	2 (18)	4 (40)	2 (20)	3 (30)	4 (40)	4 (36)	3 (33)	2 (20)
Mean temperature (°C)	17.4	13.5	13.4	15.0	17.4	17.3	18.9	20.4	23.0	21.8	19.8
Mean air velocity (m.s <sup>-1</sup> )	1.3	1.3	1.7	2.2	2.5	2.5	2.9	3.5	3.2	3.0	2.2
Mean Rh (%)	69	73	74	71	71	64	67	64	67	67	70
Mean precipitation (mm)	0.1	0.9	1.6	1.9	0.5	1.3	2.5	1.8	0.3	0.1	0.8
<b>PM<sub>2.5</sub> concentration</b>											
Mean	11.2	21.4	17.8	9.92	20.8	21.6	9.71	10.2	7.74	9.59	7.94
Median	11.0	19.9	18.8	10.4	24.1	23.2	10.3	10.5	8.55	9.79	6.70
Variance	15.1	143	86.3	16.7	74.8	47.6	15.2	15.8	16.3	3.39	20.2
Standard deviation	3.89	12.0	9.29	4.09	8.65	6.90	3.89	3.97	4.04	1.84	4.49
R.S.D (%)	34.7	56.1	52.2	41.2	41.6	31.9	40.1	38.9	52.2	19.2	56.5
Standard error	1.23	3.79	3.10	1.23	2.74	2.18	1.23	1.26	1.22	0.61	1.42
95 % confidence limit (lower)	8.79	14.0	11.7	7.51	15.4	17.3	7.30	7.73	5.35	8.39	5.16
95 % confidence limit (upper)	13.6	28.8	23.9	12.3	26.2	25.9	12.1	12.7	10.1	10.8	10.7
Range	3.82- 13.8	4.52- 39.1	4.58- 33.0	5.10- 17.6	1.17- 31.3	10.6- 32.7	3.01- 16.6	1.99- 14.6	2.66- 17.0	6.22- 12.0	1.93- 16.2
WHO exceedances	0	4	2	0	4	4	0	0	0	0	14
SA NAAQS exceedances	0	0	0	0	0	0	0	0	0	0	0
<b>Absorption coefficient</b>											
Mean	2.34	2.83	2.25	1.79	1.33	0.85	0.64	0.53	0.65	0.62	0.92
Median	2.56	2.38	1.93	1.39	1.25	0.94	0.69	0.44	0.57	0.62	0.99
Variance	0.63	3.58	1.50	1.79	0.95	0.27	0.13	0.10	0.21	0.03	0.27
Standard deviation	0.79	1.89	1.22	1.34	0.98	0.52	0.36	0.32	0.46	0.17	0.52
R.S.D (%)	33.8	66.8	54.2	74.9	73.7	61.2	56.3	60.4	70.8	27.4	56.5
Standard error	0.25	0.60	0.41	0.40	0.31	0.16	0.11	0.10	0.15	0.06	0.16
95 % confidence limit (lower)	1.85	1.65	1.45	1.01	0.72	0.54	0.42	0.33	0.36	0.50	0.63
95 % confidence limit (upper)	2.83	4.00	3.05	2.57	1.94	1.16	0.86	0.73	0.94	0.74	1.21
Range	0.37- 3.39	0.00- 5.38	0.71- 4.87	0.10- 5.17	0.13- 3.97	0.12- 1.67	0.17- 1.49	0.12- 1.06	0.16- 1.70	0.40- 0.91	0.12- 1.79

PM<sub>2.5</sub> concentrations in µg.m<sup>-3</sup> and absorption coefficient values in m<sup>-1</sup>.10<sup>-5</sup>

**APPENDIX 10 - DESCRIPTIVE STATISTICS (WEEKDAY AND WEEKEND DAY DATA)**

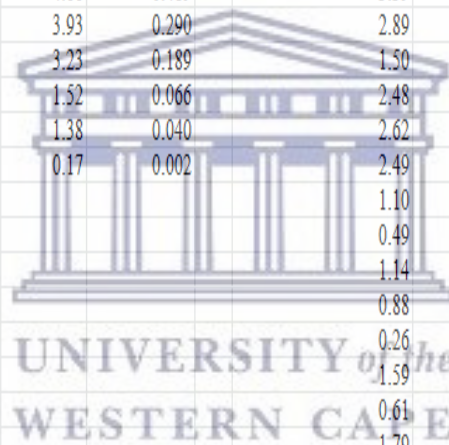
	<b>Weekday</b>	<b>Weekend day (incl. public holidays)</b>
Sample size	85	36
Percentage of total sample size	70.2	29.8
<b>PM<sub>2.5</sub> concentration</b>		
Mean	13.3	13.7
Median	11.2	10.4
Variance	57.0	91.0
Standard deviation	7.55	9.54
R.S.D (%)	56.8	69.6
Standard error	0.82	1.59
95 % confidence limit (lower)	11.7	10.6
95 % confidence limit (upper)	14.9	16.8
Range	1.17-39.1	1.99-36.9
WHO exceedances	8	6
SA NAAQS exceedances	0	0
<b>Absorption coefficient</b>		
Mean	1.41	1.24
Median	1.06	0.76
Variance	1.37	1.49
Standard deviation	1.17	1.22
R.S.D (%)	83.0	98.4
Standard error	0.13	0.20
95 % confidence limit (lower)	1.16	0.85
95 % confidence limit (upper)	1.66	1.63
Range	0.10-5.38	0.00-5.17

PM<sub>2.5</sub> concentrations in µg.m<sup>-3</sup> and absorption coefficient values in m<sup>-1</sup>.10<sup>-5</sup>



**APPENDIX 11A - SHAPIRO-WILKS NORMALITY TEST (AUTUMN)**

PM2.5 concentration	data sorted	ai	value			difference	ai*difference	Absorption coefficient	data sorted	ai	value			difference	ai*difference		
18.98	1.93	1	0.422	n	31	x31-x1	19.77	8.345	3.63	0.12	1	0.422	n	31	x31-x1	4.16	1.754
19.50	3.68	2	0.292			x30-x2	17.86	5.218	3.47	0.26	2	0.292			x30-x2	3.37	0.985
21.70	3.82	3	0.248	SS	827.03	x29-x3	15.68	3.882	4.28	0.37	3	0.248	SS	38.94	x29-x3	3.10	0.766
10.76	4.58	4	0.215	b	28.23	x28-x4	14.40	3.088	1.78	0.49	4	0.215	b	6.02	x28-x4	2.89	0.620
8.68	5.33	5	0.187	$W = b^2/SS$	0.964	x27-x5	13.54	2.537	0.54	0.54	5	0.187	$W = b^2/SS$	0.930	x27-x5	2.35	0.440
10.71	6.56	6	0.164	0.1	0.940	x26-x6	9.65	1.584	2.37	0.58	6	0.164	0.05	0.929	x26-x6	2.10	0.344
3.82	6.84	7	0.143	0.5	0.967	x25-x7	8.33	1.194	0.37	0.61	7	0.143	0.1	0.940	x25-x7	2.02	0.289
9.38	7.35	8	0.124	p-value	0.456	x24-x8	6.48	0.806	2.67	0.61	8	0.124	p-value	0.055	x24-x8	2.01	0.249
13.83	8.39	9	0.107	$\alpha$	0.05	x23-x9	5.39	0.574	2.62	0.65	9	0.107	$\alpha$	0.05	x23-x9	1.84	0.196
13.77	8.68	10	0.090	null hypothesis	do not reject	x22-x10	4.66	0.419	3.39	0.88	10	0.090	null hypothesis	do not reject	x22-x10	1.60	0.144
11.31	9.32	11	0.074			x21-x11	3.93	0.290	2.89	0.94	11	0.074			x21-x11	1.44	0.106
7.35	9.38	12	0.059			x20-x12	3.23	0.189	1.50	1.09	12	0.059			x20-x12	1.19	0.070
9.84	9.79	13	0.044			x19-x13	1.52	0.066	2.48	1.10	13	0.044			x19-x13	0.69	0.030
18.87	9.84	14	0.029			x18-x14	1.38	0.040	2.62	1.14	14	0.029			x18-x14	0.64	0.018
13.25	10.59	15	0.014			x17-x15	0.17	0.002	2.49	1.18	15	0.014			x17-x15	0.40	0.006
9.32	10.71	16	0.000						1.10	1.50	16	0.000					
4.58	10.76								0.49	1.59							
6.84	11.22								1.14	1.78							
9.79	11.31								0.88	1.79							
1.93	12.60								0.26	2.28							
15.17	13.25								1.59	2.37							
5.33	13.34								0.61	2.48							
16.22	13.77								1.79	2.49							
6.56	13.83								1.18	2.62							
3.68	15.17								0.12	2.62							
11.22	16.22								0.65	2.67							
12.60	18.87								0.61	2.89							
10.59	18.98								0.94	3.39							
8.39	19.50								0.58	3.47							
13.34	21.54								1.09	3.63							
21.54	21.70								2.28	4.28							

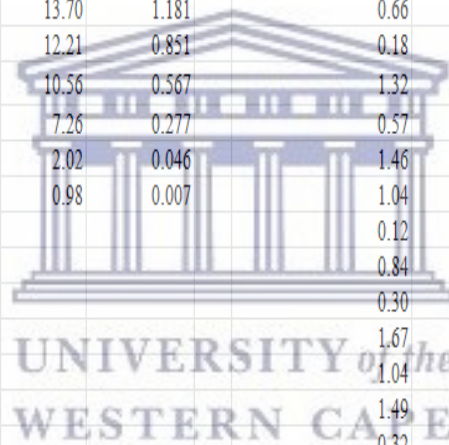


**APPENDIX 11B - SHAPIRO-WILKS NORMALITY TEST (WINTER)**

PM2.5 concentration	data sorted	ai	value			difference	ai*difference	Absorption coefficient	data sorted	ai	value			difference	ai*difference		
17.30	3.19	1	0.425	n	30	x30-x1	35.87	15.261	2.60	0.00	1	0.425	n	30	x30-x1	5.38	2.289
17.64	4.52	2	0.294			x29-x2	32.35	9.524	2.07	0.10	2	0.294			x29-x2	5.07	1.493
22.09	4.58	3	0.249	SS	3117.62	x28-x3	28.42	7.068	2.16	0.33	3	0.249	SS	66.38	x28-x3	4.70	1.168
4.52	5.10	4	0.215	b	53.14	x27-x4	25.80	5.543	0.00	0.71	4	0.215	b	7.79	x27-x4	4.16	0.895
9.15	6.04	5	0.187	$W = b^2/SS$	0.906	x26-x5	24.52	4.586	0.96	0.71	5	0.187	$W = b^2/SS$	0.915	x26-x5	3.57	0.668
36.87	6.44	6	0.163	0.01	0.900	x25-x6	22.68	3.697	4.28	0.96	6	0.163	0.02	0.912	x25-x6	2.72	0.444
30.56	6.49	7	0.142	0.02	0.912	x24-x7	17.94	2.538	5.03	0.98	7	0.142	0.05	0.927	x24-x7	1.92	0.271
39.07	6.63	8	0.122	p-value	0.015	x23-x8	15.46	1.885	2.62	1.15	8	0.122	p-value	0.026	x23-x8	1.47	0.179
30.91	8.87	9	0.104	$\alpha$	0.05	x22-x9	10.18	1.055	5.38	1.21	9	0.104	$\alpha$	0.05	x22-x9	1.38	0.143
6.04	9.15	10	0.086	null hypothesis	reject	x21-x10	9.61	0.829	0.71	1.31	10	0.086	null hypothesis	reject	x21-x10	1.13	0.098
10.25	10.25	11	0.070			x20-x11	7.39	0.515	1.21	1.39	11	0.070			x20-x11	0.97	0.068
6.49	10.43	12	0.054			x19-x12	7.18	0.385	0.71	1.45	12	0.054			x19-x12	0.88	0.047
29.11	12.08	13	0.038			x18-x13	5.22	0.199	1.93	1.68	13	0.038			x18-x13	0.48	0.018
24.43	12.34	14	0.023			x17-x14	2.14	0.048	4.87	1.78	14	0.023			x17-x14	0.37	0.008
19.05	12.69	15	0.008			x16-x15	1.04	0.008	1.68	1.93	15	0.008			x16-x15	0.15	0.001
4.58	13.73								1.45	2.07							
14.47	14.47								2.33	2.15							
18.76	17.30								2.37	2.16							
33.00	17.60								3.68	2.33							
6.44	17.64								0.33	2.37							
5.10	18.76								1.39	2.45							
12.34	19.05								2.90	2.60							
3.19	22.09								0.10	2.62							
8.87	24.43								1.78	2.90							
6.63	29.11								0.98	3.68							
13.73	30.56								5.17	4.28							
12.69	30.91								1.15	4.87							
17.60	33.00								2.45	5.03							
10.43	36.87								1.31	5.17							
12.08	39.07								2.15	5.38							

**APPENDIX 11C - SHAPIRO-WILKS NORMALITY TEST (SPRING)**

PM2.5 concentration	data sorted	ai	value			difference	ai*difference	Absorption coefficient	data sorted	ai	value			difference	ai*difference		
22.27	1.17	1	0.425	n	30	x30-x1	31.58	13.434	3.97	0.12	1	0.425	n	30	x30-x1	3.86	1.640
1.17	3.01	2	0.294			x29-x2	28.27	8.322	0.13	0.13	2	0.294			x29-x2	1.61	0.474
8.74	6.33	3	0.249	SS	2260.03	x28-x3	22.20	5.520	1.27	0.17	3	0.249	SS	16.02	x28-x3	1.50	0.372
24.88	6.42	4	0.215	b	46.30	x27-x4	20.40	4.382	1.30	0.18	4	0.215	b	3.57	x27-x4	1.32	0.283
18.57	6.89	5	0.187	$W = b^2/SS$	0.949	x26-x5	18.83	3.520	0.87	0.30	5	0.187	$W = b^2/SS$	0.798	x26-x5	1.16	0.217
23.38	8.74	6	0.163	0.1	0.939	x25-x6	16.80	2.738	1.31	0.30	6	0.163	0.01	0.900	x25-x6	1.02	0.166
26.82	9.90	7	0.142	0.5	0.967	x24-x7	15.58	2.204	0.83	0.32	7	0.142	0.01	0.900	x24-x7	0.99	0.140
31.28	10.60	8	0.122	p-value	0.243	x23-x8	14.57	1.776	1.23	0.40	8	0.122	p-value	0.010	x23-x8	0.90	0.110
25.48	10.65	9	0.104	$\alpha$	0.05	x22-x9	14.23	1.474	1.74	0.57	9	0.104	$\alpha$	0.05	x22-x9	0.70	0.072
25.17	10.90	10	0.086	null hypothesis	do not reject	x21-x10	13.70	1.181	0.66	0.66	10	0.086	null hypothesis	reject	x21-x10	0.58	0.050
17.47	11.17	11	0.070			x20-x11	12.21	0.851	0.18	0.66	11	0.070			x20-x11	0.38	0.026
28.52	11.72	12	0.054			x19-x12	10.56	0.567	1.32	0.73	12	0.054			x19-x12	0.31	0.016
18.45	14.47	13	0.038			x18-x13	7.26	0.277	0.57	0.73	13	0.038			x18-x13	0.13	0.005
21.73	16.55	14	0.023			x17-x14	2.02	0.046	1.46	0.78	14	0.023			x17-x14	0.06	0.001
32.75	17.47	15	0.008			x16-x15	0.98	0.007	1.04	0.83	15	0.008			x16-x15	0.00	0.000
10.60	18.45								0.12	0.84							
24.60	18.57								0.84	0.84							
25.54	21.73								0.30	0.87							
25.71	22.27								1.67	1.04							
10.90	23.38								1.04	1.04							
14.47	24.60								1.49	1.23							
6.42	24.88								0.32	1.27							
11.17	25.17								0.73	1.30							
16.55	25.48								0.73	1.31							
3.01	25.54								0.30	1.32							
10.65	25.71								0.84	1.46							
6.89	26.82								0.17	1.49							
6.33	28.52								0.40	1.67							
11.72	31.28								0.66	1.74							
9.90	32.75								0.78	3.97							

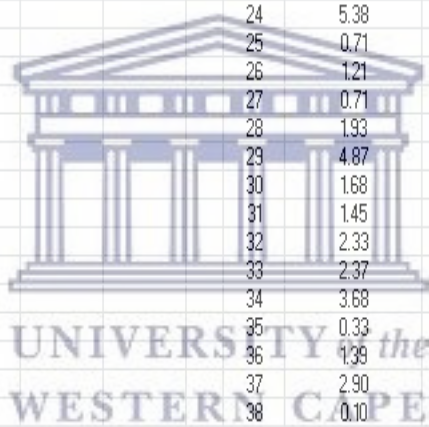


**APPENDIX 11D - SHAPIRO-WILKS NORMALITY TEST (SUMMER)**

PM2.5 concentration	data sorted	ai	value			difference	ai*difference	Absorption coefficient	data sorted	ai	value			difference	ai*difference		
6.25	1.99	1	0.425	n	30	x30-x1	15.31	6.513	0.12	0.12	1	0.425	n	30	x30-x1	1.57	0.670
11.05	2.66	2	0.294			x29-x2	11.98	3.527	1.06	0.16	2	0.294			x29-x2	1.14	0.335
14.47	2.69	3	0.249	SS	402.25	x28-x3	11.77	2.928	0.26	0.19	3	0.249	SS	3.63	x28-x3	0.87	0.216
9.43	4.69	4	0.215	b	19.85	x27-x4	9.14	1.964	0.22	0.22	4	0.215	b	1.83	x27-x4	0.74	0.160
14.64	4.80	5	0.187	$W = b^2/SS$	0.979	x26-x5	8.68	1.623	0.46	0.22	5	0.187	$W = b^2/SS$	0.923	x26-x5	0.70	0.132
1.99	6.22	6	0.163	0.5	0.967	x25-x6	5.74	0.935	0.34	0.26	6	0.163	0.02	0.912	x25-x6	0.66	0.107
13.83	6.25	7	0.142	0.9	0.983	x24-x7	5.00	0.707	0.96	0.34	7	0.142	0.05	0.927	x24-x7	0.48	0.068
6.83	6.27	8	0.122	p-value	0.800	x23-x8	4.91	0.599	0.42	0.35	8	0.122	p-value	0.042	x23-x8	0.44	0.054
10.01	6.83	9	0.104	$\alpha$	0.05	x22-x9	4.22	0.438	0.52	0.40	9	0.104	$\alpha$	0.05	x22-x9	0.33	0.035
13.48	7.22	10	0.086	null hypothesis	do not reject	x21-x10	3.72	0.320	0.93	0.42	10	0.086	null hypothesis	reject	x21-x10	0.25	0.022
4.80	8.55	11	0.070			x20-x11	2.33	0.163	0.35	0.43	11	0.070			x20-x11	0.24	0.017
8.62	8.62	12	0.054			x19-x12	1.39	0.075	0.53	0.46	12	0.054			x19-x12	0.19	0.010
2.66	8.70	13	0.038			x18-x13	1.09	0.042	0.19	0.50	13	0.038			x18-x13	0.13	0.005
8.55	9.03	14	0.023			x17-x14	0.52	0.012	1.70	0.51	14	0.023			x17-x14	0.06	0.001
6.27	9.16	15	0.008			x16-x15	0.28	0.002	0.68	0.52	15	0.008			x16-x15	0.01	0.000
17.30	9.43								1.30	0.53							
2.69	9.55								0.22	0.57							
4.69	9.79								0.16	0.62							
10.94	10.01								0.66	0.66							
9.55	10.89								0.79	0.66							
9.03	10.94								0.57	0.68							
11.25	11.05								0.50	0.74							
10.89	11.18								0.51	0.79							
11.18	11.25								0.40	0.82							
9.79	11.95								0.82	0.91							
6.22	13.48								0.66	0.93							
11.95	13.83								0.43	0.96							
8.70	14.47								0.74	1.06							
9.16	14.64								0.62	1.30							
7.22	17.30								0.91	1.70							

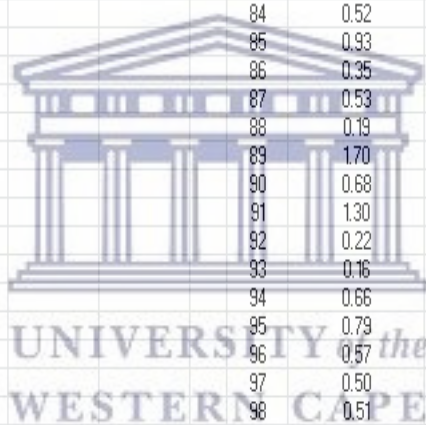
## APPENDIX 11E - SHAPIRO-WILKS NORMALITY TEST (FULL STUDY)

Index	PM2.5 concentration	data sorted	mi	ai			Index	Absorption coefficient	data sorted	mi	ai		
1	19.0	1.17	-2.565	-0.234	n	121	1	3.63	0.00	-2.565	-0.234	n	121
2	19.5	1.93	-2.214	-0.202	u	0.09	2	3.47	0.10	-2.214	-0.202	u	0.09
3	21.7	1.99	-2.021	-0.184	m	117.78	3	4.28	0.12	-2.021	-0.184	m	117.78
4	10.8	2.66	-1.882	-0.172	é	120.43	4	1.78	0.12	-1.882	-0.172	é	120.43
5	8.68	2.69	-1.773	-0.162			5	0.54	0.12	-1.773	-0.162		
6	10.7	3.01	-1.681	-0.153	W	0.92	6	2.37	0.13	-1.681	-0.153	W	0.85
7	3.82	3.19	-1.601	-0.146	mean	-4.57	7	0.37	0.16	-1.601	-0.146	mean	-4.57
8	9.38	3.68	-1.531	-0.140	sd	0.45	8	2.67	0.17	-1.531	-0.140	sd	0.45
9	13.8	3.82	-1.467	-0.134	z	4.45	9	2.62	0.18	-1.467	-0.134	z	6.02
10	13.8	4.52	-1.409	-0.128	p-value	4.22E-06	10	3.39	0.19	-1.409	-0.128	p-value	8.78E-10
11	11.3	4.58	-1.356	-0.124	α	0.05	11	2.89	0.22	-1.356	-0.124	α	0.05
12	7.35	4.58	-1.305	-0.119	null		12	1.50	0.22	-1.305	-0.119	null	
13	9.84	4.69	-1.258	-0.115	hypothesi	reject	13	2.48	0.26	-1.258	-0.115	hypothesi	reject
14	18.9	4.80	-1.214	-0.111			14	2.62	0.26	-1.214	-0.111		
15	13.3	5.10	-1.172	-0.107			15	2.49	0.30	-1.172	-0.107		
16	17.3	5.33	-1.132	-0.103			16	2.60	0.30	-1.132	-0.103		
17	17.6	6.04	-1.093	-0.100			17	2.07	0.32	-1.093	-0.100		
18	22.1	6.22	-1.057	-0.096			18	2.16	0.33	-1.057	-0.096		
19	4.52	6.25	-1.021	-0.093			19	0.00	0.34	-1.021	-0.093		
20	9.15	6.27	-0.987	-0.090			20	0.96	0.35	-0.987	-0.090		
21	36.9	6.33	-0.954	-0.087			21	4.28	0.37	-0.954	-0.087		
22	30.6	6.42	-0.922	-0.084			22	5.03	0.40	-0.922	-0.084		
23	39.1	6.44	-0.891	-0.081			23	2.62	0.40	-0.891	-0.081		
24	30.9	6.49	-0.860	-0.078			24	5.38	0.42	-0.860	-0.078		
25	6.04	6.56	-0.831	-0.076			25	0.71	0.43	-0.831	-0.076		
26	10.2	6.63	-0.802	-0.073			26	1.21	0.46	-0.802	-0.073		
27	6.49	6.83	-0.774	-0.070			27	0.71	0.49	-0.774	-0.070		
28	29.1	6.84	-0.746	-0.068			28	1.93	0.50	-0.746	-0.068		
29	24.4	6.89	-0.719	-0.066			29	4.87	0.51	-0.719	-0.066		
30	19.0	7.22	-0.692	-0.063			30	1.68	0.52	-0.692	-0.063		
31	4.58	7.35	-0.666	-0.061			31	1.45	0.53	-0.666	-0.061		
32	14.5	8.39	-0.641	-0.058			32	2.33	0.54	-0.641	-0.058		
33	18.8	8.55	-0.616	-0.056			33	2.37	0.57	-0.616	-0.056		
34	33.0	8.62	-0.591	-0.054			34	3.68	0.57	-0.591	-0.054		
35	6.44	8.68	-0.566	-0.052			35	0.33	0.58	-0.566	-0.052		
36	5.10	8.70	-0.542	-0.049			36	1.99	0.61	-0.542	-0.049		
37	12.3	8.74	-0.518	-0.047			37	2.90	0.61	-0.518	-0.047		
38	3.19	8.87	-0.495	-0.045			38	0.10	0.62	-0.495	-0.045		
39	8.87	9.03	-0.472	-0.043			39	1.78	0.65	-0.472	-0.043		
40	6.63	9.15	-0.449	-0.041			40	0.98	0.66	-0.449	-0.041		
41	13.7	9.16	-0.426	-0.039			41	5.17	0.66	-0.426	-0.039		
42	12.7	9.32	-0.403	-0.037			42	1.15	0.66	-0.403	-0.037		
43	17.6	9.38	-0.381	-0.035			43	2.45	0.66	-0.381	-0.035		
44	10.4	9.43	-0.359	-0.033			44	1.31	0.68	-0.359	-0.033		
45	12.1	9.55	-0.337	-0.031			45	2.15	0.71	-0.337	-0.031		
46	22.3	9.79	-0.315	-0.029			46	3.97	0.71	-0.315	-0.029		
47	1.17	9.79	-0.294	-0.027			47	0.13	0.73	-0.294	-0.027		
48	8.74	9.84	-0.272	-0.025			48	1.27	0.73	-0.272	-0.025		
49	24.9	9.90	-0.251	-0.023			49	1.30	0.74	-0.251	-0.023		
50	18.6	10.0	-0.229	-0.021			50	0.87	0.78	-0.229	-0.021		
51	23.4	10.2	-0.208	-0.019			51	1.31	0.79	-0.208	-0.019		
52	26.8	10.4	-0.187	-0.017			52	0.83	0.82	-0.187	-0.017		
53	31.3	10.6	-0.166	-0.015			53	1.23	0.83	-0.166	-0.015		
54	25.5	10.6	-0.145	-0.013			54	1.74	0.84	-0.145	-0.013		
55	25.2	10.6	-0.124	-0.011			55	0.66	0.84	-0.124	-0.011		
56	17.5	10.7	-0.104	-0.009			56	0.18	0.87	-0.104	-0.009		
57	28.5	10.8	-0.083	-0.008			57	1.32	0.88	-0.083	-0.008		
58	18.5	10.9	-0.062	-0.006			58	0.57	0.91	-0.062	-0.006		
59	21.7	10.9	-0.041	-0.004			59	1.46	0.93	-0.041	-0.004		
60	32.7	10.9	-0.021	-0.002			60	1.04	0.94	-0.021	-0.002		
61	10.6	11.1	0.000	0.000			61	0.12	0.96	0.000	0.000		



## APPENDIX 11E - SHAPIRO-WILKS NORMALITY TEST (FULL STUDY)

Index	PM2.5 concentration	data sorted	mi	ai			Index	Absorption coefficient	data sorted	mi	ai		
61	10.6	11.1	0.000	0.000	n	121	61	0.12	0.96	0.000	0.000	n	121
62	24.6	11.2	0.021	0.002	u	0.09	62	0.84	0.96	0.021	0.002	u	0.09
63	25.5	11.2	0.041	0.004	m	117.78	63	0.30	0.98	0.041	0.004	m	117.78
64	25.7	11.2	0.062	0.006	é	120.43	64	1.67	1.04	0.062	0.006	é	120.43
65	10.9	11.2	0.083	0.008			65	1.04	1.04	0.083	0.008		
66	14.5	11.3	0.104	0.009	w	0.92	66	1.49	1.06	0.104	0.009	w	0.85
67	6.42	11.7	0.124	0.011	mean	-4.57	67	0.32	1.09	0.124	0.011	mean	-4.57
68	11.2	12.0	0.145	0.013	sd	0.45	68	0.73	1.10	0.145	0.013	sd	0.45
69	16.6	12.1	0.166	0.015	z	4.45	69	0.73	1.14	0.166	0.015	z	6.02
70	3.01	12.3	0.187	0.017	p-value	4.22E-06	70	0.30	1.15	0.187	0.017	p-value	8.78E-10
71	10.6	12.6	0.208	0.019	a	0.05	71	0.84	1.18	0.208	0.019	a	0.05
72	6.89	12.7	0.229	0.021	null hypothesis	reject	72	0.17	1.21	0.229	0.021	null hypothesis	reject
73	6.33	13.3	0.251	0.023			73	0.40	1.23	0.251	0.023		
74	11.7	13.3	0.272	0.025			74	0.66	1.27	0.272	0.025		
75	9.90	13.5	0.294	0.027			75	0.78	1.30	0.294	0.027		
76	6.25	13.7	0.315	0.029			76	0.12	1.30	0.315	0.029		
77	11.1	13.8	0.337	0.031			77	1.06	1.31	0.337	0.031		
78	14.5	13.8	0.359	0.033			78	0.26	1.31	0.359	0.033		
79	9.43	13.8	0.381	0.035			79	0.22	1.32	0.381	0.035		
80	14.6	14.5	0.403	0.037			80	0.46	1.39	0.403	0.037		
81	1.99	14.5	0.426	0.039			81	0.34	1.45	0.426	0.039		
82	13.8	14.5	0.449	0.041			82	0.96	1.46	0.449	0.041		
83	6.83	14.6	0.472	0.043			83	0.42	1.49	0.472	0.043		
84	10.0	15.2	0.495	0.045			84	0.52	1.50	0.495	0.045		
85	13.5	16.2	0.518	0.047			85	0.93	1.59	0.518	0.047		
86	4.80	16.6	0.542	0.049			86	0.35	1.67	0.542	0.049		
87	8.62	17.3	0.566	0.052			87	0.53	1.68	0.566	0.052		
88	2.66	17.3	0.591	0.054			88	0.19	1.70	0.591	0.054		
89	8.55	17.5	0.616	0.056			89	1.70	1.74	0.616	0.056		
90	6.27	17.6	0.641	0.058			90	0.68	1.78	0.641	0.058		
91	17.3	17.6	0.666	0.061			91	1.30	1.78	0.666	0.061		
92	2.69	18.5	0.692	0.063			92	0.22	1.79	0.692	0.063		
93	4.69	18.6	0.719	0.066			93	0.16	1.93	0.719	0.066		
94	10.9	18.8	0.746	0.068			94	0.66	2.07	0.746	0.068		
95	9.55	18.9	0.774	0.070			95	0.79	2.15	0.774	0.070		
96	9.03	19.0	0.802	0.073			96	0.57	2.16	0.802	0.073		
97	11.2	19.0	0.831	0.076			97	0.50	2.28	0.831	0.076		
98	10.9	19.5	0.860	0.078			98	0.51	2.33	0.860	0.078		
99	11.2	21.5	0.891	0.081			99	0.40	2.37	0.891	0.081		
100	9.79	21.7	0.922	0.084			100	0.82	2.37	0.922	0.084		
101	6.22	21.7	0.954	0.087			101	0.66	2.45	0.954	0.087		
102	12.0	22.1	0.987	0.090			102	0.43	2.48	0.987	0.090		
103	8.70	22.3	1.021	0.093			103	0.74	2.49	1.021	0.093		
104	9.16	23.4	1.057	0.096			104	0.62	2.60	1.057	0.096		
105	7.22	24.4	1.093	0.100			105	0.91	2.62	1.093	0.100		
106	9.32	24.6	1.132	0.103			106	1.10	2.62	1.132	0.103		
107	4.58	24.9	1.172	0.107			107	0.49	2.62	1.172	0.107		
108	6.84	25.2	1.214	0.111			108	1.14	2.67	1.214	0.111		
109	9.79	25.5	1.258	0.115			109	0.88	2.89	1.258	0.115		
110	1.93	25.5	1.305	0.119			110	0.26	2.90	1.305	0.119		
111	15.2	25.7	1.356	0.124			111	1.59	3.39	1.356	0.124		
112	5.33	26.8	1.409	0.128			112	0.61	3.47	1.409	0.128		
113	16.2	28.5	1.467	0.134			113	1.79	3.63	1.467	0.134		
114	6.56	29.1	1.531	0.140			114	1.18	3.68	1.531	0.140		
115	3.68	30.6	1.601	0.146			115	0.12	3.97	1.601	0.146		
116	11.2	30.9	1.681	0.153			116	0.65	4.28	1.681	0.153		
117	12.6	31.3	1.773	0.162			117	0.61	4.28	1.773	0.162		
118	10.6	32.7	1.882	0.172			118	0.94	4.87	1.882	0.172		
119	8.39	33.0	2.021	0.184			119	0.58	5.03	2.021	0.184		
120	13.3	36.9	2.214	0.205			120	1.09	5.17	2.214	0.205		
121	21.5	39.1	2.565	0.254			121	2.28	5.38	2.565	0.254		





## APPENDIX 12 - TRAJECTORY CLUSTERS AND CORRESPONDING SAMPLING DATES

	CLUSTER			
	1	2	3	4
<b>Autumn</b>	2017/04/18	2017/04/24	2017/04/27	2017/05/06
	2017/04/21	2017/04/30	2017/05/09	2018/05/08
	2018/03/02	2017/05/03	2017/05/12	2018/03/20
	2018/03/05	2017/05/15	2017/05/18	2018/03/26
	2018/03/23	2017/05/21	2017/05/24	2018/04/07
	2018/04/01	2017/05/30	2017/05/27	
	2018/04/04	2018/04/16	2018/03/11	
	2018/04/13		2018/03/14	
			2018/03/17	
			2018/03/29	
			2018/04/10	
<b>Winter</b>	2017/06/02	2017/07/05	2017/06/17	2017/06/08
	2017/06/05	2018/08/28	2017/07/08	2017/06/11
	2017/06/14		2017/07/20	2017/06/20
	2017/06/26		2017/08/01	2017/06/23
	2017/06/29			2017/07/11
	2017/07/02			2017/07/17
	2017/07/14			2017/07/26
	2017/07/23			2017/08/13
	2017/07/29			2017/08/16
	2017/08/04			2017/08/22
	2017/08/07			2017/08/25
	2017/08/10			
	2018/08/19			
	2018/08/31			
<b>Spring</b>	2017/09/03	2017/09/06	2017/09/09	
	2017/09/15	2017/09/12	2017/09/27	
	2017/09/18	2017/10/06	2017/09/30	
	2017/09/21	2017/10/21	2017/10/12	
	2017/09/24	2017/10/24	2017/10/27	
	2017/10/03	2017/11/05	2017/11/23	
	2017/10/09	2017/11/20	2017/11/26	
	2017/10/15			
	2017/10/18			
	2017/10/30			
	2017/11/02			
	2017/11/08			
	2017/11/11			
	2017/11/14			
	2017/11/17			
	2017/11/29			
<b>Summer</b>	2017/12/02	2017/12/05	2017/12/20	2017/12/14
	2017/12/08	2017/12/11	2018/01/07	2017/12/17
	2017/12/29	2017/12/23		2017/12/26
	2018/01/04	2018/01/13		2018/01/01
	2018/01/19	2018/01/25		2018/01/10
	2018/01/22	2018/01/28		2018/01/16
	2018/02/09	2018/02/06		2018/01/31
	2018/02/12	2018/02/18		2018/02/03
	2018/02/15			2018/02/24
	2018/02/21			
	2018/02/27			

■ Duplicate sampling days

**APPENDIX 13A - AIR POLLUTION DATA FROM THE ATLANTIS AAQM STATION**

Date	SO <sub>2</sub>	O <sub>3</sub>	Date	SO <sub>2</sub>	O <sub>3</sub>	Date	SO <sub>2</sub>	O <sub>3</sub>
2017/04/18	3.76	47.6	2017/08/22	*	*	2017/12/23	0.00	*
2017/04/21	3.71	59.7	2017/08/25	*	*	2017/12/26	2.16	*
2017/04/24	3.88	54.3	2017/08/28	2.99	47.7	2017/12/29	2.32	*
2017/04/27	1.80	42.5	2017/08/31	1.32	56.6	2018/01/01	4.40	*
2017/04/30	1.12	45.5	2017/09/03	4.56	51.1	2018/01/04	0.60	*
2017/05/03	1.00	45.4	2017/09/06	4.68	72.9	2018/01/07	1.44	*
2017/05/06	1.00	49.5	2017/09/09	1.84	53.9	2018/01/10	0.64	*
2017/05/09	7.44	47.0	2017/09/12	3.68	50.6	2018/01/13	3.04	*
2017/05/12	1.00	65.0	2017/09/15	4.28	60.8	2018/01/16	3.88	*
2017/05/15	*	*	2017/09/18	3.20	55.0	2018/01/19	7.92	*
2017/05/18	*	*	2017/09/21	6.58	58.8	2018/01/22	3.18	37.4
2017/05/21	*	*	2017/09/24	1.18	54.7	2018/01/25	0.64	32.8
2017/05/24	*	*	2017/09/27	3.24	*	2018/01/28	7.00	38.4
2017/05/27	*	*	2017/09/30	5.96	*	2018/01/31	2.62	41.8
2017/05/30	*	*	2017/10/03	5.05	56.5	2018/02/03	2.67	38.6
2017/06/02	*	*	2017/10/06	1.40	56.7	2018/02/06	*	46.7
2017/06/05	*	*	2017/10/09	4.13	51.5	2018/02/09	*	28.3
2017/06/08	*	*	2017/10/12	4.00	47.2	2018/02/12	1.00	30.8
2017/06/11	*	*	2017/10/15	1.00	56.2	2018/02/15	1.44	48.7
2017/06/14	2.40	*	2017/10/18	*	51.7	2018/02/18	3.16	41.3
2017/06/17	2.28	*	2017/10/21	*	54.9	2018/02/21	2.16	33.9
2017/06/20	5.56	*	2017/10/24	*	53.4	2018/02/24	4.20	37.0
2017/06/23	7.09	41.9	2017/10/27	0.57	48.4	2018/02/27	2.04	51.6
2017/06/26	7.80	29.1	2017/10/30	0.46	52.2	2018/03/02	3.48	40.8
2017/06/29	2.84	52.4	2017/11/02	1.28	94.3	2018/03/05	2.12	36.9
2017/07/02	2.80	43.4	2017/11/05	2.33	66.5	2018/03/08	5.32	37.3
2017/07/05	*	49.9	2017/11/08	3.54	48.2	2018/03/11	*	*
2017/07/08	*	*	2017/11/11	1.13	64.8	2018/03/14	3.43	26.9
2017/07/11	*	*	2017/11/14	0.67	83.3	2018/03/17	2.16	41.3
2017/07/14	2.57	37.7	2017/11/17	5.44	52.2	2018/03/20	3.96	40.0
2017/07/17	2.84	60.0	2017/11/20	2.48	51.0	2018/03/23	3.04	40.3
2017/07/20	3.28	52.1	2017/11/23	1.42	46.7	2018/03/26	4.92	42.9
2017/07/26	5.21	49.0	2017/11/26	6.05	39.0	2018/03/29	3.84	38.9
2017/07/29	2.32	60.2	2017/11/29	2.00	46.5	2018/04/01	1.16	35.4
2017/08/01	2.44	53.5	2017/12/02	5.54	43.8	2018/04/04	1.58	64.3
2017/08/04	*	*	2017/12/05	2.80	61.8	2018/04/07	0.77	23.6
2017/08/07	3.00	46.8	2017/12/08	2.40	56.7	2018/04/10	1.27	24.6
2017/08/10	6.17	37.0	2017/12/11	2.28	54.8	2018/04/13	*	*
2017/08/13	0.92	62.6	2017/12/14	7.20	51.7	2018/04/16	*	*
2017/08/16	3.58	50.7	2017/12/17	*	*	<b>Mean</b>	<b>3.08</b>	<b>48.7</b>
2017/08/19	4.88	50.2	2017/12/20	*	*	<b>σ</b>	<b>1.88</b>	<b>11.7</b>

Concentrations in µg.m<sup>-3</sup>

\* No data

## APPENDIX 13B - AIR POLLUTION DATA FROM THE CITY HALL AAQM STATION

Date	NO <sub>2</sub>	SO <sub>2</sub>	CO	Date	NO <sub>2</sub>	SO <sub>2</sub>	CO	Date	NO <sub>2</sub>	SO <sub>2</sub>	CO
2017/04/18	*	*	*	2017/08/22	36.2	1.75	*	2017/12/23	40.0	6.00	*
2017/04/21	69.8	10.0	4.59	2017/08/25	31.8	0.56	*	2017/12/26	19.8	5.48	*
2017/04/24	56.1	10.0	4.42	2017/08/28	26.0	3.07	*	2017/12/29	28.0	7.76	*
2017/04/27	38.2	5.60	3.62	2017/08/31	36.1	4.12	*	2018/01/01	42.2	15.4	*
2017/04/30	19.1	4.32	3.15	2017/09/03	34.3	2.28	*	2018/01/04	16.2	2.20	0.00
2017/05/03	36.8	5.28	3.51	2017/09/06	51.1	5.08	*	2018/01/07	29.6	4.96	*
2017/05/06	26.6	5.60	3.02	2017/09/09	23.2	1.40	*	2018/01/10	14.8	0.76	*
2017/05/09	39.9	7.00	3.53	2017/09/12	*	*	*	2018/01/13	49.8	12.2	0.20
2017/05/12	37.6	6.12	3.51	2017/09/15	28.9	1.35	*	2018/01/16	20.3	2.96	*
2017/05/15	49.9	6.96	4.24	2017/09/18	9.78	0.43	*	2018/01/19	36.5	3.24	*
2017/05/18	49.8	8.44	3.42	2017/09/21	32.1	2.16	*	2018/01/22	11.7	1.00	*
2017/05/21	42.3	7.92	3.28	2017/09/24	27.2	1.72	*	2018/01/25	17.5	1.04	*
2017/05/24	43.6	8.28	3.15	2017/09/27	18.4	1.32	0.40	2018/01/28	21.1	*	*
2017/05/27	34.4	6.84	2.70	2017/09/30	28.1	1.84	0.34	2018/01/31	26.5	*	*
2017/05/30	43.2	8.04	3.55	2017/10/03	30.6	2.04	0.16	2018/02/03	25.1	*	*
2017/06/02	50.3	8.91	3.67	2017/10/06	21.8	0.84	0.21	2018/02/06	19.6	*	*
2017/06/05	*	*	*	2017/10/09	33.6	1.92	0.21	2018/02/09	20.6	*	*
2017/06/08	*	*	*	2017/10/12	16.1	1.60	0.14	2018/02/12	19.0	*	*
2017/06/11	15.4	0.88	1.54	2017/10/15	25.1	3.84	0.32	2018/02/15	26.6	*	*
2017/06/14	25.6	2.00	1.33	2017/10/18	19.6	1.12	0.28	2018/02/18	25.0	*	*
2017/06/17	28.7	3.12	1.71	2017/10/21	25.0	1.68	0.28	2018/02/21	17.9	*	*
2017/06/20	33.4	2.32	1.93	2017/10/24	28.7	2.46	0.20	2018/02/24	30.4	*	*
2017/06/23	38.2	3.56	2.18	2017/10/27	23.1	1.32	0.15	2018/02/27	12.2	*	*
2017/06/26	40.3	4.28	3.09	2017/10/30	30.5	1.96	0.28	2018/03/02	38.4	*	*
2017/06/29	30.9	1.12	1.45	2017/11/02	49.9	4.09	0.19	2018/03/05	35.6	*	0.16
2017/07/02	24.0	0.64	1.71	2017/11/05	44.0	1.84	0.18	2018/03/08	23.5	*	0.08
2017/07/05	39.2	2.32	3.71	2017/11/08	10.0	1.12	0.12	2018/03/11	22.2	*	0.10
2017/07/08	20.7	1.00	3.25	2017/11/11	32.8	5.44	0.36	2018/03/14	22.1	*	0.11
2017/07/11	24.0	1.00	3.50	2017/11/14	24.4	2.12	0.06	2018/03/17	35.3	*	0.15
2017/07/14	*	*	*	2017/11/17	16.0	2.00	0.21	2018/03/20	30.1	*	0.20
2017/07/17	*	*	*	2017/11/20	33.3	3.84	0.15	2018/03/23	26.3	*	0.13
2017/07/20	*	*	*	2017/11/23	22.0	2.16	0.11	2018/03/26	36.7	*	*
2017/07/26	30.8	1.22	*	2017/11/26	19.5	3.25	0.05	2018/03/29	39.4	*	*
2017/07/29	38.5	1.71	*	2017/11/29	10.7	2.28	0.12	2018/04/01	26.3	*	*
2017/08/01	35.3	1.52	*	2017/12/02	25.0	3.60	0.16	2018/04/04	*	*	*
2017/08/04	27.8	0.44	*	2017/12/05	14.4	3.32	*	2018/04/07	*	*	*
2017/08/07	19.2	0.80	*	2017/12/08	18.2	3.44	*	2018/04/10	*	*	*
2017/08/10	40.7	1.08	*	2017/12/11	27.8	4.00	*	2018/04/13	*	*	*
2017/08/13	30.1	0.10	*	2017/12/14	17.4	3.48	*	2018/04/16	*	*	*
2017/08/16	21.7	0.44	*	2017/12/17	34.6	8.68	*	<b>Mean</b>	<b>29.2</b>	<b>3.53</b>	<b>1.46</b>
2017/08/19	29.5	0.67	*	2017/12/20	9.39	4.00	*	<b>σ</b>	<b>10.9</b>	<b>2.95</b>	<b>1.54</b>

NO<sub>2</sub>/SO<sub>2</sub> concentrations in µg.m<sup>-3</sup>, CO in mg.m<sup>-3</sup>

\* No data

## APPENDIX 13C - AIR POLLUTION DATA FROM THE GOODWOOD AAQM STATION

Date	NO <sub>2</sub>	SO <sub>2</sub>	Date	NO <sub>2</sub>	SO <sub>2</sub>	Date	NO <sub>2</sub>	SO <sub>2</sub>
2017/04/18	*	*	2017/08/22	36.2	17.0	2017/12/23	23.0	*
2017/04/21	*	*	2017/08/25	18.6	5.29	2017/12/26	21.9	*
2017/04/24	*	*	2017/08/28	23.1	6.36	2017/12/29	15.4	*
2017/04/27	*	*	2017/08/31	26.0	12.6	2018/01/01	24.6	*
2017/04/30	*	*	2017/09/03	28.0	13.3	2018/01/04	22.9	2.00
2017/05/03	*	*	2017/09/06	*	13.5	2018/01/07	19.6	7.70
2017/05/06	*	*	2017/09/09	*	4.04	2018/01/10	20.2	1.80
2017/05/09	*	*	2017/09/12	15.7	6.56	2018/01/13	30.0	2.50
2017/05/12	*	*	2017/09/15	*	*	2018/01/16	16.4	1.00
2017/05/15	*	*	2017/09/18	*	*	2018/01/19	22.5	*
2017/05/18	*	*	2017/09/21	*	*	2018/01/22	16.8	*
2017/05/21	*	*	2017/09/24	*	*	2018/01/25	20.6	*
2017/05/24	*	*	2017/09/27	*	*	2018/01/28	18.9	2.20
2017/05/27	*	*	2017/09/30	*	*	2018/01/31	22.7	2.97
2017/05/30	*	*	2017/10/03	*	*	2018/02/03	21.7	2.64
2017/06/02	*	*	2017/10/06	*	*	2018/02/06	18.2	2.12
2017/06/05	*	*	2017/10/09	*	*	2018/02/09	*	*
2017/06/08	38.3	16.8	2017/10/12	*	*	2018/02/12	23.3	*
2017/06/11	12.4	6.08	2017/10/15	*	*	2018/02/15	27.5	*
2017/06/14	32.6	19.9	2017/10/18	*	*	2018/02/18	16.8	*
2017/06/17	35.4	20.1	2017/10/21	*	*	2018/02/21	19.2	*
2017/06/20	43.0	25.1	2017/10/24	*	*	2018/02/24	18.7	*
2017/06/23	46.8	29.1	2017/10/27	*	*	2018/02/27	18.8	*
2017/06/26	42.0	26.0	2017/10/30	*	*	2018/03/02	18.4	*
2017/06/29	25.1	16.2	2017/11/02	*	*	2018/03/05	21.8	3.60
2017/07/02	26.8	*	2017/11/05	*	*	2018/03/08	16.9	2.60
2017/07/05	47.9	*	2017/11/08	*	*	2018/03/11	*	5.72
2017/07/08	14.6	9.52	2017/11/11	*	*	2018/03/14	*	4.92
2017/07/11	25.4	14.0	2017/11/14	31.0	*	2018/03/17	20.9	3.56
2017/07/14	26.6	12.5	2017/11/17	31.0	*	2018/03/20	*	3.48
2017/07/17	27.1	9.00	2017/11/20	43.2	*	2018/03/23	*	5.36
2017/07/20	30.7	12.7	2017/11/23	32.0	*	2018/03/26	*	5.28
2017/07/26	21.6	9.00	2017/11/26	35.4	*	2018/03/29	*	9.48
2017/07/29	36.8	15.8	2017/11/29	24.3	*	2018/04/01	*	*
2017/08/01	21.1	10.4	2017/12/02	26.4	*	2018/04/04	*	*
2017/08/04	15.3	2.64	2017/12/05	18.6	*	2018/04/07	*	6.29
2017/08/07	20.5	3.84	2017/12/08	26.6	*	2018/04/10	*	6.76
2017/08/10	18.5	4.32	2017/12/11	29.6	*	2018/04/13	*	7.28
2017/08/13	12.0	2.00	2017/12/14	21.1	*	2018/04/16	*	6.64
2017/08/16	18.6	6.24	2017/12/17	23.0	*	<b>Mean</b>	<b>24.8</b>	<b>8.67</b>
2017/08/19	25.8	5.08	2017/12/20	17.7	*	<b>σ</b>	<b>8.11</b>	<b>6.68</b>

Concentrations in  $\mu\text{g}\cdot\text{m}^{-3}$

\* No data

## APPENDIX 13C - AIR POLLUTION DATA FROM THE GOODWOOD AAQM STATION

Date	O <sub>3</sub>	CO	Date	SO <sub>2</sub>	O <sub>3</sub>	Date	SO <sub>2</sub>	O <sub>3</sub>
2017/04/18	*	*	2017/08/22	19.1	1.52	2017/12/23	*	*
2017/04/21	*	*	2017/08/25	35.5	1.04	2017/12/26	*	*
2017/04/24	*	*	2017/08/28	27.7	1.41	2017/12/29	*	*
2017/04/27	*	*	2017/08/31	33.4	1.32	2018/01/01	*	*
2017/04/30	*	*	2017/09/03	25.3	1.77	2018/01/04	*	*
2017/05/03	*	*	2017/09/06	31.7	1.89	2018/01/07	*	*
2017/05/06	*	0.13	2017/09/09	41.0	1.25	2018/01/10	*	*
2017/05/09	*	1.00	2017/09/12	35.6	1.50	2018/01/13	*	*
2017/05/12	*	*	2017/09/15	*	*	2018/01/16	*	*
2017/05/15	*	*	2017/09/18	*	*	2018/01/19	*	*
2017/05/18	*	*	2017/09/21	*	*	2018/01/22	18.8	*
2017/05/21	*	*	2017/09/24	*	*	2018/01/25	21.0	*
2017/05/24	14.3	1.12	2017/09/27	*	*	2018/01/28	25.4	*
2017/05/27	25.2	0.81	2017/09/30	*	*	2018/01/31	26.0	*
2017/05/30	19.5	1.82	2017/10/03	*	*	2018/02/03	24.8	*
2017/06/02	20.0	1.34	2017/10/06	*	*	2018/02/06	30.9	*
2017/06/05	24.1	1.48	2017/10/09	*	*	2018/02/09	18.3	*
2017/06/08	17.3	2.03	2017/10/12	*	*	2018/02/12	20.9	*
2017/06/11	37.6	0.36	2017/10/15	*	*	2018/02/15	23.8	*
2017/06/14	25.2	1.14	2017/10/18	*	*	2018/02/18	23.4	*
2017/06/17	26.7	1.31	2017/10/21	*	*	2018/02/21	24.3	*
2017/06/20	19.9	1.63	2017/10/24	*	*	2018/02/24	25.0	*
2017/06/23	21.7	1.76	2017/10/27	*	*	2018/02/27	29.4	*
2017/06/26	17.0	1.10	2017/10/30	*	*	2018/03/02	28.7	*
2017/06/29	36.1	0.28	2017/11/02	*	*	2018/03/05	29.8	*
2017/07/02	23.8	0.63	2017/11/05	*	*	2018/03/08	24.2	*
2017/07/05	20.4	0.98	2017/11/08	*	*	2018/03/11	24.9	*
2017/07/08	35.8	0.29	2017/11/11	*	*	2018/03/14	25.2	*
2017/07/11	30.6	0.51	2017/11/14	*	*	2018/03/17	30.9	*
2017/07/14	27.9	0.60	2017/11/17	*	*	2018/03/20	30.7	*
2017/07/17	32.0	0.67	2017/11/20	*	*	2018/03/23	27.2	*
2017/07/20	16.8	1.24	2017/11/23	*	*	2018/03/26	28.2	*
2017/07/26	25.7	1.34	2017/11/26	*	*	2018/03/29	28.8	*
2017/07/29	19.3	2.14	2017/11/29	*	*	2018/04/01	*	*
2017/08/01	32.9	0.90	2017/12/02	*	*	2018/04/04	*	*
2017/08/04	34.7	0.73	2017/12/05	*	*	2018/04/07	*	*
2017/08/07	34.4	0.99	2017/12/08	*	*	2018/04/10	*	*
2017/08/10	34.6	0.86	2017/12/11	*	*	2018/04/13	*	*
2017/08/13	41.4	0.83	2017/12/14	*	*	2018/04/16	*	*
2017/08/16	35.2	1.38	2017/12/17	*	*	<b>Mean</b>	<b>27.0</b>	<b>1.13</b>
2017/08/19	29.4	1.07	2017/12/20	*	*	<b>σ</b>	<b>6.30</b>	<b>0.49</b>

O<sub>3</sub> concentrations in µg.m<sup>-3</sup>, CO in mg.m<sup>-3</sup>

\* No data

**APPENDIX 13D - AIR POLLUTION DATA FROM THE SOMERSET-WEST AAQM STATION**

Date	NO <sub>2</sub>	Date	NO <sub>2</sub>	Date	NO <sub>2</sub>
2017/04/18	5.92	2017/08/22	2.76	2017/12/23	1.64
2017/04/21	5.84	2017/08/25	2.80	2017/12/26	2.25
2017/04/24	7.24	2017/08/28	2.51	2017/12/29	2.20
2017/04/27	2.80	2017/08/31	3.48	2018/01/01	2.58
2017/04/30	3.48	2017/09/03	3.18	2018/01/04	3.38
2017/05/03	3.52	2017/09/06	2.32	2018/01/07	3.24
2017/05/06	3.08	2017/09/09	2.60	2018/01/10	2.48
2017/05/09	2.92	2017/09/12	1.71	2018/01/13	2.00
2017/05/12	3.36	2017/09/15	1.92	2018/01/16	3.40
2017/05/15	4.28	2017/09/18	3.84	2018/01/19	*
2017/05/18	2.96	2017/09/21	3.57	2018/01/22	*
2017/05/21	2.16	2017/09/24	3.88	2018/01/25	*
2017/05/24	2.56	2017/09/27	*	2018/01/28	3.05
2017/05/27	2.80	2017/09/30	*	2018/01/31	3.05
2017/05/30	4.92	2017/10/03	*	2018/02/03	2.88
2017/06/02	4.84	2017/10/06	*	2018/02/06	2.80
2017/06/05	3.64	2017/10/09	*	2018/02/09	3.20
2017/06/08	3.28	2017/10/12	*	2018/02/12	3.04
2017/06/11	3.44	2017/10/15	4.65	2018/02/15	3.60
2017/06/14	3.24	2017/10/18	3.00	2018/02/18	3.57
2017/06/17	2.92	2017/10/21	2.56	2018/02/21	3.28
2017/06/20	*	2017/10/24	1.67	2018/02/24	2.87
2017/06/23	*	2017/10/27	2.60	2018/02/27	3.46
2017/06/26	*	2017/10/30	4.08	2018/03/02	2.81
2017/06/29	*	2017/11/02	2.52	2018/03/05	1.00
2017/07/02	*	2017/11/05	1.64	2018/03/08	1.72
2017/07/05	1.94	2017/11/08	1.54	2018/03/11	1.20
2017/07/08	3.64	2017/11/11	0.95	2018/03/14	1.24
2017/07/11	3.16	2017/11/14	1.52	2018/03/17	0.80
2017/07/14	2.48	2017/11/17	1.68	2018/03/20	2.32
2017/07/17	3.04	2017/11/20	1.17	2018/03/23	1.60
2017/07/20	4.04	2017/11/23	2.44	2018/03/26	2.91
2017/07/26	2.68	2017/11/26	*	2018/03/29	2.24
2017/07/29	2.96	2017/11/29	*	2018/04/01	1.38
2017/08/01	3.52	2017/12/02	*	2018/04/04	2.23
2017/08/04	3.68	2017/12/05	2.40	2018/04/07	1.84
2017/08/07	3.64	2017/12/08	3.13	2018/04/10	1.96
2017/08/10	3.08	2017/12/11	2.68	2018/04/13	2.61
2017/08/13	3.72	2017/12/14	3.68	2018/04/16	1.87
2017/08/16	3.24	2017/12/17	2.43	<b>Mean</b>	<b>2.87</b>
2017/08/19	3.16	2017/12/20	2.54	<b>σ</b>	<b>1.03</b>

Concentrations in  $\mu\text{g.m}^{-3}$

\* No data

**APPENDIX 13E - AIR POLLUTION DATA FROM THE TABLEVIEW AAQM STATION**

Date	NO <sub>2</sub>	SO <sub>2</sub>	Date	NO <sub>2</sub>	SO <sub>2</sub>	Date	NO <sub>2</sub>	SO <sub>2</sub>
2017/04/18	32.6	15.4	2017/08/22	20.6	3.40	2017/12/23	6.00	15.0
2017/04/21	27.2	26.5	2017/08/25	12.2	1.52	2017/12/26	3.28	2.92
2017/04/24	13.0	*	2017/08/28	9.54	6.42	2017/12/29	2.12	3.21
2017/04/27	*	*	2017/08/31	12.6	1.00	2018/01/01	8.27	21.0
2017/04/30	*	*	2017/09/03	21.3	5.80	2018/01/04	3.60	2.07
2017/05/03	13.0	20.6	2017/09/06	35.0	17.63	2018/01/07	3.56	3.71
2017/05/06	2.92	1.60	2017/09/09	2.96	1.83	2018/01/10	2.60	1.42
2017/05/09	9.16	*	2017/09/12	9.08	14.1	2018/01/13	8.56	11.3
2017/05/12	11.6	*	2017/09/15	13.6	4.25	2018/01/16	2.84	3.63
2017/05/15	15.1	2.08	2017/09/18	11.8	12.5	2018/01/19	10.1	4.76
2017/05/18	14.6	38.4	2017/09/21	12.2	8.63	2018/01/22	5.60	3.60
2017/05/21	9.52	6.88	2017/09/24	10.3	3.56	2018/01/25	3.00	2.40
2017/05/24	5.72	3.88	2017/09/27	8.60	2.20	2018/01/28	6.73	2.09
2017/05/27	5.52	1.84	2017/09/30	16.8	16.2	2018/01/31	10.9	4.99
2017/05/30	16.5	2.88	2017/10/03	7.88	14.7	2018/02/03	9.44	4.42
2017/06/02	15.9	2.48	2017/10/06	2.08	2.68	2018/02/06	4.95	4.17
2017/06/05	24.4	10.1	2017/10/09	18.4	3.84	2018/02/09	8.29	1.25
2017/06/08	12.0	7.04	2017/10/12	12.0	12.8	2018/02/12	2.91	0.52
2017/06/11	2.48	1.44	2017/10/15	*	15.88	2018/02/15	16.7	14.3
2017/06/14	7.60	4.80	2017/10/18	5.48	2.08	2018/02/18	9.33	1.52
2017/06/17	14.1	7.72	2017/10/21	7.20	3.83	2018/02/21	10.4	2.67
2017/06/20	14.0	4.00	2017/10/24	8.80	4.38	2018/02/24	11.5	*
2017/06/23	19.3	3.80	2017/10/27	7.68	1.75	2018/02/27	7.80	26.3
2017/06/26	24.0	18.3	2017/10/30	15.5	18.9	2018/03/02	7.52	2.77
2017/06/29	4.32	3.88	2017/11/02	33.0	14.8	2018/03/05	11.2	7.50
2017/07/02	3.56	2.67	2017/11/05	24.8	17.7	2018/03/08	8.16	5.67
2017/07/05	16.9	4.08	2017/11/08	5.32	3.88	2018/03/11	11.1	8.42
2017/07/08	1.76	1.04	2017/11/11	6.68	*	2018/03/14	9.83	15.73
2017/07/11	*	20.3	2017/11/14	2.32	2.04	2018/03/17	11.0	7.17
2017/07/14	18.1	2.50	2017/11/17	4.52	5.50	2018/03/20	12.8	8.13
2017/07/17	16.6	1.05	2017/11/20	6.48	3.45	2018/03/23	9.64	6.60
2017/07/20	16.0	1.80	2017/11/23	2.44	1.88	2018/03/26	12.4	6.71
2017/07/26	15.9	3.83	2017/11/26	5.55	3.71	2018/03/29	12.8	8.12
2017/07/29	17.2	2.44	2017/11/29	3.50	5.14	2018/04/01	8.94	5.17
2017/08/01	15.0	12.0	2017/12/02	5.00	7.76	2018/04/04	17.5	2.95
2017/08/04	3.92	1.88	2017/12/05	1.60	2.44	2018/04/07	14.8	4.04
2017/08/07	18.1	14.3	2017/12/08	6.18	8.82	2018/04/10	8.74	2.13
2017/08/10	18.3	5.54	2017/12/11	4.43	3.04	2018/04/13	13.2	4.92
2017/08/13	3.80	2.46	2017/12/14	3.48	2.36	2018/04/16	8.28	0.96
2017/08/16	14.8	10.8	2017/12/17	4.24	5.71	<b>Mean</b>	<b>10.8</b>	<b>6.87</b>
2017/08/19	27.5	*	2017/12/20	2.68	3.75	<b>σ</b>	<b>6.97</b>	<b>6.54</b>

Concentrations in  $\mu\text{g.m}^{-3}$

\* No data

**APPENDIX 13F - AIR POLLUTION DATA FROM THE WALLACEDENE AAQM STATION**

Date	NO <sub>2</sub>	SO <sub>2</sub>	Date	NO <sub>2</sub>	SO <sub>2</sub>	Date	NO <sub>2</sub>	SO <sub>2</sub>
2017/04/18	34.2	12.3	2017/08/22	*	9.60	2017/12/23	*	11.4
2017/04/21	35.9	10.2	2017/08/25	*	4.20	2017/12/26	*	3.96
2017/04/24	32.9	12.2	2017/08/28	*	5.94	2017/12/29	*	6.88
2017/04/27	16.7	3.96	2017/08/31	*	7.16	2018/01/01	*	9.00
2017/04/30	15.5	2.96	2017/09/03	*	6.16	2018/01/04	*	3.67
2017/05/03	23.3	5.56	2017/09/06	*	9.52	2018/01/07	*	6.56
2017/05/06	12.3	2.36	2017/09/09	*	3.28	2018/01/10	*	6.88
2017/05/09	28.4	8.00	2017/09/12	*	4.22	2018/01/13	*	10.1
2017/05/12	12.0	5.96	2017/09/15	*	5.00	2018/01/16	*	4.63
2017/05/15	14.9	11.7	2017/09/18	*	4.12	2018/01/19	*	9.04
2017/05/18	12.0	7.08	2017/09/21	*	5.36	2018/01/22	*	4.71
2017/05/21	8.79	5.44	2017/09/24	*	7.72	2018/01/25	*	4.00
2017/05/24	*	5.88	2017/09/27	*	7.25	2018/01/28	*	6.00
2017/05/27	*	3.68	2017/09/30	*	8.88	2018/01/31	*	7.17
2017/05/30	42.7	9.92	2017/10/03	*	7.04	2018/02/03	*	5.79
2017/06/02	40.8	5.68	2017/10/06	*	4.84	2018/02/06	*	5.50
2017/06/05	48.5	9.12	2017/10/09	*	5.88	2018/02/09	*	6.72
2017/06/08	40.3	6.67	2017/10/12	*	5.32	2018/02/12	*	5.36
2017/06/11	12.5	1.80	2017/10/15	*	6.44	2018/02/15	*	8.54
2017/06/14	48.0	3.14	2017/10/18	*	4.84	2018/02/18	*	5.32
2017/06/17	*	4.00	2017/10/21	*	7.20	2018/02/21	*	11.8
2017/06/20	*	5.32	2017/10/24	*	5.04	2018/02/24	*	8.92
2017/06/23	*	5.67	2017/10/27	*	6.29	2018/02/27	*	5.17
2017/06/26	*	8.67	2017/10/30	*	6.76	2018/03/02	*	6.84
2017/06/29	*	3.56	2017/11/02	*	12.3	2018/03/05	*	6.40
2017/07/02	*	3.24	2017/11/05	*	8.04	2018/03/08	*	8.40
2017/07/05	*	6.40	2017/11/08	*	4.48	2018/03/11	*	*
2017/07/08	*	2.33	2017/11/11	*	7.32	2018/03/14	*	13.8
2017/07/11	*	9.36	2017/11/14	*	6.84	2018/03/17	*	7.00
2017/07/14	*	6.32	2017/11/17	*	5.24	2018/03/20	*	3.36
2017/07/17	*	4.62	2017/11/20	*	7.68	2018/03/23	*	1.32
2017/07/20	*	4.36	2017/11/23	*	9.64	2018/03/26	*	3.60
2017/07/26	*	3.92	2017/11/26	*	6.96	2018/03/29	*	2.96
2017/07/29	*	6.28	2017/11/29	*	6.84	2018/04/01	*	1.36
2017/08/01	*	4.96	2017/12/02	*	11.0	2018/04/04	*	2.92
2017/08/04	*	2.52	2017/12/05	*	6.32	2018/04/07	*	3.64
2017/08/07	*	5.64	2017/12/08	*	11.5	2018/04/10	*	2.20
2017/08/10	*	7.40	2017/12/11	*	*	2018/04/13	*	1.78
2017/08/13	*	2.75	2017/12/14	*	*	2018/04/16	*	1.70
2017/08/16	*	5.54	2017/12/17	*	6.16	<b>Mean</b>	<b>26.6</b>	<b>6.15</b>
2017/08/19	*	3.20	2017/12/20	*	2.68	<b>σ</b>	<b>13.5</b>	<b>2.67</b>

Concentrations in  $\mu\text{g.m}^{-3}$

\* No data



**APPENDIX 13F - AIR POLLUTION DATA FROM THE WALLACEDENE AAQM STATION**

Date	PM <sub>10</sub>	O <sub>3</sub>	Date	PM <sub>10</sub>	O <sub>3</sub>	Date	PM <sub>10</sub>	O <sub>3</sub>
2017/04/18	74.6	25.0	2017/08/22	73.7	22.5	2017/12/23	65.6	28.9
2017/04/21	76.1	23.6	2017/08/25	33.2	29.3	2017/12/26	22.6	34.8
2017/04/24	98.6	21.1	2017/08/28	33.1	33.9	2017/12/29	31.9	33.7
2017/04/27	34.6	30.5	2017/08/31	27.0	35.0	2018/01/01	41.9	46.1
2017/04/30	20.9	24.3	2017/09/03	35.8	26.4	2018/01/04	24.0	26.2
2017/05/03	40.4	19.4	2017/09/06	65.1	35.1	2018/01/07	29.8	42.0
2017/05/06	18.2	35.4	2017/09/09	13.0	41.8	2018/01/10	18.7	21.3
2017/05/09	45.0	17.0	2017/09/12	36.6	30.7	2018/01/13	53.6	35.8
2017/05/12	47.6	25.5	2017/09/15	40.7	20.0	2018/01/16	35.9	29.1
2017/05/15	57.3	15.8	2017/09/18	36.7	45.7	2018/01/19	48.0	42.7
2017/05/18	47.0	22.4	2017/09/21	32.3	50.8	2018/01/22	51.7	34.6
2017/05/21	30.3	27.8	2017/09/24	34.0	31.3	2018/01/25	11.5	28.9
2017/05/24	28.1	11.7	2017/09/27	28.7	33.8	2018/01/28	44.8	25.9
2017/05/27	38.3	16.0	2017/09/30	39.0	25.2	2018/01/31	37.5	34.9
2017/05/30	83.6	6.20	2017/10/03	49.0	36.2	2018/02/03	38.2	30.1
2017/06/02	63.3	17.9	2017/10/06	28.9	45.7	2018/02/06	30.7	41.5
2017/06/05	48.6	14.8	2017/10/09	29.9	43.7	2018/02/09	18.2	29.7
2017/06/08	55.0	13.7	2017/10/12	32.3	32.1	2018/02/12	32.0	24.7
2017/06/11	17.2	39.6	2017/10/15	45.1	37.3	2018/02/15	41.0	34.2
2017/06/14	29.3	19.7	2017/10/18	22.0	35.1	2018/02/18	17.8	40.5
2017/06/17	62.9	22.2	2017/10/21	16.4	42.6	2018/02/21	19.5	*
2017/06/20	53.5	22.4	2017/10/24	25.7	56.8	2018/02/24	47.9	*
2017/06/23	64.8	26.0	2017/10/27	18.9	35.8	2018/02/27	17.4	*
2017/06/26	58.5	14.9	2017/10/30	36.0	30.0	2018/03/02	37.9	*
2017/06/29	24.5	20.3	2017/11/02	68.5	50.4	2018/03/05	37.6	23.9
2017/07/02	14.7	17.5	2017/11/05	34.5	*	2018/03/08	29.0	22.1
2017/07/05	35.4	15.9	2017/11/08	31.1	*	2018/03/11	27.3	31.0
2017/07/08	10.3	33.4	2017/11/11	38.4	51.6	2018/03/14	24.4	23.5
2017/07/11	62.7	20.5	2017/11/14	29.2	56.1	2018/03/17	38.8	30.4
2017/07/14	37.2	17.8	2017/11/17	24.7	46.6	2018/03/20	51.7	27.2
2017/07/17	25.0	16.7	2017/11/20	26.7	46.4	2018/03/23	25.8	37.5
2017/07/20	58.9	12.3	2017/11/23	17.7	40.3	2018/03/26	18.3	39.4
2017/07/26	24.7	25.2	2017/11/26	16.9	38.6	2018/03/29	13.33	29.7
2017/07/29	63.3	18.8	2017/11/29	38.7	34.2	2018/04/01	7.43	18.1
2017/08/01	55.0	21.5	2017/12/02	42.4	33.2	2018/04/04	14.0	36.5
2017/08/04	5.12	39.1	2017/12/05	17.8	38.2	2018/04/07	12.2	29.6
2017/08/07	23.6	39.9	2017/12/08	41.9	36.9	2018/04/10	9.78	30.6
2017/08/10	46.2	23.2	2017/12/11	91.3	57.6	2018/04/13	8.33	27.0
2017/08/13	19.7	50.0	2017/12/14	41.8	45.8	2018/04/16	*	29.0
2017/08/16	40.4	34.5	2017/12/17	40.4	30.8	<b>Mean</b>	<b>36.5</b>	<b>31.0</b>
2017/08/19	36.6	45.9	2017/12/20	27.2	37.4	<b>σ</b>	<b>18.1</b>	<b>10.6</b>

Concentrations in  $\mu\text{g.m}^{-3}$

\* No data

**APPENDIX 14A - MEAN MONTHLY CONCENTRATIONS FOR ATLANTIS (TOP) AND CITY HALL (BOTTOM)**

	APR-17	MAY	JUN	JUL	AUG	SEPT	OCT	NOV	DEC	JAN-18	FEB	MAR	APR
PM <sub>10</sub>	NOT MONITORED												
Carbon monoxide (CO)	NOT MONITORED												
Nitrogen dioxide (NO <sub>2</sub> )	NOT MONITORED												
Ozone (O <sub>3</sub> )	52.8	48.6	46.8	52.6	52.4	54.6	55.7	51.2	54.6	47.4	41.4	39.1	40.9
Sulfur dioxide (SO <sub>2</sub> )	2.06	3.42	4.06	3.50	3.42	4.79	1.98	2.74	2.70	3.17	2.80	3.04	1.92

	APR-17	MAY	JUN	JUL	AUG	SEPT	OCT	NOV	DEC	JAN-18	FEB	MAR	APR
PM <sub>10</sub>	NOT MONITORED												
Carbon monoxide (CO)	2.95	3.35	2.13	3.15	*	0.34	0.25	0.14	*	0.1	*	0.12	*
Nitrogen dioxide (NO <sub>2</sub> )	43.9	40.9	30.2	33.0	30.7	29.7	27.4	24.2	23.6	22.7	27.2	26.7	*
Ozone (O <sub>3</sub> )	NOT MONITORED												
Sulfur dioxide (SO <sub>2</sub> )	5.62	7.42	2.77	1.55	1.12	2.03	2.12	2.96	5.69	2.82	*	*	*

\* No data recorded by AQM station

NO<sub>2</sub>/O<sub>3</sub>/PM<sub>10</sub>/SO<sub>2</sub> concentrations in µg.m<sup>-3</sup>

CO concentration in mg.m<sup>-3</sup>

The availability index shows the amount of time the station was operational and collected data

**AAQM station availability index**

- 70-100 %
- 50-69 %
- 30-49 %
- 0-29 %

**APPENDIX 14B - MEAN MONTHLY CONCENTRATIONS FOR GOODWOOD (TOP) AND SOMERSET-WEST (BOTTOM)**

	APR-17	MAY	JUN	JUL	AUG	SEPT	OCT	NOV	DEC	JAN-18	FEB	MAR	APR
PM <sub>10</sub>	NOT MONITORED												
Carbon monoxide (CO)	*	0.94	1.03	1.02	1.14	1.47	*	*	*	*	*	*	*
Nitrogen dioxide (NO <sub>2</sub> )	*	*	30.9	28.7	21.7	19.7	*	30.6	23.3	20.9	21.5	18.5	*
Ozone (O <sub>3</sub> )	*	22.0	28.3	26.3	32.0	35.4	*	*	*	23.7	26.8	26.1	*
Sulfur dioxide (SO <sub>2</sub> )	*	*	16.9	13.2	7.40	8.21	*	*	*	2.56	2.96	5.12	8.80

	APR-17	MAY	JUN	JUL	AUG	SEPT	OCT	NOV	DEC	JAN-18	FEB	MAR	APR
PM <sub>10</sub>	NOT MONITORED												
Carbon monoxide (CO)	NOT MONITORED												
Nitrogen dioxide (NO <sub>2</sub> )	NOT MONITORED												
Ozone (O <sub>3</sub> )	NOT MONITORED												
Sulfur dioxide (SO <sub>2</sub> )	4.01	3.00	3.27	3.07	3.08	2.99	2.79	1.65	2.62	2.83	3.12	1.68	2.25

\* No data recorded by AQM station

NO<sub>2</sub>/O<sub>3</sub>/PM<sub>10</sub>/SO<sub>2</sub> concentrations in µg.m<sup>-3</sup>

CO concentrations in mg.m<sup>-3</sup>

The availability index shows the amount of time the station was operational and collected data

**AAQM station availability index**

- 70-100 %
- 50-69 %
- 30-49 %
- 0-29 %

**APPENDIX 14C - MEAN MONTHLY CONCENTRATIONS FOR TABLEVIEW (TOP) AND WALLACEDENE (BOTTOM)**

	APR-17	MAY	JUN	JUL	AUG	SEPT	OCT	NOV	DEC	JAN-18	FEB	MAR	APR
PM <sub>10</sub>	NOT MONITORED												
Carbon monoxide (CO)	NOT MONITORED												
Nitrogen dioxide (NO <sub>2</sub> )	13.2	10.6	10.4	14.5	16.1	13.4	11.7	6.11	4.32	5.70	10.9	9.67	14.0
Ozone (O <sub>3</sub> )	NOT MONITORED												
Sulfur dioxide (SO <sub>2</sub> )	8.95	9.75	5.67	5.36	5.26	8.90	8.73	5.23	5.87	4.28	7.53	7.34	3.90

	APR-17	MAY	JUN	JUL	AUG	SEPT	OCT	NOV	DEC	JAN-18	FEB	MAR	APR
PM <sub>10</sub>	43.0	40.0	41.1	42.6	33.8	34.4	33.9	31.9	42.7	34.7	34.6	28.6	21.0
Carbon monoxide (CO)	NOT MONITORED												
Nitrogen dioxide (NO <sub>2</sub> )	22.5	18.4	28.1	*	*	*	*	*	*	*	*	*	*
Ozone (O <sub>3</sub> )	31.6	23.9	25.9	23.5	33.2	33.6	37.2	41.1	37.7	32.9	34.5	28.7	27.1
Sulfur dioxide (SO <sub>2</sub> )	6.19	6.36	4.74	5.40	5.14	6.33	6.60	7.48	6.17	6.03	7.09	4.91	2.96

\* No data recorded by AQM station

NO<sub>2</sub>/O<sub>3</sub>/PM<sub>10</sub>/SO<sub>2</sub> concentrations in µg.m<sup>-3</sup>

CO concentrations in mg.m<sup>-3</sup>

The availability index shows the amount of time the station was operational and collected data

**AAQM station availability index**

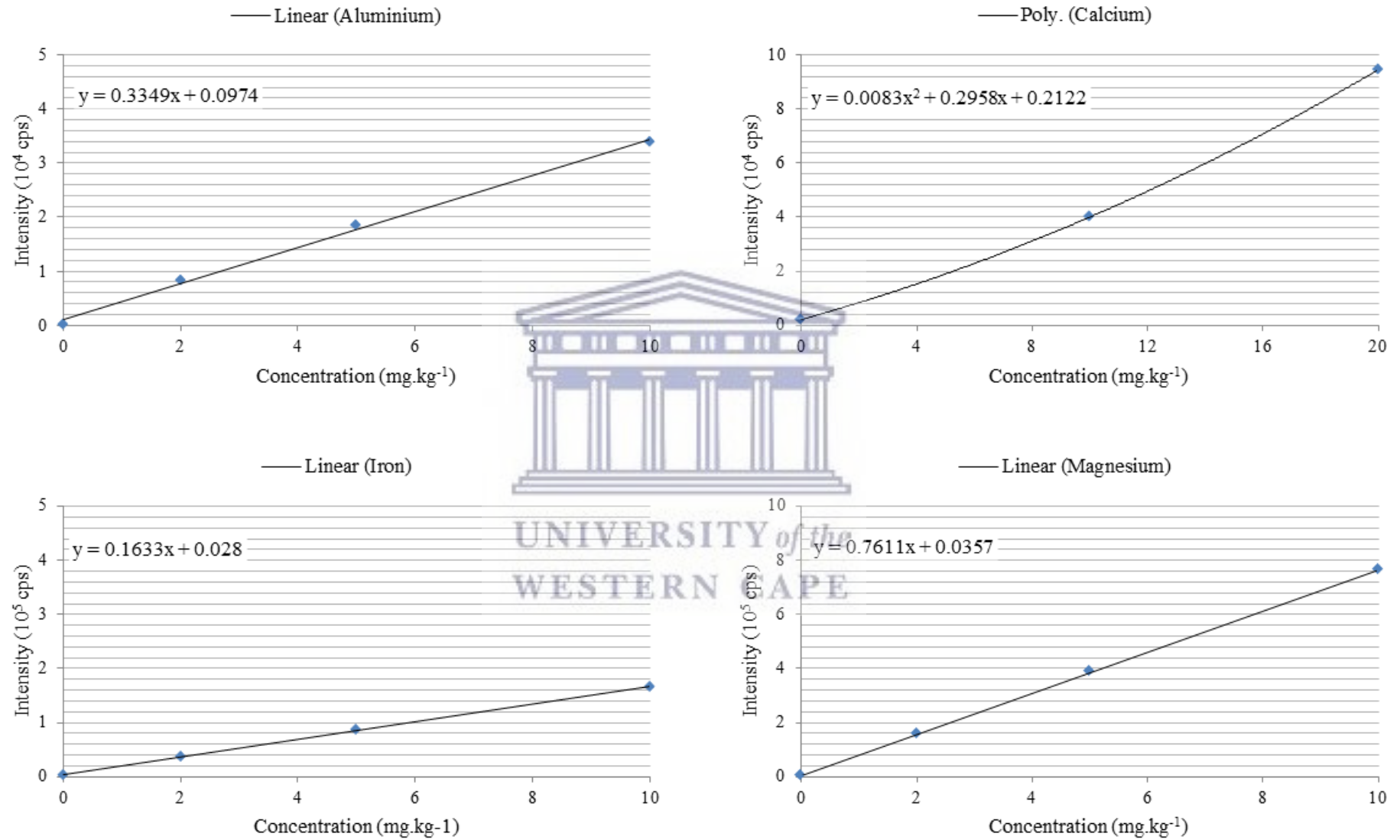
- 70-100 %
- 50-69 %
- 30-49 %
- 0-29 %

**APPENDIX 15 - METEOROLOGICAL CONDITIONS (MEAN MONTHLY VALUES) FOR SEPTEMBER 2017 AND JANUARY 2018**

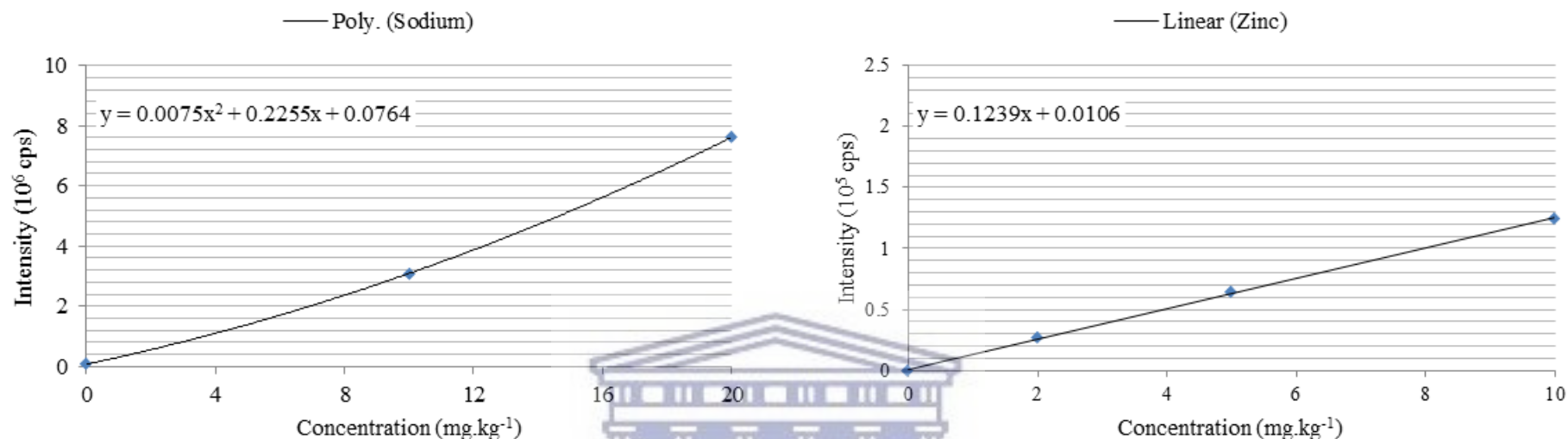
	September 2017		January 2018	
	Weekdays	Weekend days	Weekdays	Weekend days
Temperature (°C)	17.0	17.1	22.6	23.3
Rh (%)	78	66	65	71
Precipitation (mm)	1.1	0.0	0.1	0.2
UV exposure (%)	25	50	25	50
Air velocity (m.s <sup>-1</sup> )	2.4	3.3	3.3	3.5
Wind direction frequency (%)				
Northerly (N)	50	9.1	8.3	50
Easterly (E)	-	9.1	17	8.3
Southerly (S)	36	82	75	25
Westerly (W)	14	-	-	17
- No data				



## APPENDIX 16 - STANDARDISATION CURVES (ICP-OES)



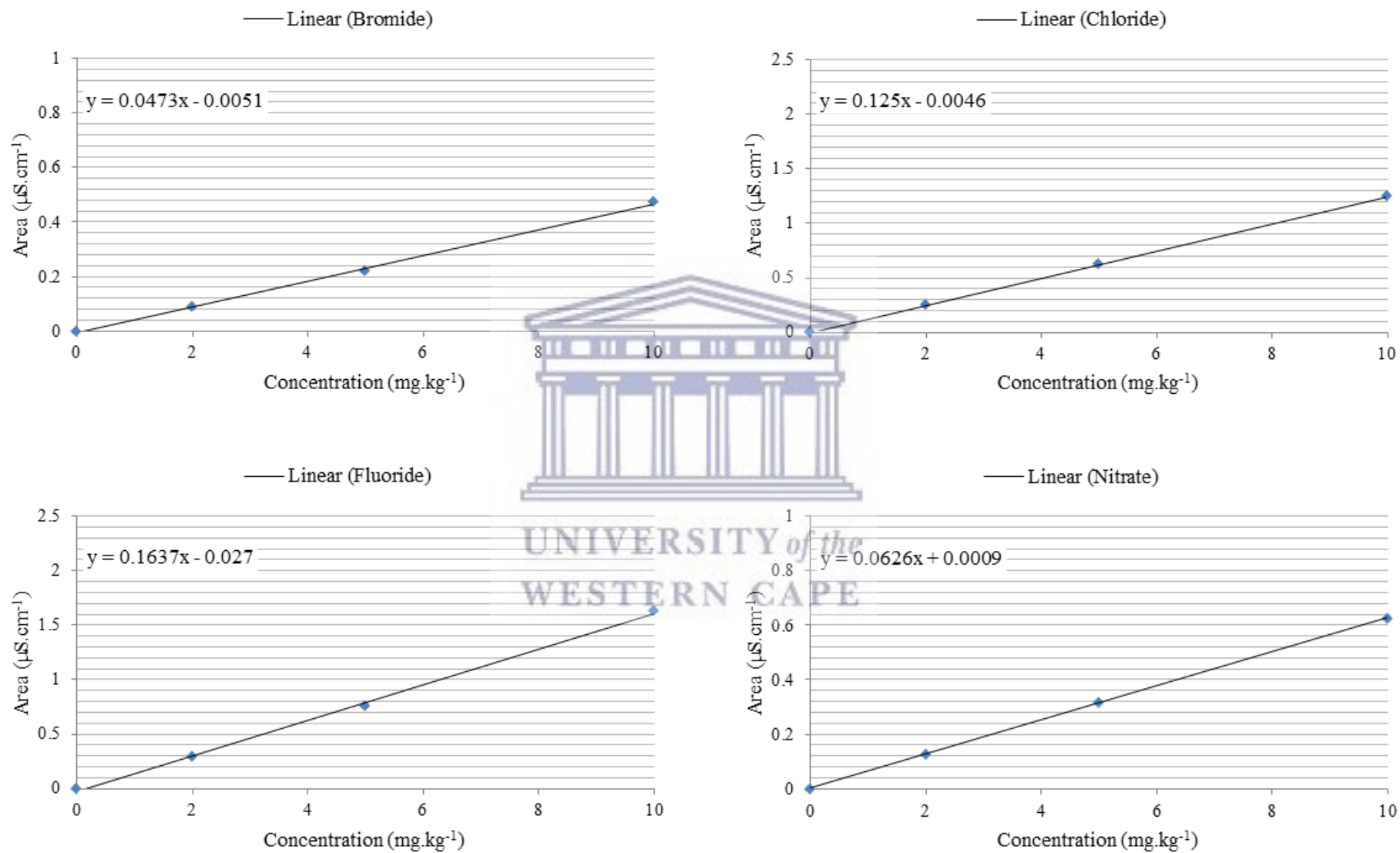
## APPENDIX 16 - STANDARDISATION CURVES (ICP-OES)



	RSD (%)					
	Aluminium	*Calcium	Iron	Magnesium	*Sodium	Zinc
Standard 1 (2.00 mg.kg <sup>-1</sup> and *10.0 mg.kg <sup>-1</sup> )	1.63	0.51	0.74	0.56	1.41	1.59
Standard 2 (5.00 mg.kg <sup>-1</sup> and *20.0 mg.kg <sup>-1</sup> )	1.42	0.60	0.45	0.22	0.54	0.28
Standard 3 (10.0 mg.kg <sup>-1</sup> )	0.63	-	0.48	0.74	-	0.48

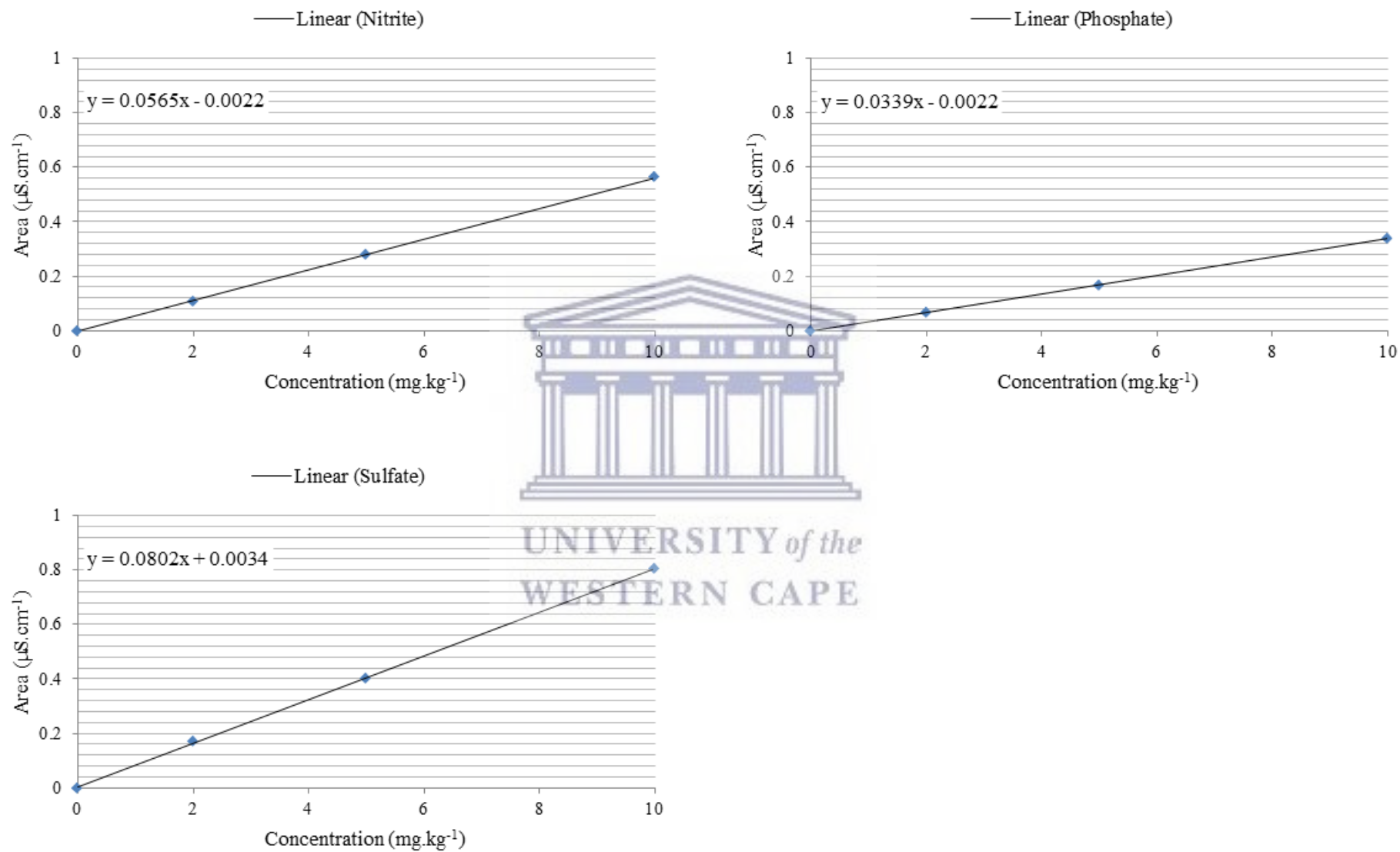
Note: Only two standards of calcium and sodium (10.0 and 20.0 mg.kg<sup>-1</sup>) were used for instrument standardisation compared to three standards for aluminium, iron, magnesium and zinc (2.00, 5.00 and 10.0 mg.kg<sup>-1</sup>). Calcium and sodium stock standard solutions were ten times more concentrated (1,000 mg.kg<sup>-1</sup>) than the four latter elements (100 mg.kg<sup>-1</sup>). Technician used the protocol for ICP-OES standardisation.

## APPENDIX 17 - STANDARDISATION CURVES (IC)



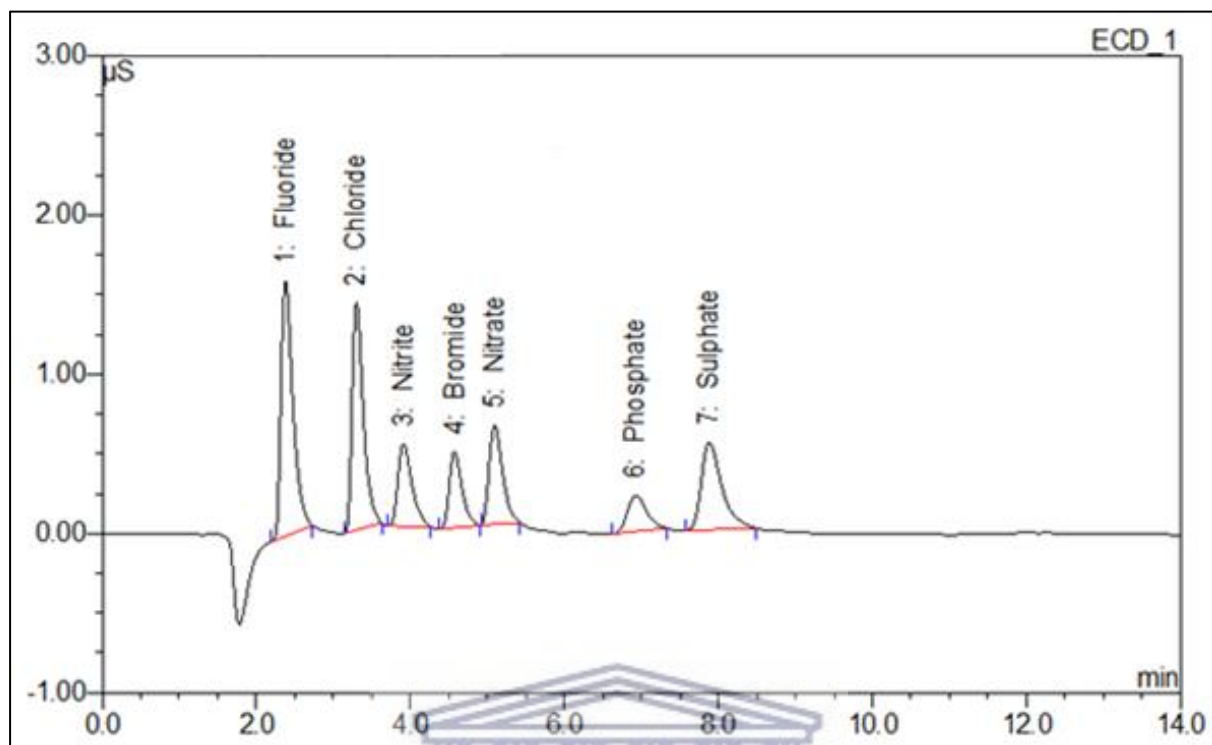


## APPENDIX 17 - STANDARDISATION CURVES (IC)



## APPENDIX 18 - CHROMATOGRAMS (IC)

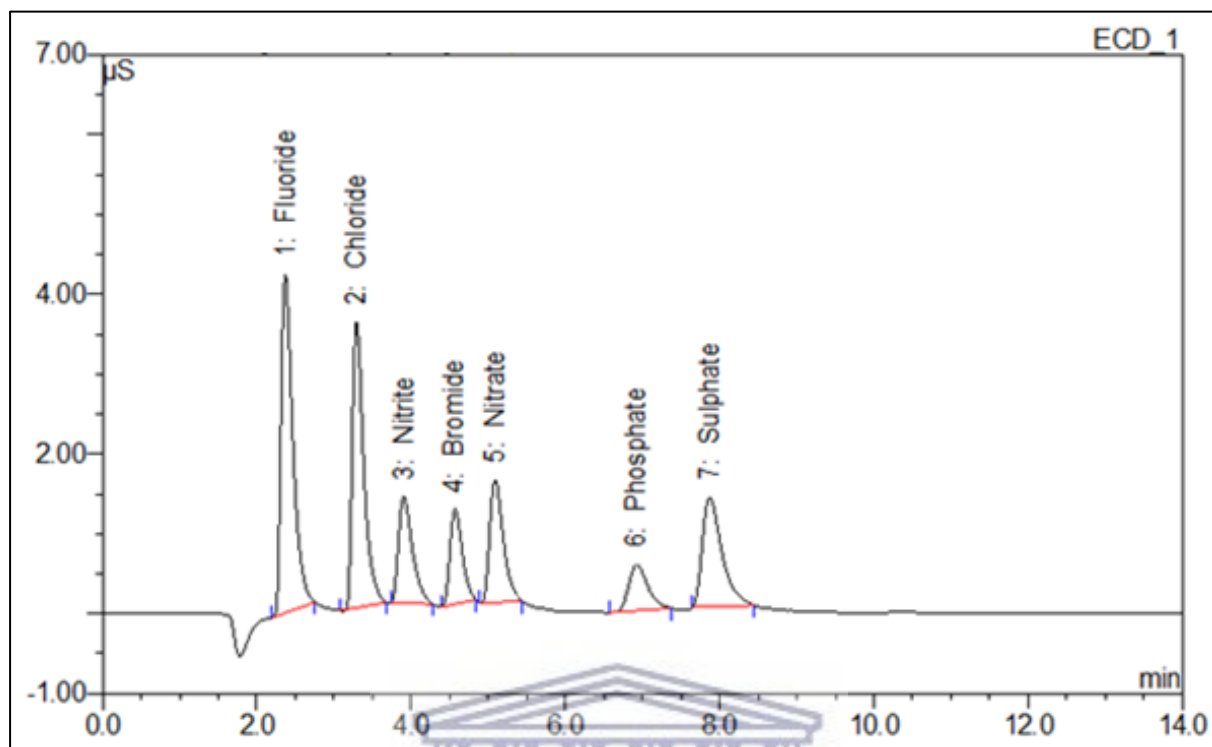
Standard 1 (2.00 mg.kg<sup>-1</sup>)



Peak no.	Component name	Retention time	Area (μS.cm-1)	Height (μS)	Amount (mg.kg <sup>-1</sup> )
1	Fluoride	2.38	0.29	1.60	1.80
2	Chloride	3.30	0.24	1.42	1.94
3	Nitrite	3.91	0.11	0.52	1.95
4	Bromide	4.57	0.09	0.48	1.95
5	Nitrate	5.09	0.13	0.62	2.01
6	Phosphate	6.93	0.07	0.23	1.93
7	Sulfate	7.88	0.17	0.55	2.10

## APPENDIX 18 - CHROMATOGRAMS (IC)

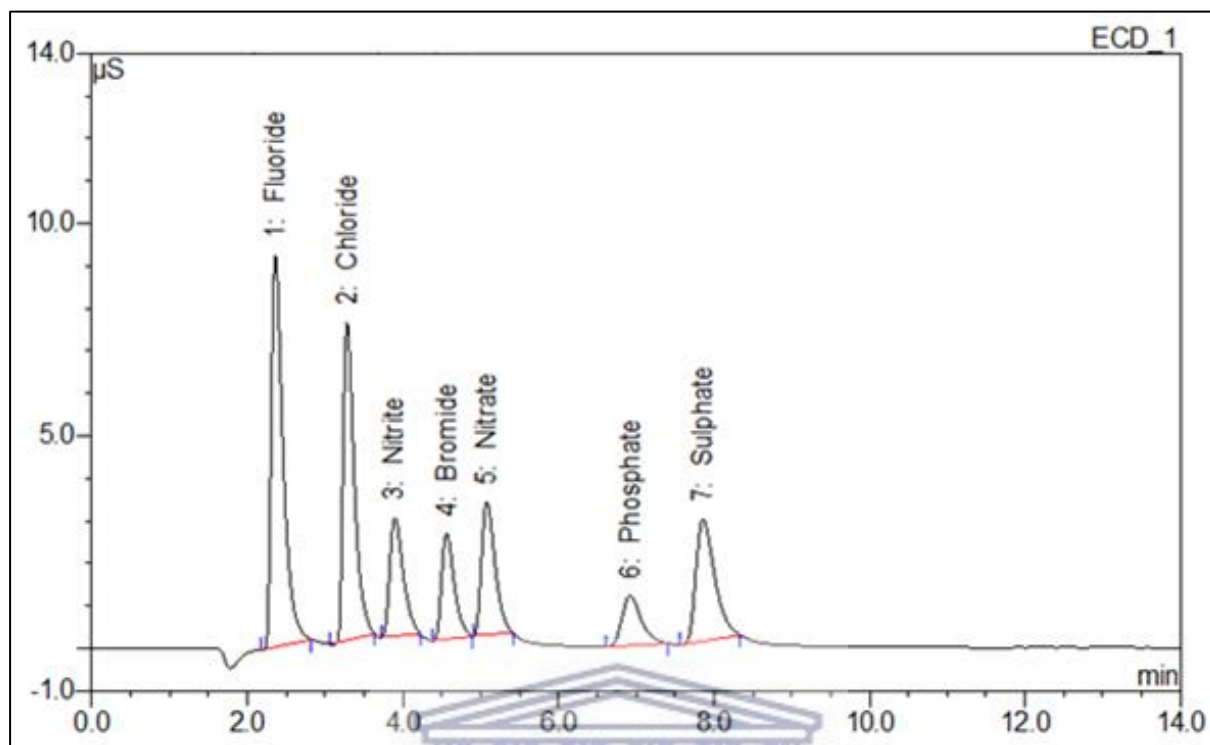
Standard 2 (5.00 mg.kg<sup>-1</sup>)



Peak no.	Component name	Retention time	Area (μS.cm-1)	Height (μS)	Amount (mg.kg <sup>-1</sup> )
1	Fluoride	2.37	0.76	4.23	4.72
2	Chloride	3.29	0.62	3.58	4.95
3	Nitrite	3.91	0.28	1.33	4.95
4	Bromide	4.57	0.22	1.19	4.69
5	Nitrate	5.09	0.32	1.54	5.03
6	Phosphate	6.93	0.16	0.57	4.89
7	Sulfate	7.87	0.40	1.37	4.99

## APPENDIX 18 - CHROMATOGRAMS (IC)

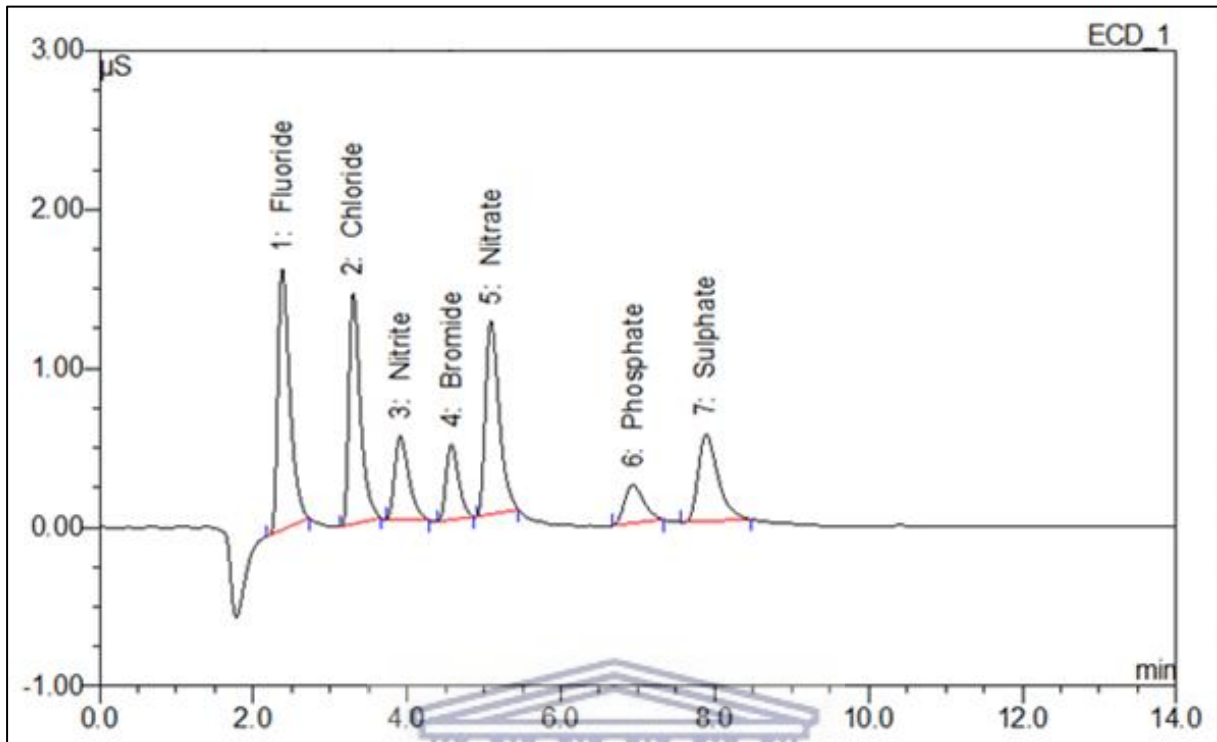
Standard 3 (10.0 mg.kg<sup>-1</sup>)



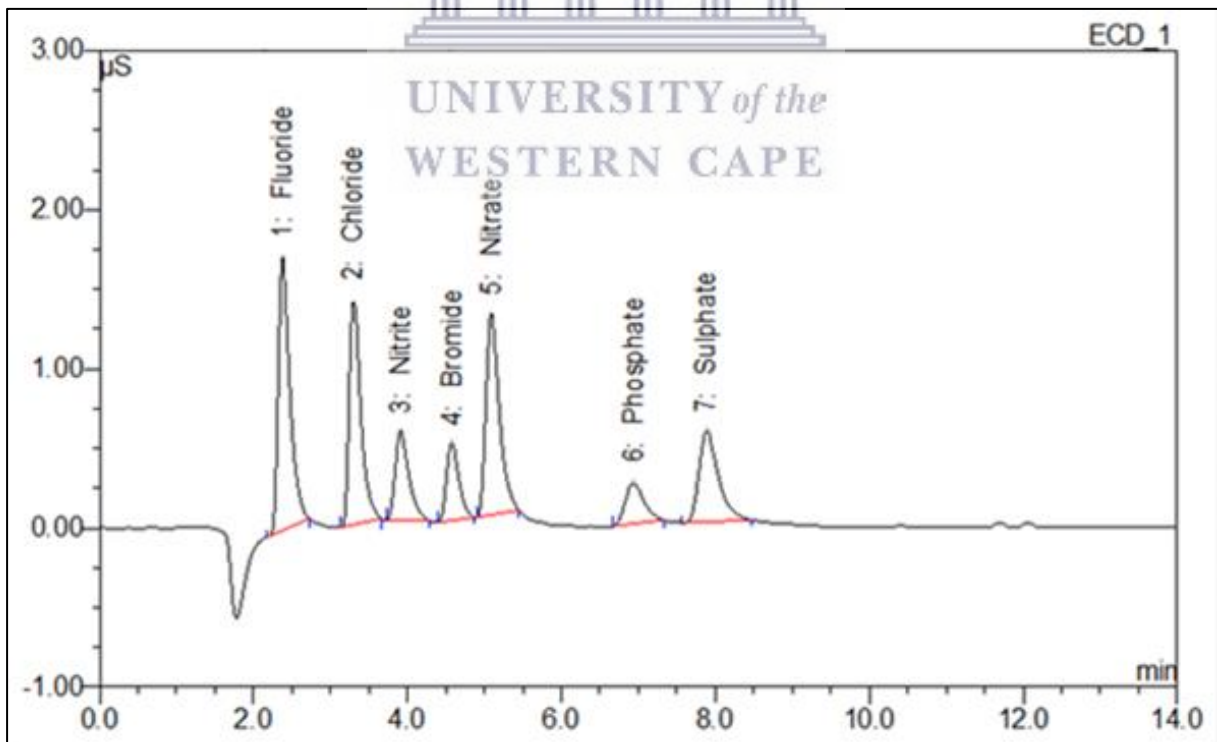
Peak no.	Component name	Retention time	Area (μS.cm-1)	Height (μS)	Amount (mg.kg <sup>-1</sup> )
1	Fluoride	2.36	1.63	9.21	10.2
2	Chloride	3.28	1.25	7.48	10.0
3	Nitrite	3.90	0.56	2.80	10.0
4	Bromide	4.56	0.47	2.50	10.2
5	Nitrate	5.08	0.63	3.13	9.98
6	Phosphate	6.92	0.34	1.18	10.1
7	Sulfate	7.86	0.81	2.88	9.98

## APPENDIX 18 - CHROMATOGRAMS (IC)

Control solution (2.00 mg.kg<sup>-1</sup>, pre-sample analysis)

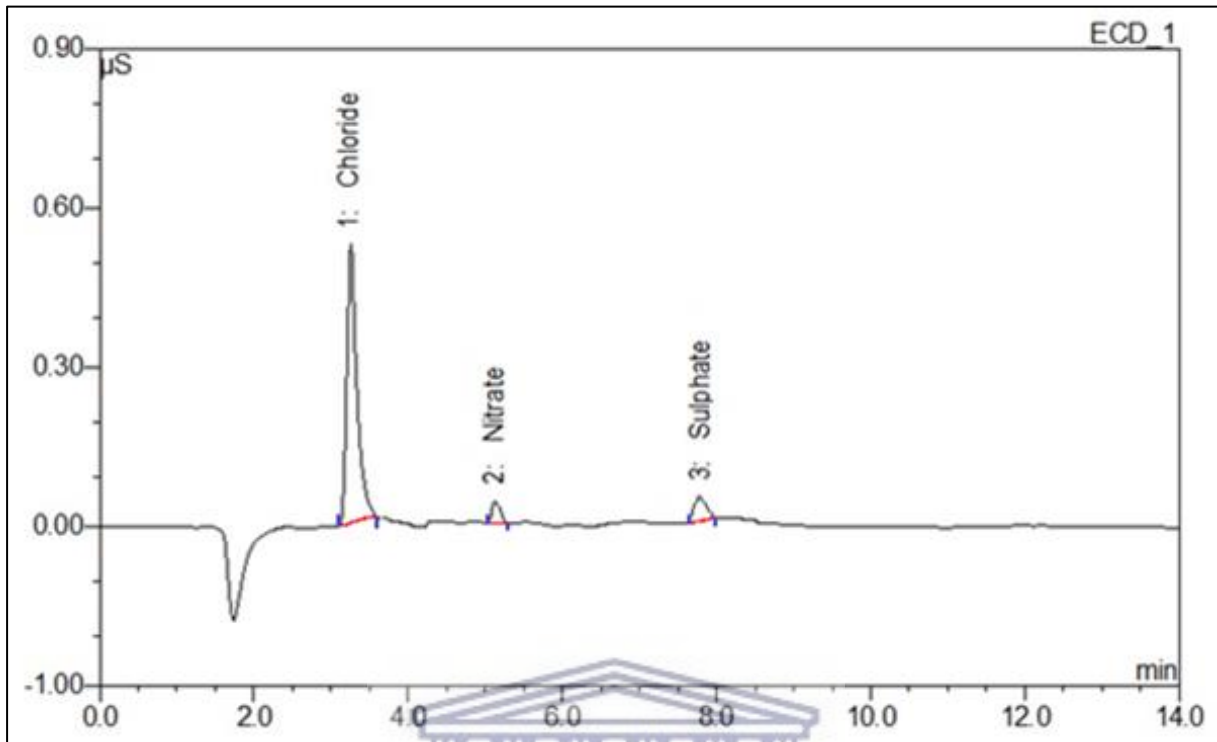


Control solution (2.00 mg.kg<sup>-1</sup>, post-sample analysis)

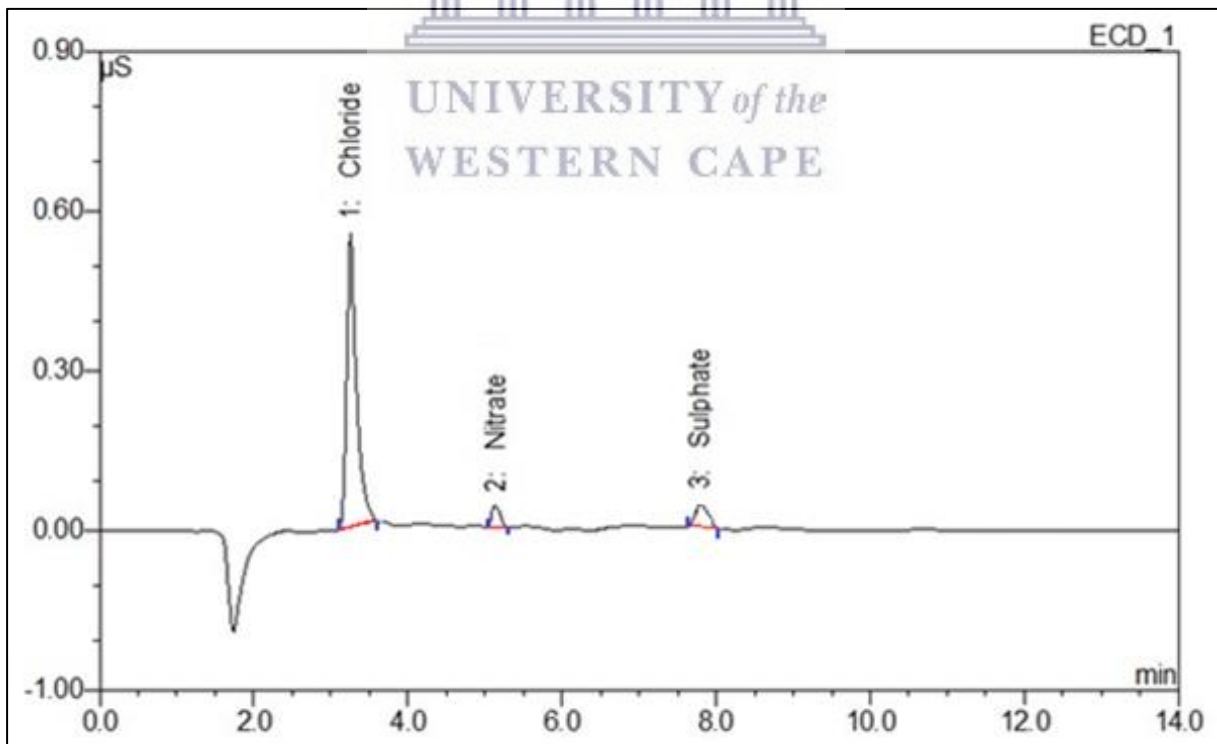


## APPENDIX 18 - CHROMATOGRAMS (IC)

Sample solution (September 2017, weekday)

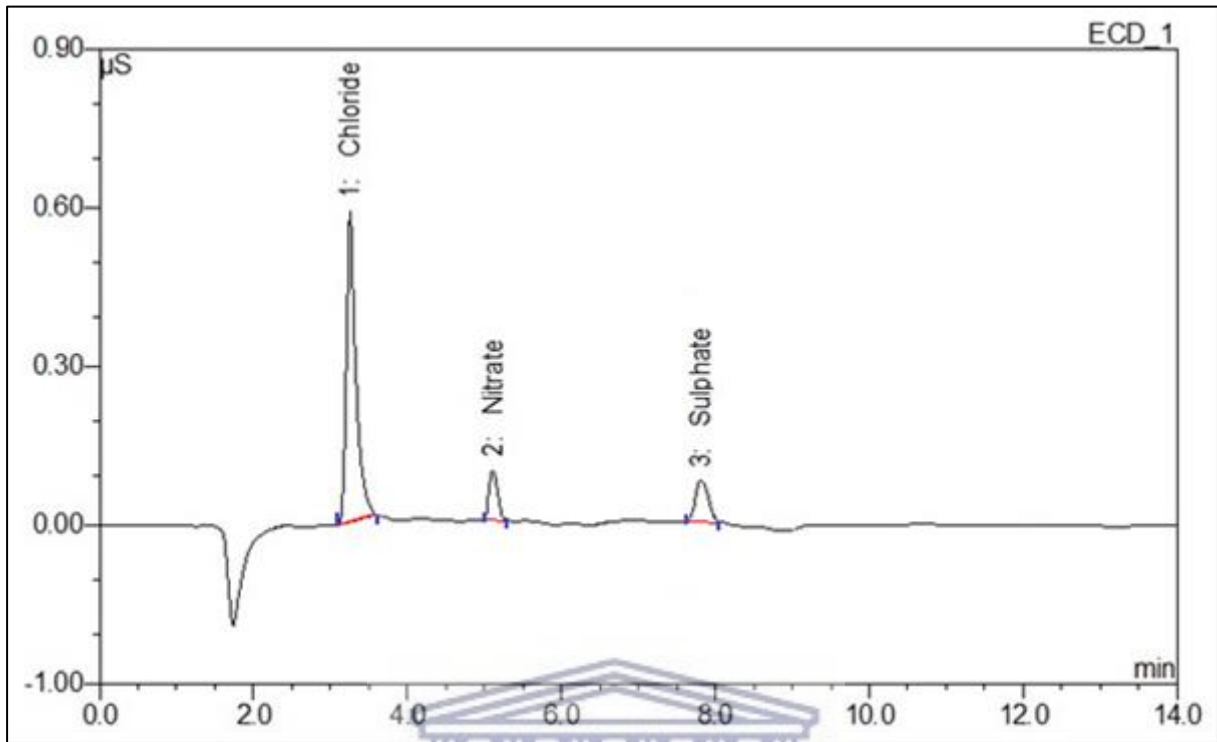


Sample solution (September 2017, weekend day)



## APPENDIX 18 - CHROMATOGRAMS (IC)

Sample solution (January 2018, weekday)



Sample solution (January 2018, weekend day)

